Synthesis of bioactive surfaces for the control of stem cells differentiation

Émilie Prouvé

THÈSE EN COTUTELLE PRÉSENTÉE

POUR OBTENIR LE GRADE DE

DOCTEUR DE L'UNIVERSITÉ DE BORDEAUX ET DE L'UNIVERSITÉ LAVAL

ÉCOLE DOCTORALE DES SCIENCES CHIMIQUES

PROGRAMME DE DOCTORAT EN GÉNIE DES MATÉRIAUX ET DE LA MÉTALLURGIE

SPÉCIALITÉ : CHIMIE ET TECHNOLOGIES POUR LE VIVANT

par

Émilie PROUVÉ

Synthesis of bioactive surfaces for the control of stem cells differentiation

---

Soutenue le 12 Octobre 2021 devant la commission d'examen formée de :

M. G. SUBRA	Professeur, Université de Montpellier	Président du Jury
Mme M. CERRUTI	Professeur, Université McGill	Rapporteur
Mme M. CUCCHIARINI	Professeur, Université de la Sarre	Examinateur
M. J. RUEL	Professeur, Université Laval	Examinateur
Mme M.-C. DURRIEU	Directrice de recherche, Université de Bordeaux	Directrice de thèse
M. G. LAROCHE	Professeur, Université Laval	Co-Directeur de thèse

Synthèse de surfaces bioactives pour le contrôle de la différenciation des cellules souches

Résumé

La réparation des défauts osseux de taille importante (fracture, tumeur, nécrose de l'os) pour lesquelles une partie de l'os est manquante et doit être remplacée, demeure un défi important pour le domaine médical. Des matériaux synthétiques, comme des matériaux céramiques, métalliques, et polymères, sont ainsi développés comme substituts osseux. Mais ces matériaux n'interagissent pas suffisamment avec l'os du patient et finissent par être encapsulés par une couche de tissu fibreux, ce qui peut résulter en une fracture de l'os, de l'implant, ou de l'interface entre les deux. La recherche vise donc à étudier et comprendre les interactions entre les cellules et les matériaux, afin de développer des matériaux capables d'interagir avec les cellules, et de mettre au point des implants combinant un matériau bioactif, des cellules, et des facteurs bioactifs permettant la reconstruction du tissu osseux.

Dans ce contexte, les cellules souches mésenchymateuses (MSCs) ont gagné en popularité en médecine régénératrice compte tenu de leur capacité d'auto-renouvellement, leur multipotence, et leur taux de prolifération élevé. Cependant, une fois extraites du patient et cultivées in vitro, les MSCs ont tendance à se différencier de manière aléatoire, ce qui conduit à une population hétérogène de cellules avec laquelle il est difficile de reconstruire un tissu. Bien que les MSCs soient utilisées en clinique pour le traitement de diverses pathologies, une meilleure compréhension de leur comportement reste nécessaire pour permettre de contrôler leur différenciation vers une lignée spécifique et ainsi améliorer leurs performances en clinique.

Les hydrogels ont émergé comme matériaux prometteurs pour la culture cellulaire puisqu'ils permettent de mimer la matrice extracellulaire naturelle des cellules. Notamment, de nombreuses études ont évalué l'impact de la rigidité des hydrogels sur la différenciation des MSCs et ont montré qu'une rigidité proche de celle d'un tissu naturel favorise la différenciation vers les cellules de ce tissu. Cependant, il est maintenant reconnu que les hydrogels et les tissus naturels ne sont pas caractérisés uniquement par leur rigidité, mais aussi par leur viscoélasticité. Or peu d'études ont été menées sur l'impact des propriétés viscoélastiques des hydrogels sur la différenciation des MSCs (15 articles sur les cinq dernières années via PubMed).

Dans ce projet, il a été montré qu'il était possible de synthétiser des hydrogels de poly(acrylamide-co-acide acrylique) avec une rigidité et une viscoélasticité contrôlées, mesurées par compression et par AFM. Cinq hydrogels ont été choisis pour étudier l'impact des propriétés mécaniques sur la différenciation ostéogénique des MSCs en variant la rigidité et le pourcentage de relaxation : 15 kPa-15%, 60 kPa-15%, 140 kPa-15%, 100 kPa-30%, et 140 kPa-70%. Il a été montré que la fonctionnalisation de surface de ces hydrogels avec un peptide

mimétique de la protéine BMP-2 a mené à une forme cellulaire étoilée après deux semaines de différenciation, sauf pour la rigidité la plus basse (15 kPa). Cette forme cellulaire étoilée correspondrait à une forme d'ostéocyte, qui est le dernier stade de différenciation ostéogénique des MSCs, et qui n'a jamais été obtenu in vitro à notre connaissance. De plus, une rigidité de 60 kPa a mené à une plus forte expression de marqueurs de différenciation ostéocytaires par rapport à des rigidités de 15 et 140 kPa, pour une même relaxation de 15%. Enfin, la plus forte expression de marqueurs de différenciation d'ostéoblastes et d'ostéocytes a été observée pour l'hydrogel présentant 70% de relaxation et une rigidité de 140 kPa. Ceci semble montrer qu'une viscoélasticité élevée favorise la différenciation ostéogénique des MSCs, même si elle est associée à une rigidité qui n'est pas la plus favorable. Ainsi, les propriétés viscoélastiques de la matrice auraient un impact non négligeable sur la différenciation des MSCs et devraient être considérées à l'avenir.

Mots clés :

Hydrogels, rigidité, viscoelasticité, BMP-2, cellules souches mésenchymateuses, différenciation ostéogénique, ostéocytes.

Synthesis of bioactive surfaces for the control of stem cells differentiation

Abstract

The repair of large bone defects, including large fracture, tumor, and necrosis for which a part of the bone is missing and has to be replaced, is still a challenge for the medical field. Synthetic materials, such as ceramic, metallic, and polymeric materials, have been developed as bone substitutes. However, these materials do not interact with the bone of the patient and generally end up being encapsulated by a layer of fibrous tissue, that might result in the fracture of the bone, the implant, or the interface between the two. The research therefore aims at studying and understanding cell-material interactions in order to develop materials capable of interacting with cells, and to create new implants combining a carrier material, cells, and bioactive factors, allowing bone reconstruction.

In this context, mesenchymal stem cells (MSCs) have gained high interest in regenerative medicine considering their self-renewal ability, multipotency, and high proliferative rate. However, once extracted from the patient and cultivated in vitro, MSCs tend to differentiate randomly, which leads to a heterogeneous population of cells with which it is difficult to reconstruct any tissue. Therefore, although MSCs are used in clinics for the treatment of various pathologies, a better understanding of their biological behavior is still required to provide the ability to control their in vitro differentiation into a specific lineage and improve their clinical performance.

Hydrogels have emerged as promising materials for cell culture as they allow to mimic the natural extracellular matrix of cells. Particularly, many studies have evaluated the impact of hydrogels stiffness on MSCs differentiation and showed that a stiffness close to that of a biological tissue leads to a differentiation towards cells of this tissue. Nevertheless, it is now recognized that hydrogels as well as biological tissues are not only described by their stiffness, but also by their viscoelastic properties. However, only few studies have been conducted on the impact of hydrogels viscoelastic properties on MSCs differentiation (15 articles over the past five years from PubMed).

In this project, it has been shown that it was possible to synthesize poly(acrylamide-co-acrylic acid) hydrogels with different controlled stiffness and viscoelasticity, evaluated using compression and AFM. Five hydrogels have been chosen to study the impact of hydrogels mechanical properties on MSCs osteogenic differentiation by varying the stiffness and the relaxation percent : 15 kPa-15%, 60 kPa-15%, 140 kPa-15%, 100 kPa-30%, and 140 kPa-70%. It has been shown that the surface functionalization of these hydrogels with a mimetic peptide of the BMP-2 protein led to star-like cells, except for the lowest stiffness (15 kPa). This star-

like shape would correspond to the shape of osteocytes, which is the last stage of osteogenic differentiation, and which has never been obtained in vitro to our knowledge. Moreover, a stiffness of 60 kPa led to a higher expression of osteocyte markers as compared to stiffnesses of 15 and 140 kPa, for a constant low relaxation of 15%. Finally, the strongest expression of osteoblast and osteocyte differentiation markers has been observed for the hydrogel with a high relaxation of 70% and a stiffness of 140 kPa. This shows that a high viscoelasticity would favor MSCs osteogenic differentiation, even if it is associated with a stiffness that is not the most favorable. Thus, the viscoelastic properties of the matrix would have a significant impact on MSCs differentiation and should be considered in the future.

Key words :

Hydrogels, stiffness, viscoelasticity, BMP-2, mesenchymal stem cells, osteogenic differentiation, osteocytes.

Unités de recherche

3 BIOs group : BIOactive surfaces, BIOmaterials and BIOmimetic tissue- engineered products
Institut de Chimie et Biologie des Membranes et des Nano-objects (CNRS UMR5248 CBMN)
Allée Geoffroy Saint Hilaire - Bât. B14, 33600 Pessac, France

Laboratoire d'Ingénierie de Surface (LIS)
Centre de recherche du CHU de Québec
Hôpital Saint-François d'Assise, 10 rue de l'Espinay, Québec (Québec) Canada G1L 3L5

Synthèse de surfaces bioactives pour le contrôle de la différenciation des cellules souches

Résumé étendu

La réparation des défauts osseux de taille importante, comme une fracture, une tumeur, ou une nécrose de l'os pour lesquelles une partie de l'os est manquante et doit être remplacée, demeure un défi important pour le domaine médical. Les os sont des matériaux composites puisqu'ils sont composés d'une phase organique, principalement constituée de fibres de collagène de type I, et d'une phase minérale, formée de cristaux d'hydroxyapatite déposés entre les fibres de collagène.[1, 2]

Les os contiennent également différents types de cellules comme les cellules souches mésenchymateuses (MSCs) qui peuvent se différencier en cellules du tissu adipeux (adipocytes), en cellules du cartilage (chondrocytes), ou encore en cellules osseuses (ostéoblastes).[3] Les ostéoclastes sont responsables de la résorption de l'os. En effet, ils sécrètent de l'acide chlorhydrique capable de dissoudre l'hydroxyapatite, et des enzymes capables de dégrader les protéines.[2] Les ostéoblastes proviennent de la différenciation des MSCs et leur principale fonction est de synthétiser la matrice extracellulaire osseuse, appelée ostéoïde, et de promouvoir sa minéralisation.[4] Les ostéoblastes peuvent ensuite se retrouver encastrés dans l'os et peuvent devenir des ostéocytes. Les ostéocytes forment un réseau tri-dimensionnel de cellules connectées par leurs dendrites. Puisque les ostéocytes sont distribués à travers tout l'os, ces cellules ressentent les déformations physiques de l'os.[5] Ceci leur permet de savoir quand il est nécessaire de résorber ou de former de l'os, et ainsi de réguler le recrutement des ostéoclastes pour la résorption de l'os et de réguler la minéralisation de l'os.[6]

La réparation des défauts osseux de taille importante nécessite un remplissage du défaut afin de retrouver le fonctionnement normal de l'os. Ainsi, la méthode la plus utilisée actuellement pour le traitement des défauts osseux est la greffe osseuse. La greffe osseuse consiste à prélever du tissu osseux sain, chez le patient lui-même (greffe autologue) ou chez un autre individu (greffe allogénique), et de l'implanter au niveau de défaut osseux.[1, 7] Cependant, la greffe autologue peut causer des complications au niveau du site de prélèvement, comme de la douleur et des infections, le temps opératoire est allongé, et la quantité d'os disponible est limitée, tandis que la greffe allogénique peut causer une réaction immunitaire et/ou inflammatoire chez le patient, qui va nuire à la reconstruction de l'os.[1] Pour pallier ces inconvénients, des matériaux synthétiques sont développés comme substituts osseux, comme des matériaux céramiques, métalliques, et polymères. Les matériaux céramiques peuvent intéragir avec l'os du patient et être bien intégrés dans l'os, ils sont aussi résorbables et peuvent donc être progressivement éliminés pour laisser place à du nouveau tissu osseux. Mais leur vitesse de résorption est difficile à contrôler et la fragilité de ces matériaux pose problème pour la réparation des os qui supportent des charges importantes.[8, 9] Les matériaux métalliques sont moins fragiles

que les céramiques, mais leur rigidité est généralement très supérieure à celle de l'os, ce qui peut résulter en un effet de "stress-shielding". Le "stress-shielding" se produit lorsque l'implant subit les charges à la place de l'os à certains endroits et concentre la charge sur l'os à d'autres endroits, ce qui peut endommager l'os et/ou l'implant et causer une fracture de l'un ou l'autre, ou de l'interface entre les deux.[10, 11] Les matériaux polymères présentent l'avantage d'avoir des propriétés facilement modulables selon l'application souhaitée, mais leurs propriétés mécaniques sont généralement plus faibles que celles de l'os[12, 13], et, tout comme les métaux, ces matériaux n'interagissent pas suffisamment avec l'os du patient et finissent par être encapsulés par une couche de tissu fibreux, ce qui peut résulter en une fracture de l'os, de l'implant, ou de l'interface entre les deux. Ainsi, les matériaux utilisés actuellement ne possèdent pas encore toutes les qualités requises pour faire de bons substituts osseux.

Les facteurs de croissance jouent un rôle important dans la modulation de l'activité cellulaire puisqu'ils peuvent interagir avec les récepteurs cellulaires et ainsi déterminer la réponse biologique.[14] Parmi les facteurs de croissance impliqués dans la reconstruction osseuse, les BMPs sont particulièrement étudiées et utilisées, et notamment la BMP-2. La BMP-2 joue un rôle significatif dans la stimulation de la différenciation des MSCs en ostéoblastes, et dans la transcription de gènes reliés à la formation du tissu osseux.[15] L'utilisation de BMP-2 recombinante humaine en clinique est actuellement autorisée par l'EMA (European Medicines Agency) et la FDA (Food and Drug Administration) pour le traitement des fractures du tibia par exemple.[16] La BMP-2 est généralement administrée contenue dans une éponge de collagène pour éviter qu'elle ne soit trop rapidement éliminée par le corps, comme c'est le cas lorsqu'elle est administrée par injection.[16] Cependant, une administration locale de BMP-2 à une concentration supérieure à la concentration physiologique peut causer des complications, comme la formation osseuse ectopique, qui est la formation de tissu osseux sur des tissus mous, donc ailleurs que sur le squelette.[17]

Pour pallier les inconvénients des méthodes actuelles, la recherche vise à développer une nouvelle stratégie pour la reconstruction tissulaire, appelée ingénierie tissulaire. L'ingénierie tissulaire est basée sur la combinaison de (1) un matériau support qui mime la matrice extracellulaire naturelle et qui est biodégradable pour laisser progressivement la place au nouveau tissu, (2) des cellules ostéogéniques pour former le nouveau tissu, et (3) des agents bioactifs, comme les facteurs de croissance par exemple, qui vont diriger les cellules vers le phénotype souhaité et qui vont promouvoir la vascularisation du tissu formé.[18, 19] Un des défis majeurs pour mettre en place cette stratégie consiste à **comprendre et optimiser les interactions entre les cellules et le matériau pour guider le comportement cellulaire et obtenir la réponse cellulaire adéquate pour la régénération du tissu**.[20, 21, 22]

Pour régénérer du tissu osseux, la première stratégie serait de collecter et d'utiliser des ostéoblastes car cela permettrait d'obtenir rapidement du tissu osseux. Cependant, la collection des cellules osseuses peut causer des complications au niveau du site de prélèvement et

la prolifération des ostéoblastes étant limitée, il est difficile d'obtenir le nombre important de cellules requis pour régénérer un gros fragment d'os.[20, 23, 24] Dans ce contexte, les cellules souches constituent un candidat prometteur pour l'ingénierie tissulaire, et plus particulièrement les MSCs. Les MSCs sont des cellules souches adultes multipotentes qui ont un taux de prolifération élevé, et qui peuvent se différencier en chondrocytes, adipocytes, et ostéoblastes.[25] Les MSCs peuvent être isolées de plusieurs tissus comme la moëlle osseuse, le tissu adipeux, la pulpe dentaire, la peau, le sang de cordon ombilical, et le cartilage par exemple.[26] Les MSCs issues de la moëlle osseuse sont actuellement les MSCs les plus étudiées et utilisées de part leur facilité d'accès, leur capacité de prolifération élevée, et le fait qu'elles jouent un rôle important dans la formation et la réparation du tissu osseux.[20, 27] La différenciation ostéogénique des MSCs passe par différents stades. Les MSCs sont d'abord dans une phase de prolifération lorsqu'elles s'engagent vers des cellules pré-ostéoblastiques. Ensuite, les pré-ostéoblastes maturent en ostéoblastes, qui présentent une prolifération réduite, et qui sécrètent et minéralisent la matrice extracellulaire. Une fois la matrice extracellulaire formée, les ostéoblastes peuvent être inclus dans la matrice et devenir des ostéocytes.[2, 4, 28, 29]
Les MSCs issues de moëlle osseuse ont été testées en clinique pour la régénération du squelette après diverses fractures ou pathologies, comme l'arthrose, les fractures qui ne guérissent pas, les fractures dues à l'ostéoporose, la nécrose de l'os, ou encore l'inégalité de la longueur des jambes.[30, 31] Les MSCs sont généralement administrées par injection d'aspirat de moëlle osseuse ou par injection de MSCs cultivées in vitro.[30] Plusieurs dispositifs médicaux contenant des MSCs sont actuellement utilisés en clinique pour le traitement de diverses pathologies comme l'arthrose, l'infarctus du myocarde, la réaction d'une greffe contre l'hôte, ou encore la reconstruction de défauts du squelette.[30, 32] Pour une application en régénération osseuse, le but serait de faire se différencier les MSCs en ostéoblastes afin de reconstruire la matrice osseuse. Cependant, quand les MSCs sont extraites et cultivées in vitro pour les faire proliférer, elles ont tendance à se différencier de manière aléatoire, ce qui donne une population hétérogène de cellules.[3, 33, 34] Ainsi, ce travail de thèse vise à essayer de **contrôler la différenciation ostéogénique des MSCs** afin d'obtenir une population homogène de cellules. Ceci passe par la **conception d'un matériau interagissant avec les cellules et favorisant une différenciation vers la lignée ostéoblastique**.
Alors que la compréhension actuelle des processus cellulaires est principalement basée sur des expériences menées sur des matériaux plats et rigides, comme le polystyrène et le verre, il est devenu évident que ces matériaux ne sont pas représentatifs de l'environnement physiologique des cellules et que le développement de systèmes de culture plus représentatifs de l'environnement naturel des cellules in vivo est nécessaire.[35] Ainsi, les hydrogels ont émergé comme matériaux prometteurs pour la culture cellulaire puisqu'ils permettent de mimer la matrice extracellulaire naturelle des cellules. En effet, les hydrogels sont des réseaux tri-dimensionnels formés par la réticulation de polymères hydrophiles, ce qui leur donne la capacité d'absorber de grandes quantités d'eau et ainsi de mimer les tissus biologiques.[36, 37, 38]

Les polymères utilisés pour la fabrication des hydrogels peuvent être des polymères naturels, comme l'alginate, le collagène, le chitosan, la gélatine, l'acide hyaluronique, la cellulose et l'agarose. Ces polymères sont abondants, biocompatibles, et certains d'entre eux possèdent des sites qui leur permettent d'interagir avec les cellules. Cependant, ces polymères présentent quelques désavantages comme le manque de stabilité, des propriétés mécaniques basses et une dégradation rapide.[36] De manière différente des polymères naturels, la chimie des polymères synthétiques est modulable, ce qui offre la possibilité d'optimiser les propriétés physico-chimiques et mécaniques des hydrogels à base de polymères synthétiques en fonction de l'application visée.[36] Les polymères synthétiques les plus utilisés pour la fabrication d'hydrogels sont le polyacrylamide, le poly(éthylène glycol), le poly(alcool vinylique) et le poly(méthacrylate d'hydroxyéthyle). Cependant, le manque de sites d'adhésion pour les cellules, le manque de biocompatibilité et les produits de dégradation potentiellement toxiques sont des inconvénients des polymères synthétiques.[39]

Les hydrogels constituent un outil puissant pour évaluer les interactions entre les cellules et le matériau, en étudiant la réponse des cellules à différentes caractéristiques du matériau, comme la topographie, la porosité, les propriétés mécaniques, et la présentation et la distribution de biomolécules. La possibilité d'encapsuler les cellules dans les hydrogels permet également de comparer le comportement cellulaire entre un environnement en deux ou trois dimensions.[36] Il a été montré dans la littérature que la topographie de surface des hydrogels influence l'adhésion et la différenciation des MSCs. En effet, la réalisation de sillons sur l'hydrogel entraine l'alignement des cellules le long des sillons[40, 41], ce qui pourrait favoriser une différenciation en cellules neuronales[40], tandis que des pilliers favorisent l'étalement des cellules et la différenciation ostéogénique.[40] La rugosité de surface du gel peut aussi influencer la différenciation des MSCs, puisqu'il a été montré que la différenciation ostéogénique des MSCs est optimale pour une rugosité de surface de 500 nm pour un gel avec une rigidité de 31 kPa.[42]
S'inspirant de la tridimensionnalité de l'environnement naturel des cellules, des études ont été menées dans le but de comparer le comportement des MSCs lorsqu'elles sont cultivées en 2 dimensions, i.e. à la surface du gel, ou en 3 dimensions, i.e. encapsulées dans le gel. Tout d'abord, l'encapsulation des MSCs dans des hydrogels dans lesquels les cellules sont entièrement encapsulées et immobilisées en contact avec le substrat s'est révélée favorable à la différenciation chondrogénique.[43, 44] En effet, l'encapsulation en 3D conduit à des cellules qui présentent une morphologie ronde et favorise les interactions entre les cellules, ce qui mène à l'obtention de chondrocytes.[43, 45, 46] Une étude a montré que l'encapsulation de MSCs dans des gels avec une réticulation permanente (qui ne peut pas être clivée par les cellules) mène à des cellules rondes et favorise une différenciation adipogénique, tandis que pour un hydrogel avec une réticulation qui peut être clivée par les cellules, une différenciation ostéogénique est favorisée grâce à la possibilité pour les cellules de déformer la matrice et de s'étaler.[47, 48]

Les cellules peuvent également être encapsulées dans des gels macro-poreux, c'est-à-dire qui présentent des pores interconnectés avec une taille de pore de l'ordre de la taille d'une cellule ou supérieure (>50 μm).[49] Il a été montré que l'étalement et la différenciation ostéogénique de MSCs était plus importante pour des gels avec des pores orientés de manière aléatoire qu'avec des pores lamellaires parallèles entre eux.[50] Il a également été montré qu'un gel avec une porosité de 40% augmente la viabilité cellulaire et la différenciation ostéogénique des MSCs par rapport à une porosité de 0% ou 20%, grâce à un meilleur transfert des nutriments à travers le gel.[51]

De nombreuses études ont évalué l'impact des propriétés mécaniques des hydrogels sur la différenciation des MSCs, et notamment de la rigidité, et ont montré qu'une rigidité proche de celle d'un tissu naturel favorise la différenciation vers les cellules de ce tissu. Ainsi, les différenciations neurogénique[52, 53] et adipogénique[54, 55, 56] sont prédominantes sur des matrices à faible rigidité (de 0.1 à 5 kPa), la différenciation myogénique est encouragée pour des rigidités entre 8 et 40 kPa[52, 53, 55], alors que la différenciation ténogénique est favorisée entre 30 et 50 kPa.[57] Les résultats obtenus pour la différenciation chondrogénique et ostéogénique sont plus hétérogènes, avec une différenciation chondrogénique rapportée à la fois pour des faibles rigidités (0.5 - 1.5 kPa)[58, 59] et des matrices plus rigides (80 kPa)[60], et une différenciation ostéogénique mentionnée pour une large gamme de rigidités allant de 1.5 kPa à 190 kPa[52, 54, 56, 61], bien qu'elle soit majoritairement mentionnée entre 20 et 60 kPa.[52, 55, 56, 57, 58, 62, 63] **En effet, il faut bien distinguer la rigidité de l'os, qui est très élevée, de l'ordre de 30-50 GPa pour l'os cortical**[11]**, de la rigidité de la matrice extracellulaire osseuse produite par les ostéoblastes, qui serait de l'ordre de 30 kPa**[52]. Les MSCs sont capables de sentir la rigidité du substrat en exerçant des forces contractiles sur la matrice grâce aux récepteurs cellulaires comme les intégrines par exemple.[64] Ainsi, selon la rigidité du gel, les forces exercées par les cellules sont différentes, ce qui conduit à une morphologie cellulaire et une organisation du cytosquelette différentes. Le cytosquelette étant relié au noyau, une organisation différente amène à une expression des gènes différente et donc à une différenciation différente.[65, 66] Cependant, il est maintenant reconnu que les hydrogels et les tissus naturels ne sont pas caractérisés uniquement par leur rigidité, mais aussi par leurs propriétés viscoélastiques. Par exemple, il a été montré que la différenciation adipogénique, myogénique et ostéogénique étaient favorisées en augmentant le module visqueux des gels (de 1 à 130 Pa) pour une rigidité constante à 5 kPa.[67] Une autre étude a montré que la différenciation adipogénique des MSCs était favorisée pour une rigidité de 9 kPa et des temps de relaxation longs (140, 200 et 2300 s), alors que la différenciation ostéogénique était favorisée pour une rigidité de 17 kPa et des temps de relaxation courts (60, 140 et 200 s).[68] Malheureusement, peu d'informations supplémentaires sont disponibles sur l'impact des propriétés viscoélastiques des hydrogels sur la différenciation des MSCs (15 articles sur les cinq dernières années via PubMed, avec les mots clés hydrogel viscoelasticity mesenchymal stem cell differentiation).

Enfin, la présence et la distribution de biomolécules sur le gel peuvent influencer le

comportement cellulaire. Une étude a montré que parmi quatre protéines, le collagène I, le collagène IV, la fibronectine et la laminine, la différenciation ostéogénique des MSCs est prédominante avec le collagène I et une rigidité de 80 kPa, tandis que la différenciation myogénique est favorisée avec la fibronectine et une rigidité de 25 kPa.[69] De plus, la combinaison de plusieurs protéines à la surface du gel, comme la fibronectine, la laminine et l'ostéopontine, favoriserait la différenciation ostéogénique des MSCs par rapport à ces différentes protéines seules.[70] Des peptides issus des protéines de la matrice extracellulaire sont également utilisés pour fonctionnaliser les hydrogels. Ces peptides sont facilement accessibles par synthèse et avec une haute pureté, et leur structure peut être conçue selon l'effet souhaité.[71] Ainsi, la séquence peptidique correspondant aux acides aminés 73 à 92 de la BMP-2 recombinante humaine favoriserait la différenciation ostéogénique des MSCs par rapport à un peptide d'adhésion RGD.[72] L'association du peptide mimétique de la BMP-2 avec le peptide RGD permettrait d'améliorer la différenciation ostéogénique des MSCs par rapport aux peptides seuls.[73] Des motifs de peptides ou de protéines de différentes tailles et formes peuvent aussi influencer la différenciation des MSCs. Les MSCs se dirigeraient vers la lignée adipogénique pour des petits motifs (entre 177 et 1413 μm^2), et vers la lignée ostéogénique pour des plus gros motifs (entre 2826 et 5652 μm^2).[74] Une autre étude a montré que des motifs circulaires encouragent la différenciation ostéogénique, tandis que des motifs anisotropiques, comme une étoile à 4 branches, favorisent la différenciation neurogénique.[75] Il a également été montré que les motifs circulaires mènent à un cytosquelette désordonné et l'absence de différenciation ostéogénique, tandis que des motifs qui favorisent la tension du cytosquelette, comme un ovale très allongé ou des formes concaves, favorisent l'expression de marqueurs ostéogéniques.[76] Ainsi, la compréhension de l'influence des propriétés physiques, spatiales et biochimiques des matériaux sur le devenir des cellules permettra le développement de matériaux avec des propriétés sur mesure adaptées pour des applications spécifiques en médecine régénératrice.

Comme énoncé précédemment, ce travail de thèse vise à essayer de contrôler la différenciation ostéogénique des MSCs par le biais d'interactions avec un matériau. Les précédents travaux des deux équipes de recherche s'étant déroulés avec des matériaux rigides, comme le titane, le verre, le silicium, et le PET (poly(téréphtalate d'éthylène)), ce projet se base sur l'utilisation d'hydrogels comme support de culture cellulaire afin de mimer l'environnement naturel des cellules et d'évaluer l'impact des propriétés mécaniques de la matrice sur la différenciation ostéogénique des MSCs. Pour ce faire, des hydrogels à base d'acrylamide ont été utilisés comme support de culture de MSCs humaines provenant de moëlle osseuse, de part leur facilité de synthèse et leur rigidité hautement modulable. Cependant, ces hydrogels sont considérés comme étant principalement élastiques. Ainsi, des hydrogels de copolymère d'acrylamide et d'acide acrylique ont été synthétisés en variant leur formulation afin de moduler à la fois la rigidité des gels, mais aussi leur comportement viscoélastique. Fournir des hydrogels avec une rigidité et une viscoélasticité contrôlées permettra d'aller plus loin que la littérature

actuelle sur l'évaluation de l'impact des propriétés mécaniques sur la différenciation des MSCs, en incluant la dimension viscoélastique des matériaux.

La première partie du projet a consisté à synthétiser des hydrogels en variant leur formulation, et à caractériser leurs propriétés physico-chimiques et mécaniques.[77] Seize formulations de gel ont été synthétisées en variant la quantité d'agent réticulant (0.03%, 0.24%, 0.36% et 0.48%) et le ratio entre l'acrylamide et l'acide acrylique (100/0%, 95/5%, 90/10% et 82/18%). Les spectres infrarouge de ces hydrogels sont marqués par les pics caractéristiques des fonctions -CH, -CH_2, -NH, -NH_2 et -C=O. De plus, les gels avec acide acrylique mènent à l'apparition d'un pic à 1560 cm^{-1} qui correspond aux fonctions carboxylates (-COO^-) apportées par l'acide acrylique.[78, 79, 80] L'intensité de ce pic augmente avec la quantité d'acide acrylique dans le gels, ce qui signifie que l'acide acrylique est bien intégré dans le gel et en proportion variable. L'augmentation de la quantité d'agent réticulant conduit à une diminution de la capacité d'absorption de fluide des gels. Ceci s'explique par le fait qu'une augmentation de la réticulation crée un réseau plus dense dans lequel le liquide, ici une solution tampon (PBS, Phosphate Buffered Saline, pH 7.4), a plus de difficulté à pénétrer.[80, 81] En revanche, une augmentation de la quantité d'acide acrylique conduit à une augmentation de la capacité d'absorption de fluide des gels. Avec un pKa autour de 5, les polymères d'acide acrylique sont négativement chargés à pH neutre, ce qui crée des répulsions électrostatiques entre les chaines polymères et augmente le gonflement des gels.[81, 82] Cette hypothèse a été confirmée en montrant que le gonflement de gels de polyacrylamide ne varie pas selon le pH (pH 3, 5, 7 et 10), alors que le gonflement de gels de poly(acrylamide-co-acide acrylique) diminue à pH 3, et ce d'autant plus que la quantité d'acide acrylique dans le gel est élevée. Des tests de relaxation de contrainte en compression non confinée ont permis d'accéder aux propriétés mécaniques des 16 formulations de gel. Avec les formulations étudiées, le module élastique des gels a été mesuré entre 5 et 145 kPa. Le module augmente avec la quantité d'agent réticulant, puisque l'augmentation de la réticulation crée un réseau plus dense, mais diminue lorsque la quantité d'acide acrylique augmente, car les répulsions électrostatiques diminuent la densité du réseau. Ensuite, il a été montré que le pourcentage de relaxation des gels, qui correspond au pourcentage de la contrainte maximale qui est dissipé lors de la relaxation, augmente avec la quantité d'acide acrylique puisqu'il est aux alentours de 15% pour des gels de polyacrylamide et atteint jusqu'à 70% pour des gels de copolymère avec 18% d'acide acrylique, pour une déformation du gel de 6%. Ceci est lié à la présence des charges négatives apportées par l'acide acrylique qui favorisent le réarrangement des chaines polymères, et donc la dissipation de la contrainte lors de la relaxation, grâce aux répulsions électrostatiques. Cette hypothèse a été confirmée en montrant que la relaxation de gels de polyacrylamide ne varie pas selon le pH (pH 3, 7 et 10), alors que la relaxation de gels de poly(acrylamide-co-acide acrylique) diminue considérablement à pH 3, pour se retrouver au même niveau que le gel de polyacrylamide. Enfin, il a été observé par microscopie électronique que la taille des pores diminue lorsque la quantité

d'agent réticulant augmente, puisque le diamètre moyen des pores de gels de polyacrylamide est de 4.4 μm pour 0.03% d'agent réticulant et de 0.8 μm pour 0.36% d'agent réticulant. Les hydrogels de polyacrylamide présentent une structure de pores ronde ou ovale avec des parois de gel séparant distinctement les pores, tandis qu'un gel avec 18% d'acide acrylique présente une forme de pores irrégulière avec une séparation moins marquée entre les pores, ce qui pourrait suggérer un degré plus élevé d'interconnexion entre les pores. Ceci pourrait favoriser la migration de fluide dans le gel et donc participer à expliquer la relaxation plus importante des gels contenant de l'acide acrylique. Ainsi, il a été démontré que la rigidité et les propriétés viscoélastiques, et particulièrement le pourcentage de relaxation, pouvaient être contrôlés en variant la formulation d'hydrogels de poly(acrylamide-co-acide acrylique).

Puisque les cellules n'adhèrent pas sur ces hydrogels, comme en surface d'une majorité d'hydrogels synthétiques, la deuxième partie du projet a consisté à fonctionnaliser les hydrogels avec des molécules bioactives afin de permettre l'adhésion des MSCs. Dans ce projet, un peptide mimétique de la protéine BMP-2 (KRKIPKASSVPTELSAISMLYLC), développé et breveté par l'équipe 3BIO's[83], a été immobilisé de façon covalente à la surface des gels grâce à un bras d'ancrage appelé Sulfo-SANPAH. Il a été montré que ce peptide favorise la différenciation ostéogénique des MSCs lorsqu'il est immobilisé sur différents matériaux comme du verre ou du poly(téréphtalate d'éthylène).[83, 84, 85, 86] Les hydrogels ont également été fonctionnalisés avec du collagène de type I, étant le composant majoritaire de la matrice extracellulaire osseuse et étant traditionnellement utilisé dans la littérature pour fonctionnaliser les hydrogels de polyacrylamide lors des études sur l'impact de la rigidité du gel sur la différenciation des MSCs.[52, 55, 56] Ceci permettra également d'évaluer l'impact de la biofonctionnalisation de l'hydrogel sur la différenciation ostéogénique des MSCs. En fonctionnalisant les hydrogels avec un peptide BMP-2 portant une molécule fluorescente (TAMRA) et en les observant en microscopie confocale, il a été montré que le protocole utilisé permet une fonctionnalisation homogène et localisée en surface des gels. La densité de peptide sur les gels a été estimée autour de 1.5-2 pmol/mm^2, ou 1 molécule/nm^2. En marquant les gels fonctionnalisés avec le collagène I avec un anticorps anti-collagène I, puis avec un anticorps fluorescent, et en observant les gels en microscopie confocale, il a été observé que la fonctionnalisation est également homogène et localisée en surface des gels et l'intensité de fluorescence est similaire entre les gels. La densité de collagène sur les gels a été évaluée autour de 8 pmol/cm^2, soit une densité inférieure à celle du peptide BMP-2. Il a été montré que l'intensité de fluorescence de gels immergés dans une solution de peptide fluorescent ou de collagène (qui est ensuite marqué par immunofluorescence), sans activation préalable du gel avec Sulfo-SANPAH, est moindre par rapport à celle des gels activés, ce qui confirme l'immobilisation covalente des biomolécules grâce au Sulfo-SANPAH. Enfin, une étude préliminaire a montré qu'une fonctionnalisation avec le peptide BMP-2 favorise l'expression de marqueurs de différenciation (ostéopontine, E11, DMP1, sclérostine) par rapport à une fonctionnalisation avec le collagène.

Suite aux essais de compression réalisés dans la première partie du projet, 5 gels ont été sélectionnés pour évaluer l'impact des propriétés mécaniques sur la différenciation des MSCs (rigidité - relaxation) : 5 kPa-15%, 55 kPa-15%, 145 kPa-15%, 55 kPa-30%, et 55 kPa-70%. Ces gels devraient permettre d'évaluer l'impact de la rigidité pour une relaxation constante, et l'impact de la relaxation pour une rigidité constante, sur la différenciation ostéogénique des MSCs. Les propriétés mécaniques de ces 5 gels ont également été mesurées par Microscopie à Force Atomique (AFM). En effet, la compression et l'AFM étant les deux méthodes les plus utilisées pour mesurer la rigidité des hydrogels dans les études sur l'impact de la rigidité sur le comportement cellulaire, il est intéressant de les comparer afin de voir si des études utilisant ces deux techniques sont comparables entre elles. De plus, ces deux techniques sont complémentaires puisque la compression permet de mesurer les propriétés mécaniques de l'ensemble du gel, sur des centaines de μm à plusieurs mm, tandis que l'AFM permet de mesurer les propriétés mécaniques de surface des gels, sur des centaines de nm. Avec les paramètres utilisés, les valeurs de rigidité mesurées en AFM sont similaires à celles mesurées en compression, ce qui montre que le module de l'ensemble du gel est comparable au module de surface. Il est tout de même à noter que le module du gel le moins rigide a été évalué à 5 kPa par compression et à 15 kPa par AFM. Ceci est dû au fait que le découpage des gels a mené à une forme particulièrement conique du gel le moins rigide, qui a vu sa rigidité sous-estimée lors des mesures en compression. Des mesures préliminaires de relaxation de contrainte ont également été effectuées par AFM afin d'évaluer la faisabilité de la technique et de comparer la relaxation de l'ensemble du gel à celle de la surface du gel. Les essais ont été effectués sur les gels 55 kPa-15% et 55 kPa-30%, et ont mené à des pourcentages de relaxation de 8% et 50%, pour ces deux gels, respectivement. Ainsi, il serait possible de mesurer la relaxation de surface des gels par AFM et de voir des différences entre les formulations de gel, bien que les valeurs numériques ne soient pas identiques à celles mesurées en compression du fait de la vitesse d'approche de la pointe AFM qui est différente de la vitesse utilisée en compression.

Par la suite, la question suivante s'est posée : les propriétés mécaniques des gels vierges sont-elles équivalentes à celles des gels fonctionnalisés, et donc, sont-elles les propriétés mécaniques que vont sentir les cellules ? Pour répondre à cette question, les propriétés mécaniques des gels ont été mesurées par compression et par AFM après la fonctionnalisation avec le peptide BMP-2. Aucune différence de rigidité ou de relaxation entre des gels vierges et des gels fonctionnalisés n'a été mesurée par compression. Ceci était attendu car il a été montré que la fonctionnalisation avec le peptide BMP-2 s'étend sur une profondeur d'environ 25 μm, alors que les essais compression ont été menés avec une déformation du gel de 6%, soit sur une profondeur d'environ 300 μm. Les mesures par AFM ont révélé que la rigidité des gels ne contenant pas d'acide acrylique (15 kPa-15%, 55 kPa-15%, 145 kPa-15%) reste inchangée après la fonctionnalisation, tandis que la rigidité des gels contenant de l'acide acrylique (55 kPa-30% et 55 kPa-70%) augmente significativement après fonctionnalisation. De plus, cet

effet est plus prononcé pour le gel contenant la plus forte quantité d'acide acrylique puisque les gels contenant 10% et 18% d'acide acrylique présentent une rigidité similaire autour de 55-60 kPa avant la fonctionnalisation, et une rigidité de 100 kPa et 140 kPa, respectivement, après la fonctionnalisation. Ceci s'explique par le fait que le poly(acide acrylique) est connu pour former des réticulations sous lumière UV, même sans la présence d'un photo-initiateur.[87, 88, 89] Ainsi, l'irradiation UV des gels, pratiquée lors de la fonctionnalisation afin d'activer le Sulfo-SANPAH, augmente la réticulation des gels avec acide acrylique, causant ainsi une augmentation de leur rigidité. Enfin, il a également été montré, pour la première fois, que la fonctionnalisation de surface des gels avec le peptide BMP-2 ne modifie pas les propriétés viscoélastiques des gels mesurées par AFM, donc à l'échelle microscopique. Plusieurs études ont montré que certaines cellules, dont les MSCs, sont capables de ressentir les propriétés mécaniques du substrat sur lequel elles sont jusqu'à une profondeur de 5 μm.[52, 90, 91, 92, 93] Ainsi, il semble que mesurer les propriétés mécaniques des gels par compression ne permette pas d'évaluer les propriétés mécaniques que les cellules vont réellement sentir. Cette étude fournit donc une comparaison claire entre la compression et l'AFM, qui manque encore dans la littérature, et qui semble montrer que la caractérisation des propriétés mécaniques de surface des gels par AFM est cruciale pour évaluer l'impact des propriétés mécaniques sur le comportement cellulaire pour des études en 2 dimensions. Ainsi, la rigidité des gels après fonctionnalisation et mesurée par AFM a été considérée pour la suite du projet, tandis que la relaxation des gels mesurée par compression a été conservée, puisqu'il a été montré que la fonctionnalisation n'avait pas d'impact sur la relaxation des gels à l'échelle microscopique. Les 5 gels considérés présentent donc les propriétés mécaniques suivantes : 15 kPa-15%, 60 kPa-15%, 140 kPa-15%, 100 kPa-30%, et 140 kPa-70%.

Enfin, des cellules souches mésenchymateuses humaines de moëlle osseuse ont été mises en culture sur ces hydrogels pendant 24h et 2 semaines dans du milieu de culture ostéogénique. L'aire cellulaire a été évaluée après 24h et il a été montré que celle-ci augmente avec la rigidité du gel, pour une même relaxation autour de 15%. Ceci est cohérent avec les observations faites dans la littérature[52, 55, 56, 58, 62, 69] et confirme l'hypothèse que les cellules ont besoin d'être moins contractiles sur les gels mous que sur les gels rigides pour adhérer à la matrice. Les cellules sur les gels présentant 30% et 70% de relaxation présentent une aire cellulaire plus faible que celles sur le gel 60 kPa-15%, bien que ces deux gels possèdent des rigidités plus élevées de 100 et 140 kPa. Ceci indique qu'une augmentation de la relaxation des gels mène à une diminution de l'aire cellulaire. Plusieurs études ont également observé ce phénomène[94, 95, 96, 97] et ont émis l'hypothèse que les forces de traction développées par la cellule à l'interface avec le substrat sont faibles à cause de la relaxation, et donc de la dissipation de ces forces par le substrat, ce qui limite l'étalement des cellules[94, 97].
Après 24h de culture, l'expression d'ostéopontine est plus importante pour les gels 60 kPa-15% et 140 kPa-15%, ce qui est cohérent avec le fait que les cellules sont plus étalées sur

ces gels et qu'une aire cellulaire plus importante favorise la différenciation des MSCs en ostéoblastes.[62, 69, 74, 76] Pour une même relaxation de 15%, l'expression de marqueurs ostéocytaires (E11, DMP1, et sclérostine) est plus importante pour une rigidité de 60 kPa, que pour des rigidités de 15 et 140 kPa. Enfin, les gels 100 kPa-30% et 140 kPa-70% ont mené à la plus forte expression des trois marqueurs ostéocytaires après seulement 24h de culture.
Après deux semaines de culture en milieu ostéogénique, les MSCs cultivées sur du verre sont très étalées et présentent une morphologie cuboïdale, caractéristique des ostéoblastes[98, 99] alors que les cellules sur les hydrogels présentent un corps cellulaire plus petit et une morphologie dendritique, caractéristique des ostéocytes[5, 6, 99], excepté sur le gel le moins rigide. De même manière qu'à 24h de culture, l'expression de marqueurs ostéocytaires (E11, DMP1, et sclérostine) après 2 semaines est plus importante pour une rigidité de 60 kPa, que pour des rigidités de 15 et 140 kPa, pour une même relaxation de 15%. Ces résultats sont cohérents avec le fait qu'une rigidité comprise entre 30 et 60 kPa favoriserait la différenciation ostéogénique des MSCs.[52, 55, 56, 57, 58, 62, 63] Enfin, le gel 140 kPa-70% a mené à la plus forte expression des trois marqueurs ostéocytaires après 2 semaines de culture, ce qui semble montrer que la relaxation du gel a un impact non négligeable sur la différenciation ostéocytaire des MSCs. De plus, cela semble indiquer qu'une relaxation élevée favorise la différenciation ostéocytaire des MSCs, et ce, même si la rigidité du gel est élevée et n'est donc pas la plus favorable. L'hypothèse principale pour expliquer ces résultats est que l'augmentation de la viscoélasticité du substrat donne plus de possibilités aux cellules de remodeler la matrice, ce qui favorise la différenciation.[100] Ainsi, ce projet apporte un nouveau regard sur l'impact des propriétés viscoélastiques des hydrogels sur la différenciation ostéogénique des MSCs, et souligne l'importance de considérer ces propriétés pour la conception de matériaux efficaces pour promouvoir la régénération osseuse. De plus, les résultats présentés sont particulièrement prometteurs pour l'étude de la différenciation des MSCs vers des ostéocytes, qui est encore une processus relativement peu connu, et pour l'étude des ostéocytes, qui est une tâche difficile compte tenu du fait que ces cellules sont particulièrement difficiles à extraire.

Table of contents

List of figures

List of tables

Abbreviations

2D	Two Dimension
3D	Three Dimension
AD-MSCs, ASCs	Adipose tissue derived MSCs
AFM	Atomic Force Microscopy
ALP	Alkaline Phosphatase
APS	Ammonium Persulfate
β-TCP	β-Tricalcium Phosphate
BMP	Bone Morphogenetic Protein
BM MSCs	Bone Marrow Mesenchymal Stem Cells
BSA	Bovine Serum Albumin
BSP	Bone Sialoprotein
CC	Cleavable Crosslinks
CMS	Cyclic Mechanical Loading
COL1	Collagen I
CS	Chondroitin sulfate
DAPI	4',6-diamidino-2-phenylindole
DBM	Demineralized Bone Matrix
DMP1	Dentin Matrix Protein-1
ECM	Extracellular Matrix
EDTA	Ethylenediaminetetraacetic Acid
EMA	European Medicines Agency
ESCs	Embryonic Stem Cells
FABP	Fatty Acid Binding Protein
FAC	Fluid Absorption Capacity
FBS	Fetal Bovine Serum
FDA	Food and Drug Administration
FGF	Fibroblast Growth Factor
FN	Fibronectin
FTIR	Fourier-Transform Infrared Spectroscopy
GAG	Glycosaminoglycan
GelMA	Gelatin-Methacryloyl
GvHD	Graft versus Host Disease
HA	Hyaluronic Acid
HAp	Hydroxyapatite
hFOB	human osteoblasts
hMSCs	human Mesenchymal Stem Cells
HPA	Hydroxyphenyl Propionic Acid
HSCs	Hematopoietic Stem Cells
IGFs	Insulin-like Growth Factors
iPSCs	Induced Pluripotent Stem Cells
LN	Laminin
MeHA	Methacrylated Hyaluronic Acid
MEPE	Matrix Extracellular Phosphoglycoprotein
mRNA	messenger Ribonucleic Acid
MSCs	Mesenchymal Stem Cells
NiTi	Nickel-Titanium

OCN	Osteocalcin
OPN	Osteopontin
ORO	Oil Red O
PAM	Polyacrylamide
PBS	Phosphate Buffered Saline
PC	Permanent Crosslinks
PCL	Poly(ϵ-caprolactone)
PDGF	Platelet-Derived Growth Factor
PDMS	Polydimethylsiloxane
PEEK	Poly(ether-ether-ketone)
PEG	Polyethylene Glycol
PEO	Polyethylene Oxide
PET	Polyethylene Terephtalate
PGA	Polyglycolic Acid
pHEMA	Poly(hydroxyethyl methacrylate)
PLA	Polylactic Acid
PLGA	Poly(lactic-co-glycolic acid)
PMMA	Poly(methylmethacrylate)
PNIPAAm	Poly(N-isopropylacrylamide)
PRP	Platelet-Rich Plasma
PVA	Poly(vinyl alcohol)
qRT-PCR	quantitative Real Time Polymerase Chain Reaction
Runx-2	Runt-related transcription factor 2
SEM	Scanning Electron Microscopy
SIBLINGs	Small Integrin-Binding Ligand N-Linked Glycoproteins
SLRPs	Small Leucine-Rich Proteoglycans
SOST	Sclerostin
TAMRA	5-(and-6)-carboxytetramethylrhodamine
TEMED	Tetramethylethylenediamine
TGF-β	Transforming Growth Factor β
UHMWPE	Ultra-High Molecular Weight Polyethylene
VEGF	Vascular Endothelial Growth Factor
vSMCs	vascular Smooth Muscle Cells

Acknowledgements

Je remercie chaleureusement les membres du jury qui ont accepté d'évaluer mon travail. Je tiens à remercier mes directeurs de thèse, Marie-Christine Durrieu et Gaétan Laroche, pour cette belle expérience de thèse en co-tutelle. Cela a été vraiment plaisant de travailler avec deux directeurs qui s'entendent aussi bien, et j'espère que les aventures en co-tutelle entre la chaleur de Bordeaux et le grand froid de Québec seront encore nombreuses après moi. Je vous remercie pour la confiance et la liberté que vous m'avez accordées pour mener ces travaux de thèse. Cela n'a pas toujours été facile mais j'ai énormément grandi à vos côtés durant ces quatre années. Je suis heureuse de voir que malgré le caractère parfois capricieux de mes hydrogels, vous avez voulu poursuivre les recherches dans cette voie avec les futurs étudiants. Je vous suis très reconnaissante également pour m'avoir donné la possibilité de participer à d'autres activités pendant ma thèse, comme le concours "Ma thèse en 180s", l'encadrement de stagiaires de la licence au master, et de nombreux congrès nationaux et internationaux. Gardez votre optimisme, votre dynamisme, et votre passion. Merci à mes collaborateurs préférés.

Une thèse en co-tutelle signifie deux pays, deux laboratoires, deux diplômes, mais aussi deux fois plus de belles rencontres et de remerciements.

Du côté de Bordeaux, je remercie Delphine Maurel à Biotis pour ses conseils qui m'ont permis de me lancer dans l'évaluation de la différenciation ostéocytaire.
Je remercie Cécile Feuillie et Michael Molinari pour leur bonne humeur, leur disponibilité, leur pédagogie et les heures passées à l'AFM sur mes gels.
Dans l'équipe 3BIO's, je remercie évidemment Christel Chanseau et Murielle Rémy. Merci pour votre bonne humeur, votre écoute, vos encouragements, votre soutien et votre aide scientifique. Christel, c'est toujours un plaisir de discuter avec toi, continue ton combat pour l'écologie et merci pour les évènements sociaux que tu organises à CBMN. Murielle, ça a été un plaisir de t'accueillir dans l'équipe, j'espère que tu t'y plais et que tu pourras t'y épanouir.
J'ai une pensée pour les anciens étudiants, Ibrahim, Caroline, Catarina, Bruno, Jian Qiao. Merci pour vos conseils et pour le savoir que vous m'avez transmis, et bien sûr merci pour les bons moments que j'ai passés avec chacun de vous (les bières, les soirées, le week-end escapade à Québec, le Zombicide).
Merci à Emilie pour le soutien mutuel et bon courage pour la fin de ta thèse.
Je souhaite à Yujie et Cristina de la réussite dans leur thèse. J'espère avoir pu vous aider et vous faire profiter de mon expérience.

Un immense merci à mes amis, rencontrés en thèse ou bien avant. Merci à Baba qui pense toujours à venir faire un coucou quand il passe par Bordeaux. Merci à Yoann et Malou pour les soirées et les activités en tout genre. Merci à Antoine pour son humour et son coaching pour MT180.
Merci à Manon, la plus décidée d'entre nous. Merci à Myriam, et à son quad. Merci à Boubou, qui me soutient en tant qu'amateur de Ricard. Je suis extrêmement heureuse et reconnaissante de vous avoir rencontrés et d'avoir vécu cette aventure avec vous. J'espère que notre amitié se poursuivra, même quand on aura une vie normale. Merci à Gui, le pro des montages photo, qui a dû supporter les plaintes de tous ces étudiants en thèse et qui a su nous faire rire.
Et évidemment merci à Esther, mon amie, ma confidente, ma soeur, ma maman. Cela fait maintenant 9 ans qu'on se suit et qu'on vit les mêmes épreuves, et je ne compte plus le nombre de fois où tu m'as écoutée, soutenue, encouragée, fait rire. Merci d'être entrée dans ma vie, pour le meilleur et pour le pire.

Du côté de Québec, je remercie chaleureusement Bernard Drouin pour son aide précieuse sur la caractérisation des propriétés mécaniques des hydrogels.
Je remercie Andrée-Anne pour sa gentillesse et le temps qu'elle m'a accordé lors de mon dernier séjour à Québec, même si mon séjour a été écourté.
Mille mercis à Pascale pour ton soutien scientifique et psychologique, je suis très heureuse de t'avoir rencontrée. On doit te le dire souvent mais tu es un peu la maman des étudiants, ce qui implique à la fois de nous réprimander quand on fait une bêtise et de nous pousser vers le haut quand on a un coup de mou. Bon courage à toi pour la suite et merci encore.
Merci aux étudiants du groupe de Gaétan et du goupe de Diego, Alex, Amna, Natalia, Nawel, Souhaila, Dimitria, Carolina, Sergio, Leticia, Federica, Sara, pour les moments de convivialité partagés.
Un grand merci à Sergio, Francesco, Linda, Morgane, Sébastien, Simon, Gabriel, Nooman. J'ai adoré les mois que j'ai passés à vos côtés y compris les jeux de société divers, les soirées parfois improbables mais d'autant plus incroyables, les escapades..., bref les vacances à Québec. Sergio tu as été une formidable rencontre, j'espère avoir des occasions de te revoir, y la cortina nunca esta cerrada para ti.

Pour finir, je tiens à remercier mes proches qui m'ont soutenue du mieux qu'ils pouvaient pendant ces quatre ans. Ma Maman, ma soeur Cassandra, qui sont toujours là quoi qu'il arrive et quelles que soient les épreuves qui nous attendent. Vous savez qu'on peut tout réussir toutes les trois. Merci à mon Papa, mes frères et soeurs Thomas et Clara, ma belle-mère Lucie. Merci pour votre soutien et vos blagues malgré la distance, vous me manquez (et non je ne fais pas des potions comme Harry Potter même si j'aimerais bien). Un grand merci à ma belle famille pour leur écoute, leurs encouragements, leurs conseils et leur bienveillance. Et enfin merci à mon chéri Axel qui me supporte depuis 8 ans maintenant, ce qui n'est pas une mince affaire.

Merci d'être l'épaule solide sur laquelle je peux me reposer. Je suis heureuse que nous ayons vécu nos 8 années d'études ensemble et que nous continuions à partager de nouvelles choses tous les jours. Si je suis arrivée jusque là c'est parce que tu m'en as donné la force. La vie est devant nous maintenant. Et merci à nos petits rats qui vont me manquer.

Ceux qui me connaissent bien savent que je n'ai pas pu arriver jusque là sans verser une (grosse) larme. Merci à vous tous.

Foreword

This thesis includes three articles that I wrote as the first author. The first article is a book chapter about the impact of hydrogels properties on the behavior of mesenchymal stem cells, while the two other articles present the main results obtained during this PhD. Some details regarding the articles achieved during the four years of the thesis as well as the role of the co-authors in the accomplishment of this work are given bellow.

Paper 1 :
Title : Hydrogels for mesenchymal stem cell behavior study.
Authors : E. Prouvé, G. Laroche, M. C. Durrieu.
Book : Superabsorbent Polymers : Chemical Design, Processing and Applications. DeGruyter.
State : Published 2021, Feb 22^{th}.
Author's contribution : The first author performed the bibliographical research and wrote the manuscript. All the authors reviewed the manuscript.

Paper 2 :
Title : Evaluating poly(acrylamide-co-acrylic acid) hydrogels stress relaxation to direct the osteogenic differentiation of mesenchymal stem cells.
Authors : E. Prouvé, B. Drouin, P. Chevallier, M. Rémy, M. C. Durrieu, G. Laroche.
Journal : Macromolecular Bioscience.
State : Submitted 2021, Feb 25^{th}. Published 2021, April 14^{th}.
Author's contribution : The first author designed the experiments based on the discussion with all the authors. The first author performed all the experiments, analyzed and interpreted the data, and drafted the manuscript. P. Chevallier performed the Scanning Electron Microscopy on the hydrogel samples as well as the mechanical tests depending on the pH. All the authors reviewed the manuscript.

Paper 3 :
Title : Interplay of matrix stiffness and stress relaxation in directing Mesenchymal Stem Cells osteogenic differentiation.
Authors : E. Prouvé, M. Rémy, C. Feuillie, M. Molinari, P. Chevallier, B. Drouin, G. Laroche, M. C. Durrieu.
Journal : Biomaterials.
State : Under preparation.
Author's contribution : The first author designed the experiments based on the discussion with all the authors. The first author performed all the experiments, analyzed and interpreted the data, and drafted the manuscript. C. Feuillie and M. Molinari designed the AFM experiments and C. Feuillie performed all the AFM measurements. All the authors reviewed the manuscript.

Introduction

It is estimated that 1.6 million bone grafts are used annually in the U.S. for degenerative diseases, injuries, tumors, and infections, accounting for approximately $244 billion.[20] The reconstruction of damaged bone therefore constitutes an area of general interest and remains a real clinical issue, especially in the case of large bone loss. Indeed, while the bone graft is the gold standard for the repair of bone defects, the quantity of available grafts is limited and might fail to meet the growing demand.[1] To overcome this problem, synthetic materials, such as ceramic, metallic, and polymeric materials, have been developed as bone substitutes. However, these materials generally do not interact with the bone of the patient and end up being surrounded by a layer of fibrous tissue, that might result in the fracture of the bone or the implant, and in the need for new surgery.[8, 11]

In this context, tissue engineering is emerging as a new strategy for bone repair. Bone tissue engineering consists in combining (1) a biocompatible scaffold that closely mimics the natural bone extracellular matrix and that degrades over time to be replaced by newly formed bone tissue, (2) osteogenic cells that produce the bone tissue matrix, and (3) bioactive agents that help to direct the cells to the phenotypically desirable type.[18, 19, 20] Considering this strategy, mesenchymal stem cells (MSCs) constitute an interesting candidate for bone tissue engineering. Indeed, they are self-renewable, multipotent, easily accessible from bone marrow, and they can differentiate into different types of cells, including bone cells (osteoblasts).[101] However, the clinical use of MSCs is hindered by their tendency to uncontrollably proliferate and differentiate, when cultivated in vitro.[32] Therefore, one of the major challenges to implement bone tissue engineering is to understand and optimize the interactions between MSCs and materials, in order to guide MSCs behavior and obtain the appropriate cellular response for tissue regeneration.[20, 21, 22]

The 3BIO's research team (Bordeaux) and the LIS laboratory (Québec) have a long-term expertise in studying the impact of the surface properties of materials on MSCs behavior, including for example the presence and distribution of various biomolecules [84, 85, 102, 103, 104], as well as nanotopographies[105, 106, 107, 108, 109]. However, these studies were conducted on hard materials such as titanium, glass, silicon, and PET (polyethylene terephthalate), and it is now recognized that the properties of these materials, and especially

their mechanical properties, do not match the properties of the native cell extracellular matrix. Therefore, transfering this expertise of surface properties from hard materials to hydrogels, that better mimic the natural cell growth environment, could be a promising approach to further control MSCs differentiation.

One objective of this PhD project is to develop hydrogels with controlled mechanical properties, in terms of stiffness and viscoelastic properties, and to assess their impact on MSCs osteogenic differentiation. In the literature, it is believed that mimicking the mechanical properties of cells natural extracellular matrix would be favorable for the control of cell fate. In addition, the optimal mechanical properties to direct MSCs osteogenic differentiation are still to be determined, and particularly there is still very little information regarding the impact of the viscoelastic properties of the matrix on MSCs differentiation. Considering that cells extracellular matrix is composed of many different proteins, a second objective of this project is to assess the impact of hydrogels biofunctionalization on MSCs osteogenic differentiation, by comparing a mimetic peptide of the BMP-2 protein and type I collagen, and to determine if varying hydrogels biofunctionalization might change the way cells feel the mechanical properties of the matrix.

The first chapter focuses on the composition of bone and the processes of bone repair, as these constitute important knowledge for the development of effective strategies for bone repair. Then, the different strategies currently used in clinics for bone repair and their limitations are presented.

The second chapter presents different types of stem cells that can be used for bone tissue engineering, with a particular focus on mesenchymal stem cells (MSCs). Then, the use of MSCs in various clinical applications and their limitations is mentioned. Subsequently, the influence of the in vitro culture conditions of MSCs on their osteogenic differentiation is discussed. Finally, hydrogels are presented as an interesting platform for cell culture, and the principal polymers that can be used to synthesize hydrogels are reviewed.

The third chapter aims at gathering the accumulated knowledge on the control of MSCs behavior by varying hydrogels properties such as topography, porosity, mechanical properties, and biomolecules presentation.

The fourth chapter describes the obectives of this project and the main strategy followed to achieve these objectives.

The fifth chapter presents a first result article about the synthesis of hydrogels with controlled mechanical properties, and their chemical, structural, and mechanical characterization. This chapter also includes preliminary results about the impact of hydrogels stress relaxation on human bone marrow MSCs osteogenic differentiation.

Chapter 6 presents a second result article describing hydrogels surface functionalization with a mimetic peptide of the BMP-2 protein, as well as the impact of the surface functionalization on hydrogels surface mechanical properties. Subsequently, the impact of hydrogels stiffness and stress relaxation on MSCs osteogenic differentiation is presented and discussed.

Chapter 7 shows supplementary studies about the evaluation of hydrogels cytotoxicity, the surface functionalization of hydrogels with type I collagen, and preliminary results about the impact of hydrogels functionalization with a BMP-2 mimetic peptide or with type I collagen on MSCs osteogenic differentiation.

Finally, chapter 8 is a general discussion about all the results obtained in this PhD work and their significance for the control of MSCs osteogenic differentiation and the design of materials capable of interacting with cells.

LITERATURE REVIEW

Chapter 1

Bone physiology and repair

This first chapter focuses on the composition of bone and the processes of bone repair as these constitute important knowledge for the development of effective strategies for bone repair. Then, the different strategies currently used in clinics for bone repair and their limitations are presented, including bone graft, synthetic bone substitutes, and biological subsitutes.

1.1 Bone composition

1.1.1 Bone structure

In order to develop effective strategies for bone regeneration, it is important to consider bone structure and composition. Bones constitute an essential element of the human body as they form the framework of the body, they protect intern organs, they allow movement, and they provide minerals.[1] Bones are composite materials as they are composed of an organic phase, mainly formed of type I collagen fibers, and a mineral phase, made of hydroxyapatite (HAp) crystals located between the collagen fibers (Figure 1.1).[1, 2] However, the process of hydroxyapatite crystals deposition on the type I collagen matrix is a complex process that is still not fully understood.[28] In addition to collagen, it is reported that well-over 100 extracellular matrix proteins are present in bone.[28] The organic phase provides elasticity to bones, while the mineral phase brings them rigidity.[2] Indeed, a load applied on the bone is first resisted by the stiffness of the bone, provided by the mineral phase. Then, when the load exceeds a critical value, the energy is dissipated by the organic phase thanks to stretching and/or rupture of molecules and chemical bonds.[28]

Two types of structures can be found in bones (Figure 1.1). Cortical bone counts for 80% of the skeleton. It is highly dense and organized in concentric lamellae, called osteons, which form a channel to allow the passage of the blood vessels. Trabecular bone, also called cancellous bone or spongy bone, is much less dense and presents a higher surface area due to its high porosity, which brings lightness to bones. Trabecular bone can be found at the center of long

bones, such as the femur and the shin, in flat bones like the shoulder blades and the ribs, and in vertebrae.[2, 4] Bones also contain bone marrow for which the distinction should be made between red bone marrow, located within the pores of trabecular bone, and yellow bone marrow, which can be found at the center of long bones.[4] They have a very important role within the organism as they are the source of various types of stem cells which participate in the renewal of several populations of cells. Indeed, stem cells have the ability to proliferate almost endlessly to maintain stem cells population, or they have the possibility to differentiate into different types of cells to renew the population.[3] Thus, red bone marrow contains hematopoietic stem cells (HSCs) that can differentiate into all types of blood cells, such as red and white blood cells, and platelets[4], while yellow bone marrow contains mesenchymal stem cells (MSCs) which can differentiate into fat cells (adipocytes), cartilage cells (chondrocytes), and bone cells (osteoblasts).[3]

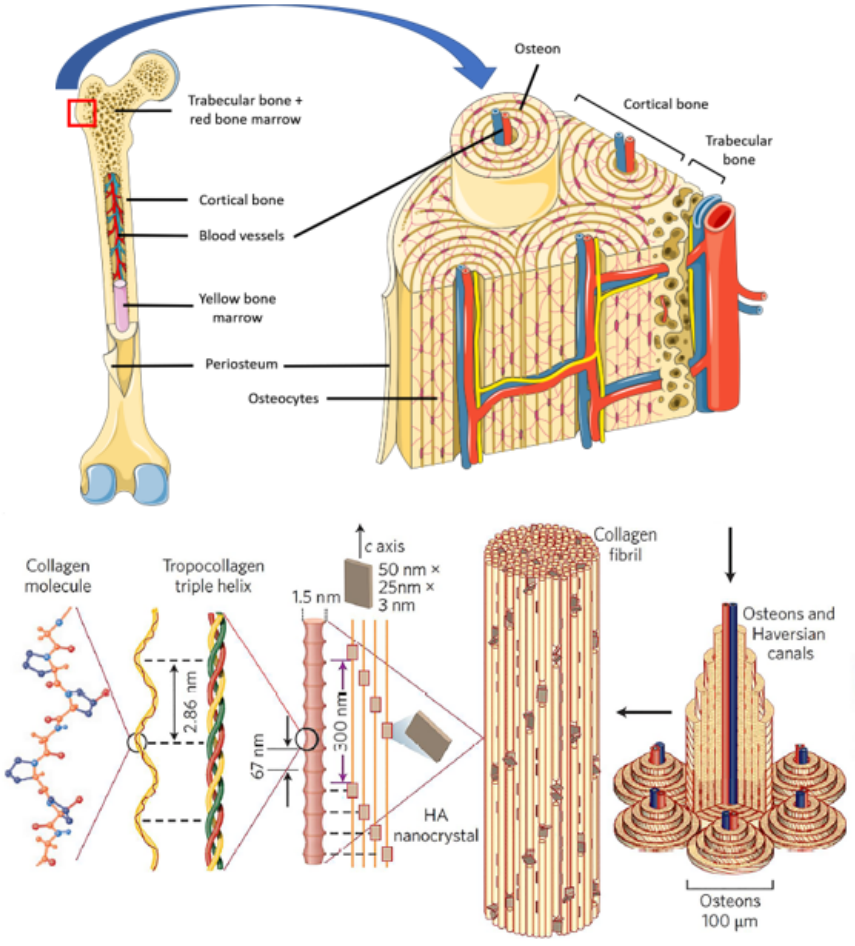

FIGURE 1.1 – The hierarchical structure and main nanostructure of human bone. The macrostructure of bone consists of trabecular (spongy) bone and cortical (compact) bone, with bone and Haversian canals around blood vessels. At the micro level, bone tissue is mainly a three-dimensional nanostructure composed of nanohydroxyapatite and self-assembled collagen fibres.[13]

1.1.2 Cellular components

As previously mentioned, in addition to organic and inorganic materials, bones are composed of different types of cells that can be divided into two categories, stem cells (HSCs and MSCs) and cells forming bone tissue. The latter are composed of three different types of cells, namely osteoclasts, osteoblasts and osteocytes (Figure 1.2.)[1, 2, 4, 23]

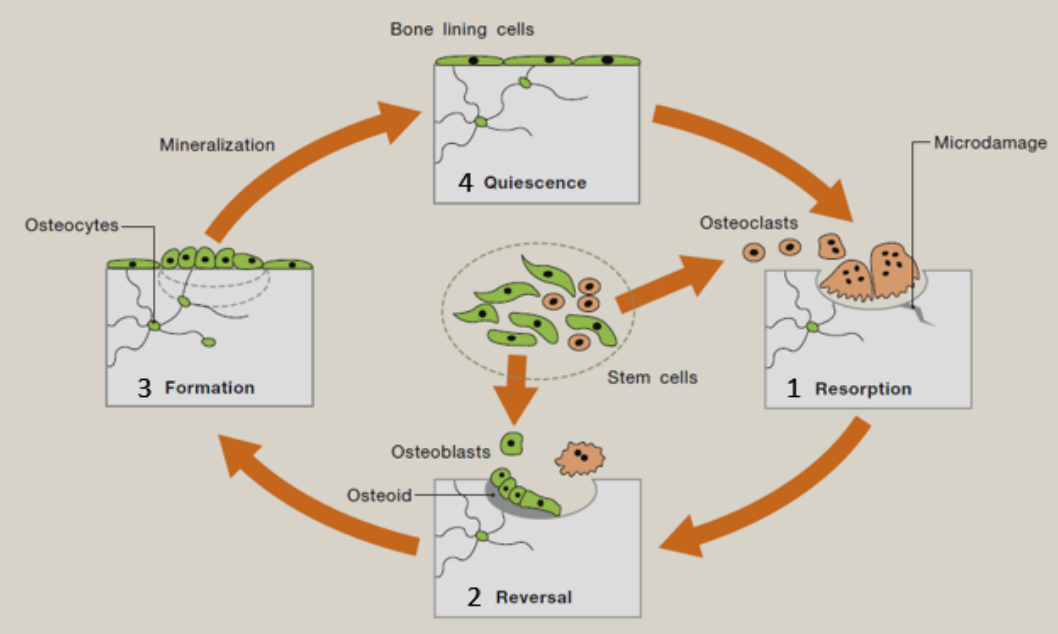

FIGURE 1.2 – Bone remodelling cycle.[2]

Osteoclasts are multi-nucleated cells formed from the differentiation of HSCs and that are responsible for bone resorption.[2, 4, 23] Indeed, it has to be noted that bone is a dynamic tissue as about 2.5% of cortical bone and 25% of trabecular bone are renewed every year.[4] Osteoclasts attach to bone surface and secrete hydrochloric acid capable of dissolving hydroxyapatite, as well as proteolytic enzymes which degrade proteins, resulting in bone resorption.[2]

Osteoblasts are mono-nucleated cells[23] resulting of the differentiation of MSCs, and whose principal function is to synthesize bone extracellular matrix and promote its mineralization.[4] Osteoblasts produce a matrix called osteoid that is deposited at the surface of bone.[2, 3] This matrix is mainly composed of type I collagen, as well as other proteins such as fibronectin, osteopontin, osteonectin, and osteocalcin.[23, 110] Osteoblasts then perform matrix mineralization by transferring calcium and phosphate ions from the extracellular medium to the matrix. Once this process is achieved, osteoblasts can become bone lining cells and form a layer of cells at the surface of bone, or be progressively included into cortical bone and differentiate into osteocytes, or else undergo apoptosis.[2, 4, 28, 29]

Osteocytes represent one of the terminal fates of osteoblasts and form the most abundant cells in

bone. They are embedded within bone in a lacunocanalicular system and form a tridimensional network of interconnected cells which makes them sensitive to mechanical stress and bone micro-damages.[2, 4, 23, 28] Indeed, when a bone is mechanically loaded, there are several possible stimuli that could be detected by osteocytes.[5] First, because osteocytes are distributed throughout the bone matrix, they will experience and sense the physical deformation of the bone matrix. Then, the load-induced flow of canalicular fluid through the lacunocanalicular network results in fluid flow shear stress that will also be sensed by osteocytes. Finally, electrical potentials that are generated from the flow of the canalicular fluid (which is an ionic solution) through the charged surfaces of the lacunocanalicular walls could also be sensed by osteocytes.[5] This sensitivity helps osteocytes to regulate osteoclasts recruitment for bone resorption, as well as regulate bone mineralization.[6]

1.1.3 Bone extracellular matrix

As highlighted in the previous sections, the extracellular matrix of bone is composed of an inorganic phase, made of hydroxyapatite (HAp) crystals, and an organic phase comprising many proteins that have different roles.

The bone extracellular matrix (ECM) is composed at 90% of dense and highly crosslinked type I collagen fibers.[111] It has been found that the quantity and structure of type I collagen was critical to maintain proper bone strength[28], as the lack of type I collagen or mutation of collagen structure are involved in the osteogenesis imperfecta disease (brittle bone disease)[111, 112], while crosslinking defects are related to osteoporosis.[111] Collagen types III and V are also present in bone ECM, and regulate the fiber diameter and fibrillogenesis of type I collagen.[112] Collagen modulates osteogenesis by binding with integrins of osteoblast progenitors. It also provides a matrix for anchoring cells and therefore regulates the growth and osteogenic properties of osteoblasts.[112]
Small leucine-rich proteoglycans (SLRPs), such as biglycan, decorin, keratocan, and asporin, can also be found in bone. These molecules are secreted extracellular proteins that regulate cellular behaviors and participate in all stages of bone formation, including cell proliferation, osteogenesis, mineral deposition, and bone remodeling.[112]
Glycoproteins, such as osteonectin and sclerostin, are also present in the bone ECM. Osteonectin regulates the calcium release by binding collagen and HAp crystals, thereby influencing the mineralization of collagen during bone formation.[112] Sclerostin, produced by osteocytes, would be an inhibitor of osteoblast matrix production.[28]
Many other proteins are present in bone and form approximately 5% of the matrix. The most studied are osteopontin (OPN) and osteocalcin (OCN) which participate to matrix mineralization.[111] OCN has the ability to bind calcium and mediate its association with

hydroxyapatite, while OPN regulates bone formation, mineralization, and resorption.[112] They would also be implicated as contributors to the strengthening mechanism of bone by forming a tether between collagen fibrils and mineral crystals.[28] OCN would promote the differentiation of MSCs into osteoblasts. OPN would increase the proliferation capacity of MSCs in a dose dependent manner, and would also induce MSCs migration.[112] OPN is part of the SIBLINGs (Small Integrin-Binding Ligand N-Linked Glycoproteins) family, a family of glycophosphoproteins found in mature and mineralized bone. This family also comprises other proteins such as bone sialoprotein (BSP), dentin matrix protein-1 (DMP1), and matrix extracellular phosphoglycoprotein (MEPE).[112] BSP promotes osteoblast differentiation and initiates matrix mineralization in bone tissue, while DMP1 and MEPE, produced by osteocytes, regulate matrix mineralization and phosphate metabolism.[112] DMP1 would be a negative regulator of MSCs differentiation, but would inhibit the apoptosis of osteocytes, enhance bone mineralization, and prevent the disintegration of the osteocyte network.[28, 112]

Although they are not directly deposited into the ECM, many growth factors exist in bone and can be trapped within the ECM, which can falicitate their interaction with different cell types. The main growth factors influencing bone formation and repair are presented later in this chapter.

1.2 Bone development and repair

1.2.1 Physiology of bone development

The earliest forms of skeleton, that form during embryogenesis, are the mesenchymal condensations that form when undifferentiated mesenchymal cells migrate into areas destined to become bone. These mesenchymal condensations can then become bone through two distinct processes.

The first process is intramembranous ossification. This process is involved in the formation of the bones in the cranial vault, parts of the jaw, and the medial part of the clavicle.[113, 114] During this process, mesenchymal stem cells gather together in a fibrous connective tissue membrane made of collagen fibers, and begin to differentiate into osteoblasts to form an ossification center. Bone matrix (osteoid) is then secreted by the osteoblasts within the fibrous membrane. Finally, osteoid is mineralized within a few days and trapped osteoblast become osteocytes, while the remaining osteoblasts continue producing osteoid to increase bone size. As bone matrix mineralization makes bones relatively impermeable to nutrients and metabolic waste, blood vessels are trapped within the bone during its formation to supply nutrients to osteocytes as well as bone tissue and to eliminate waste products.[115]

The second process is called endochondral ossification, as it is a two-step process involving chondrogenesis and osteogenesis (Figure 1.3). Indeed, the cells in mesenchymal condensations first differentiate into chondrocytes to create a cartilaginous template of the future bone. These chondrocytes then undergo hypertrophy as they stop dividing, they enlarge, and become hypertrophic chondrocytes, a subpopulation of chondrocytes surrounded by a calcified ECM. The cartilage continues to grow longitudinally, and continually deposits hypertrophic chondrocytes. Subsequently, a vascular invasion brings osteoblast progenitors that will form a primary ossification center, as they will differentiate into mature osteoblasts that secrete the bone ECM that will replace the cartilaginous ECM.[113, 114] A secondary ossification center then arises within the end of the bone, and the cartilage tissue is progressively replaced by bone.[114]

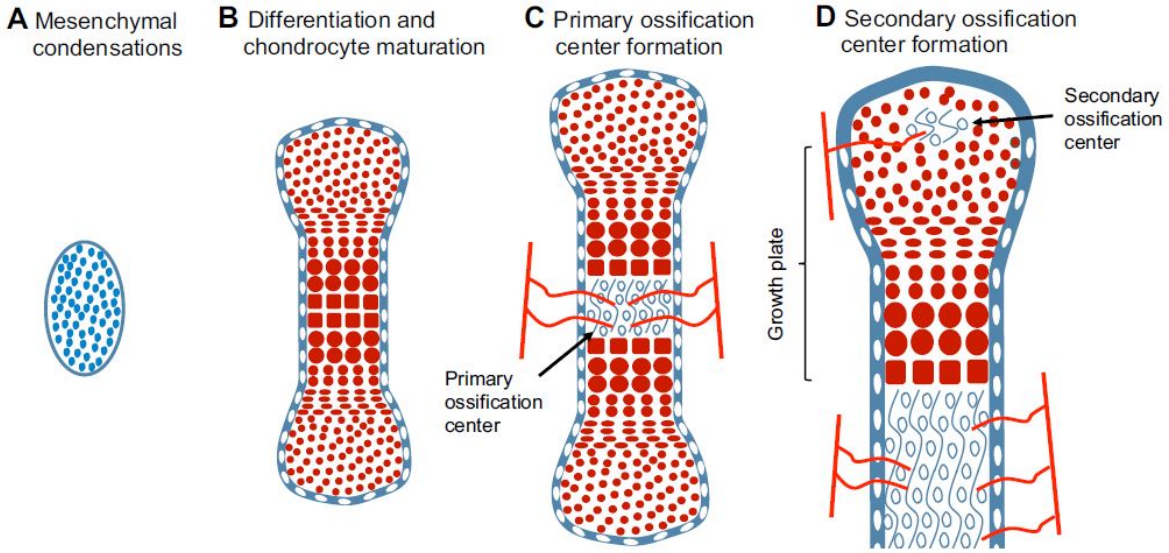

FIGURE 1.3 – A) Schematic representation of mesenchymal cells (blue) that begin to form condensations. B) Mesenchymal cells differentiate into chondrocytes (red cells), and the process of chondrocyte maturation and hypertrophy initiates. The cartilage template is surrounded by a layer of perichondrium (white cells). C) Vascularization (represented by red lines) takes place in the center of the cartilage template, resulting in replacement of chondrocytes with endochondral bone (open circles) in the primary ossification center. D) The secondary ossification center forms and also becomes vascularized.[114]

1.2.2 Bone repair

Bone repair can occur by different mechanisms, that can be similar to bone formation during embryogenesis.

Endochondral bone repair describes bone repair which occurs in an environment of micromotion between the fragments, such as with fractures treated in a cast. After injury there is extensive bleeding with the formation of a large haematoma, followed by the formation of a fibrinous blood clot. During the first few days post-fracture, the body also triggers an inflammatory response. It is thought that molecules associated with the inflammatory phase and blood clot formation are essential for initiating the correct repair response. Similarly to endochondral ossification, the relative movement of the repair environment and the relative tissue hypoxia due to damage to the blood supply leads to the formation of a large cartilaginous mass, called a callus, by undifferentiated mesenchymal cells, that will stabilize the fracture site. Subsequently, the chondrocytes undergo hypertrophy, the callus is invaded by osteoprogenitor cells and blood vessels, and bone tissue is formed on the cartilage.[116]

When a stable environment for repair is established by early surgical fixation of the fragments, the cartilage callus is no longer needed for bone repair. Primary bone repair, also referred to as contact healing, occurs in situations where the fracture is rigidly compressed with no interfragmentary gap. Since a dense and normally oriented scaffold for repair exists, in the form of the original bone held by rigid compression fixation, surface osteoblasts are sufficient for bone repair. Indeed, they perform bone repair by depositing lamellar bone (i.e. bone with parallel collagen fibers) directly parallel to the long axis of the bone.[116] Direct bone repair, or gap repair, occurs when the fracture is rigidly compressed but with an interfragmentory space from 0.2 mm to a few mm. In this case, the central part of the defect is filled with mesenchymal stem cells that progressively differentiate into osteoblasts to recreate bone. The repair is more advanced at the periphery of the defect than in the center, as mesenchymal stem cells differentiate into osteoblasts that produce woven bone (i.e. bone with randomly oriented collagen fibers). Then, as woven bone is progressively produced towards the center of the defect, the woven bone at the periphery is replaced by lamellar bone. Rapidly, the proportion of lamellar bone increases in all the defect and osteons are recreated.[116]

Finally, distraction osteogenesis occurs in a stable environment due to external fixation but with an intermittent or continuous incremental lengthening of the fixation. In this case, the healing process is similar to direct bone repair, but with the longitudinal distraction helping the collagen fibers of the woven bone to align along the long axis of the bone. This technique allows bone repair to occur without the need for internal stabilization or bone grafting.[116]

1.3 Strategies for bone regeneration

As previously mentioned, different strategies already exist and are efficient for the repair of small bone defects (cast, surgical fixation) but are still insufficient for the repair of large defects such as large fractures, bone tumor, or bone necrosis, for which a large part of the bone is missing. These defects must be filled to get the normal function of bone back. The filling material has to provide mechanical support and allow for bone reconstruction, which requires three important properties : osteoconduction, osteoinduction, and osteogenesis (Figure 1.4). Osteoconduction is the ability to support the adhesion and growth of osteoblasts and osteoprogenitors. Osteoinduction describes the ability to recruit undifferentiated cells and stimulate their development into pre-osteoblasts. Osteogenesis includes osteogenic differentiation and new bone formation. Ideally, the filling material should progressively resorb to be replaced by bone tissue. In the case of implanted materials that replace bone, like a hip prosthesis for example, osseointegration, which describes a stable anchoring of the implanted material by a direct contact with bone, is also an important requirement.[1]

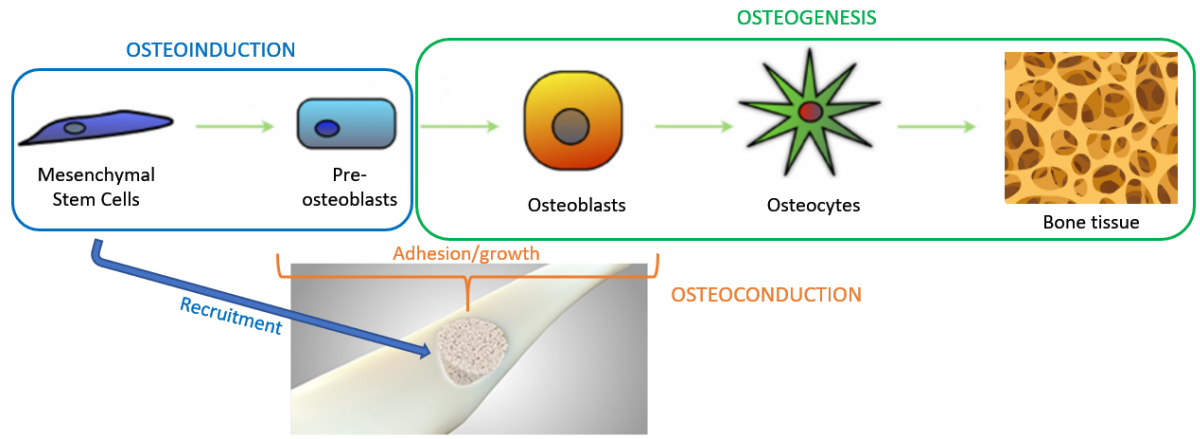

FIGURE 1.4 – The essential properties of bone filling materials : osteoconduction, osteoinduction and osteogenesis.

1.3.1 Bone grafts

Currently, bone graft is the most widely used method for the treatment of bone defects. More than two million of bone grafts would be performed every year worldwide, which represents the second most frequent transplant, after blood transfusion.[1, 7] A bone graft consists in collecting healthy bone tissue and implanting it at the location of the bone defect. Three types of grafts can be distinguished : autologous graft, allogeneic graft, and xenotransplantation.

Xenotransplantation consists in implanting an organ or cells from animals to humans. This approach would circumvent the lack of organs from human origin, but the immunologic differences between the species generally result in graft rejection.[1]

Autologous graft (or autograft) consists in collecting healthy bone tissue from the patient, generally in the hip, and reimplanting it at the location of the bone defect. This method is considered as the gold standard for the treatment of bone defects as the graft presents the required properties of osteoinduction, osteoconduction, and osteogenesis, and is directly compatible with the patient as it comes from the patient himself. Cancellous (trabecular) autografts are the most commonly used form of autologous bone grafts. They present few osteoblasts and osteocytes, but are abundant in mesenchymal stem cells which help maintain the osteogenic potential and the ability to generate new bone from the graft. Additionally, the large surface area of a cancellous autograft facilitates the revascularization and incorporation of the graft locally to the host bone. While cortical autografts possess better structural integrity and are mechanically supportive. Nevertheless, autologous graft suffers from several disadvantages, such as complications, pain and infection that can occur where the bone is collected, a longer operating time and a limited volume of available bone.[1]

Allogeneic transplant (or allograft) is the transplantation of tissue collected on another individual of the same species. Cancellous allografts are the most common types of commercial allogeneic grafts and are supplied predominately in the form of cuboid blocks. Because of their low mechanical properties and their relative poor healing promoting ability, cancellous allografts are mainly applied for spinal fusion augmentation and for filling small cavitary skeletal defects. Cortical allografts confer rigid mechanical properties and are mainly applied for filling large skeletal defects where immediate loading-bearing resistance is required. Allograft is an alternative to autograft but this method also presents some disadvantages. The success rate is lower than for the autograft, as it is thought that the initial osteoinduction phase would be destroyed by immune response and inflammatory cells, which could quickly surround the neo-vasculature, causing the necrosis of osteo-progenitor cells. Allograft also presents a risk of virus transmission.[1]

1.3.2 Synthetic bone substitutes

The complications that may occur for the different types of bone grafts and the inability to meet the growing demand for bone initiated the development of synthetic bone substitutes. The bone substitutes currently used in clinics can be divided into four groups : ceramics, bioactive glasses, metallic materials, and polymeric materials.[1, 7]

Ceramics

Ceramic materials exhibit great compression strength and high Young's modulus, together with high wetting degrees and surface tensions, which would favor the adhesion of proteins, cells, and other biological moieties, which make them interesting candidates as bone substitutes.[8]

The most widely used ceramics are alumina (Al_2O_3) and zirconia (ZrO_2) because of their high strength, good corrosion and wear resistances, stability, and non-toxicity. Alumina has been used in total hip arthoplasties, in total knee prosthesis, and in dentistry for making screws, blades, and ceramic crowns. Because of its enhanced mechanical properties when compared to alumina, zirconia has replaced alumina in ceramic femoral heads. In addition, due to its white color, zirconia has often been used to make dental implants. However, these ceramics can be qualified as biologically inert (bioinert) materials as they do not interact with the host bone, which elicits a foreign body reaction. As a defense mechanism, the host body will surround the implant by an acellular collagen capsule, to isolate it from the body. This capsule of fibrous tissue can provoke interfacial micromovements that grow with time and eventually results in the failure of the prosthesis.[8]

In order to avoid the formation of a capsule around the implant and to obtain favorable interactions with the living body (bioactive response or degradation), ceramics made of calcium phosphates or sulfates are now clinically used for bone tissue augmentation, with different sizes and shapes (Figure 1.5), as bone cements, or for metallic implant coatings.[8, 9]
Being the principal component of bone, special attention has been paid to hydroxyapatite (HAp, $Ca_5(PO_4)_3OH$).[8, 9] The ability of hydroxyapatite to host ions in its structure allows the design of synthetic calcium phosphates with tunable properties such as degradation, surface structure, and electric charge. In addition, the presence of certain chemical elements (Sr, Zn, silicates) that are released during ceramic resorption would facilitate bone regeneration carried out by osteoblasts.[8] Hydroxyapatite has osteoconduction and osseointegration properties, but lacks osteoinduction and osteogenesis properties. In addition, this material resorbs too slowly to allow osseous repair.[7, 9, 117]
Calcium Sulfate ($CaSO_4$) has been used for the first time in 1892 to fill bone defects. The

dihydrate form of the compound has the ability to harden by exposure to moisture. It is therefore possible to control the porosity of the material by varying the exposure to moisture.[7] Calcium sulfate offers many advantages as it presents a structure similar to bone, it is osteoconductive, and inexpensive.[118] The material has a highly crystalline structure which allows to resist compression forces. However, if the material is more resistant than trabecular bone, it is seven times less resistant than cortical bone.[7] In addition, this material resorbs very fast and can resorb before a complete bone reconstruction.[7, 118]
Finally, β-tricalcium phosphate (β-TCP, $Ca_3(PO_4)_2$) can also be used. This material resorbs faster than hydroxyapatite but slower than calcium sulfate. However, tricalcium phosphate is contra-indicated in case of infection and for the replacement of long bones, as it is not strong enough to survive physiologic loading.[7, 117]
Considering the faster resorption of β-TCP as compared to HAp, and the better mechanical properties of HAp, these two materials are often used together to create composite ceramics that enable a faster and higher bone ingrowth rate than using HAp alone, while offering better mechanical properties than β-TCP alone.[8, 118] But despite the improvement of mechanical properties of β-TCP by the incorporation of HAp, the strength of the composite ceramics is still lower than cortical bone compression strength.[118]
Cements based on calcium phosphates, calcium carbonates, or calcium sulfates are also under investigation as it would provide mouldable and even injectable pastes that are able to harden within the body. The physical-chemical properties of these materials, such as the setting time, porosity, and mechanical behavior, depend on cement formulation and the presence of additives, and would therefore be tunable. However, some aspects still need to be improved and are related to their mechanical toughness, curing time, application technique on the osseous defect, and the final biological properties.[8, 9]

It is recognized that the main disadvantage of ceramic materials is their brittleness that makes them not suitable for load-bearing applications.[8, 9] To overcome this drawback, coatings of hydroxyapatite and other calcium phosphates over metallic substrates are developped. But the resorbable nature of these materials causes a loosening of the coating over time. In addition, other aspects still have to be solved including adherence of the ceramic to the metallic substrate.[8]
In addition, the porosity of ceramic implants is adjusted to enhance biological performance, as interconnected macropores > 100 μm would be required to allow tissue ingrowth and neovascularization, and to ensure a fast healing response.[8, 9] However, adding porosity to the material further decreases its mechanical properties. Although there have been several attempts to improve the mechanical properties of ceramics by combining them with polymers, at the moment no biodegradable composites have been obtained with a combination of strength, ductility and toughness close to that of cortical bone.[9]

FIGURE 1.5 – Synthetic materials made from hydroxyapatite and tricalcium phosphate produced by the company Biomatlante and used as bone grafts. They are composed of macro- and micropores, with a porosity of 70%, which allows cell and nutrients transport. From biomatlante.com

Bioactive glasses

Bioactive glasses (or bioglasses) are originally silicates that are coupled to other minerals naturally found in the body (Ca, Na_2O, H, and P).[118] Bioactive glasses have the ability to degrade chemically and convert to hydroxyapatite which can subsequently bond to host bone.[117, 119, 120] Indeed, sodium, silica, calcium, and phosphate ions are released from the surface, forming a silica gel layer on the glass surface, allowing amorphous calcium phosphates to precipitate on this layer. These amorphous structures then crystalize to natural hydroxyapatite, which activates osteoblasts for the formation of new bone. Because of the continuous reactions and layer formation, the glass will finally be absorbed and therefore constitutes a bioresorbable material.[120] Bioactive glasses would also posses antibacterial properties as a result of a local pH increase caused by the exchange of alkali ions with protons in body fluid. The release of salt ions also contributes to a higher osmotic pressure, which is an antimicrobial factor.[120] These features make bioglasses interesting candidates for bone regeneration purposes.

S53P4 bioactive glass, composed of 53% SiO_2, 4% P_2O_5, 23% Na_2O, and 20% CaO (by weight), is increasingly used in clinical practice in various bone graft applications and in treatment of osteomyelitis. This bioactive glass is mostly used in a granular form (Figure 1.6) and has been found to be an interesting alternative to autologous bone graft for the repair of several small bone defects, such as defect reconstruction of facial bones, frontal sinus fracture obliteration, nasal septal perforation repair, mastoid obliteration for the treatment of chronic otitis, tibial plateau fracture repair, and bone repair after small tumor resection. Although this material degrades slowly, as it can remain present in the body fourteen years after implantation, it has been found that bone incorporates well with the bioglass and that the newly formed bone tissue is stable, with clinical success rates at least comparable to the gold standard procedure (autologous bone graft).[120] The use of bioglass could therefore replace the autologous bone graft and would circumvent a second operating site in the patient, providing more comfort for the patient and the surgeon. Thanks to its antimicrobial properties, S53P4 bioactive glass is also a promising candidate for the treatment of osteomyelitis, which is an infection of

bone and bone marrow. Osteomyelitis is commonly treated with surgical implantation of non degradable polymeric beads loaded with antibiotics, that must be removed by subsequent surgical intervention, usually after two weeks. The use of resorbable bioglass would therefore avoid a second surgical intervention.[120]

However, the low strength and the brittleness of bioactive glass have largely hindered the development of bioactive glass scaffolds for repairing segmental defects in structural (load-bearing) bones, also called structural bone defects.[117] Synthetic scaffolds for bone repair should be osteoconductive and osteoinductive, and they should have a 3D microstructure capable of supporting new bone infiltration and angiogenesis (blood vessels formation and growth) to sustain new bone growth, which goes through an interconnected porous network. The scaffold should also be bioactive, with the ability to convert to hydroxyapatite at a rate comparable to new bone ingrowth.[117] In this context, mesoporous bioglasses are being developped, with highly ordered interconnected mesopore channels of pore size ranging from several nm to hundreds of μm, which provides bioglasses with higher specific surface area, improving the colonization by the host bone.[117, 119] However, making porous bioactive glass further decreases the mechanical properties of the scaffold. Therefore, combining bioglass with other materials, such as polymers, is currently under investigation to create composite scaffolds with suitable mechanical properties for the repair of structural bone defects, but this still requires improvements before being applied in clinics.[117] Finally, bioactive glasses can be used as coatings on prostheses, but because of their resorbable nature, the prosthesis will lose the coating over time.[7]

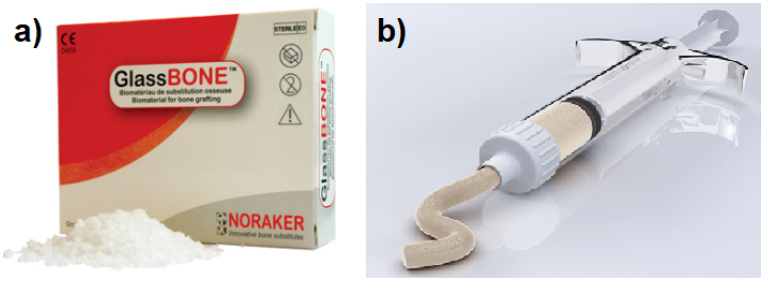

FIGURE 1.6 – Bioactive glasses used for orthopedic, maxilla facial and spine surgery a) in the form of granules or b) in the form of a paste that can be injected. From noraker.com

Metallic materials

Metallic materials have been widely used in orthopedic surgery for making temporary devices, such as plates, pins, and screws, or permanent implants for total joint replacement. They are also used in dentistry as tooth fillings for example.[10, 11] Due to their high mechanical strength and fracture toughness, they are useful for load-bearing applications.[10] Metallic

biomaterials can be divided into four groups depending on their composition : stainless steels, cobalt-based alloys, titanium-based alloys and other materials, such as shape memory nickel-titanium alloys (nitinol) and degradable magnesium alloys. If medical implants made of the metallic materials in the first three groups have been approved by the FDA (United States Food and Drug Administration) and are routinely used in orthopedic practice, it is not the case for the last group.[11]

Stainless steel is the generic name for a number of iron-based alloys that contain a high percentage (11-30 wt%) of chromium and varying amounts of nickel. Chromium and nickel contribute to increased corrosion resistance by forming a protective oxide film on the surface of the alloy. The addition of other alloying elements, such as molybdenum, may enhance resistance to specific corrosion mechanisms, or develop desired mechanical and physical properties. However, it has been found that the stainless steels alloys generally used in clinical applications were not sufficiently corrosion resistant for long-term use (Figure 1.7a). In addition, these alloys also present a poor fatigue and wear resistance, leading to fractures several months or years after implantation (Figure 1.7b), and present toxicity and carcinogenicity due to the release of nickel and chromium. Nowadays, stainless steels are rarely used in any permanent implant devices, except for Orthinox stainless steels, which are high-nitrogen, nickel-free stainless steels, that are used to make permanent hip prostheses.[11]

Cobalt-chromium based alloys are superior to stainless steels in corrosion resistance, thanks to the high chromium content that leads to spontaneous formation of a passive oxide (Cr_2O_3) layer. The corrosion resistance is also improved by adding molybdenum and nickel. They present superior mechanical properties over stainless steels, with better fatigue resistance, making them an ideal choice of materials for total joint replacements[11], although fracture of the prosthesis can occur (Figure 1.7d).[121] However, cobalt-chromium alloys are expensive, and similarly to stainless steels, there are concerns about the toxicity of the elements released from cobalt-based alloys (Ni, Cr, and Co).[11]

The use of titanium alloys as biomaterials has been increasing, notably Ti-6Al-4V alloys, due to their lower modulus (closer to the modulus of bone), superior biocompatibility and enhanced corrosion resistance as compared to stainless steels and cobalt based alloys. In addition, titanium alloys would have the ability to bond with bone. In general, once a material is implanted into the bone, the body naturally forms a capsule around that material in recognition of it as a foreign body, and the formation of this capsule tissue contributes to the loosening of permanent implants. But in the case of titanium alloys, the implants demonstrate intimate integration with host bone tissue. This is thought to be due to the formation of titanate (Na_2TiO_3) on the surface of Ti alloy, which progresses further to result in the formation of carbonated apatite (hydroxyapatite with PO_4^{3-} substituted by CO_3^{2-}). Subsequently, collagen fibers of the

host bone would insert into the carbonated apatite layer on the implant, forming a bond between the implant and the host tissue. This bonding can be a problem for temporary implants or implants that need to be retrieved due to rupture. As such, titanium alloys are primarily used in permanent implants or short-term temporary devices that will be retrieved before bone bonding is formed. Titanium alloys suffer from poor shear strength and wear resistance that often cause premature rupture of the implant(Figure 1.7c). In addition, different alloys are being developped as the release of Al and V from Ti-6Al-4V alloys would be involved in long-term health problems such as Alzheimer's disease, other neuropathies and osteomalacia (disease characterized by the softening of the bones).[11]

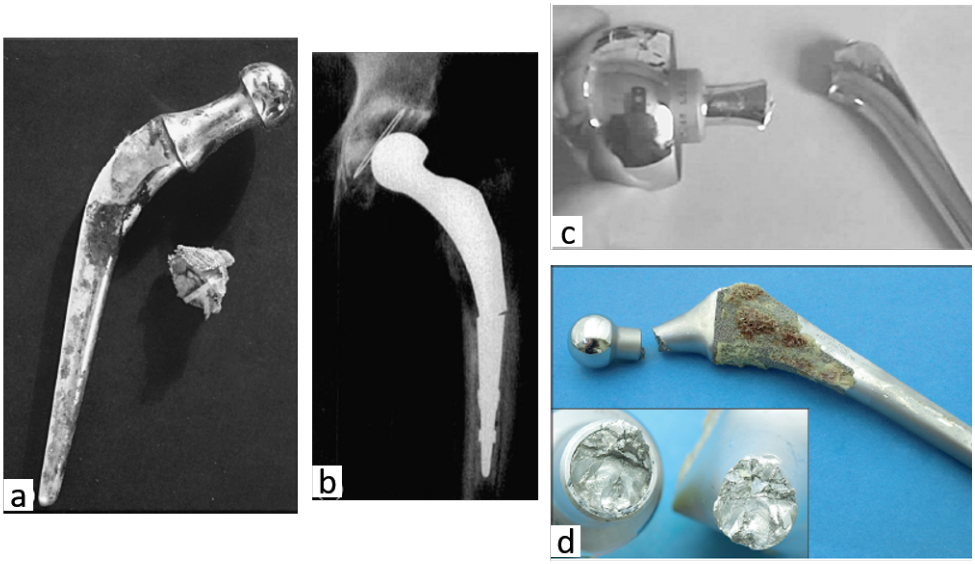

FIGURE 1.7 – Examples of failure of metallic prostheses for total hip replacement. Stainless steel prostheses a) corrosion and b) failure after 9 years of implantation. c) Typical titanium (Ti-6Al-4V) prosthesis and d) cobalt-chromium prosthesis premature failure of the neck after 10 to 15 years of implantation.[11, 121]

It has to be noted that stainless steel, cobalt-based alloys and titanium-based alloys have much higher Young's modulus than that of bone (4 times to 20 times higher) resulting in a stress-shielding effect. Stress-shielding occurs as the implant may shield parts of the surrounding bones from load and concentrate forces in other parts. If the stress is concentrated in areas that have not previously been exposed to high loads, these areas can be damaged, which results in bone fracture. Then, if stress-shielding reduces the load previously seen in areas around the implant, those areas may remodel in response, by producing a smaller amount of bone tissue and a less dense bone tissue. The interface between the bone and the implant is therefore deteriorated as the bone is weakened, with potential loosening and fracture of the bone, the interface, or the implant.[10, 11]

The use of magnesium alloys as orthopedic implant materials is currently under investigation as it would present several benefits. Magnesium has a similar density and Young's modulus to that of bone, which would avoid any stress-shielding effect. Magnesium alloys have controllable corrosion rates, and thus resorbability, in physiological media, which would provide resorbable implants allowing native tissue to integrate with the implant and eventually replace it. In addition, the major alloying elements used (Mg and Ca) can be tolerated by the body at relatively high levels. However, the main issue of these alloys is the fact that the degradation of Mg alloys leads to the formation of hydrogen gas that accumulates around the implant. Magnesium glasses are investigated as an alternative to crystalline alloys to address the issue associated with the hydrogen bubble effect.[11]
The first widespread medical application of nickel-titanium alloys, also called nitinol, was for the fabrication of intra-vascular stents. This has been driven by their good workability, good resistance to corrosion, and shape memory effect. Shape memory is the ability of nitinol to undergo deformation at one temperature, stay in its deformed shape when the external force is removed, then recover its original, undeformed shape upon heating. The stent can therefore be deformed to get smaller and more easily introduced into a blood vessel, and subsequently return to its undeformed shape and maintain the structure of the blood vessel. Their use as orthopedic implant materials to make correction rods for scoliosis and fixation staples for long bones is also investigated. Indeed, NiTi alloys are interesting as they would have a better corrosion resistance than Cobalt-chromium alloys or stainless steels, and they would possess the closest Young's modulus to that of cortical bone of human (30-50 GPa). However, their fatigue resistance would be lower than that of stainless steels, cobalt and titanium based alloys, and there is still no convinving evidence that NiTi alloys are better than the existing competitors.[11]

Polymeric materials

Polymeric materials are gaining interest for bone replacement because their physical characteristics can be molded according to their application as they can be produced in a more porous or smooth form, they are easily manipulated, and they are lighter than metals. However, their main disadvantage is their inferior mechanical properties as compared to ceramics, bioglasses, metals, and bone. In addition, they generally lack adhesion to the living tissues.[12, 13]

Poly(methylmethacrylate) (PMMA) is a biocompatible, biologically inert, and hydrophobic polymer. PMMA is used as cement for orthopedic prostheses fixation, such as hip prostheses, for filling craniofacial defects (Figure 1.8), for repairing fractured vertebrae, and in dentistry.[12] Commercial cements are sold as a powder containing linear PMMA, a polymerization initiator (benzoyl peroxide), radio-opacifiers (barium sulphate $BaSO_4$, zirconia ZrO_2), and antibiotics like gentamycin, and a liquid containing methyl methacrylate monomers, a catalyst (N,N-

dimethyl para-toluidine), and a stabilizer (hydroquinone).[122] The cement is prepared at the time of the surgery by mixing the powder with the liquid phase which form a paste that can be casted around the prosthesis and subsequently hardens. Being a plastic material, PMMA does not have osteoinduction, osteoconduction, and osteogenesis properties[7, 122], although making a porous material can improve the osteoconductivity.[7] Its compressive strength is similar to bone, but it is not resorbable and the on-site preparation before the surgery can lead to significant variations between patients.[7] In addition, PMMA cements suffer from several other drawbacks such as the presence of residual monomer that can enter the bloodstream and cause embolism, the high temperature released during cement mixing that can produce thermal necrosis in the bone or adjacent tissues, the shrinkage of cement during polymerization that can produce free spaces and loss of contact between cement and prosthesis/bone, the excess of tension that can cause cement fractures and release of cement particles, which can subsequently interact with the surrounding tissues, generating an inflammatory reaction.[12, 122]

Poly(ether-ether-ketone) (PEEK) is a biocompatible and chemically resistant polymer that has found several applications for bone repair. PEEK is implanted as spinal cages or spacers in patients suffering from spinal diseases (Figure 1.8). It is also used as screws for the fixation of bone fracture repair devices, as well as for making partial dentures. The main drawback of PEEK is the fact that it is biologically inert, therfore not providing a good interaction with the bone tissues surrounding the implant, which can trigger implant failure.[12]

Ultra-high molecular weight polyethylene (UHMWPE) is widely used to fabricate components of hip, knee, and shoulder prostheses[123] (Figure 1.8) considering that UHMWPE has an elastic modulus closer to the bone than other materials commonly used in prostheses such as cobalt and titanium alloys. Nevertheless, UHMWPE is a bioinert material, and its fixation to the bone is only possible using PMMA as bone cement. In addition, during joint movements, wear of the polymer surface occurs which releases residues of the polymeric material and may cause osteolysis (bone resorption), aseptic loosening, and inflammation at the implant interface, leading to the need for surgical revision.[12]

As previously mentioned, some efforts are dedicated to making composite materials by combining polymers and ceramics such as hydroxyapatite. The polymer would provide improved mechanical properties as compared to the ceramic alone, while hydroxyapatite would provide greater integration between the bone tissue and the implant. Nonetheless, such composites still have drawbacks such as the formation of wear particles and the material's poor fatigue resistance.[12]

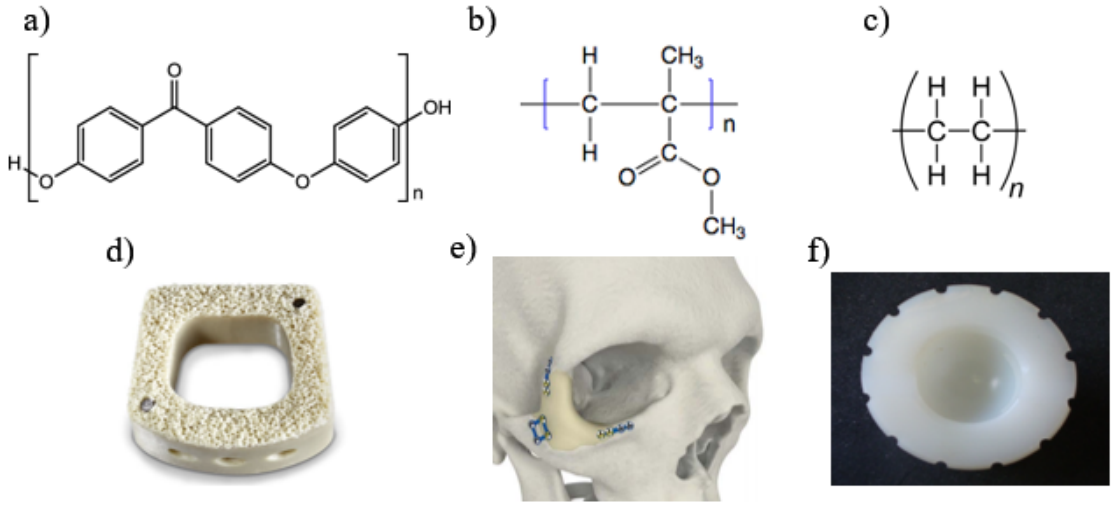

FIGURE 1.8 – Polymeric materials used for bone repair. Chemical structure of a) poly(ether-ether-ketone) (PEEK), b) poly(methylmethacrylate) (PMMA), and c) polyethylene. Examples of use of polymeric materials for bone repair. d) Porous PEEK cervical cage. From odtmag.com. e) PMMA customized implant to correct trauma and/or defects in maxillofacial or craniofacial bone. From Stryker.com. f) Cup fabricated from ultra high molecular weight polyethylene used as articulating surface of a total artificial hip prosthesis.[123]

While the previously mentioned polymers are not degradable, researchers are now focusing on the use of biodegradable polymers for bone defect repair, as the implanted material could degrade over time and progressively be replaced by bone tissue. These polymers can be natural polymers, such as chitosan, silk fibroin, fibrinogen, collagen, and hyaluronic acid. They have been extensively studied as bone defect repair materials due to their biodegradability, bioactivity, and biocompatibility. In addition, some of them have natural adhesion ligands, such as GFOGER, DGEA, and RGD amino-acid sequences, that can promote cell adhesion. However, they also have some shortcomings such as high water solubility, poor mechanical properties, possible denaturation during processing, and batch-to-batch variability and possible immunogenicity depending on their source.[13] Synthetic polymers offer the advantage of having controllable design and synthesis parameters, which can provide biomaterials with tunable properties. In recent years, the most studied synthetic degradable polymers are aliphatic polyesters, such as poly(ϵ-caprolactone) (PCL), polylactic acid (PLA), polyglycolic acid (PGA) (Figure 1.9) and copolymer of poly(lactic-co-glycolic acid) (PLGA). However, PCL showing a slow degradation rate and poor mechanical properties, it is not an ideal bone defect repair material. While PGA has been used as the first biodegradable suture in clinical practice, its excessively rapid degradation rate in vivo makes it not suitable for repairing bone defects. Because of its high mechanical strength and porous structure, PLA is widely studied for bone repair applications. PLGA copolymers also attract the interest as their properties, such as the degradation rate and the mechanical properties, can be modulated by changing the ratio of PLA and PGA. However, the utility of PLGA is limited in bone repair because of poor

osteoconductivity and hydrophobicity.[13] In addition, PLA and PGA degrade into their original monomers, lactic acid and glycolic acid respectively, which decreases the pH in the surrounding tissues, leading to local inflammatory reaction and poor tissue regeneration.[124]

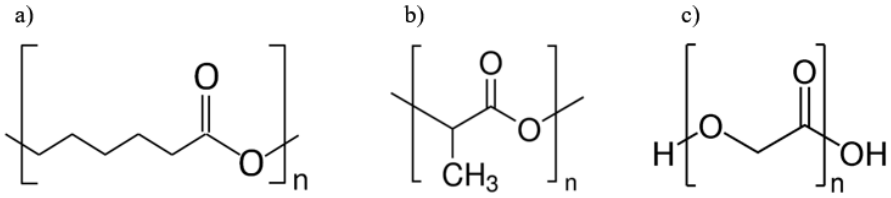

FIGURE 1.9 – Synthetic degradable polymeric materials investigated for use in bone repair. Chemical structure of a) poly(ϵ-caprolactone) (PCL), b) polylactic acid (PLA), and c) polyglycolic acid (PGA).

1.3.3 Bone repair by using biological products

As the use of autografts and allografts is related to many complications such as donor site morbidity, infection, immune response, and virus transmission, while synthetic grafts are not performant enough in terms of osteoinduction, osteoconduction, and osteogenesis, other strategies are developed which consist in using biological products and molecules naturally found in the body that are involved in bone physiology.

Demineralized bone matrix

Demineralized bone matrix (DBM) is bone that has been acid-treated in order to remove the mineral matrix, while maintaining the organic matrix (mainly collagen with some non-collagen proteins), growth factors, and residual calcium phosphate mineral (1-6%). As the remaining collagen proteins in DBM can provide a 3D configuration for ingrowth of host capillaries and osteoprogenitor cells into the graft, DBM has been demonstrated to be an osteoconductive and osteoinductive substitute.[1, 118, 125] Nevertheless, a large rate of the osteogenic capacity of bone is lost during its processing. In the meantime, the original cells and possible bacteria in the allogeneic bone are killed during the acidic treatment, which could reduce the risks of immune rejection and infection.[1, 118, 125]
Currently the most popular DBM product is a moldable bone paste, which can be casted into the defect site. These moldable DBM product are made of the combination of DBM powder/particles with biocompatible viscous carriers, which provides a stable suspension of DBM powder/particles.[125] DBM can also be provided as blocks, strips, and putty, of various shapes and sizes (Figure 1.10). However, considering the low mechanical properties of such

material, DBM is only used for filling purposes and generally not as a stand-alone bone substitute.[118]

FIGURE 1.10 – Examples of bone grafts substitutes made from demineralized bone matrix. The products are designed with different shapes and sizes and can be blocks or strips of pure demineralized bone matrix (porous white materials), or a mixture of demineralized bone matrix and a viscous phase that provides a putty or a paste that can be molded into the bone defect (yellow materials). From zimmerbiomet.com

Platelet-rich plasma

Platelet-rich plasma (PRP) is obtained by centrifugation of blood to obtain blood platelets, that are subsequently mixed with thrombin and calcium chloride to form a gel.[14, 118, 126] Thrombin is a stimulator of platelet activation, as it causes a burst release of platelet contents (70% within 10 minutes), such as cytokines and growth factors, while the association of thrombin with calcium chloride ($CaCl_2$) produces a gel that slightly slowers down the release. Indeed, during the lifespan of the platelets, they continue to synthesize and secrete additional growth factors that will be released progressively thanks to the gel. Upon activation of platelets, they release their growth factors and cytokines that regulate the inflammatory phase of bone healing and subsequently modulate callus formation and bone remodeling, as well as regulate cell proliferation and differentiation.[126]
PRP therapy constitutes a cost-effective, safe, reliable, and easy method for accelerating and improving tissue healing and regeneration. Furthermore, PRP can be made from the blood of the patient, therefore eliminating the issues of immunogenicity and disease transmission related to allogenous bone grafts. In addition to the soft tissues, PRP has been used in the treatment of osteoarthritis (degradation of cartilage tissue in the joints), oral and maxillary surgery, and repair of large bone defects. However, the platelet lifespan is approximately 7 to 10 days which is less than that of bone healing. Consequently, PRP is supposed to influence early bone healing rather than late bone formation.[126] In addition, it does not present any mechanical resistance. PRP is therefore not validated as a stand-alone bone substitute, but is rather used as a supplement to other materials such as bone grafts.[118]

Growth factors

As previously mentioned, growth factors play an important role in modulating cellular activities. Indeed, growth factors bind to target cell receptors and induce an intracellular signal transduction that reaches the nucleus and determines the biological response. Since growth factors are involved in all phases of bone repair, increasing attention is brought to the use of growth factors for the treatment of bone defects. The main growth factors acting on the skeleton are fibroblast growth factor (FGF), vascular endothelial growth factor (VEGF), platelet-derived growth factor (PDGF), insulin-like growth factors (IGFs), transforming growth factor-β (TGF-β), and bone morphogenetic proteins (BMPs).[14] Considering that only BMPs, and especially BMP-2 and BMP-7, are currently used in clinics for bone regeneration, they will be presented in a separate section.

The fibroblast growth factor (FGF) family comprises 22 members that have different roles and modes of action.[127, 128] Indeed, FGFs have various biological functions that occur both in vivo and in vitro, including roles in mitogenesis, cellular migration, differentiation, angiogenesis and wound healing.[127] Among the 22 members of the FGF ligand family, it has been found that FGF-2, -9 and -18 in particular have important roles during bone development.[127, 128] FGF-2 would be the most common FGF ligand used in the regenerative medicine field including bone regeneration. FGF-2 would enhance osteoprogenitor cells proliferation and differentiation towards osteoblasts, similarly to FGF-9 and -18[127, 128], and induce angiogenesis.[128] FGF-9 would also promote chondrocyte hypertrophy and neovascularization during bone healing.[128]

Vascular endothelial growth factor (VEGF) is an important growth factor that stimulates the growth of new blood vessels as it regulates the proliferation, migration and activation of endothelial cells constituting blood vessels. VEGF therefore indirectly contributes to bone formation and regeneration as angiogenesis will bring bone-forming progenitor cells as well as nutrients, oxygen, and minerals necessary for mineralization. During endochondral bone formation and repair, VEGF would actively contribute to bone synthesis by inducing the migration of osteoblastic cells into the primary ossification center together with blood vessels, osteoclasts and hematopoietic stem cells. It would also regulate the differentiation of stem cells from bone marrow into either chondrocytes or osteoblasts.[127, 129]

Platelet-derived growth factor (PDGF) is involved in bone regeneration as it increases the numbers of mesenchymal stem cells in the defect site by recruiting them and increasing their proliferation. The bone regeneration is facilited by the initiation of mitosis in stem cells and endothelial cells, as well as the activation of osteoblasts and vascular growth directed by PDGF.[127, 130]

Insulin growth factors (IGFs) are polypeptides with high sequence similarity to insulin. Among them, IGF-I is the most abundant in skeletal tissues. IGF-I has been found to regulate the

growth, proliferation, survival, and differentiation of osteoblasts, as well as the differentiation of osteoclasts, therefore playing an important role in skeletal growth. IGF-I would also promote angiogenesis which is a key event in bone regeneration.[127, 131]
The transforming growth factor-beta (TGF-β) superfamily is comprised of over forty members that have been found to promote osteoprogenitor proliferation, early differentiation, and commitment to the osteoblastic lineage. They would be involved in endochondral and intramembranous ossification, as mice deficient of one or several TGF-β isoforms display reduced bone growth and mineralization. Finally, TGF-β signaling would play an essential role in coupling bone formation and bone resorption and maintaining normal bone homeostasis.[132]

Although growth factors present multiple interesting effects in bone growth and regeneration, their short biological half-life, lack of long-term stability and tissue selectivity, and possible toxicity and risk of tumor-promoting activity limit their therapeutic application and require controllable and sustainable delivery. Indeed, a direct injection of growth factors in soluble form into a regeneration site is generally not effective, due to rapid diffusion of growth factors away from the injection site, which can result in ectopic bone formation, which is the formation of bone in soft tissues outside the skeletal tissue. Therefore, delivery to the bone regeneration site through a carrier matrix would be more appropriate.[14, 127]

Bone Morphogenetic proteins

Bone Morphogenetic proteins (BMPs) belong to the transforming growth factor (TGF-β) superfamily. To date, over 20 BMPs have been recognized.[15, 16, 133, 134] Based on the sequence homology and the known functions, BMP family members are generally classified into four categories : BMP-2/4, BMP-5/6/7/8, BMP-9/10 and BMP-12/13/14[15, 133], while other BMPs do not have proven osteogenic properties.[133] BMPs play important roles in maintaining bone mass by inducing the differentiation of mesenchymal stem cells into osteoblasts and thus, increasing the number of mature osteoblasts.[15, 133] Among the BMPs, BMP-2, BMP-4, BMP-6, BMP-7, and BMP-9 would play more important roles in ossification.[15]
Human BMP-2 is an acidic glycoprotein with molecular weight of approximately 32 kDa and containing 114 amino acid residues. BMP-2 plays a significant role in stimulating the differentiation of mesenchymal cells into osteoblasts, and regulating the transcription of osteogenesis-related genes such as ALP (Alkaline Phosphatase), type-I collagen, osteocalcin, and bone sialoprotein genes. BMP-4 would be a stimulating factor during early stage ossification as it would cooperate with VEGF to stimulate the gather of mesenchymal stem cells, enhancing their survival capability and enlarging bone formation.[15] BMP-6 plays a role in inducing the differentiation of mesenchymal stem cells into osteoblasts and stimulating

calcification of the cellular matrix.[15] The major biological functions of BMP-7 would be to induce the differentiation of mesenchymal stem cells surrounding the bone fracture site into chondrocytes and osteoclasts, and stimulating the expression of different substances needed for induction of osteogenesis.[15] Finally, BMP-9 induces the differentiation of mesenchymal stem cells into osteoblasts and osteoclasts.[15]

As previously mentioned, among BMPs, only recombinant human BMP-2 and BMP-7 are currently used in clinics (recombinant proteins are produced by a cell whose genetic material has been modified by genetic recombination). They have been tested in several preclinical studies showing the ability to induce bone regeneration, and evaluated in clinical trials to treat various bone disorders such as non-unions (fracture that fail to heal without a surgical intervention), open fractures, and osteonecrosis.[16] The use of BMP-2 has been approved in 2002 by the European Medicines Agency (EMA) for the treatment of lumbar spine fusion and acute tibial fractures in adults. Later the same year, the American Food and Drug Administration (FDA) approved the use of BMP-2 for the treatment of open tibial fractures.[16, 17, 133] In 2007, FDA approved the use of BMP-2 for maxillary sinus and alveolar ridge augmentation to enable installation of dental implants.[17, 133] BMP-7 received official approval by EMA in 2004 for the treatment of recalcitrant long bone non-unions.[16, 17, 133] It has to be noted that BMPs are relatively soluble in aqueous media and would therefore be rapidly cleared from the defect site and diffuse into adjacent tissues if not maintained by an appropriate carrier. Several materials have been tested in pre-clinical settings for the release of BMPs, such as collagen, calcium phosphate ceramics, and synthetic polymers, but only bovine collagen based BMPs delivery devices are used in clinics (Figure 1.11).[16]

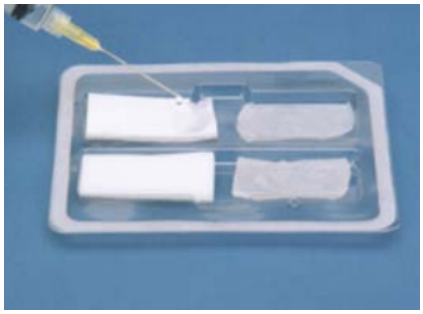

FIGURE 1.11 – Infuse^{TM} Bone graft is composed of human bone morphogenetic protein-2 applied to an absorbable collagen sponge carrier. The BMP-2 containing solution has to be applied on the collagen sponge carrier before the surgery. The collagen sponge carrier exists in different sizes. From Medtronic.com

However, the local delivery of BMPs at supra-physiological concentration can cause several complications. Considering the more intensive clinical use of BMP-2 than BMP-7, the complications related to the use of BMP-2 for bone repair are well documented.
The most recognized adverse event related to BMP-2 use is ectopic bone formation (the formation of bone in soft tissues outside the skeletal tissue).[16, 17, 133, 134] This is due to BMP-2 leakage outside the implant site, which causes multiple non-osteoblastic cells to undergo osteogenic programming when exposed to BMP-2, and therefore produce bone tissue outside of bone.[17]
As BMP-2 enhances osteoclastic activity, it might lead to osteolysis (bone resorption), and further to implant displacement or loosening.[16, 17, 133, 134] In addition, BMP-2 has also been found to promote adipogenesis, which might cause lipid deposition in the forming bone, providing bone with poor mineral quality and poor density.[17]
Local inflammation secondary to BMP-2 implantation could also cause seroma[16, 17, 134] (accumulation of blood plasma) that can be harmful depending on its location, radiculitis[16, 17] (inflammation of spinal nerve root), as well as swelling of the neck and throat tissues when used for spine fusion[17, 133, 134], resulting in compression of the airway and neurological structures of the neck, and difficulty breathing or speaking.[17] Wound complications and infection have also been reported.[16, 17, 134]
Finally, some concerns are brought about the role of BMP-2 in cancer as BMP-2 is generally upregulated in diverse tumors and is associated with tumor cell proliferation and invasion. However, there is no formal evidence yet that the use of BMP-2 increases the risk of cancer.[17, 134]

The use of BMPs in clinical applications therefore still requires optimization of the concentration and dose of BMP, to try to reduce the clinical complications related to their supra-physiological concentration, the control of BMP delivery, and the carriers used to deliver BMPs.[16, 17, 134]

1.3.4 Bone tissue engineering

It is estimated that 1.6 million bone grafts are used annually in the U.S. for degenerative diseases, injuries, tumors, and infections, accounting for approximately $244 billion, with trauma and fracture management representing almost 40% of those costs.[20] The reconstruction of damaged bone therefore constitutes an area of general interest and remains a real clinical issue, especially in the case of large bone loss. Although autografts constitute the gold standard for bone repair, they have several drawbacks such as donor site morbidity and surgical complications including pain, hemorrhage, infection, and nerve injury at the donor site.[20] To overcome that, synthetic and natural bone substitutes have been developed and

applied in clinics. However, as previously mentioned, the use of these bone substitutes alone is not sufficient to induce proper bone reconstruction. After 10 years of incorporation, as high as 60% of grafts may fail to integrate, leading to non-unions and late graft fractures.[20] Consequently, a new strategy, called tissue engineering, has emerged for tissue regeneration by trying to exploit the regenerative properties of bone physiological processes.
Tissue engineering approach is based on the combination of (1) a biocompatible scaffold that closely mimics the natural bone extracellular matrix niche, (2) osteogenic cells to lay down the bone tissue matrix, (3) signals (bioactive agents) that help to direct the cells to the phenotypically desirable type and promote sufficient vascularization to meet the growing tissue nutrient supply and clearance needs (Figure 1.12).[18, 19, 20, 21, 135, 136]

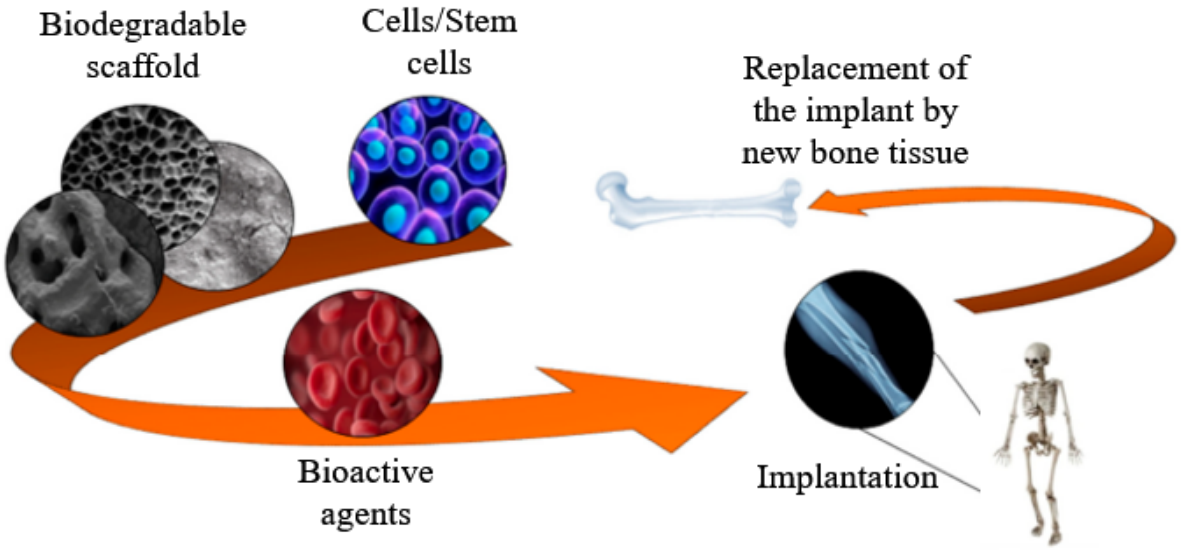

FIGURE 1.12 – Tissue engineering approach is based on the combination of (1) a biocompatible scaffold that closely mimics the natural bone extracellular matrix niche and degrades over time, (2) osteogenic cells to lay down the bone tissue matrix, (3) bioactive agents that help to direct the cells to the phenotypically desirable type and promote sufficient vascularization to meet the growing tissue nutrient supply and clearance needs.[18]

The scaffold plays a crucial role in bone tissue engineering as its purpose is to mimic the structure and function of the natural bone extracellular matrix, which can provide a three-dimensional environment to promote the adhesion, proliferation, and differentiation of cells and to have adequate physical properties, such as porosity to promote the colonization of the scaffold by cells and blood vessels, and mechanical properties for bone repair.[19, 21] The scaffold should be degradable in order to gradually degrade until the new bone tissue completely replaces it.[19, 136] Bioresorbable biomaterials investigated for bone tissue engineering are generally natural polymers (such as collagen, gelatin, silk fibroin, and chitosan), synthetic polymers (such as PLA, PGA, and PCL) and ceramics (such as hydroxyapatite, β-TCP, and bioactive glasses).[18, 19, 20, 22]

It is known that, in vivo, biochemical signals (growth factors, hormones, and cytokines), secreted locally at the injury sites, cause the migration of inflammatory and precursor cells and/or the differentiation of mesenchymal stem cells, and activation of osteoblasts and osteoclasts. Including growth factors in the scaffold, such as BMP-2, BMP-7, VEGF, PDGF, TGF-β, would greatly help in directing cell behavior to promote bone tissue and blood vessels production.[18, 20, 22, 135] In addition, physical entrapment or covalent binding to the scaffold would be an appropriate approach when a prolonged, more controlled, or on-demand release of the growth factor is required[21], and might be more efficient than the collagen sponges loaded with BMP-2 already used in clinics.

Osteoblasts being regulators of bone deposition, modeling, and remodeling, they represent an excellent cell source for a successful cell-based skeletal treatment. In addition, the risk of rejection of the tissue engineered construct might be reduced by using autologous cells (cells of the patient).[21] However, technical difficulties associated with their harvesting, expansion into meaningful numbers and phenotypic maintenance undermine the benefits of using primary cells. Consequently, various types of stem cells (embryonic stem cells, induced pluripotent stem cells, mesenchymal stem cells) have been largely proposed as a viable and easy source of osteoblast progenitors during the creation of engineered bone implants.[20] Among them, mesenchymal stem cells are highly studied, as they are directly involved in bone formation and regeneration. The recruitment of endogenous MSCs (MSCs from the body) to bone defect sites could be triggered by local injection of growth factors or implantation of a scaffold carrying growth factors. In such cases, the ex vivo MSC manipulation, that can affect their phenotypic and molecular profiles, would not be required. However, in some cases the recruitment of endogenous MSCs might not be adequate as the MSC functionality has been shown to be affected by intrinsic factors such as patient's pathological conditions. For example, patients with non-unions (fracture that fail to heal without a surgical intervention) were shown to exhibit a decreased pool of bone marrow MSCs, as well as changes in the serum levels of hormones and growth factors required for MSCs recruitment and proliferation.[20] The combination of MSCs to the scaffold carrying growth factors therefore seems to be a better approach to effectively stimulate bone regeneration.

Finally, if the tissue engineered construct could be directly implanted into the body, the use of bioreactor cultivating systems for three dimensional cell-scaffold constructs has been proposed to achieve homogeneous bone tissue development at clinically relevant sizes. By enabling reproducible and controlled changes of specific environmental factors (pH, temperature, pressure, nutrient supply and waste removal), bioreactors would allow for automated and standardized tissue manufacturing.[135]

Although tissue engineering constitutes a promising approach for the regeneration of damaged tissue, including bone, many challenges remain to be elucidated in order to translate tissue engineering from the laboratory to the clinics. For example, vascularization remains a challenging technical obstacle in bio-fabrication that has prevented the development of clinically successful engineered constructs.[21] In addition, it is recognized that several factors contribute to mediating cell-material interaction. A major challenge is therefore to elucidate the cellular and molecular mechanisms of stem cell actions in bone defect therapeutics, as well as optimize cell-material interactions in order to guide cell behavior and obtain the desired cell response for bone reconstruction.[20, 21, 22]

Chapter 2

Mesenchymal stem cells and hydrogels for bone repair

This chapter presents different types of stem cells that can be used for bone tissue engineering, with a particular focus on mesenchymal stem cells (MSCs). Then, the use of MSCs in various clinical applications and their limitations is mentioned. Subsequently, the influence of the in vitro culture conditions of MSCs on their osteogenic differentiation is discussed. Finally, hydrogels are presented as a better platform for cell culture and for the understanding of cell-material interactions, that is crucial for the development of effective strategies for bone regeneration, as compared to the traditionally used materials (plastic, glass...).

2.1 Stem cells as a new strategy for bone repair

One key element of current research is to use the cells of the patient to regenerate defective or missing organs. To regenerate bone, the first strategy would therefore be to directly collect and use pre-differentiated cells (preosteoblasts) or osteoblasts. This would allow to quickly obtain functional bone cells synthesizing extracellular matrix. However, similarly to bone collection for a bone graft, bone cells collection can cause complications at the collection site. In addition, osteoblasts proliferation remaining limited, it is difficult to obtain the high number of cells needed to regenerate an important bone fragment.[20, 23, 24] In this context, stem cells constitute promising candidates for tissue engineering and regenerative medicine. Stem cells are undifferentiated cells that can, under particular conditions, differentiate into specialized cell types.[3]

2.1.1 Embryonic stem cells

Embryonic stem cells (ESCs) are pluripotent stem cells, i.e. cells that have the ability to undergo self-renewal and to give rise to all cells of the tissues of the body[137], which makes them highly attractive for regenerative medicine in general. Indeed, because ESCs are pluripotent, with high proliferative activity, they can potentially be used as a single source for the derivation of multiple lineages present in adult bone, including osteogenic cells, vascular cells, osteoclasts, and nerve cells for bone regeneration.[135] There have been multiple studies demonstrating that human ESCs treated with osteogenic factors (β-glycerophosphate, ascorbic acid and dexamethasone) undergo differentiation toward an osteogenic lineage.[20, 135] However, ESCs require complex proliferative culture conditions, including various growth factors, feeder cell layers (layer of cells unable to divide, which provides extracellular secretions to help another cell to proliferate), specific culture media and/or coated culture plates.[20, 135] In addition, their use in research and clinics is limited, or even prohibited, due to ethical considerations, for human embryos. Furthermore, their implantation can lead to an immune response of the patient, as the cells come from another individual, or to tumor formation when they are cultivated in vitro and implanted in vivo.[3, 20, 135]

2.1.2 Induced pluripotent stem cells

Induced pluripotent stem cells (iPSCs) constitute an ethical alternative to embryonic stem cells. iPSCs are pluripotent stem cells that are artificially derived from a non-pluripotent cell via the induction of a "forced" expression of specific genes.[135] iPSCs were first produced from mouse fibroblasts by retroviral delivery of four transcription factors (Oct4, Sox2, Klf4, and Myc) in 2006, which induced a pluripotent state comparable to ESCs.[20, 135] The reprogrammed cells can even be those of the patient to avoid any immune response.[3, 20, 138] However, the reprogramming efficiency is quite low and the expansion time of the cells is high. In addition, their use in clinics is still limited due to the little knowledge and hindsight about their handling and behavior.[3, 20, 138] For example, the potential formation of teratomas (tumors formed by pluripotent cells that differentiate into cells that produce mature tissues in inappropriate places in the body) after implantation of iPSCs is of clinical concern.[20, 135] Additional research is also needed to determine the best starting cell for iPSC generation for human clinical applications.[135]

2.1.3 Mesenchymal stem cells

Adult stem cells therefore constitute an alternative to ESCs and iPSCs. Adult stem cells can be found in various adult tissues but have a limited differentiation capacity. They are highly used for regenerative medicine as they can be extracted from the patient, cultivated in vitro, exposed to the appropriate factors to direct their differentiation, and implanted to the patient without any immunogenicity considerations.[3]

Mesenchymal stem cells are adult multipotent stem cells that can differentiate in vivo into mesoderm-type cells such as osteoblasts (bone cells), chondrocytes (cartilage cells), and adipocytes (fat cells) (Figure 2.1).[25] In addition, MSCs differentiation into other cell types such as neurons, smooth muscle cells and hepatocytes has also been reported when the cells were cultured in vitro.[25] MSCs can be isolated from many different tissues such as bone marrow, adipose tissue, dental pulp, skeletal muscle, skin, umbilical cord blood, cartilage, and others.[26]

Bone marrow-derived stem cells (BMSCs) are currently the most commonly utilized and researched source of adult mesenchymal stem cells due to their relatively easy harvesting, high proliferative capacity, and established regenerative potential.[20, 27] In addition, orthopedic surgeons might be more comfortable with the concept of using marrow-derived MSCs because cancellous bone is frequently used as autograft material in bone regeneration.[27] Nevertheless, some studies are conducted on the comparison of MSCs from different sources and tend to show that the frequency of MSCs in adipose tissue would exceed the frequency of MSCs in bone marrow.[139, 140, 141] In addition, bone marrow MSCs would have similarities in capacity for multilineage differentiation and secretion of bioactive factors with MSCs from adipose tissue[142, 143] or cartilage[143] for example. Han et al. also showed that bone marrow MSCs and adipose tissue MSCs have almost the same bone regeneration ability for the repair of rabbit cranial defects.[144] However, contradictory results have also been obtained, showing that MSCs from adipose tissue may have an inferior potential for both osteogenesis and chondrogenesis as compared to bone marrow MSCs.[145] Therefore, there are still no clear guidelines indicating which sources of MSCs are the most suitable for bone regeneration.

Finally, MSCs can also be obtained from the reprogramming of iPSCs. This strategy presents several advantages as iPSCs can be easily generated in sufficient quantities from skin-derived fibroblasts for example, and they present a high therapeutic potential regardless of the donor's age, which is not the case for bone marrow or adipose tissue MSCs, as iPSCs undergo rejuvenation when they are reprogrammed.[141] Nevertheless, more studies are required to evaluate the therapeutic potential of MSCs obtained from iPSCs derived from various origins in order to treat specific diseases.[141]

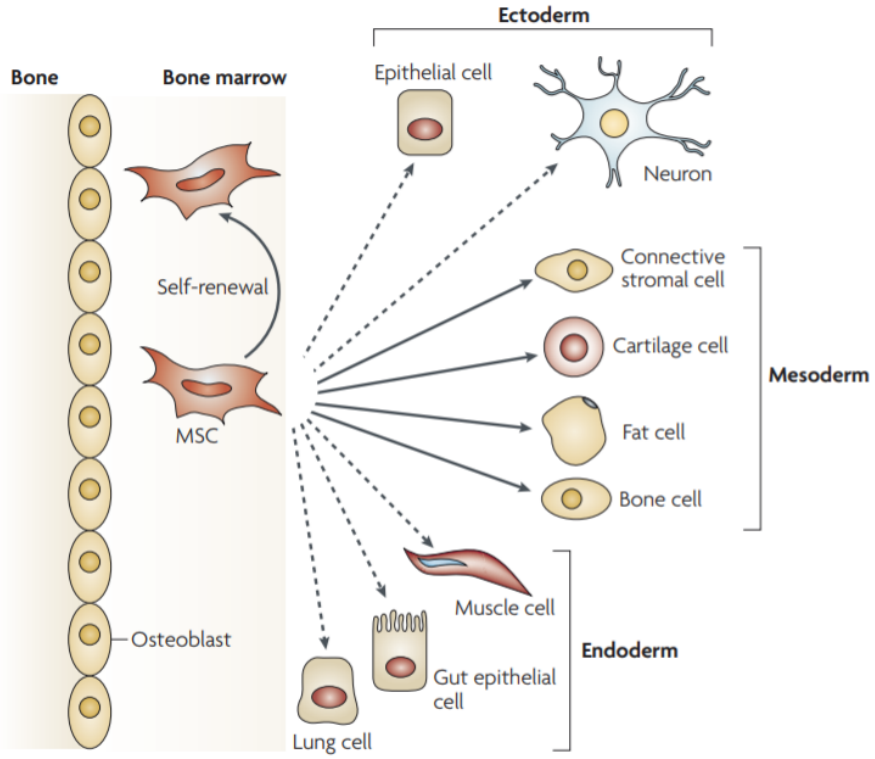

FIGURE 2.1 – Bone marrow MSCs have the ability to self-renew and differentiate into mesoderm type cells. They would also have the ability to differentiate into other cell types when cultured in vitro.[25]

Even though human mesenchymal stem cells can be extracted from different tissues, they are all defined by expression of CD73, CD90, and CD105, by lack of expression of a series of other cell surface markers such as CD11b, CD34, and CD45, by a fibroblastoid appearance (spindle-shaped cells), and trilineage differentiation potential to generate chondrocytes, osteoblasts, or adipocytes.[26]

MSCs osteogenic differentiation goes through different stages (Figure 2.2). MSCs are first in a proliferative phase as they engage to pre-osteoblastic cells. Then, pre-osteoblasts mature into osteoblasts that stop proliferating, and are involved into secretion, maturation, and mineralization (calcium deposition) of the extracellular matrix (ECM). Once the ECM is formed, osteoblasts can be embeded in the matrix and become osteocytes, or they can become inactive cells that constitute a bone coating (bone lining cells), or else they can die by apoptosis.[2, 4, 28, 29]

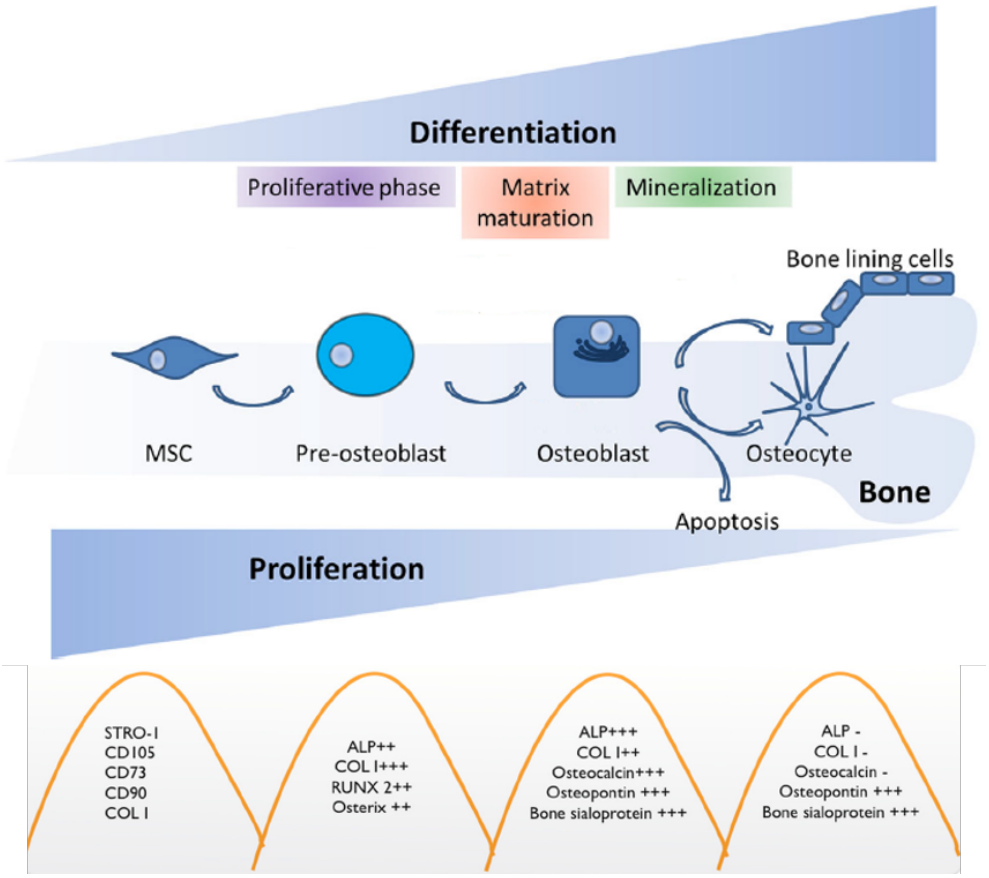

FIGURE 2.2 – Stages of MSCs osteogenic differentation and expression of differentiation markers. Adapted from [29, 146]

During the differentiation, the shape of the cells is found to vary. MSCs are long and narrow cells, while osteoblasts are known as cuboidal cells, and osteocytes present a star-like shape (Figure 7.5). Indeed, during the transition from osteoblasts to osteocytes, the cells undergo a dramatic transformation from a polygonal cell to a cell with a reduced cytoplasmic volume and extending dendrites.[147, 148]

As previously mentioned, bone formation is induced by MSCs condensation, with cells forming three-dimensional structures called bone nodules. These nodules are generated by the proliferation and condensation of osteoprogenitors, which further differentiate into osteoblasts. Subsequently, the cells forming the nodule start producing the extracellular matrix, before mineralizing it. At the beginning, these nodules are formed of 5 to 35 cells.[149] Their size and thickness increase as a function of time and differentiation, although this increase is not infinite. After 20 days, bone nodules are constituted of approximately a hundred of cells, with a thickness of 70 to 100 μm. However, the in vitro observation of these nodules is far from being systematic.[149] Indeed, many parameters have been found to influence bone nodules formation, including the donor's health status, gender, and age, the cell harvesting protocol, and the properties of the culture substrate, such as its topography and composition.[149]

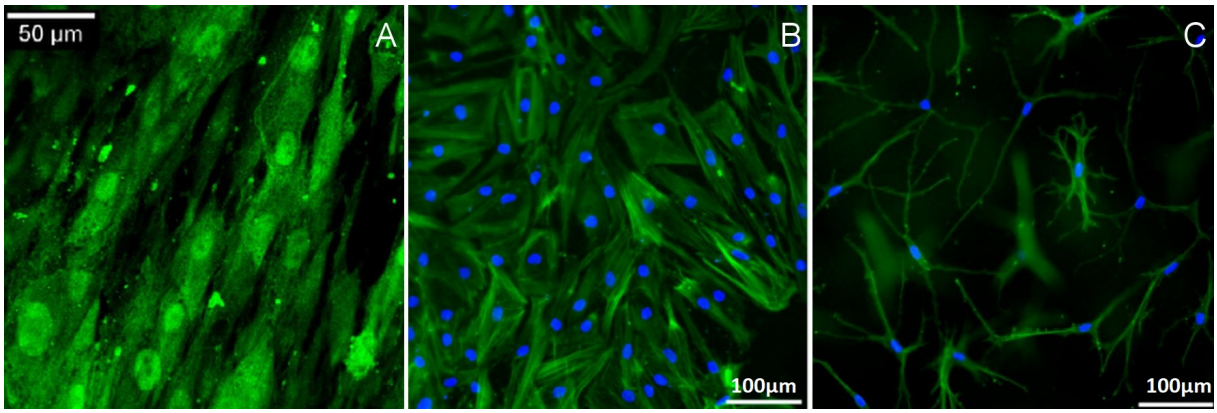

FIGURE 2.3 – Fluorescence microscopy images of cells at different stages of osteogenic differentiation. Cytoskeleton in green, nucleus in blue. A. Human MSCs are long and narrow cells.[150] B. Human osteoblasts are cuboidal cells.[98] C. Human osteocytes have a star-like shape.[29]

Specific factors and proteins are also expressed by the cells at the different stages of differentiation (Figure 2.2). The main factors and proteins used to evaluate MSCs osteogenic differentiation are listed below.

The markers STRO-1, CD105, and CD90 are cell surface proteins expressed by MSCs.[26]

Runx-2, also called Cbfα1, and Osterix are proteins that play the role of transcription factors, which means that they regulate the transcription of specific genes, which are associated with the osteogenic differentiation in their case. Runx-2 has been identified as an important differentiation regulator in the osteoblast lineage, as an inactivation of Runx-2 in mice leads to a delay in osteoblast differentiation, or even to the absence of osteoblasts. Runx-2 is expressed at high levels in osteoblasts, as well as in all mesenchymal condensations that form to become bone. Osterix is an osteoblast differentiation transcription factor that is expressed specifically in osteoblasts.[113]

The markers collagen I (COL1), osteopontin (OPN), osteocalcin (OCN), and bone sialoprotein (BSP) are proteins produced by osteoblasts and constituting the extracellular matrix, as previously mentioned.[111]

Alkaline phosphatase (ALP) is an enzyme involved in the ECM mineralization. ALP is expressed in early development of bone and calcifying cartilage. Human ALP is categorized into four groups, depending on where they are predominantly expressed, with the tissue-non specific alkaline phosphatase being found in hypertrophic chondrocytes and osteoblasts cell membranes. During mineralization, ALP hydrolyzes extracellular inorganic pyrophosphate to supply inorganic phosphate for hydroxyapatite production.[151, 152]

The markers E11, dentin matrix protein (DMP1), and sclerostin (SOST) are proteins expressed by osteocytes.[153] E11, also called podoplanin, is a transmembrane glycoprotein and is the earliest osteocyte-selective protein to be expressed as osteoblasts differentiate into osteocytes.[147, 148] E11 is distributed along the osteocyte cell body and along the dendritic

processes of the osteocyte,[154] and it has been found to play a role in dendrite formation in osteocytes.[147, 154] These markers present different levels of expression depending on the differentiation stage of the cell (Figure 2.4).[5] While E11 and DMP1 are early osteocyte markers, sclerostin is expressed by mature osteocytes.[5] Nevertheless, the knowledge about the transition of osteoblasts towards osteocytes is mainly based on in vivo observations from the staining of histological sections. In addition, the in vitro study of osteocytes is still challenging as isolating osteocytes from bone is a complex process, leading to very low yields, high cell heterogeneity, and cells that may not express markers normally found in osteocytes, such as sclerostin.[155, 156]

A

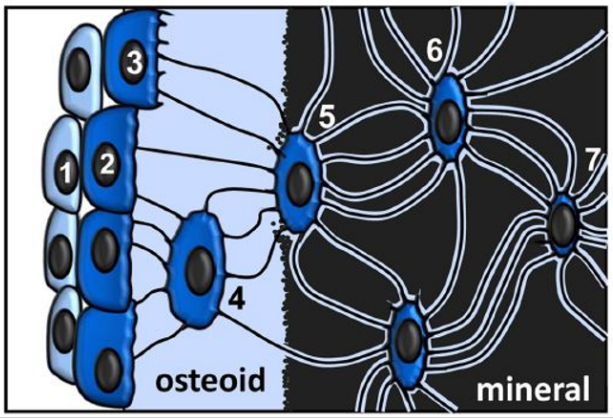

B

	1	2	3	4	5	6
RUNX2	+	+	-	-	-	-
OCN	-	+	+	+	+	-
E11	-	-	+	+	+	-
DMP1	-	-	+	+	+	+
PHEX	-	-	+	+	+	+
MEPE	-	-	-	+	+	+
Sclerostin	-	-	-	-	-	+
CapG	-	-	+	+	+	+
ORP150	-	-	-	-	-	+

FIGURE 2.4 – A) Schematic diagram depicting the transitional stages that occur as osteoblasts differentiate into mature osteocytes. During this process, the volume of the cell body and the number of cell organelles decreases. 1=preosteoblast; 2=osteoblast; 3=embedding osteoblast; 4=osteoid osteocyte; 5=mineralizing osteocyte; 6, 7=mature osteocytes. C) Table illustrating the relative temporal expression of various osteogenic markers during the in vivo transition from osteoblast to osteocyte as depicted in A). RUNX2 directs early osteoblast differentiation and is expressed in both preosteoblasts and osteoblasts. OCN is expressed by mature osteoblasts and early osteocytes. E11 is the earliest osteocyte marker to be expressed during differentiation, but is not found in mature osteocytes in vivo. DMP1, CapG and MEPE expression is observed in mineralizing and mature osteocytes, whereas sclerostin expression is confined to mature osteocytes. Adapted from [5]

2.1.4 The use of mesenchymal stem cells in clinics

Mesenchymal stem cells have attracted much attention from researchers for their therapeutic potential, mainly due to four unique properties. Firstly, their ability to migrate to sites of inflammation following tissue injury when injected in the body, although the precise mechanisms by which MSCs are able to migrate to and engraft in sites of injury remain not fully understood. Secondly, their ability to differentiate into various cell types, which has

prompted studies using transplanted MSCs to replace damaged or injured cells. Thirdly, their ability to secrete multiple bioactive molecules (growth factors, cytokines, chemokines) capable of stimulating recovery of injured cells and inhibiting inflammation. And finally, their lack of immunogenicity and ability to perform immunomodulatory functions, as they could interact with and modulate various types of immune cells.[30, 31]
In 2014, there were 425 clinical trials involving the use of MSCs, with 76% of them using autologous MSCs. With regard to MSC type, bone marrow MSCs were the most used. The main diseases applying MSCs for treatment were bone/cartilage disease, heart disease and graft-versus host disease.[30] MSCs have been tested clinically for several regenerative approaches in the skeletal system including osteoarthritis (deterioration of the protective cartilage at the end of bones), non-union fractures, osteoporotic fractures, bone necrosis, leg length inequality, and osteodysplasia (abnormalities of bone growth) (Table 2.1).[30, 31] In these clinical trials, MSCs are generally administered by injection of MSC-enriched bone marrow aspirate or injection of ex vivo expanded MSCs. They can also be loaded into various biomaterials (calcium phosphate ceramics or collagen sponges) that will subsequently be implanted.[30]

Pathology	**Cell source**	**Clinical trial phase**	**Number of patients**	**Route of administration**
Osteoarthritis	Autologous BM-MSCs	I/II	30	Intra-articular injection
Osteoarthritis	Umbilical cord MSCs	III	104	Cartilage tissue lesion injection
Knee Osteoarthritis	Autologous BM-MSCs	I	6	Not mentioned
Hip Osteoarthritis	BM-MSCs	I	6	Intra-articular injection
Non-union fracture	BM-MSCs	II	19	Non-union site injection
Osteoporotic fracture	Autologous AD-MSCs	II	8	Implanted at the bone void
Tibial fracture	Autlogous BM-MSCs	I/II	24	Implanted at the fracture site
Osteonecrosis of the femoral head	Autologous BM-MSCs	/	50	Femoral head injection

TABLE 2.1 – Examples of clinical trials involving MSCs administration for bone repair. BM-MSCs = bone marrow derived MSCs, AD-MSCs = adipose tissue derived MSCs. Adapted from [30]

In addition to their differentiation potential, MSCs also influence the immune response by modulating all types of immune cells.[32] This aspect makes them very attractive for various clinical applications. Indeed, many clinical trials have been conducted with MSCs

to treat various pathologies, and some examples are presented in Table 2.2. Osteogenesis imperfecta, also called "brittle bone disease", is a genetic disease causing an alteration of type I collagen produced by osteoblasts, and resulting in bones fragility and deformation.[33] GvHD, or Graft versus Host Disease, is a complication that may occur for patients that receive a tissue transplant. The immune cells of the implanted tissue recognize the patient as being another individual and therefore react against him (contrary to graft rejection for which the immune cells of the patient react against the implanted tissue).[33] Myocardial infarction is caused by an obstruction of an artery resulting in the necrosis of cardiac tissue. Thanks to their immunomodulatory abilities, MSCs would favor cardiac tissue repair.[33] Lupus erythematosus is an auto-immune disease, which means that the immune system of the patient is turning against him.[33]

Pathology	**Clinical trial phase**	**Number of patients**	**Route of administration**
Osteogenesis imperfecta	I	6	Intravenous
Osteogenesis imperfecta	I	1	In utero
Cartilage defect	I	24	Intra-articular cartilage
GvHD	II	55	Intravenous
GvHD	II	32	Intravenous
GvHD	II	37	Intravenous
Myocardial infarction	I	69	Intra-coronary
Myocardial infarction	I	53	Intravenous
Lupus erythematosus	I	15	Intravenous

TABLE 2.2 – Examples of clinical trials involving bone marrow MSCs for their immunomodulatory behavior. The administered MSCs were coming from a donor different from the patient. Adapted from [33]

Currently, different MSC-based products have been approved by several countries for the treatment of different diseases such as degenerative arthritis, myocardial infarction, GvHD, and reconstruction of skeletal defects.

CARTISTEM, is a combination of human umbilical cord MSCs and sodium hyaluronate which is intended to be used as a therapeutic agent for cartilage regeneration in cartilage defects of the knee.[32]

CardioRel is an autologous product designed for patients suffering from myocardial infarction that provides mesenchymal stem cells for cardiac regeneration. Hearticellgram-AMI are bone marrow-derived MSCs used to treat acute myocardial infarction through intracoronary injection.[32]

Trinity Evolution is an allograft of cancellous bone containing viable adult stem cells and osteoprogenitor cells within the matrix and a demineralized bone component. Trinity Evolution is intended for the treatment of musculoskeletal defects.[30, 32] Osteocel Plus

is made from bone matrix that retains its native bone forming cells, including MSCs and osteoprogenitors. Osteocel Plus is intended for the repair, replacement, and reconstruction of skeletal defects.[30, 32] AlloStem is partially demineralized allograft bone combined with adipose derived MSCs.[32]
Prochymal is the first stem cell therapy approved for use in Canada for acute GvHD. It is an allogeneic therapy based on MSCs derived from the bone marrow of adult donors.[32]

However, the current knowledge is not sufficient to predict the action of MSCs for the treatment of these different pathologies. In addition, it has been reported that the quality and therapeutic efficacy of MSCs depend on several parameters such as the isolation and culture methods, as well as the age, genetic traits, and medical history of the donor.[157, 158] For example, freshly isolated cells and cells from younger donor would have better performance than in vitro cultured cells or cells from older donor.[157] Many questions remain also unanswered regarding the safety of using MSCs as a therapy.[32] Considering that the most common method of administration of MSCs is intravenous infusion, the majority of the cells are trapped within capillaries of various organs, especially in the lungs, before the cells reach their target. Therefore, only a small fraction of the injected cells will reach the lesion site. Furthermore, this route of delivery can cause occlusion of small blood vessels and pulmonary embolism due to the accumulation of cells in the lung region.[157] Multiple studies would also suggest that besides the potential effect of MSCs on tissue regeneration, these cells may also be significantly involved in the process of heterotopic ossification (ectopic bone formation).[158] The risk associated with tumorigenesis after stem cell transplantation is also widely discussed in the literature. Some data indicate that MSCs can be associated with tumor progression by the secretion of proangiogenic factors, while other studies suggest that factors secreted by MSCs may have antitumor properties. The implication of MSCs in tumorigenesis would depend on the type of tumor, the method of culture, cell heterogeneity, dose, secreted molecules, and probably many other factors.[157] Although MSCs present a great therapeutic potential for the treatment of various diseases, the optimal dose, the route of cell administration, and protocols for MSC isolation and ex vivo preparation are still to be optimized.[158]
For bone regeneration purposes, the aim would be to make MSCs evolve into osteoblasts, whether they would be injected or implanted into a scaffold, since only they are capable of recreating bone matrix. However, the in vivo bone regeneration mechanisms involving MSCs being still poorly understood, it is difficult to obtain and maintain a stable cell phenotype in vitro. Once extracted and cultivated in vitro to make them proliferate, MSCs tend to differentiate randomly, which leads to a heterogeneous population of cells.[3, 33, 34] It is then complicated to use this heterogeneous population of cells for the reconstruction of any tissue. Although several techniques, such as magnetic-activated cell sorting and flow cytometry sorting, could be used to sort the cells and keep only a defined cell population, most of these methods have not gained widespread acceptance so far because of the high expense, technical difficulties,

and great damage to cells.[159] Research therefore aims at developing techniques allowing to control MSCs differentiation and to obtain a homogeneous cell population (differentiated cells or cells that maintain ther stemness). This goes through the study of the impact of many different parameters on MSCs differentiation, also trying to identify the cellular mechanisms involved.

2.2 The influence of the culture conditions on mesenchymal stem cells osteogenic differentiation

2.2.1 Culture medium

Once the cells are extracted from their in vivo environment, they are cultivated in vitro under the appropriate conditions for their survival and proliferation. Basic environmental requirements for cells to grow optimally include controlled temperature, a substrate for cell attachment (if the cells are adherent cells, which is the case for MSCs), and appropriate growth medium. Cell culture media generally comprise amino acids, vitamins, inorganic salts, glucose, and serum as a source of growth factors, hormones, and attachment factors. In addition to nutrients, the medium also helps to maintain pH and osmolarity. Depending on its formulation, the culture medium can also direct the differentiation of MSCs towards a particular lineage. If growth factors such as those mentioned in the first chapter can be added to the culture medium to direct MSCs osteogenic differentiation, the addition of small natural or synthetic molecules is more conventional as they are easier to obtain, they can be manufactured at a low cost, and they exert their effects in a potent, rapid and reversible way.[160] As such, osteogenic differentiation culture media generally include dexamethasone, ascorbic acid, and β-glycerophosphate to induce osteogenesis of bone marrow MSCs in vitro.[160, 161, 162] Ascorbic acid was found to initiate the formation of a collagenous extracellular matrix, which further leads to the upregulation of alkaline phosphatase and osteocalcin. Dexamethasone promotes cell proliferation, ALP activity and mineral deposition. While β-glycerophosphate provides a high concentration of phosphate ions for mineralization.[160, 161, 162]

For example, Nishimura et al. showed that growth medium supplemented with 50 nM dexamethasone, 0.2 mM ascorbic acid, and 10 mM β-glycerophosphate leads to a higher expression of ALP of human bone marrow MSCs after 7 and 14 days, so a higher osteogenic differentiation, as compared to basic growth medium.[163] If the addition of these molecules can affect MSCs differentiation, their concentration can also be an important factor to consider. Honda et al. developed a systematic and computational approach for designing cocktails of different factors with varying concentration with the aim to stably achieve osteogenic commitment of mouse and human bone marrow MSCs. The tested cocktails contained

ascorbic acid, calcitriol (the active form of vitamin D), BMP-2, heparin, dexamethasone, and β-glycerophosphate with varying concentration. Among 100 tested cocktails with mouse MSCs, only 14 cocktails demonstrated in vitro calcium precipitation within 7 days, achieving greater than 50% of the calcium precipitation of the reference medium containing 50 mM ascorbic acid, 10 mM β-glycerophosphate, 100 nM dexamethasone, and 100 ng/ml BMP-2. Two cocktails were selected for further investigation (m4 and m8, Table 2.3). The reference medium and the two cocktails induced the early expression of Runx-2 and Osterix at day 1 and the delayed expression of osteocalcin at day 7, confirming the osteogenic fate of mouse MSCs. However, it has been observed that the reference medium and the cocktail m8 induced in vitro calcium deposition of human MSCs after 15 days, while the cocktail m4 did not.[164] These findings tend to show that there is no unique culture medium composition to direct MSCs osteogenic differentiation. In addition, the effects of a particular composition can vary between different species. Moreover, there are probably many synergies that exist between these molecules and that are not fully understood. For example, Hildebrandt et al. showed that supplementing the culture medium with 10^{-8} M of dexamethasone promoted umbilical cord blood MSCs mineralization only in combination with BMP-2 (10^{-7} M), while a concentration of 10^{-7} M dexamethasone led to a high amount of mineralization and expression of collagen-I independently of BMP-2 addition.[165] Finally, it can be seen from these examples that the concentration of dexamethasone, ascorbic acid, and β-glycerophosphate used might significantly vary between the studies, which constitutes a limitation to compare the results.

Chemical factor	**Differentiation medium**	**m4 cocktail**	**m8 cocktail**
Ascorbic acid (μM)	50	50	50
Vitamin D (nM)	0	0	0.08
BMP-2 (ng/mL)	100	12.5	0.39
Heparin (μg/mL)	0	0	0.39
Dexamethasone (nM)	100	0.39	200
β-glycerophosphate (mM)	10	10	10

TABLE 2.3 – Culture medium containing various cocktails of osteogenic factors to promote mouse and human MSCs osteogenic differentiation. Adapted from [164]

One way to standardize the experiments could be to use commercially available osteogenic differentiation medium. Nevertheless, their composition is generally secret and they might not all have the same efficiency in directing MSCs osteogenic differentiation as shown by Okajcekova et al. By comparing three different commercial osteogenic differentiation media, they showed that one medium, that had the particularity to be exempt of animal serum supplement, led to a stronger calcium mineral deposition of dental pulp MSCs as compared to the two other osteogenic media or to growth medium (Figure 2.5).[166] Other factors,

such as the source of serum, might influence MSCs differentiation. While fetal bovine serum (FBS) is routinely used for cell culture, Popov et al. demonstrated that human serum led to higher expression of ALP than FBS in human bone marrow MSCs, even in the absence of any osteogenic supplement.[167] Finally, even though various compositions of culture medium have shown to guide and enhance MSCs osteogenic differentiation, it is not certain that the differentiation is homogeneous between the cells or that the cells have reached the osteoblast stage. Consequently, although osteogenic culture medium might guide MSCs towards the osteogenic commitment, it is not possible to only rely on the use of osteogenic culture medium to control MSCs osteogenic differentiation.

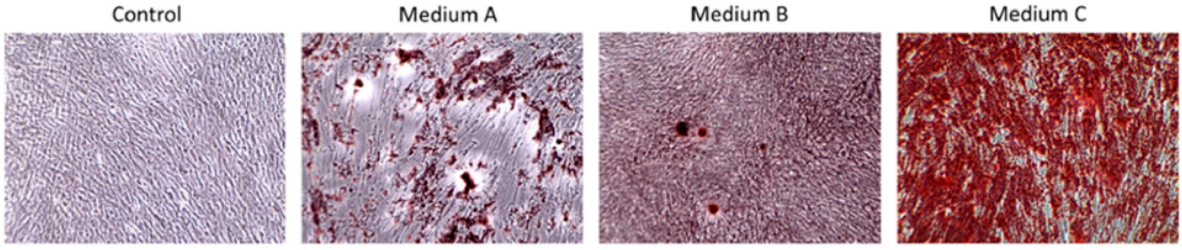

FIGURE 2.5 – Alizarin red staining for the evaluation of calcium deposition during osteogenic differentiation of dental pulp MSCs exposed to different culture media for 15 days. Control group was cultured in basic growth media. The culture media A, B, and C were commercial osteogenic differentiation media from different companies : Medium A) StemPro Osteogenesis Differentiation Kit (ThermoFischer, USA), Medium B) Mesenchymal Stem Cell Osteogenic Differentiation Medium (PromoCell, Germany) and Medium C) OsteoMAX-XFTM Differentiation Medium (Sigma-Aldrich, USA). The culture medium C led to strongest calcium deposition. Magnification 100x. Adapted from [166]

2.2.2 Number of passages and age of the donor

Passaging, or subculturing, of cells is a procedure wherein cells from a given culture are divided into new cultures and fed with fresh culture medium to allow further expansion of the cells. Due to the rareness and high heterogeneity of freshly isolated MSCs, extensive in vitro passage is required to expand their populations prior to clinical use. However, several studies have shown that long-term in vitro culture of MSCs might alter their proliferation and differentiation potential. Twenty years ago, Banfi et al. indicated that, after in vitro culture, the population of expanded human bone marrow MSCs progressively lost their ability to proliferate and differentiate in multiple mesenchymal lineages, already after passage 1 or 2.[168] More recently, Yang et al. found that human bone marrow MSCs had a reduced proliferative capability when increasing the passage number, but this effect was observed after passage 3 or 5 depending on the culture medium used. They also observed that MSCs maintained their normal spindle shape in the early passages up to passage 5, but exhibited irregular flattened geometry and

enlarged size at later passages. Finally, the number of passages also affected MSCs osteogenic differentiation capacity as the intensity of calcium staining increased over time in the cultures at passage 4, while calcium deposition was not detectable in the cultures at passage 8.[169] Similar results were obtained for rat bone marrow MSCs as the cells had a uniform spindle shape till passage 3, while they presented more flatten, larger, and polygonal phenotypes at higher passage. The doubling time of cells at passages 1-3 was within 20-30 hours, whereas passage 5 showed an extreme doubling time of 130 hours. Cells at passage 5 were also found to express a senescence marker, indicating a possible degradation of the functional characteristics of the cells, while cells at passage 2 did not express this marker.[170]
Some studies also highlighted that MSCs proliferation and differentiation could be affected by both the age of the donor and the number of passages. Kretlow et al. showed that mouse bone marrow MSCs adhesion and proliferation was decreasing as the age of the donor was increasing (6-day-old, 6-weeks-old, and 1-year-old mice). A decreased osteogenic potential was also found with increased donor age. Finally, no significant differences in osteogenic potential for cultures at different passages were found for old donors (6-week-old and 1-year-old mice), while the osteogenic potential was reduced between passage 1 and 6 for young donors (6-days-old mice).[171] Zaim et al. found that human bone marrow MSCs harvested from adult donors (25-50 years) stopped proliferating at about passage 15, MSCs from old donors (over 60 years) stopped proliferating at passage 7, while cells from child donors (0-12 years) reached their maximal life span at passage 24. Similarly, MSCs from child, adult, and old donors gradually lost their fibroblast like morphology and started to gain an irregular and flat shape when they were at passage 15, 9, and 5, respectively. In addition, they demonstrated that a great number of MSCs lost their osteogenic differentiation potential due to increasing donor age.[172] These results are in agreement with the observations made by our team, as Pedrosa et al. showed that human bone marrow MSCs from young (36 years old) or old (65 years old) donors had markedly different responses to varying nanotopographies. In addition, the population of cells from the old donor exhibited a more heterogeneous expression of osteogenic differentiation markers.[105]

2.2.3 Cell seeding density

In addition to culture medium, number of passages, and age of the donor, the initial cell seeding density would also have an impact on MSCs proliferation and differentiation. It is believed that starting with a low cell seeding density and gradually increasing it, until reaching an optimal cell seeding density, would enhance cell functions and biosynthesis due to cell-cell interactions, increased intercellular signaling via endogenous signal molecules, and increased secretion of ECM by neighboring cells which helps other cells to attach. However, once the cell seeding density exceeds the optimal density, contact-inhibition via intercellular communication

between adjacent cells starts to suppress cell proliferation. In addition, limited nutrients to be shared by many more cells, hypoxia of overly crowded cells, and insufficient waste removal, results in a decrease in cell function.[173] Several studies have evaluated the impact of MSCs seeding density on their proliferation and differentiation potential. Nevertheless, they can lead to very different results depending on the source of the cells (human cells or animal cells), the material used for cell culture, and the dimensionality of the culture system (two-dimensional or three-dimensional cell culture).

In two-dimensional systems, the studies of Kim et al. and Luo et al. both showed that increasing rat bone marrow MSCs seeding density leads to a decrease in the cells proliferation rate.[174, 175] Regarding their osteogenic differentiation, Luo et al. showed that a moderate initial cell seeding density (10,000 cells/cm^2) promoted a higher osteogenic differentiation than lower (5,000 cells/cm^2) or higher (25,000 and 50,000 cells/cm^2) density, when the cells were cultivated on composite nanofibers made of molybdenum disulphide and polyacrylonitrile.[175] While Kim et al. observed that late stage osteogenic differentiation was enhanced for higher cell seeding density (150,000 cells/cm^2), while cell proliferation and early osteogenic differentiation were stimulated by lower cell seeding density (30,000 cells/cm^2), when the cells were cultivated on poly(propylene fumarate).[174] When studying human bone marrow MSCs, Eyckmans et al. found that a high seeding density (80,000 cells/cm^2) resulted in a higher expression of osteogenic genes after two weeks as compared to lower seeding densities (5,000 and 25,000 cells/cm^2), when the cells were cultivated in classical plastic well-plates (Figure 2.6 part i).[176] However, these results contradict the study of McBeath et al. which demonstrated that human bone marrow MSCs osteogenic differentiation was favored at low cell seeding density (1,000 and 3,000 cells/cm^2), while adipogenic differentiation was favored at high cell seeding density (21,000 and 25,000 cells/cm^2) (Figure 2.6 part ii).[177] Finally, Bhat et al. reported that human bone marrow MSCs cultured with the seeding densities of 1,000 and 5,000 cells/cm^2 demonstrated equivalent cell yield and viability, surface marker expression, as the expression of positive MSCs markers (CD73, CD90 and CD105) was more than 90% and that of negative markers (CD34, CD45) was less than 5%, and equivalent tri-lineage differentiation potential.[178] All the studies presented in this section used osteogenic differentiation medium to direct MSCs osteogenic differentiation.

In conclusion, it appears that the initial cell seeding density affects MSCs differentiation. However, the optimal cell seeding density is likely to depend on many different parameters, such as the source of the cells, the material used for cell culture, the composition of the osteogenic differentiation medium, the duration of the cell culture experiment, and probably other factors.

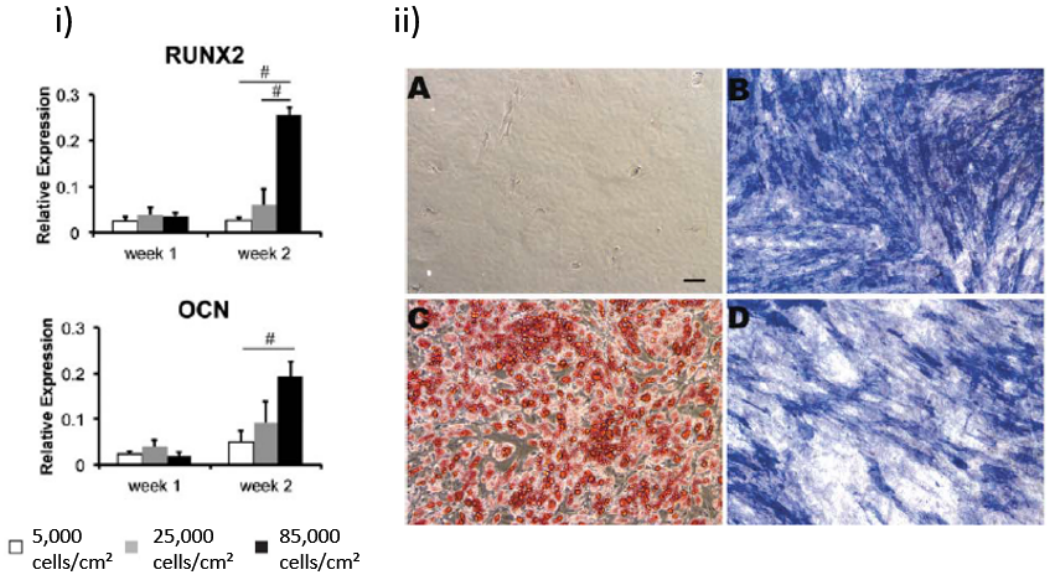

FIGURE 2.6 – Impact of cell seeding density on mesenchymal stem cells differentiation. i) Gene expression of the bone markers, Runx-2 and osteocalcin (OCN) for human bone marrow MSCs seeded at different densities and cultured for one or two weeks in osteogenic culture medium. Adapted from [176] ii) Brightfield images of human bone marrow MSCs plated at 1,000 cells/cm^2 (A and B) or 25,000 cells/cm^2 (C and D), cultured for 4 weeks in adipogenic (A and C) or 3 weeks in osteogenic (B and D) differentiation media, and stained for the presence of lipids (A and C) or alkaline phosphatase (B and D). Scale bar = 200 μm. Adapted from [177]

2.2.4 Application of stimuli

During the early stage of bone defect healing, hypoxia would enhance the migration of osteogenic and angiogenic precursor cells as well as osteogenesis and angiogenesis. Then, newly formed vessels around the bone defect would eliminate the hypoxic condition as the healing process continues. If the cells are generally cultured in the presence of 21% O_2, physiologic oxygen pressure is lower and varies from tissue to tissue between 1% and 13%, and would be comprised between 1% and 7% in bone marrow. Therefore, different studies aimed at evaluating the impact of hypoxia on MSCs differentiation. Yu et al. showed that inducing mouse MSCs hypoxia via $CoCl_2$ for 3 days led to an increase in the expression of osteogenic genes (ColI, Runx-2, ALP, Osterix, osteopontin, osteocalcin) and calcium deposition (Figure 2.7a-d) as compared to 1, 5, or 7 days of hypoxia or to normoxia (standard culture condition with 21% O_2).[179] Hung et al. demonstrated that human bone marrow MSCs cultivated at 1% O_2 for 4 weeks expressed higher levels of ALP, osteopontin, and osteocalcin, and showed increased mineralization than MSCs cultured with 21% O_2. These results indicate that hypoxia would favor osteogenesis. However, it has been found that chondrogenesis and adipogenesis were inhibited in hypoxic conditions.[180] Similarly, Cicione et al. found that 1% O_2 inhibited adipogenesis and chondrogenesis of human bone marrow MSCs. Nevertheless, they observed that osteogenesis was also impaired under hypoxic conditions, as the expression

of ALP and osteopontin, and calcium deposition (Figure 2.7e) were significantly reduced under hypoxia.[181] Finally, Ding et al. noted that 1% O_2 led to a decrease in the expression of osteogenic markers (Runx-2, ALP, osteopontin, osteocalcin) in rat bone marrow MSCs after 3, 7, 14, and 21 days, as compared to 21% O_2. Curiously, they observed a higher calcium deposition for cells cultured under hypoxia after 3, 7, and 14 days, but not after 21 days.[182] The exact influence of hypoxia on MSCs differentiation therefore still remains inconclusive due to these contradictory reports in the literature.

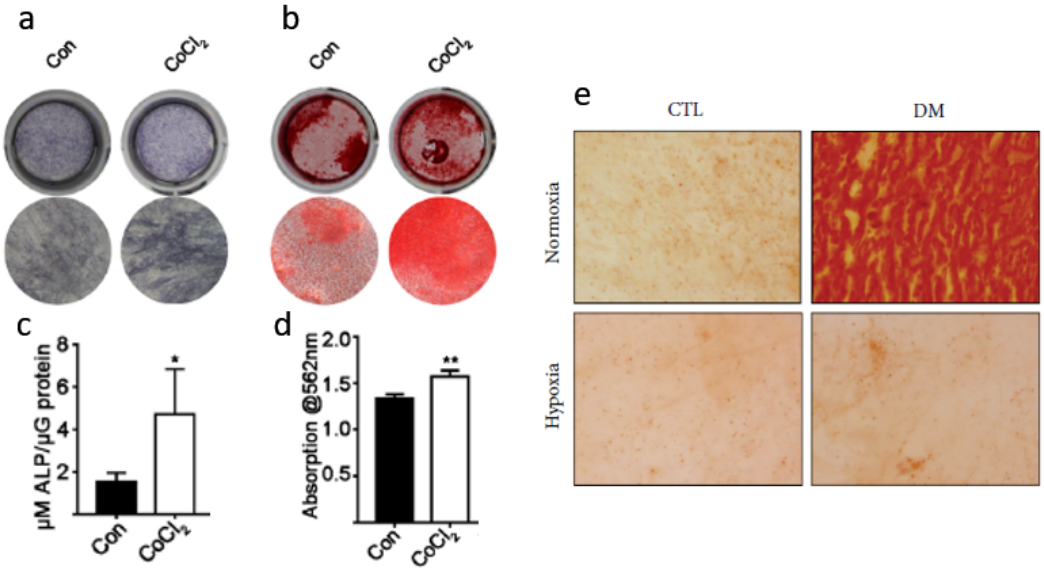

FIGURE 2.7 – Mouse MSCs cultured under normoxia or hypoxia induced by $CoCl_2$ treatment. a) ALP staining on day 7. b) Matrix mineralization (alizarin red staining) on day 14. c) ALP activity on day 7. d) Quantitative analysis of alizarin red staining. Osteogenesis was favored by hypoxic conditions. Adapted from [179] e) Alizarin red staining of human bone marrow MSCs cultured in normoxic (21% O_2) or hypoxic (1% O_2) conditions in osteogenic differentiation medium (DM) or normal growth medium (CTL). Osteogenesis was inhibited by hypoxia. Adapted from [181]

During normal development, organisms are exposed to a variety of mechanical stimuli that promote and regulate tissue development. For example, physiological loading is widely believed to be beneficial in maintaining skeletal integrity. As such, several studies have investigated MSCs osteogenic differentiation in response to mechanical solicitation. For example, rat bone marrow MSCs have been submitted to uniaxial cyclic strain with a strain magnitude of 8% and a frequency of 1 Hz during 16 hours intermittently (cycles of 15 min stretching and 15 min resting). After 16 hours of stretching, cells were elongated and perpendicularly aligned to the stretching direction, while unstrained cells presented random orientation. After 7 days in osteogenic or adipogenic differentiation medium, strained cells exhibited a higher expression of ALP and a lower expression of ORO (oil red O) as compared to unstrained cells, showing that mechanical solicitation enhances osteogenesis but impairs adipogenesis.[183] Similarly,

Li et al. applied a cylic strain (5% strain magnitude) to rat bone marrow MSCs during 6 hours per day and observed that the cells became oriented perpendicular to the axis of strain. In addition, the expression of osteogenic markers was higher for strained cells after 3 and 5 days, while the expression of adipogenic markers was lower for strained cells as compared to unstrained cells.[184] After applying cyclic mechanical stretch (10% elongation, 0.5 Hz) to human bone marrow MSCs for 3 weeks, Wang et al. showed that the expression of ALP, Runx-2, osteocalcin, and collagen I, as well as calcium deposition, were increased in strained cells as compared to the non-loaded control cells (Figure 2.8).[185] Finally, Chen et al. demonstrated that submitting human bone marrow MSCs to mechanical stretch (12% at 0.5 Hz) resulted in increased expression of ALP, Runx-2, and Osterix, and higher calcium deposition than non-loaded cells.[186] As MSCs fate is believed to be related with cell cytoskeleton tension, and that increased tension would result in osteogenic fate of MSCs[187], it can be postulated that the increase in generated tension on the cytoskeleton by mechanical loading would be favorable for MSCs osteogenic differentiation.

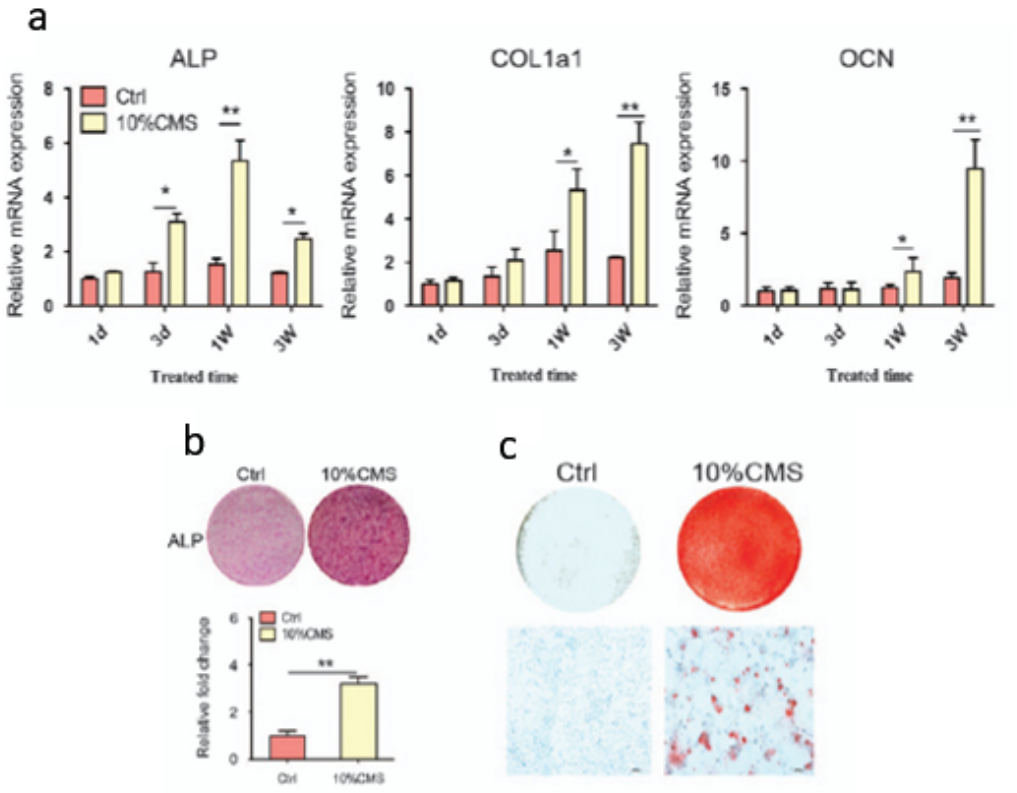

FIGURE 2.8 – Cyclic mechanical loading could regulate osteogenic differentiation in human bone marrow MSCs. a) qRT-PCR analysis of osteogenic differentiation markers ALP, COL1a1 (type I collagen), and OCN (osteocalcin) in MSCs after treatment with 10% CMS (Cyclic Mechanical Loading) for 3 weeks compared with static control cells. b) Representative images of ALP staining (including quantitative analysis) and c) Alizarin red staining of MSCs after treatment with 10% CMS for 3 weeks compared with static control cells. Adapted from [188]

2.3 Hydrogels : a material of choice for cell culture

Considering that MSCs are adherent cells, the in vitro culture of MSCs is traditionally performed in two dimensions on plastic materials (polystyrene). Indeed, the majority of the previously mentioned studies evaluated the impact of different parameters (culture medium, number of cell passages, cell seeding density, application of stimuli) on MSCs behavior when cultivated on plastic cell culture plates. However, it is now recognized that the surface properties of the material could greatly influence MSCs adhesion, proliferation, and differentiation. For example, it has been reported that the surface charge[189], the surface chemistry[190], the roughness[191], the topography[105, 192, 193], as well as the presence and distribution of biomolecules[84, 102] could significantly alter MSCs osteogenic commitment. In addition, flat and stiff materials, such as polystyrene and glass, are far from being representative of the physiological environment of cells.[35] Therefore, hydrogels have emerged as promising materials for cell culture since they mimic the essential elements of native cell extracellular matrices.[35] Hydrogels are three-dimensional systems created by the crosslinking of hydrophilic polymer chains, which gives them the ability to absorb large amounts of fluid and therefore mimic biological tissues.[36, 37, 38] Hydrogels crosslinking can be achieved either by physical or chemical crosslinking. Physical hydrogels result from ionic bonding, hydrogen bonding, physical interactions or molecular entanglements between the polymer chains, which are reversible by application of force or environmental changes.[37] The presence of reversible crosslinks might be of particular interest for cell culture, as providing a matrix that can be deformed by cells may favor their differentiation.[47, 48] This will be discussed in more details in the chapter 3. Physical gels have become the center of attention of many researchers because of their relatively facile production, although they tend to be more fragile than chemical hydrogels.[38] Chemical hydrogels are obtained via the creation of covalent bonds between the polymer chains.[37, 38] Chemically crosslinked hydrogels are often used due to their good mechanical strength[194], their homogeneity at the microscale and the ease to control their physical and chemical properties, such as matrix elasticity and porosity.[68] Because of hydrogels special traits, such as modifiable chemical properties, biocompatibility, elasticity, porosity, and the capability to allow nutrients and growth factors circulation, they have broad uses in biomedical research that goes from drug delivery to regenerative medicine and tissue engineering.[36] Hydrogels are also gaining attention due to their ability to encapsulate cells.[36] Hydrogels are generally classified in two categories depending on the source of the polymers, i.e. natural and synthetic polymers. A few typically used natural and synthetic based hydrogels are discussed in the following sections.

2.3.1 Hydrogels made of natural polymers

Many polymers used for hydrogel fabrication are natural polymers, including alginate, collagen, chitosan, gelatin, hyaluronic acid, cellulose, and agarose. These polymers are abundant in source and present inherent biocompatibility. Some of the natural polymer based constructs contain degradable moieties such as hydrolysable ester groups and enzyme-mediated hydrolytic amide groups, as well as natural binding sites, which provide interactions between cells and hydrogels. However, low stability, poor mechanical properties, and rapid degradation rate are major disadvantages of the natural-based hydrogels.[36] In addition, procedures for the isolation and purification of natural polymers can be expensive, and can lead to batch-to-batch variations that may decrease the reproducibility of materials properties and functions.[39]

Type I collagen being the major structural component of many tissues, including bone, it constitutes an attractive material for cell studies. Collagen hydrogels are typically formed via physical crosslinking by raising the temperature and the pH to initiate collagen fibril self-assembly. The gelation occurs rapidly (about 30 minutes under physiological conditions) and the gel can be molded in various shapes.[35] Collagen hydrogels already present cell adhesion sites without modification, such as GFOGER, DGEA, and RGD amino-acid sequences[195], and present a native viscoelastic environment for cells.[35] However, collagen gels suffer from some drawbacks including low stiffness, limited long-term stability, batch-to-batch variability, and immunogenicity problems due to the presence of antigens from the original tissue.[35, 196] The physical crosslinking and the degradability of collagen hydrogels also result in significant contraction of the matrix by the cells during long-term cell culture.[35] This effect might be circumvented by chemical crosslinking.[36]

Gelatin can be obtained by partial hydrolysis of collagen.[36] Similarly to collagen, gelatin is rich in RGD sequences (Arg-Gly-Asp) (Figure 2.9a)[197], which constitutes the minimal binding domain to the integrin receptor[195], and therefore enables cell adhesion. Gelatin's thermoresponsive characteristics enable it to undergo a sol-gel transition based on the environmental temperature. If the temperature drops below ambient temperature, the transition takes place from solution to gel, and can be reversed by heating the solution to physiological temperature.[37] However, gelatin has poor mechanical properties as well as high degradation rate, and therefore requires extensive crosslinking, including physical, chemical, or enzymatic crosslinking, before being used for cell culture experiments.[37, 197]

Hyaluronic acid is a native polysaccharide component of connective tissue and ECM (Figure 2.9b). Hyaluronic acid constitutes an interesting candidate for drug delivery as it is a negatively charged polymer which is able to bind with positively charged molecules, such as drugs or bioactive compounds, that can subsequently be released in the body by ion exchange or polymer disintegration.[37] Being a glycosaminoglycan (GAG) consisting of repeating units that are widely distributed in cartilage, hyaluronic acid hydrogels have shown great

potential for cartilage tissue repair. In addition, hyaluronic acid is capable of interacting with various cell receptors.[198] However, because of non-specific protein adsorption on hyaluronic acid-based scaffolds in vivo, it can induce foreign body reaction. In addition, a wide range of cells (monocytes, leukocytes, and platelets) can stick to the surface of hyaluronic acid-scaffolds and may lead to the release of cytokines and pro-inflammatory mediators that induce inflammation.[199] Finally, one of the challenges of hyaluronic acid is hyaluronidase, which causes a high degradation rate in vivo.[36]

Cellulose represents the most abundant naturally occurring biopolymer (Figure 2.9e). Cellulose can be obtained from plants and natural fibers such as cotton and linen, as well as from some bacteria.[200, 201] Cellulose present many advantages including biocompatibility, biodegradability, non-toxicity, mechanical and thermal stability, and cost-efficiency.[201] Hydrogels can be obtained either directly from native cellulose or from cellulose derivatives such as methylcellulose, carboxymethyl cellulose, hydroxypropyl methylcellulose, dialdehyde cellulose, cellulose acetate, and others.[200, 201] Cellulose-based hydrogels can be obtained through physical crosslinking thanks to the presence of hydroxyl groups in cellulose that can easily form crosslinks through hydrogen bonding.[200] Hydrogels from cellulose derivatives can be obtained through physical crosslinking, via ionic bonding or hydrogen bonding, or through chemical crosslinking, with a functionalized crosslinker or under UV irradiation.[200] Nevertheless, the main limitations of cellulose-based hydrogels is the low solubility of cellulose in both water and most organic solvents due to the hydrogen-bonded structure, and the poor reactivity of cellulose.[202]

Alginate is a polysaccharide extracted from brown algae. It is a natural anionic copolymer composed of two monosaccharides; α-L-guluronic acid (G units) and β-D-mannuronic acid (M units) (Figure 2.9d).[35, 36, 37] Because of its abundance, inexpensiveness, and biocompatibility, alginate has been increasingly used for cell studies.[36] In addition, alginate has the particular ability to form ionic crosslinks by interacting with divalent cations, such as Ca^{2+}, Sr^{2+} and Ba^{2+}, that promote the formation of ionic bridges between alginate G units.[35, 36, 37] This particularity made alginate very popular for studying cell-material interaction in 3D as it allows easy encapsulation of the cells in the hydrogel.[35] However, because of the poor adhesion properties of alginate-based hydrogels, adhesion peptides such as RGD are generally used to improve cell adhesion.[35, 36]

Chitosan, the deacetylated form of chitin, is a naturally linear cationic heteropolymer extracted from the shrimp or crab shells (Figure 2.9c).[36, 203] It has analogous composition and structure to glycosaminoglycans[203], and possesses high biocompatibility, good biodegradability, and non-toxicity.[37, 203] In addition, owing to its cationic nature, chitosan would present antimicrobial activity against both Gram-positive and Gram-negative bacteria. Chitosan can be crosslinked either by physical or chemical crosslinking. However, because its mechanical properties are weak, chitosan should be combined with other functional materials to promote the osteogenic differentiation and tissue regeneration.[203] Moreoever, unmodified

chitosan is both insoluble in water and organic solvents due to its crystalline arrangement, making it difficult to apply in pharmaceutical and tissue engineering applications without modification.[37]

Agarose is a biocompatible polysaccharide extracted from marine red algae.[204, 205] Agarose is the main component of agar, attained by extraction of agaropectin from agar (Figure 2.9f).[204] Agarose has been widely used in biomedical applications because of its controlled self-gelling properties, water-solubility, adjustable mechanical properties, and non-immunogenic properties.[204, 205] Agarose dissolves in hot water to form a gel when cooled to below an upper critical solution temperature.[205] Agarose is an attractive platform for cell encapsulation because it undergoes gelation through the formation of extensive intermolecular hydrogen bonds resulting in double helical structures of polymer chains and in the formation of a gel.[39, 204] The concentration of agarose in the solution determines the stiffness of the hydrogel.[205] Finally, agarose is non degradable and has to be combined with adhesion peptides or other polymers to enable cell adhesion.[204]

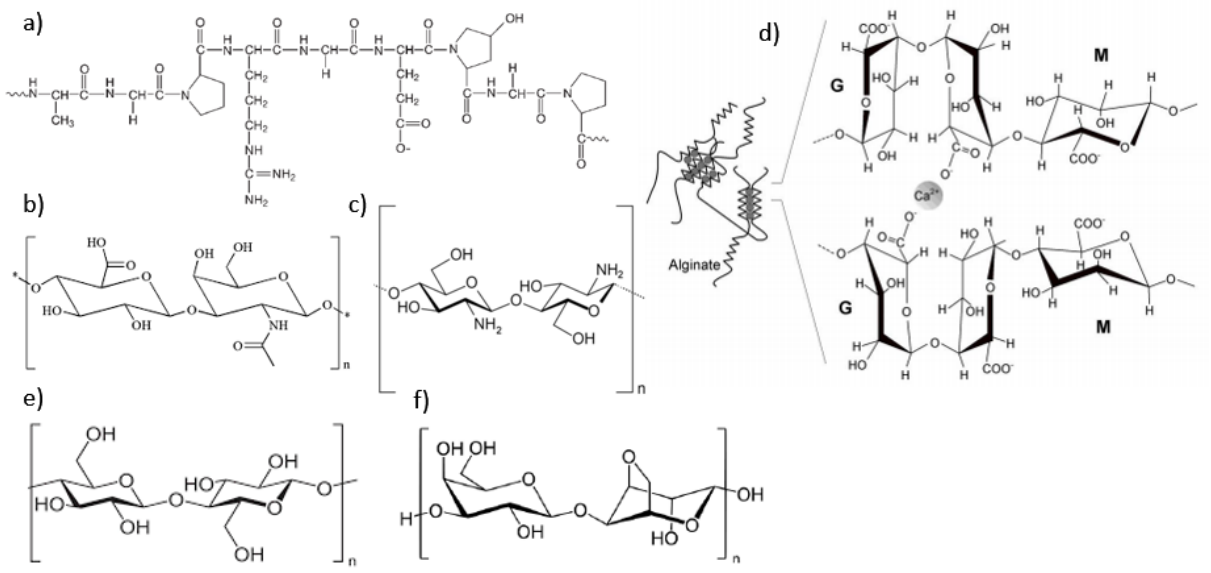

FIGURE 2.9 – Chemical structure of several natural polymers used for the preparation of hydrogels. a) Gelatin, b) Hyaluronic acid, c) Chitosan (the amine groups are protonated at pH > 6.5), d) Alginate containing α-L-guluronic acid (G units) and β-D-mannuronic acid (M units), and physical crosslinking by interaction of the G units with Ca^{2+} ions, e) Cellulose, f) Agarose.

2.3.2 Hydrogels made of synthetic polymers

Different from natural polymers, the chemistry of synthetic polymers is tunable, providing the ability to optimize the physicochemical and mechanical properties of synthetic polymer based hydrogels. Additionally, diverse molecular weights, block structures, and degradable linkages can lead to tunable mechanical properties and degradation rate. Nevertheless, lack of adhesion sites, lack of biocompatibility, and potentially toxic degradation products are some disadvantages of synthetic based hydrogels.[36] In addition, the mesh size of many commonly used synthetic hydrogels is on the order of nanometers, which is several orders of magnitude smaller than cells (microns), and can alter the transport of large solute molecules and limit cellular migration and cell-cell interactions.[39]

Polyacrylamide (PAM) (Figure 2.10a) based hydrogels have been widely used in the biomedical field, for drug delivery, and for biosensors in recent years. The highly tunable mechanical properties is the crucial factor that makes PAM stands out from other materials, as the hydrogel stiffness can be tuned from less than 1 kPa to several hundreds of kPa.[36, 206] PAM hydrogels are chemically crosslinked hydrogels produced by reacting acrylamide monomer and bis-acrylamide crosslinker via radical polymerization.[35] Nevertheless, PAM presents poor cell adhesion and the presence of unreacted monomers might lead to toxicity, which are concerns in biomedical use.[36] The existence of well-established protocols for the fabrication of hydrogels with tunable stiffness and for the coupling of proteins or peptides circumvent the lack of adhesion of PAM hydrogels and contribute to their appeal for cell culture. Indeed, the ability to independently modulate hydrogel stiffness and adhesive ligand presentation can lead to more complete understanding of complex cell responses to these inputs and is difficult to accomplish with natural materials. However, one major disadvantage is that PAM cannot be used to encapsulate cells in 3D, due to toxicity of the hydrogel precursors.[35] Temperature responsive hydrogels can be synthesized from acrylamide derivatives such as poly(N-isopropylacrylamide) hydrogels (PNIPAAm) (Figure 2.10b) that are extensively studied for making injectable hydrogels that undergo gelation at body temperature and can subsequently release various molecules in the body.[207]

Polyethylene glycol (PEG) (Figure 2.10c), also known as polyethylene oxide (PEO), is a synthetic material with tremendous biocompatibility, low cost, water solubility, and that has been approved by the food and drug administration (FDA) for use in various biomedical applications.[36, 37] PEG can be modified with a wealth of different functional groups which provides the ability to form chemical hydrogels using a variety of polymerization techniques, giving high design flexibility.[35] Pure PEG based hydrogels do not support cell adhesion and proliferation and have to be functionalized with adhesion proteins or peptides.[37] One advantage of PEG hydrogels is the possibility to encapsulate cells for studies in three dimensions.[208]

Poly(vinyl alcohol) (PVA) (Figure 2.10e) is prepared by a partial or complete hydrolysis of poly(vinyl acetate).[39] It is a synthetic polymer with hydrophilicity (-OH groups), biodegradability, and biocompatibility.[209] Different crosslinking techniques can be used to obtain PVA hydrogels. The physical crosslinking technique involves the strong hydrogen bonding among polymer chains. For chemical crosslinking, it is necessary to promote covalent bonding between pendant hydroxyl (-OH) groups present in PVA chains by using crosslinking agents. Irradiative crosslinking can also be performed using electron beam or gamma radiation.[208, 209] PVA normally presents little cell adhesion properties but could easily be modified with cell adhesion peptides thanks to the multiple available hydroxyl groups on the polymer chains.[36]

Poly(hydroxyethyl methacrylate) (pHEMA) (Figure 2.10d) hydrogels are highly investigated for biomedical applications due to their non-toxicity, biocompatibility, high water absorption capacity, tunable mechanical properties, and capability to encapsulate cells.[37, 208] PHEMA hydrogels are generally synthesised via the free radical polymerization of methacrylates. Many studies aim to modify the properties of pHEMA to improve the degree of hydration, degradation, and mechanical properties of the hydrogels.[39] It is believed that, because pHEMA hydrogels possess a property called non-fouling which prevents the adsorption of non-specific proteins at the surface of the material, they would avoid the immune reaction of the body and therefore avoid the formation of a thick collagenous substance around the material when implanted in vivo.[37]

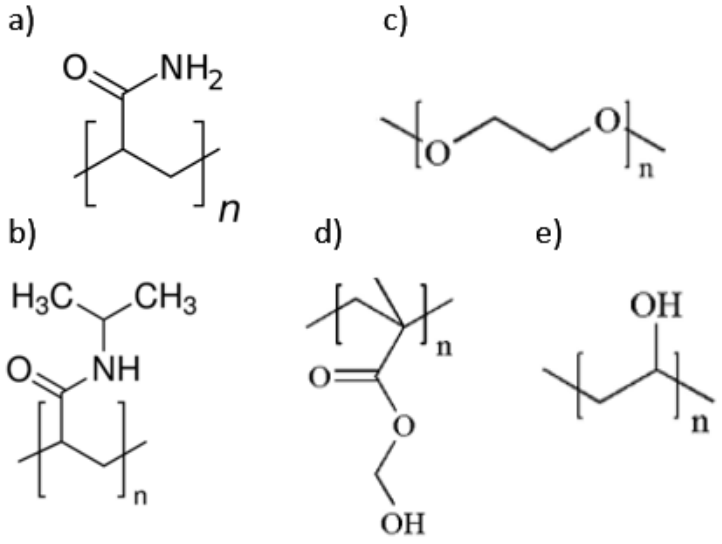

FIGURE 2.10 – Chemical structure of several chemical polymers used for the preparation of hydrogels. a) polyacrylamide, b) poly(N-isopropylacrylamide), c) polyethylene glycol, d) poly(hydroxyethyl mathacrylate), e) poly(vinyl alcohol).

Of course, it is possible to combine several polymers and their advantages to create hydrogels with particular features. For example, copolymerization of various synthetic monomers can lead to copolymeric hydrogels with block copolymers, alternating or random copolymers, that allow to tune hydrogels properties. In addition, because using purely biological or synthetic materials has limitations in creating cell encapsulation systems, many efforts are dedicated to the development of biosynthetic gels that combine the bulk properties of synthetic polymers and the attributes of natural polymers. Hydrogels therefore constitute particularly interesting materials for cell culture either in two or three dimensions. Many properties of hydrogels can be modulated to study their impact on cell behavior, including cell adhesion, proliferation, and differentiation. The impact of hydrogels properties on MSCs behavior is covered in the next chapter.

Chapter 3

Hydrogels for mesenchymal stem cell behavior study

Emilie Prouvé[a,b,c,d,e], Gaétan Laroche[a,b*†], and Marie-Christine Durrieu[c,d,e*†]

[a]Laboratoire d'Ingénierie de Surface, Centre de Recherche sur les Matériaux Avancés, Département de Génie des Mines, de la Métallurgie et des Matériaux, Université Laval, 1065 Avenue de la médecine, Québec G1V 0A6, Canada
[b]Axe Médecine Régénératrice, Centre de Recherche du Centre Hospitalier Universitaire de Québec, Hôpital St-François d'Assise, 10 rue de l'Espinay, Québec G1L 3L5, Canada
[c]Université de Bordeaux, Chimie et Biologie des Membranes et Nano-Objets (UMR5248 CBMN), Allée Geoffroy Saint Hilaire - Bât B14, 33600 Pessac, France
[d]CNRS, CBMN UMR5248, Allée Geoffroy Saint Hilaire - Bât B14, 33600 Pessac, France
[e]Bordeaux INP, CBMN UMR5248, Allée Geoffroy Saint Hilaire - Bât B14, 33600 Pessac, France

†These authors contributed equally.

*Corresponding authors :
Gaetan.Laroche@gmn.ulaval.ca Phone : +1 (418) 656-7983 Fax : (418) 656-5343
marie-christine.durrieu@inserm.fr Phone : +33 5 40 00 30 37 Fax : +33 5 40 00 30 68

This work has been published in the book : *Superabsorbent Polymers : Chemical Design, Processing and Applications. DeGruyter. 2021.*

3.1 Résumé

Les hydrogels ont été identifiés comme un outil prometteur pour mimer les propriétés de la matrice extracellulaire native des cellules et pour étudier la réponse des cellules à de nombreuses propriétés. En effet, les propriétés des hydrogels, comme la topographie, la porosité, les propriétés mécaniques et la présentation de biomolécules, sont facilement modulables et peuvent mener à un comportement cellulaire significativement différent en termes d'adhésion, prolifération et différenciation. De plus, les hydrogels offrent la possibilité d'encapsuler les cellules, et ainsi comparer les réponses cellulaires entre un environnement en deux dimensions, généralement utilisé pour les expériences traditionnelles de culture cellulaire, à un environnement en trois dimensions, plus représentatif de l'environnement in vivo des cellules. Ainsi, ce chapitre vise à rassembler les connaissances accumulées sur le contrôle du comportement des MSCs en utilisant les hydrogels en tant que support de culture, ce qui pourrait aider à développer des biomatériaux appropriés pour des applications cliniques.

3.2 Abstract

Mesenchymal stem cells (MSCs) are self-renewing, multipotent stem cells with the ability to differentiate into mesoderm-type cells, such as adipocytes, osteocytes, and chondrocytes. MSCs have also been reported to differentiate into other cell types such as neurons, smooth muscle cells and hepatocytes in vitro. Consequently, they constitute an interesting candidate for tissue engineering and regenerative medicine purposes. However, the perfect control of MSCs commitment towards a desired lineage has still not been achieved, which is an obstacle for their use in clinical applications. In this context, hydrogels have been identified as a promising tool to mimic the properties of the native extracellular matrix of cells and to investigate the response of cells to many different features. Indeed, hydrogels properties, such as topography, porosity, mechanical properties, and biomolecules presentation, are easily tunable and can lead to significantly different cell behavior in terms of cellular attachment, proliferation and differentiation. In addition, hydrogels offer the possibility to encapsulate cells, and therefore compare cell response between two dimensional environments, typically used in traditional cell culture experiments, and three dimensional environments, more representative of the cell in vivo environment. Therefore, this chapter aims at gathering the accumulated knowledge on the control of MSC behavior by using hydrogels as cell culture material, which might help designing appropriate biomaterials for clinical applications.

3.3 Introduction

The interest in hydrogel materials is growing rapidly considering their unique swelling properties, coupled with a high versatility and a high tunability of materials features, which opened the door to many applications such as disposable diapers, filters for water purification, separation materials for chromatography and electrophoresis, biosensors, cosmetic products and drug delivery.[38] In particular, hydrogels have broad uses in biomedical research that include regenerative medicine and tissue engineering.[36] Indeed, while most of the current understanding of cell processes is based on experiments performed on flat and stiff materials, such as polystyrene and glass, it became clear that these materials are not representative of the physiological environment of cells, and that culture systems that better mimic cells native in vivo environments were needed.[35] In this context, hydrogels have proven useful in many cell culture applications, shedding light on mechanisms regulating cell behavior and providing the appropriate conditions for the expansion and controlled differentiation of various cell types. Hydrogels constitute a powerful tool to mimic the properties of the native extracellular matrix (ECM) of cells and to investigate the response of cells to many different features such as topography, porosity, mechanical properties, and biomolecules presentation. They are also gaining attention due to their ability to encapsulate cells[36], and therefore compare cell response between two dimensional (2D) and three dimensional (3D) environments.

Because of their self-renewal ability and potential to differentiate into multilineages, stem cells became a prominent subject in medical research for regenerative medicine and tissue engineering purposes.[101] Among stem cells, pluripotent stem cells, such as embryonic stem cells (ESCs) or induced pluripotent stem cells (iPSCs) are attractive because they can give rise to all the cell types in the body.[101] However, the use of ESCs in research and clinic is restricted due to ethical considerations. In addition, they can cause an immune response of the patient, as the cells come from another person, and they can form tumors after they are cultivated in vitro and subsequently implanted in vivo.[3] Induced pluripotent stem cells are an ethical alternative to ESCs as they can be obtained by reprogramming adult cells. Nevertheless, the cell reprogramming efficiency is quite low and the use of iPSCs in clinic is still limited because of the lack of knowledge regarding their manipulation and behavior.[3, 138] Considering the need for stable, safe, and highly accessible stem cell sources, adult stem cells, and particularly mesenchymal stem cells (MSCs), constitute interesting candidates. Indeed, they are self-renewable, multipotent, easily accessible and they can be expanded in vitro with high genomic stability, and few ethical issues.[101] MSCs can be extracted from various tissues like bone marrow, adipose tissue, and dental pulp, and they are capable of in vivo differentiation into mesoderm-type cells such as osteoblasts, chondrocytes, and adipocytes, as well as other cell types such as neurons, smooth muscle cells, and hepatocytes when cultured in vitro.[101] Although MSCs exhibit several advantages, their clinical use is hindered by their tendency to uncontrollably proliferate and differentiate which can lead to tumor formation.[32] Moreover,

the perfect control of MSCs differentiation towards a desired lineage has still not been achieved. Consequently, a better understanding of their biological behavior is required to provide tools to control their fate and allow their use in clinical applications.
Therefore, the objective of this chapter is to provide a broad overview of the use of hydrogels as cell culture substrate and the modulation of hydrogels properties to study and direct MSCs adhesion, proliferation, and differentiation.

3.4 Impact of hydrogels properties on mesenchymal stem cells fate

3.4.1 Surface topography

In vivo, stem cells behavior is controlled by the interplay of many different signals coming from cells surrounding microenvironment. This microenvironment is composed of chemical and mechanical cues, which will be reviewed in the following sections, as well as topographical cues at the micro- and nanoscale.[210] Surface topography is therefore considered as an interesting tool to alter cell growth, morphology, and differentiation. Indeed, micron scale topographic features such as ridges, grooves, and pillars have been shown to influence cell spreading, migration, and differentiation.[106, 211, 212] Nanostructures including pits, pillars, and grooves have also been shown to elicit specific cell responses on several materials.[105, 192, 213] However, most of the studies performed so far have been conducted with solid substrates. Consequently, new methods have been developed for the fabrication of micro- and nanotopographies on the surface of hydrogel substrates, as hydrogels present the benefit of having similar features to ECM. The strategy consists in fabricating hydrogel substrates with micro- or nanotopographical patterns, on which the cells spread, elongate, and align through a phenomenon called contact guidance[41], which will determine cell shape and differentiation.

Li et al. developed different topographies on polyacrylamide hydrogels functionalized with type I collagen to promote cell adhesion, to study the effect on rat bone marrow MSCs spreading, proliferation, and differentiation.[40] Substrate topography was set in square pillars or grooves, with three sets of dimensions. The width of the patterns and the distance between them were set to 5/15, 10/10, or 15/5 μm, for both squares and grooves. In addition, substrate stiffness was varied to 6 kPa (soft) and 47 kPa (stiff). This research team showed that both stiffness and dimension affect MSCs proliferation, as stiffer and more unevenly dimensioned substrates (15/5 μm) lead to more cell growth. However, there was no difference in the multiplication rate between square pillars and grooves. Substrate topography is a key factor to regulate MSCs morphology as a grooved topography promotes the directed alignment of

cells and a reduced cell area compared to square pillars (Figure 3.1a and b). Finally, it has been shown that osteogenic differentiation was promoted on the stiff substrate with uneven square pillars (15/5 μm), while neurogenic differentiation was predominant on the soft substrate with evenly dimensioned grooves (10/10 μm), as grooved topography favors cell alignment and axon growth.[40] Similarly, Hu et al. molded rectangular microplates onto poly(2-hydroxyethyl methacrylate) (pHEMA) hydrogels.[41] The dimensions of the hydrogel microplates were 20 μm in height and 2 μm in width, and the length was varied from 10, 25, and 50 μm. The interplate spacing was varied between 5 to 10 μm and the intercolumn spacing was 5 μm. It has been observed that human MSCs adhered and spread on a regular cell culture Petri-dish but did not spread on a flat pHEMA hydrogel, due to the hydrophilicity of the pHEMA hydrogels and the lack of anchor point on the flat surface. However, cells adhered on microstructured pHEMA hydrogels and spread into elongated geometries in response to the topographical cues, as observed in the previous study, staying in between the parallel plates and conforming to the gaps (Figure 3.1c). Cell length increased as the interplate spacing decreased, as cells need to stretch more in the longitudinal direction to fit into a smaller space between the parallel plates. In addition, the cells tended to elongate more on longer plates. Finally, after 32 days of culture, the cells formed a dense and interconnected layer, with cells connecting in vertical direction through the intercolumn spacing. This is one of the advantages of having plate-patterned substrate over groove-patterned substrate, as it allows cell-cell connections and interactions (Figure 3.1c).[41] Although many studies focused on polygonal patterns, as squares, grooves, and plates, some researchers also investigated the impact of circular patterns on cell behavior. For example, Yang et al. produced chitosan hydrogels with uniform micro-hills of 10 μm and dispersed micro-hills of 5 to 30 μm in diameter.[214] Spacing between micro-hills were determined as 4 μm for uniform hills and 14 μm for dispersed hills. They observed that rat MSCs on uniform hills were flat, polygonal and well spread, while the majority of MSCs on dispersed hills was fusiform with cells that adhered to the hills, forming a bridge-like structure across the hills, or that fell between the hills. Therefore, cells on dispersed hills would spread and migrate along the spacing between micro-hills, leading to orientation by contact guidance. No difference in cell adhesion was found between flat and patterned hydrogels, however MSCs proliferation was higher for dispersed hills followed by uniform hills and lastly flat hydrogels.[214] Although the spatially and dimensionally dispersed micro-hills were found to promote MSCs alignment and proliferation, it is not certain whether this effect is due to micro-hills size, shape, or to the spacing between the hills.

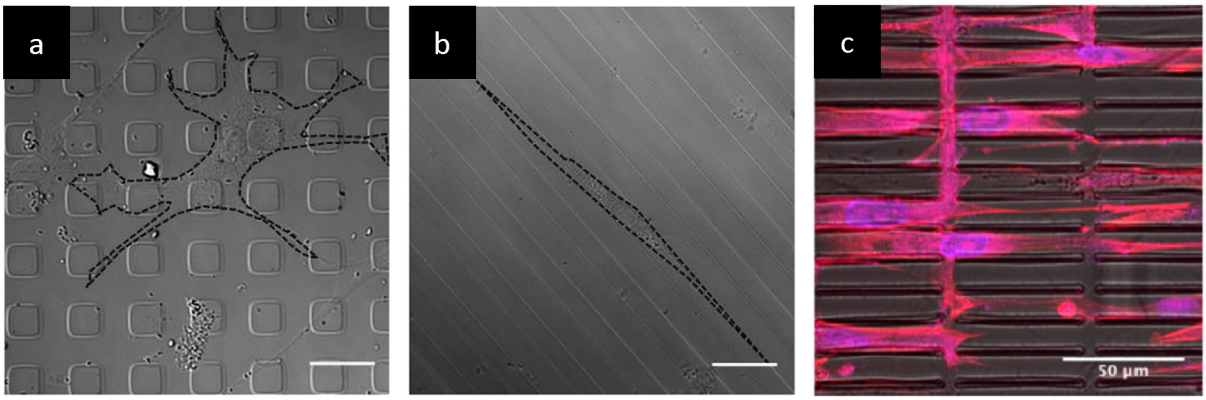

FIGURE 3.1 – a, b) Spreading of rat MSCs on a stiff (47 kPa) polyacrylamide hydrogel patterned with square pillars (a) or (b) grooves. The grooved topography promoted cell alignment by contact guidance and led to a reduced cell area compared to square pillars. Scale bars, 20 μm. Adapted from [40] c) Human MSCs cultured on a microplate patterned pHEMA hydrogel substrate. After 7 days of culture, cells elongated and aligned along the direction parallel to the plates and connected through the intercolumn spaces. Adapted from [41]

Besides pillars and grooves, other hydrogel topographies consisting in wrinkles and cavities with various shapes have been studied. Poellmann et al. prepared polyacrylamide hydrogels with square or hexagonal cavities, varying the size of the cavities (from 3 to 20 μm) and the width of the borders separating the cavities (from 1 to 20 μm).[215] They observed that the proportion of well spread mouse bone marrow MSCs was higher for 10 and 15 μm borders than for 1 and 2 μm borders, with no effect of cavity shape and size. However, cell area was higher for square patterns with large borders (15-20 μm) than for hexagonal patterns or small borders (2-5 μm). Finally, square patterns induced cell alignment along the borders, with cells on smaller borders becoming more elongated, while they did not align on substrates with hexagonal cavities. This is explained by the fact that borders on square substrates are similar to continuous grooves, which is consistent with the results of the precedent studies, while borders between hexagonal cavities frequently change direction on a scale shorter than most cells.[215] Guvendiren et al. investigated the effects of pattern geometry and size on stem cell morphology and spreading by molding lamellar and hexagonal patterns with a periodicity (λ) of 50 or 100 μm and a height of 20 μm on pHEMA hydrogels.[216] For lamellar patterns with λ = 50 μm, most of the cells formed bridges between the patterns and spread randomly without recognizing the pattern, while for λ = 100 μm the majority of cells aligned themselves along the patterns. For hexagonal patterns with λ = 50 μm, one third of the cells attached inside the patterns and remained rounded, while for λ = 100 μm the majority of the cells were found to be inside the patterns with a round morphology but a larger cell area. Lamellar patterns with λ = 100 μm and hexagonal patterns with λ = 50 μm were chosen to study human MSCs differentiation as they induced aligned cells which could stimulate osteogenesis and round cells which could favor adipogenesis, respectively. The differentiation on patterned surfaces was also

compared to that observed on flat surfaces. As expected, MSCs osteogenic differentiation was found to be up-regulated for lamellar patterns, while adipogenic differentiation was higher for hexagonal patterns. In addition, osteogenesis was found only for cells that were elongated and aligned by taking the shape of the lamellar pattern, whereas only cells inside the hexagonal patterns which remained round with low spread area stained positive for adipogenesis.[216] These observations confirm that surface topography can direct cell shape which in turn modulates cell differentiation. Finally, Randriantsilefisoa et al. synthesized polyethylene glycol hydrogels presenting both micro- and nanowrinkles or creases to study the morphology of human MSCs.[217] On wrinkled hydrogels, cells developed a branched morphology with many cell interconnections and created additional wrinkles due to cell contractile forces. For hydrogels presenting creases, the cells were preferentially oriented and gathered along the creases, promoting a tissue-like formation by being close to one another.[217]

Finally, less defined structures, such as random surface roughness might also influence cell spreading and differentiation. For example, Hou et al. developed gelatin-methacryloyl (GelMA) hydrogels with two different values of stiffness (4 kPa as soft gel and 31 kPa as stiff gel) and with varying surface roughness (Rs) from the nano- to microscale (from 200 nm to 1.1 μm) to study the effect on human MSCs adhesion, spreading, and osteogenic differentiation.[42] They found that cell spreading area on soft hydrogels increased with increasing surface roughness, and that cells presented defined and aligned actin stress fibers for a roughness greater than 500 nm. On stiff hydrogels, the spreading of MSCs was slightly enhanced by increasing the roughness from 200 to 500 nm, but was restricted for higher roughness. In addition, focal adhesions were observed on soft gels from a roughness of 500 nm, whereas on the stiff gels the maximum size of focal adhesions was obtained for an intermediate roughness of 500 nm. These results are correlated with MSCs osteogenic differentiation (Figure 3.2) as the increase of surface roughness on soft hydrogels induced a higher expression of osteogenic markers. On the stiff hydrogels, the osteogenic differentiation increased linearly with the surface roughness, but decreased for roughness greater than 500 nm. Thus, the highest levels of osteogenic differentiation were observed for the conditions inducing the highest cytoskeletal and nuclear tension.[42]

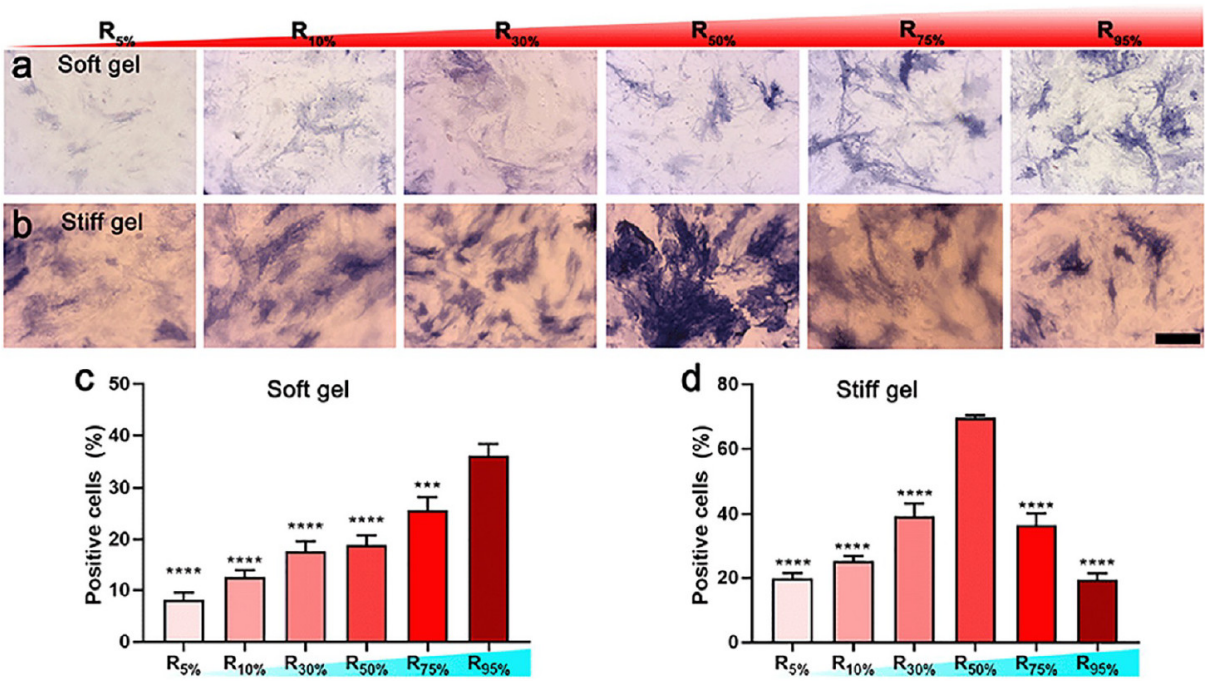

FIGURE 3.2 – Osteogenic differentiation of human MSCs on roughness gradient hydrogels. Alkaline phosphatase staining of MSCs cultured on (a) soft (4 kPa) and (b) stiff (31 kPa) hydrogels in osteogenic induced media for 7 days. Quantification of ALP positive cells on (c) soft and (d) stiff hydrogels. Scale bar, 200 μm. The designations R5%, R10%, R30%, R50%, R75% and R95% refer to roughness values (Rs) of 200, 300, 400, 500, 700 and 1100 nm. On soft gels, MSCs osteogenic differentiation increased with the roughness. On stiff gels, the differentiation was maximal for an intermediate roughness of 500 nm.[42]

3.4.2 Two-dimensional VS three-dimensional culture systems

As previously mentioned, hydrogel materials are gaining popularity for cell culture applications, thanks to their ability to encapsulate cells[36], which allows cell response comparison between 2D and 3D environments. Expansion of MSCs is typically being conducted using traditional two-dimensional (2D) adherent culture conditions. This technique is relatively easy, but it has been demonstrated that cells produced in this manner eventually lose their stemness and differentiation potential, which is accompanied by replicative cell senescence and reduced paracrine capabilities.[218] Drawing inspiration from the native stem cell microenvironment, hydrogel platforms have been developed to drive stem cells fate by controlling parameters such as matrix mechanical properties, degradability, presence of cell-adhesive ligand, local microstructure, and cell-cell interactions.[219, 220] Consequently, the understanding of the differences in cell behavior as cell cultures are shifted from 2D surfaces to 3D substrates is highly needed. In general, 3D culture systems can be divided into two categories. The first category includes macro-porous substrates which present interconnected pores with a pore size on the length scale of a single cell or greater (>10 μm).[49] In these substrates, the pore size and architecture can influence cell behavior in terms of migration and

differentiation.[49, 221] The second category comprises non-macro-porous substrates for which cells are fully encapsulated within the 3D substrate and are immobilized by contact with the substrate. Depending on the stiffness of the substrate and the ability of cells to degrade the hydrogel, the possibilities for cells to migrate or probe the surrounding environment will vary, which is likely to influence stem cell fate.[49]

Non-macro-porous substrates have been proven useful for MSCs chondrogenic differentiation as 3D cell encapsulation would allow rounded cell morphology and particular cell/cell or cell/matrix interactions which are critical to obtain chondrocytes.[43, 45, 46] Merceron et al. used cellulose based hydrogels to study the chondrogenic differentiation of human adipose tissue MSCs when cultured in 2D or 3D environments in vitro and in vivo.[43] After 3 weeks of culture in monolayers on top of the gel (2D) or encapsulated in gel pellets (3D) and in the presence of control or chondrogenic culture media, this team of scientists found that the expression level of four different chondrogenic markers was the highest for cells cultured in pellets and in the presence of chondrogenic medium. In addition, it has been shown that only 3D culture in the presence of chondrogenic medium supported the production of both GAG (glycosaminoglycan) and type II collagen, normally found in cartilage matrix. This study therefore demonstrated that 3D culture of MSCs was more suitable for chondrogenic differentiation in vitro, although a chondrogenic medium was required. Cells from the in vitro experiment were then collected and encapsulated in the hydrogels before being subcutaneously injected to mice, to ascertain whether cells were able to form cartilaginous tissue in vivo. After 5 weeks of implantation, cartilaginous tissue formation was achieved for MSCs treated with a chondrogenic medium in both 2D monolayer and 3D pellet cultures. While MSCs cultured in 2D chondrogenic medium failed to achieve chondrogenic differentiation in vitro, they formed a cartilaginous tissue to the same extent as MSCs pre-cultured in 3D once transferred in 3D structures and implanted in vivo.[43] Although cells cultured in 2D and 3D led to the same result in vivo after 5 weeks of implantation, studying tissue formation at shorter time points might have revealed differences in tissue formation rate. Another study, conducted by Varghese et al., showed the benefit of 3D culture for MSCs chondrogenic differentiation.[44] Nevertheless, this study highlighted that 3D culture alone was not sufficient to direct MSCs differentiation towards the chondrogenic phenotype and that the physicochemical properties of the matrix were determinant to guide cell fate. Indeed, by encapsulating goat MSCs into PEG hydrogels or PEG hydrogels containing chondroitin sulfate (CS) moieties, it has been shown that PEG-CS hydrogels promoted self-aggregated cell clusters homogeneously distributed within the hydrogels and producing cartilaginous tissues, while no cell aggregation was observed for PEG hydrogels. Cell aggregation was correlated with chondrogenic differentiation as MSCs in PEG-CS hydrogels exhibited earlier activation and higher expression of chondrogenic markers compared to MSCs in PEG hydrogels. The authors explained these observations by the fact that CS moieties enhanced the aggregation of cells, possibly by interacting with various growth

factors from the culture medium and enhancing their activity, leading to the formation of large cell clusters, which is recognized as a requirement for chondrogenesis. In addition, they showed that the immobilized CS segments of the scaffold underwent degradation in response to the cellular processes, which facilitated large cell cluster growth and matrix deposition.[44] Besides the presence of specific chemical moieties, the addition of ECM proteins or peptides into the 3D environment can also influence cell differentiation. For example, Jung et al. entrapped different proteins such as type I collagen, laminin, and fibronectin into PEG hydrogels, allowing cell encapsulation to study human MSCs differentiation in 3D environments versus the situation where cells were cultured on 2D protein films.[222] For 2D culture after 14 days, they found that myogenic differentiation was enhanced for a film of fibronectin as compared to cells cultured on plastic dishes in the presence of differentiation medium, while none of the protein films was able to promote osteogenic, adipogenic, and chondrogenic differentiations to higher levels than the differentiation medium. For 3D matrices after 28 days, hydrogels containing collagen were found to upregulate the expression of each lineage gene (myogenic, osteogenic, adipogenic, and chondrogenic) compared to hydrogels with laminin and fibronectin. In addition, ECM proteins in a 3D environment stimulated adipogenic and osteogenic differentiation at higher levels than in 2D culture.[222] However, even within a 3D environment, cell differentiation might not be homogeneous. Song et al. encapsulated human bone marrow MSCs within alginate hydrogels and directed their differentiation using osteogenic or adipogenic culture medium.[223] After 3 and 7 days, they observed homogeneous osteogenesis with similar amounts of calcium deposition through the hydrogel. Conversely, in the case of adipogenesis, more lipids were observed in the bottom of the gel than in the top.[223] Finally, while the above studies have been conducted using covalently crosslinked hydrogels, the question arises whether the type of crosslinking (chemical or physical) could impact stem cell fate when encapsulated within the hydrogel. Huebsch et al. showed that within non-degradable, ionically crosslinked alginate hydrogels functionalized with RGD (Arg-Gly-Asp) peptides, encapsulated MSCs differentiation was dictated by matrix stiffness with osteogenic commitment occurring primarily at intermediate stiffness (11-30 kPa) and adipogenic lineage predominating in softer (2.5-5 kPa) microenvironments (Figure 3.3a).[54] These observations were explained by two phenomena. First, it appeared that cell interaction with integrins was different depending on hydrogel stiffness, with for example a higher number of integrin α5-RGD bonds for a stiffness of 22 kPa. Second, it has been shown that cells used traction forces to mechanically reorganize the RGD peptides presented within these hydrogel matrices. These tractions forces are dependent on matrix stiffness as cells cultured on very compliant substrates cannot assemble their cytoskeleton and adhesion complexes while this is required to exert the so-called traction forces. On the contrary, on very rigid substrates, the cells cannot generate enough force to deform the matrix, which in turn will influence stem cell fate.[54] The possibility for cells to generate forces when encapsulated within these hydrogels is likely to be attributed to the physical crosslinking of alginate which allows matrix reorganization as physical crosslinks

can break and re-form.[45] On the contrary, the study of Khetan et al. showed that human MSCs encapsulated within covalently crosslinked RGD-modified methacrylated hyaluronic acid (MeHA) hydrogels underwent almost exclusively adipogenesis relative to osteogenesis for all the tested stiffnesses from 4 to 91 kPa (Figure 3.3b and c).[47] In addition, MSCs showed limited focal adhesion formation and unpolymerized actin in 3D matrices, while MSCs seeded on 2D MeHA gels of similar elastic modulus (25 kPa) exhibited focal adhesion and underwent primarily osteogenic differentiation. These results are correlated with the measurement of very minimal deformation of the surrounding gels by encapsulated MSCs in all formulations. To confirm that cell differentiation was related to the ability of cells to deform the matrix, MSCs were encapsulated in hydrogels with cleavable crosslinks allowing cell degradation (CC) or with permanent crosslinks inhibiting cell degradation (PC). MSCs in CC gels developed a robust network of stress fibers and focal adhesions which were not observed in PC gels. In addition, MSCs spread within CC gels and deformed the surrounding matrix to a greater extent than in PC gels. When switching the culture medium to a mixed adipogenic/osteogenic medium, MSCs in CC and PC gels underwent primarily osteogenesis and adipogenesis, respectively (Figure 3.3d). Thus, for hydrogels of the same stiffness, osteogenesis was favored when cells were able to spread and pull on the surrounding matrix, and adipogenesis was favored when cells remained rounded and were unable to displace the surrounding matrix.[47, 48] Stem cell fate is therefore regulated by cell-generated tension, that can be disabled by the presence of non-degradable covalent crosslinks, which indicates that stem cells response to biophysical cues is highly dependent on the type of hydrogel used, as well as the dimensionality of the system.

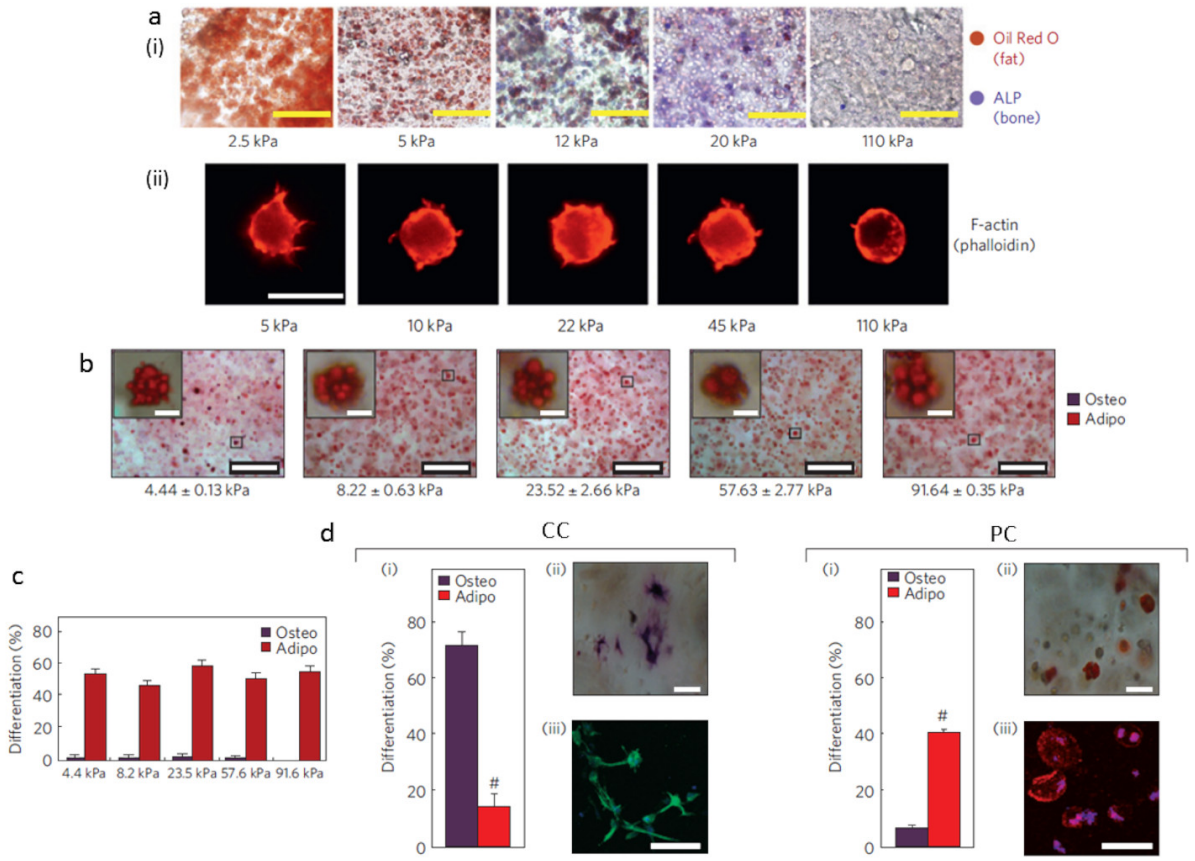

FIGURE 3.3 – a) (i) Staining of encapsulated mouse MSCs for ALP activity (Fast Blue; osteogenic marker, blue) and neutral lipid accumulation (Oil Red O; adipogenic marker, red) after 1 week of culture in the presence of combined osteogenic and adipogenic culture medium within RGD-modified alginate hydrogels with different stiffness. Adipogenesis was favored for soft substrates while osteogenesis occurred at intermediate stiffnesses. (ii) Actin staining of mouse MSCs 2 h after encapsulation into alginate matrices with varying stiffnesses. MSCs differentiation was dictated by matrix stiffness irrespective of cell morphology as MSCs remained rounded independently of stiffness. Scale bars, 100 μm (i) and 10 μm (ii). Adapted from [54] b) Representative bright-field images and c) percentage differentiation of human MSCs within MeHA gels following 7 days of incubation in mixed osteogenic/adipogenic culture medium. Adipogenesis was predominant regardless of the stiffness. Scale bars, 100 μm and 5 μm (insets). d) (i) Percentage of human MSCs differentiation towards osteogenic or adipogenic lineages in gels with cleavable crosslinks (CC) or permanent crosslinks (PC) (# $p<0.005$) (ii) Representative bright-field images of MSC staining for ALP (osteogenesis) and lipid droplets (adipogenesis) in CC or PC hydrogels. (iii) Representative immunocytochemistry for osteocalcin (OC, osteogenesis, green) and fatty acid binding protein (FABP, adipogenesis, red) of MSCs in CC or PC hydrogels. Osteogenesis was favored for CC gels where cells were able to pull on the surrounding matrix, and adipogenesis was favored for PC gels where cells were unable to displace the surrounding matrix. Scale bars, 25 μm (ii) and 20 μm (iii). Adapted from [47]

In the case of macro-porous substrates, the size and the architecture of pores are likely to affect MSCs differentiation. For example, Phadke et al. fabricated poly(ethylene glycol) diacrylate-co-N-acryloyl 6-aminocaproic acid hydrogels with either randomly oriented pores of 50 to 60 μm (spongy gel) or lamellar pores of 100 to 150 μm (columnar gel) and showed that human MSCs cultured in spongy gels presented a more spread morphology as compared to cells seeded in columnar gels, which tended to form small cellular aggregates along the pore walls.[50] Although both pore architectures supported MSCs osteogenic differentiation, cells in spongy gels exhibited significantly higher expression of several osteogenic markers and higher calcium deposition, suggesting that the spongy gels promoted faster osteogenic differentiation than the columnar gels. The enhanced osteogenic differentiation of MSCs in spongy gels could be explained by the highly interconnected porous network which facilitated nutrients transport. The difference in tortuosity of the pores might also influence cell differentiation. Finally, the higher pore surface area in the spongy gels allowed for increased available area for cell spreading, leading to more spread cells which favors osteogenesis.[50] In another study, oligo(poly(ethylene glycol) fumarate) hydrogels were synthesized with a fixed pore size (50-100 μm) and with varying porosity of 0, 20, and 40%. It has been found that the gel with 40% porosity prolonged cell viability, which has been accounted for enhanced nutrient transfer. In addition, ALP (Alkaline Phosphatase) activity of rat bone marrow MSCs was higher for a porosity of 40% after 8 days, showing that greater porosity enhances osteogenic differentiation.[51] Using the same hydrogels but with constant porosity of 75% and pore size of 100, 300, and 400 μm, Dadstean et al. showed that rat bone marrow MSCs tended to aggregate on the edge and inside the pores of the interconnected porous network.[224] ALP activity and calcium deposition after 14 days were found to be significantly higher within porous hydrogels than on regular tissue culture plastic, but no difference was observed for the various pore sizes.[224] In addition to osteogenesis, hydrogel porosity has been found to influence chondrogenesis. Recently, Yang et al. developed covalently crosslinked type I collagen hydrogels with different pore architecture to study the impact on rat bone marrow MSCs chondrogenesis.[225] They fabricated hydrogels presenting a porous network with large and solid walls (the P group) with a pore size of 35 μm for P1 and 20 μm for P2, or hydrogels displaying a fibrous network with abundant micropores (the F group) with a median pore size of 0.7 μm for F1 and 0.3 μm for F2 (Figure 3.4a). MSCs were found to form clusters for all samples, but with larger clusters within the F2 gel. Cell proliferation was faster for the F group than for the P group, with F2 promoting the fastest proliferation. On the contrary, the cell area was higher for the P group, with a well-organized actin network after 7 days of culture, while cells presented a round morphology for the F group after 1 day and more spread cells but with dispersed actin cytoskeleton after 7 days (Figure 3.4b), indicating that chondrogenic phenotype was favored in the F group. Regarding cell differentiation, the expression of five different chondrogenic markers was higher in the F group after 7 days, with the highest gene expression observed for F2. Furthermore, glycosaminoglycans and collagen II, produced in cartilage, were

found in the F group but much less in the P group, suggesting a more chondrogenic cell type in the F group. Finally, cells in the P group presented calcium deposition indicating that more MSCs in the P group underwent osteogenic differentiation than in the F group. Similar observations were made in vivo, leading to the conclusion that the F group hydrogels facilitated chondrogenesis. In a similar way to previous studies, the higher cell proliferation rate of the F group was explained by the abundant well-interconnected micropores facilitating proteins and cell metabolic wastes circulation. In addition, the dense porous network of F group hydrogels provided a confined space for cells which resulted in cells with decreased spreading area, dispersed actin cytoskeleton, and spherical morphology, directing cells towards the chondrocyte phenotype. On the contrary, the P group hydrogels had a larger porous network with relatively flat pore walls, providing flat surfaces for cells to spread, which was beneficial for osteogenic differentiation. This study also confirmed the results obtained by Khetan et al.[47] showing that MSCs tended to undergo osteogenic differentiation in degradable three-dimensional hydrogels, as hydrogels from the P group exhibited faster degradation and higher osteogenic differentiation.[225] Finally, collagen-hyaluronic acid hydrogels with three distinct mean pore sizes (94, 130, and 300 μm) allowed an increase in rat bone marrow MSCs attachment by increasing the pore size.[226] In addition, for smaller pore size, cells adopted a flat morphology, whereas cells presented a rounded morphology for a larger pore size of 300 μm, which is correlated with a higher expression of chondrogenic markers for the largest pores. The chondrogenic differentiation occurring preferably for the largest pores can be explained by a better transport of chondrogenic factors and nutrients, as well as a lower specific surface area which would result in lower cell adhesion ligand density, promoting rounded morphologies and therefore directing cells towards the chondrocyte phenotype.[226]

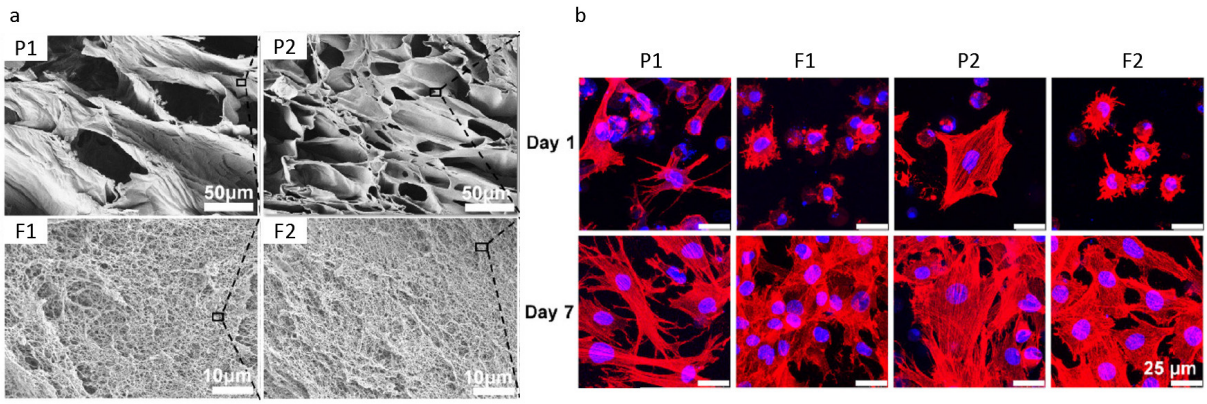

FIGURE 3.4 – a) SEM images of covalently crosslinked type I collagen hydrogels with different pore architecture. Hydrogels of the P group presented a porous network with large and solid walls (pore size of 35 μm for P1 and 20 μm for P2) and hydrogels from the F group displayed a fibrous network with abundant micropores (median pore size of 0.7 μm for F1 and 0.3 μm for F2). b) Phalloidin (cytoskeleton in red)/DAPI (nuclei in blue) staining of rat bone marrow MSCs encapsulated in the hydrogels. Cell area was higher in hydrogels from the P group. Scale bars, 25 μm. Adapted from [225]

3.4.3 Mechanical properties

The key to control and direct stem cell commitment into specific cell types required for regenerative medicine is thought to lie in mimicking the properties of the extracellular matrix (ECM) of cells. This goes through surface conjugation with biomolecules, which will be discussed in the next section, and the control of the mechanical properties of the matrix. Indeed, considering that cells mechanical microenvironments can be as physically diverse as brain, muscle, cartilage or bone, it is thought that glass or plastic dishes, commonly used for standard in vitro cell culture, fail to provide proper environment for cell growth and differentiation.[227] Hence, over the past 15 years, a particular effort has been devoted to the development of hydrogels with tunable stiffness mimicking native tissues to study the impact of stiffness on cell adhesion, proliferation, and stem cells differentiation.

In particular, covalently crosslinked polyacrylamide hydrogels have been extensively used for such studies, as they offer the possibility to simply modulate hydrogel stiffness by varying their crosslinker content.[206] In pioneering work, Engler and colleagues synthesized polyacrylamide gels with varying stiffness and coated them with type I collagen to evaluate the effect of stiffness on human bone marrow MSCs differentiation (Figure 3.5a).[52] They demonstrated that MSCs grown on soft matrices mimicking brain tissue (0.1 - 1 kPa) tended to develop branched morphology and to express higher level of neurogenic differentiation markers, whereas on matrices with intermediate stiffness close to the modulus of muscle (8 - 17 kPa), cells exhibited a spindle-shape typical of myoblasts, with greater expression of myogenic markers.[52] Finally, MSCs cultured on more rigid matrices mimicking the stiffness of osteoid (25 - 40 kPa), a collagen matrix secreted by osteoblasts, became polygonal in shape, similar to osteoblasts and showed an up-regulation of osteogenic markers.[52] These results suggest that optimizing the matrix mechanical properties could be a powerful tool to direct stem cells differentiation into a specific lineage. This hypothesis has been confirmed ever since by many other studies which are summarized in Table 1. Briefly, neurogenic[52, 53, 60, 62] and adipogenic[54, 55, 56, 61, 228] differentiation have been found to be predominant on soft matrices (from 0.1 to 5 kPa), myogenic commitment has been shown to be mostly encouraged for stiffnesses between 8 and 40 kPa[52, 53, 55, 60, 69, 229], while tenogenic differentiation was favored for stiffnesses between 30 and 50 kPa.[57] In addition, Yang et al. demonstrated that a soft matrix, with a stiffness close to that of bone marrow (2 kPa), would allow MSCs to maintain their stem cell phenotype.[230] Finally, the results obtained for chondrogenic and osteogenic differentiation were more heterogeneous, with chondrogenic differentiation reported both on soft matrices (0.5 - 1.5 kPa)[58, 59] and stiffer matrices (80 kPa)[60], and osteogenic differentiation mentioned for a wide range of stiffnesses going from 1.5 up to 190 kPa[52, 54, 56, 57, 58, 59, 60, 61, 62, 63, 69, 228, 230, 231, 232, 233], although it would be predominant between 20 and 60 kPa. Such inhomogeneity in the results could be explained by the use of a broad range of techniques to evaluate hydrogels stiffness, which complicates

the comparison between the different studies. In addition, Trappmann et al. showed different results depending on the substrate used, as they obtained a stronger adipogenic differentiation of MSCs on soft polyacrylamide gels (0.5 kPa) and a stronger osteogenic differentiation for stiffer matrices (20 and 115 kPa) (Figure 3.5b and c), but they did not observe any effect of the stiffness on MSCs differentiation for PDMS substrates.[55] These results have been explained by the fact that cells do not pull directly the hydrogel matrix, but the covalently attached collagen on the surface of the gel. Consequently, the strains applied by cells are resisted by the attached collagen and the resistance is correlated to the number of anchorage points of collagen on the underlying matrix. Thus, by reducing the anchoring density of collagen on a gel with a stiffness of 20 kPa, cells did not exhibit the typical behavior for a stiffness of 20 kPa but behaved as if they were on a gel with a stiffness of 2 kPa.[55] These findings can explain the different behavior of cells between polyacrylamide hydrogels and PDMS, as well as the discrepancies observed over the literature. Finally, as most in vitro studies focused on cell state under static conditions at a particular time point, Lee et al. studied whether changing the biophysical aspects of the substrate could modulate the degree of MSCs lineage specification.[62] They explored MSCs osteogenic and neurogenic differentiation on soft (0.5 kPa) or stiff (40 kPa) hydrogels followed by transfer of the cells to gels of the opposite stiffness. They observed that transferred MSCs, from soft to stiff gels, tended to decrease the expression of neurogenic markers and to increase the levels of osteogenic markers to levels that were comparable to cells that were cultured on the stiff gels alone. In the same way transferred MSCs from stiff to soft gels showed a decreased expression of osteogenic markers and an increased expression of neurogenic markers as compared to cells maintained in culture on stiff substrates which mostly express osteogenic markers. Though, the expression of osteogenic marker remained elevated compared to MSCs that were cultured on soft gels, indicating that transferring MSCs from stiff to soft substrates does not lead to a complete lineage reversal.[62]

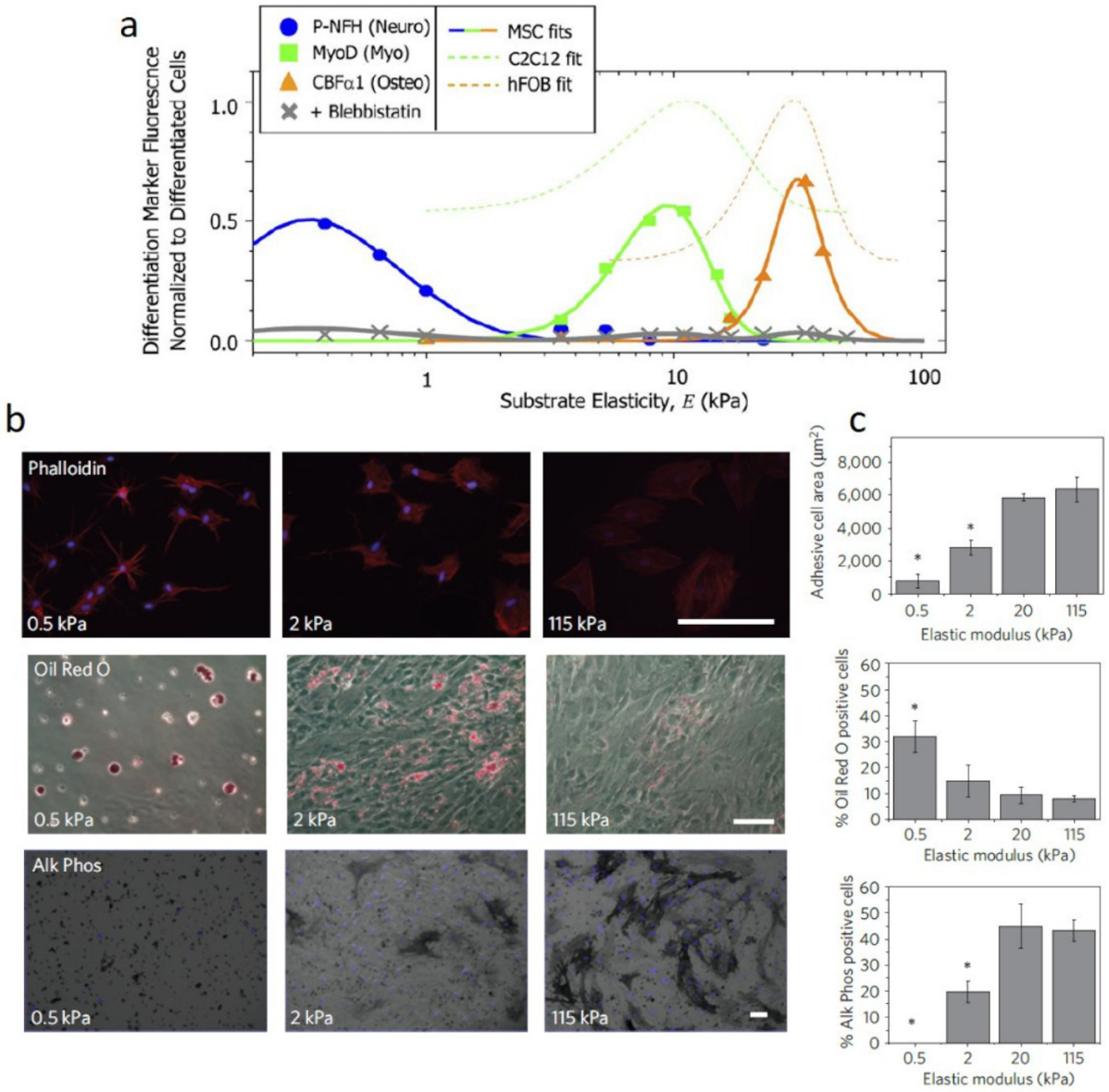

FIGURE 3.5 – a) Fluorescence intensity of human bone marrow MSCs differentiation markers versus substrate elasticity revealed maximal lineage specification at the stiffness typical of each tissue type. Average intensity was normalized to peak expression of control cells (murine myoblasts C2C12 or human osteoblasts hFOB). Blebbistatin blocked all marker expression in MSCs. Adapted from [52] b) F-actin staining (phalloidin staining ; red), Oil Red O and alkaline phosphatase (Alk Phos) staining of human MSCs on polyacrylamide hydrogels. Nuclei were counterstained with DAPI (blue). Scale bars, 200 μm. c) Quantification of MSCs spreading after 24 h and differentiation after 7 days (Oil Red O for adipogenic differentiation and Alk Phos for osteogenic differentiation) in culture on polyacrylamide hydrogels (* $p<0.05$). Cell spread area and osteogenic differentiation increased with hydrogel stiffness but remained constant from a stiffness of 20 kPa, while adipogenic differentiation increased for decreasing stiffness. Adapted from [55]

Stem cell source	Hydrogel	Surface coating	Culture medium	Stiffness	Differentiation	Ref.
h-BM MSCs	PAM	type I collagen	Growth medium	0.1-1 kPa 8-17 kPa 25-40 kPa	Neurogenic 0.1-1 kPa Myogenic 8-17 kPa Osteogenic 25-40 kPa	[52]
h-BM MSCs	PAM	type I collagen	Growth medium	0.7 - 9 - 25 - 80 kPa	Myogenic 25-80 kPa Osteogenic 80 kPa	[69]
h-BM MSCs	PAM	type I collagen	Growth medium	7 - 19 - 27 - 42 kPa	Osteogenic 42 kPa	[63]
h-BM MSCs	PAM	type I collagen	Growth medium	1 - 3 - 7 - 15 kPa	Adipogenic 1 kPa Myogenic 15 kPa	[61]
h-MSCs	PAM	type I collagen	Mixed osteogenic and adipogenic medium	0.5 - 2 - 20 - 115 kPa	Adipogenic 1 kPa Osteogenic 20 - 115 kPa	[55]
	PDMS			0.1 - 40 - 800 kPa	No impact	
h-BM MSCs	PAM	type I collagen	Growth medium	gradients 10 to 30 30 to 50 70 to 90 kPa	Tenogenic 30 to 50 kPa Osteogenic 70 to 90 kPa Osteogenic 30 to 50 kPa and 70 to 90 kPa	[57]
		fibronectin				
h-BM MSCs	PAM	type I collagen	Osteogenic medium	1.5 - 26 kPa	Osteogenic 26 kPa	[231]
h-MSCs	PAM	type I collagen	Growth medium	1.6 - 40 kPa	Chondrogenic 1.6 kPa Osteogenic 40 kPa	[58]
h-ASCs	PAM	type I collagen	Growth medium	4 - 13 - 30 kPa	Adipogenic 4 kPa Osteogenic 30 kPa	[56]
h-BM MSCs	PAM	fibronectin	Growth medium	0.5 - 40 kPa	Neurogenic 0.5 kPa Osteogenic 40 kPa	[62]
h-MSCs	PAM	fibronectin	Growth medium	15 - 37 - 50 - 63 kPa	Osteogenic 63 kPa	[233]
mouse-BM MSCs	PAM	fibronectin	Growth medium	15 - 50 - 63 kPa	Osteogenic 63 kPa	[232]
h-MSCs	gelatin-HPA	/	Growth medium	0.6 - 2.5 - 8 - 13 kPa	Neurogenic 0.6 kPa Myogenic 13 kPa	[53]

mouse-MSCs / h-MSCs	alginate	RGD peptide	Mixed osteogenic and adipogenic medium	2.5 - 5 - 12 - 20 - 110 kPa	Adipogenic 2.5 - 5 kPa Osteogenic 12 - 20 kPa	[54]
rat-BM MSCs	collagen-GAG	/	Growth medium	0.5 - 1 - 1.5 kPa	Chondrogenic 0.5 kPa Osteogenic 1.5 kPa	[59]
h-BM MSCs	gelatin-HA	/	Adipogenic or osteogenic medium	0.15 - 1.5 - 4 kPa	Adipogenic 4 kPa Osteogenic 4 kPa	[228]
h-MSCs	silk fibroin	/	Growth medium	6 - 20 - 33 - 64 kPa	Myogenic 33 kPa	[229]
h-BM MSCs	PEG	RGD peptide	Mixed osteogenic and adipogenic medium	2 - 12 kPa	Stem cell 2 kPa Osteogenic 12 kPa	[230]
h-BM MSCs	PVA-HA	/	Growth medium	gradient 20 to 200 kPa	Neurogenic 20 kPa Myogenic 40 kPa Chondrogenic 80 kPa Osteogenic 190 kPa	[60]

TABLE 3.1 – Differentiation of mesenchymal stem cells seeded on hydrogels with varying stiffness. h = human, BM MSCs = bone marrow mesenchymal stem cells, ASCs = adipose stem cells, PAM = polyacrylamide, PDMS = polydimethylsiloxane, HPA = hydroxyphenyl propionic acid, GAG = glycosaminoglycan, HA = hyaluronic acid, PEG = polyethylene glycol, PVA = polyvinyl alcohol.

Besides cell differentiation, it has been shown that matrix stiffness has a great impact on cell adhesion, spreading and proliferation. Many studies agree on the fact that cell area increases with matrix stiffness, with small and round cells with few stress fibers and focal adhesions on soft substrates, and highly spread cells with organized actin cytoskeleton and focal adhesions on stiff substrates.[52, 58, 61, 69, 230, 234] In addition, cell attachment and proliferation have been reported to be greater on stiffer matrices.[53, 58, 69, 229, 232] These observations would be explained by the fact that MSCs, as well as other cell types, can sense the rigidity of the substrate by exerting contractile forces, thanks to cell receptors as integrins, which can cluster into complexes known as focal adhesions that allow cell adhesion to the matrix. Focal adhesions can connect the substrate to cell cytoskeleton, providing physical links between mechanical environment and intracellular contractile architecture.[64] It is believed that cells on soft gels need to be less contractile than on stiff gels to adhere to the matrix. This is correlated with highly spread cells with organized actin cytoskeleton and stable focal adhesions

on stiff gels, which maintain cell contractility, and more round cells with dynamic adhesions and no cytoskeleton organization on soft substrates.[65] Finally, as the cytoskeleton is associated with nuclear structures, the physical properties of cells are linked to gene expression.[66] In summary, matrix stiffness influences cell spreading and cytoskeleton organization which, in turn, drives cell differentiation through different pathways that have unfortunately not all been elucidated yet.

In this context, hydrogel substrates can also serve as a powerful tool for the measurement of traction forces exerted by cells on the extracellular matrix. The general method consists in cultivating cells on top of hydrogels containing thousands of fluorescent beads and following the displacements of the beads to calculate cell generated forces. For example, polyacrylamide[235, 236] or agarose[237] hydrogels have been used to study the distribution of forces exerted by fibroblasts or even metastatic breast adenocarcinoma cells in 2D culture. This method enabled to follow the dynamic mechanical interaction of the cells and their substrate and to characterize the location and magnitude of the traction forces. The same methodology was applied for 3D cell culture as it is more representative of the in vivo cell behavior. As such, Legant et al. encapsulated fibroblasts in 3D polyethylene glycol hydrogels containing around 70000 fluorescent beads and tracked the displacements of the beads in the vicinity of each cell to obtain a three-dimensional map of cell induced deformations.[238] Although these studies can provide useful results for the understanding of cell-matrix interactions, they have been conducted mainly with fully differentiated fibroblasts. Consequently, individual studies are required to investigate the behavior of different cell types, as the results obtained with fibroblasts are not directly transposable to other cells.

Although it is clear that matrix stiffness has a great impact on stem cell fate, it is now acknowledged that the mechanical properties of hydrogels and living tissues are not limited to elasticity, but include viscoelastic properties. Viscoelastic materials first resist to cell generated forces because of their elasticity, and then dissipate the applied forces over time due to their viscoelastic response, which can dramatically alter cell behavior.[66] However, only few studies investigated the impact of hydrogels viscoelastic properties on cell adhesion, proliferation, and stem cell differentiation. For example, Cameron et al. varied the formulation of polyacrylamide hydrogels to obtain matrices with a constant elastic modulus (4.7 kPa) and with varying viscous modulus (1, 10, 130 Pa).[67] They showed that human bone marrow MSCs spread area and proliferation increase with the viscous modulus. In addition, adipogenic, myogenic, and osteogenic differentiation were enhanced for the highest viscous modulus, in the presence of differentiation supplements.[67] Similarly, Charrier et al. developed polyacrylamide hydrogels with a constant elastic modulus (5 kPa) with varying viscous modulus (0, 200, 500 Pa) by entrapping linear polyacrylamide into the hydrogel network.[94] They observed that mouse fibroblasts had overall smaller areas on viscoelastic gels

than on purely elastic gels. In addition, they showed that the percentage of rat hepatic stellate cells undergoing myofibroblast differentiation decreased as the viscous modulus increased, and that differentiated cells had the ability to de-differentiate on substrates with higher viscous modulus.[94] Chaudhuri and colleagues compared the effect of covalently crosslinked alginate hydrogels (elastic substrates) and chemically crosslinked alginate hydrogels (stress relaxing substrates) of varying elastic modulus (1.5, 3, 9 kPa) on the spreading of human osteosarcoma cells and mouse fibroblasts.[95] They confirmed that the cell-spreading area increases with the hydrogel stiffness and they observed enhanced cell spreading on stress-relaxing substrates relative to elastic substrates, with greater cell focal adhesion formation and higher number of cells forming stress fibers.[95] Using similar hydrogels, Bauer et al. showed that mouse myoblasts had a significantly higher cell-spreading area as the elastic modulus was increased from 2.8 kPa to 49.5 kPa on elastic gels, while for stress-relaxing gels, the cell-spreading area increased from 2.8 to 12.2 kPa, but did not further increase with higher modulus.[96] However, myoblast proliferation was higher on stress-relaxing substrates as compared to elastic substrates for all investigated elastic moduli.[96] In another study, Chaudhuri et al. developed alginate hydrogels using different molecular weight polymers in combination with different crosslinking densities of calcium to obtain matrices with constant elastic modulus but different relaxation time.[68] They evidenced that both spreading and proliferation of mouse fibroblasts increase with faster stress relaxation, for a constant elastic modulus of 9 kPa. Moreover, they observed adipogenic differentiation of human MSCs for an elastic modulus of 9 kPa, with the level of adipogenesis decreasing in rapidly relaxing gels, and very low levels of osteogenic differentiation. In contrast, no adipogenic differentiation was observed for a higher initial elastic modulus of 17 kPa, while osteogenic differentiation was significantly enhanced in gels with faster stress relaxation (Figure 3.6).[68] These studies highlight the importance of considering the effect of both elasticity and viscoelastic properties on cell behavior, as they can have a great impact on cell adhesion, proliferation, and differentiation. In addition, these results seem to show that cell response to varying viscoelastic properties might depend on cell type. Consequently, more efforts should be dedicated to such studies in order to provide tools for the control of cell behavior for regenerative medicine purposes, as they are still lacking today. Finally, hydrogel materials offer many possibilities for mimicking the mechanical properties of the extracellular matrix and providing a suitable environment for controlled cell growth and fate.

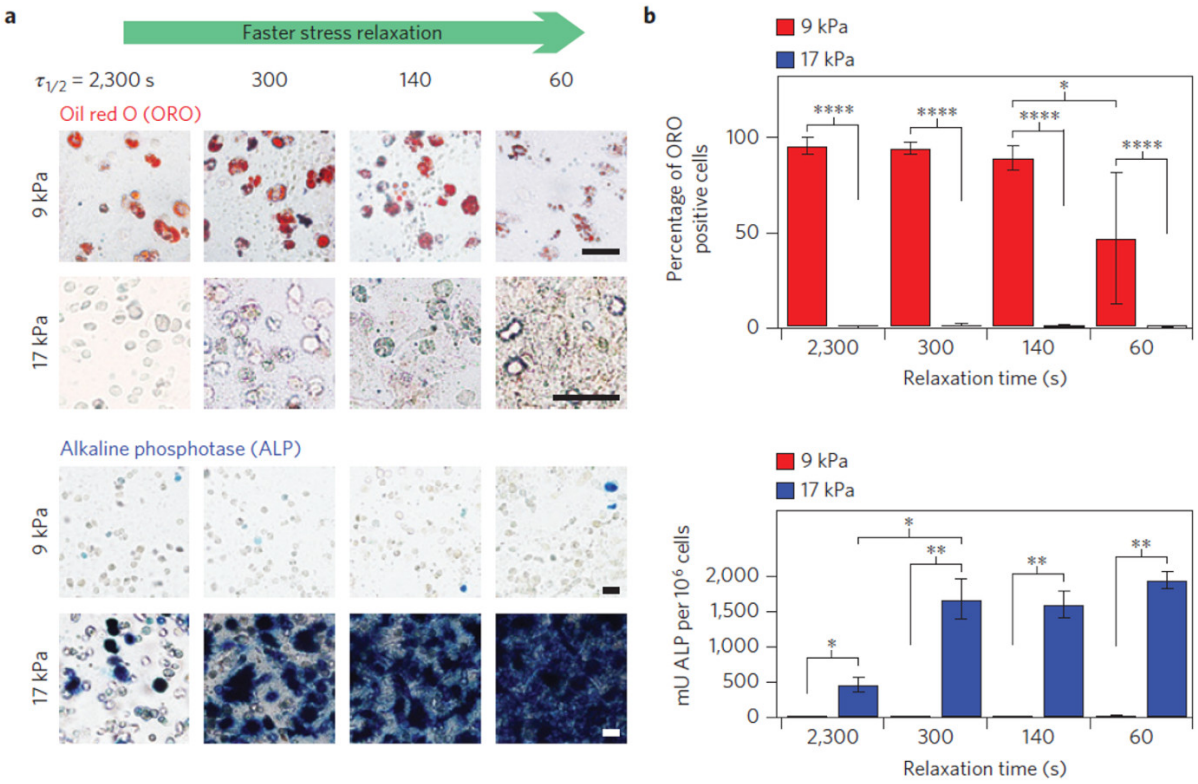

FIGURE 3.6 – a) Representative images of Oil Red O (ORO) staining (red), indicating adipogenic differentiation, and alkaline phosphatase (ALP) staining (blue), indicating early osteogenic differentiation, for human MSCs cultured in alginate gels of indicated modulus and timescale of stress relaxation for 7 days. Gels were functionalized with RGD peptide to promote cell adhesion. Scale bars, 25 μm. b) Quantification of the percentage of cells staining positive for ORO, and a quantitative assay for alkaline phosphatase activity from lysates of cells in gels from the indicated conditions at 7 days in culture. *, **, and **** indicate $p < 0.05$, 0.01, and 0.0001 respectively. Adipogenesis occurred preferably for a soft gel with long relaxation times, while osteogenesis was favored on a stiffer gel with short relaxation times. Adapted from [68]

3.4.4 Bio-functionalization

Over the past years, the conception of biomaterials has evolved from inert materials, which do not interact with the cells of the host organism, into sophisticated substrates with the capability to communicate with cells and direct their fate.[71, 239] Specifically, tuning the biochemical cues of the substrate has been identified as a promising way to direct cell fate. Many studies have therefore investigated the impact of several signaling molecules, such as growth factors, extracellular matrix proteins, and peptides, on cell behavior in terms of adhesion, spreading, and differentiation.[239] If these cues can be presented to cells in a soluble form, their immobilization on the material generally improves their stability and provides better control over their density and orientation.[71, 239] In the natural in vivo environment, it is acknowledged that cell adhesion and differentiation are partly mediated by the interaction with various proteins anchored in the ECM, which is mainly driven by

integrin receptors.[71] MSCs reside in a niche made up of neighboring cells and the ECM infused with autocrine and paracrine soluble growth factors notably.[240] Cellular behavior depends on the abundance and distribution of bioactive factors in the ECM, which undergoes remodeling[241] as a result of cells self-renewal and differentiation.[242] For instance, during MSCs proliferation, the native ECM has a higher concentration in fibroblast growth factor-2 (FGF-2)[243], while the ECM is richer in bone morphogenic protein-2 (BMP-2) during osteogenic differentiation. Therefore, the classical approach in materials biofunctionalization consists in mimicking the cellular microenvironment through interaction with growth factors, proteins, and peptides.[71] Growth factors are soluble molecules that stimulate cell growth, differentiation, survival, and tissue repair through specific binding of transmembrane receptors on target cells.[136] The immobilization of growth factors and proteins to biomaterials prevents the loss of bioactivity caused by their progressive release from the material in the soluble form.[136] Nevertheless, the use of full-length proteins is limited by the complexity and high costs of production and purification, as well as their lack of stability, as they are very susceptible to changes of pH, temperature, and solvents-induced conformational changes.[71] In addition, proteins generally present different binding sites that interact with various cell receptors and might trigger unwanted cellular responses.[239] The use of synthetic peptides, derived from a particular sequence of a full-length protein, might circumvent these limitations as they can be produced in large quantities with high purity and at low cost. Moreover, they are more stable to pH and temperature changes, and they can be tuned to introduce anchoring units to allow their binding to the surfaces without losing their biological activity.[71] Finally, besides biomolecules, some attention is also given to studying the effect of different chemical functional groups on cell behavior.

If it is known that the ECM is composed of different proteins, it can also be considered at a smaller scale as it contains specific chemical functional groups depending on the type of tissue. Indeed, carboxylic acid functionalities are typical of cartilage, as it is rich in glycosaminoglycans, while phosphates are highly present in mineralized tissue forming bone, and hydrophobic functional groups are characteristics of adipose cells as they are rich in lipids and release fatty acids.[244] For example, Wang et al. synthesized PEG hydrogels (PEG), PEG hydrogels containing phosphate groups (PhosPEG), or copolymer hydrogels of PEG and PhosPEG (PhosPEG-PEG), and showed that only PhosPEG-PEG gels promoted osteonectin, collagen I and ALP production of goat MSCs, indicating an enhanced osteogenic differentiation.[245] In addition, calcium deposition was higher for the copolymer hydrogels. The authors explained these differences by the degradation rate of the various hydrogels, arguing that the presence of cleavable phosphoesters allowed PhosPEG-PEG hydrogels degradation which promoted mineralization by converting the phosphoesters into insoluble calcium phosphate, which did not occur for PEG gels. Finally, for PhosPEG gels, the degradation rate might be too high to promote differentiation and matrix deposition.[245]

Using polyacrylamide hydrogels modified by plasma treatment to create surfaces with amino groups, carboxyl groups, or phosphate groups, Lanniel et al. evidenced that human MSCs differentiation was impacted by the combination of surface chemistry and matrix stiffness.[246] MSCs exhibited higher neurogenic differentiation for matrices with carboxyl groups and a stiffness of 6.5 kPa, while myogenic differentiation was enhanced for a stiffness of 10 kPa and carboxyl groups, and osteogenic differentiation was favored for a stiffness of 41 kPa and phosphate groups.[246] Similarly, Benoit et al. demonstrated that human MSCs cultured on PEG hydrogels carrying acid, phosphate, and t-butyl groups tended to differentiate into chondrocytes, osteoblasts, and adipocytes, respectively.[244] However, it is not clear whether these observations are due to direct interactions with the functional groups or with proteins that would be preferentially adsorbed on materials presenting specific chemical environments. Indeed, it has been demonstrated that human bone marrow MSCs had limited attachment on PEG hydrogels or phosphate functionalized PEG hydrogels (PhosPEG) without serum in the culture medium, while PhosPEG gels promoted significantly higher cell attachment and spreading in the presence of serum compared to control PEG hydrogels, as PhosPEG hydrogels promoted higher protein adsorption.[247] In the same way, Ayala et al. controlled surface hydrophobicity of polyacrylamide based hydrogels by varying the alkyl chain length of pendant side chains, terminated by a carboxylic acid function, to evaluate the impact on human MSCs behavior and protein adsorption.[248] It has been observed that cell adhesion and cell surface area increased progressively when increasing the length of the alkyl chain from one carbon (C1) to five carbons (C5), but decreased for six (C6), seven (C7), or ten carbons (C10). After 14 days of culture in osteogenic culture medium, several osteogenic markers were expressed for cells on C5 hydrogels while they were not detected for cells on C3 hydrogels (Figure 3.7). When cultured with myogenic culture medium, MSCs stained positive for myogenic markers on C5 hydrogels, while they underwent cell death on C3 hydrogels. These results were correlated with protein adsorption as these hydrogels were found to selectively adsorb fibronectin and laminin from the serum, with little proteins found on C1, C3, and C7 hydrogels, and abundant proteins adsorbed on C5 hydrogels. These observations were explained by the fact that the side chain must be sufficiently long to allow the terminal carboxyl groups to reach the binding sites on the proteins, explaining the small adsorption of proteins for hydrogels with short alkyl chains. However, when the side chains are too long, they become more hydrophobic and collapse onto the surface of the hydrogel, decreasing the accessibility of carboxyl groups for binding.[248] Therefore, MSCs response to surface chemistry is likely to be attributed to differences in protein adsorption rather than direct interaction with varying chemical groups (acid, phosphate, t-butyl groups, and alkyl chains).

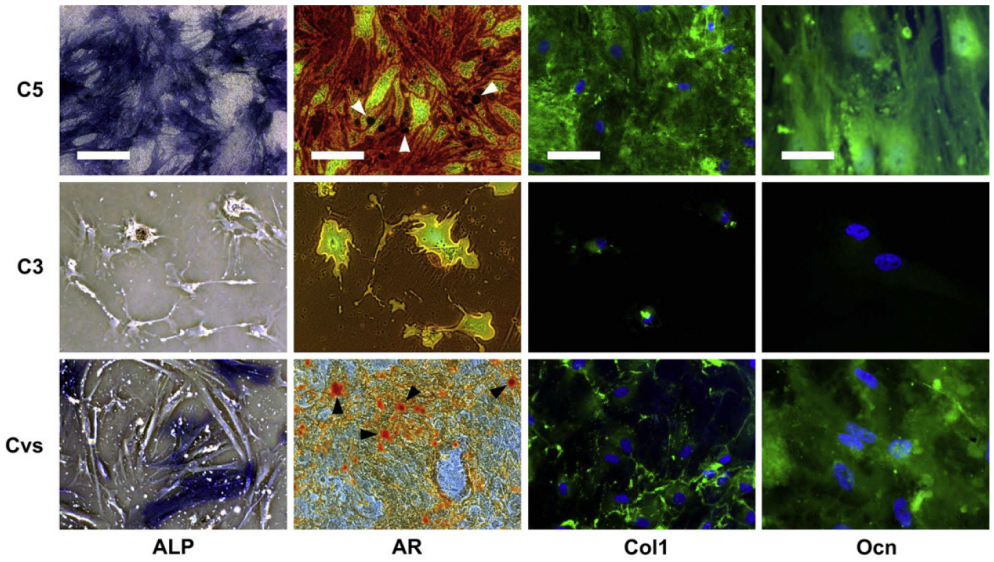

FIGURE 3.7 – Osteogenic differentiation of human MSCs cultured on polyacrylamide based hydrogels carrying surface alkyl chains with 3 (C3) or 5 (C5) carbons and on glass coverslips (Cvs). Alkaline phosphatase (ALP) staining at 14 days in osteogenic medium. Alizarin red S (AR) and immunofluorescent (green) staining for collagen I (Col1) and osteocalcin (Ocn) after 21 days. White (C5 hydrogels) and black (glass coverslips) arrowheads, in alizarin red S staining, point to calcium nodules. Scale bars, 200 μm (ALP), 100 μm (AR and Col1), and 50 μm (Ocn). The C5 hydrogels led to higher osteogenesis. Adapted from [248]

The ECM is composed of different proteins, which interact with cell surface receptors, as well as growth factors. If growth factors are usually solubilized in the culture medium for in vitro culture, the in vivo configuration is different as these molecules are sequestered in the ECM and interact with nearby cells.[249] In addition, as proteins and growth factors have short serum half-lives, their immobilization can increase the persistence of signaling and allows control of the delivered dose.[249] For example, Rowlands et al. immobilized various ECM proteins (collagen I, collagen IV, fibronectin, and laminin) on polyacrylamide hydrogels with varying stiffness (0.7, 9, 25, and 80 kPa) and studied the impact on myogenic and osteogenic differentiation of human bone marrow MSCs (Figure 3.8).[69] It has been found that MSCs osteogenic differentiation occurred predominantly on the stiffest gel (80 kPa) coated with collagen I, which may be attributed to the fact that this combination best mimics the natural microenvironment of bone. The osteogenic marker expression was very low on both collagen IV and laminin coated gels, regardless of gel stiffness, which suggests that cell differentiation is mediated by substrate stiffness in combination with the presented ECM molecule. For myogenic differentiation, the maximum expression of myogenic marker occurred on fibronectin coated gel with a stiffness of 25 kPa. Moreover, it has been observed that collagen I and laminin coated gels showed the highest expression at a stiffness of 80 kPa, while cells cultured on fibronectin and collagen IV coated gels had the greatest expression for a stiffness of 25 kPa, which confirms the interplay between stiffness and adhesive ligand presentation.[69] As different proteins

and different combinations of proteins are susceptible to influence the cell fate, Dolatshahi-Pirouz et al. developed miniaturized human MSC-laden gelatin hydrogel constructs entrapping various proteins, including fibronectin (FN), laminin (LN) and osteocalcin (OCN), to study the impact of these proteins on MSCs osteogenic differentiation.[70] They evidenced that constructs combining several proteins, and especially FN-OCN and LN-FN-OCN, resulted in higher ALP expression and calcium deposition, as compared to individual incorporation of ECM proteins. The authors explained that the functional properties of ECM proteins can be changed through protein-protein interactions, as it causes structural alterations that might expose hidden osteogenic regions on combined proteins, thereby enhancing the osteogenic differentiation of MSCs.[70] While functionalizing the hydrogel with ECM proteins is an approach to direct cell differentiation, the strategy of Benoit et al. consisted in immobilizing heparin on a PEG hydrogel, as heparin is capable of interacting with numerous proteins associated with osteogenic differentiation.[250] The authors showed that hydrogels functionalized with heparin led to higher expression of osteogenic markers of human MSCs as compared to functionalization with RGD peptide (a cell adhesion peptide present in several matrix proteins such as fibronectin, vitronectin, osteopontin and bone sialoprotein[251]) or with both heparin and RGD. These results were explained by a higher binding affinity of heparin with the proteins and growth factors from the culture medium, therefore promoting osteogenic differentiation.[250] The immobilization of growth factors such as transforming growth factor β (TGF-β), which regulates multiple biological processes including embryonic development, adult stem cell differentiation, immune regulation, wound healing, and inflammation[252], was also studied for its potential to direct cell fate. For example, Kopesky et al. observed that adsorbed TGF-β1 onto peptide or agarose hydrogels induced increased chondrogenesis of equine and bovine MSCs over MSCs cultured in TGF-β1-free conditions, and similar chondrogenesis to MSCs cultured with TGF-β1 in the culture medium.[253] In addition, agarose hydrogels with adsorbed TGF-β1 stimulated the production of full-length aggrecan, a constituent of cartilage, while the presence of TGF-β1 in the culture medium led to aggrecan cleavage. However, tethered TGF-β1 neither stimulated accumulation of cartilage components nor induced proliferation of MSCs encapsulated in hydrogels, which might be explained by a lower accessibility of TGF-β1 and by the accumulation of newly secreted matrix proteins that may block tethered TGF-β1 from cell receptors.[253] On the contrary, McCall et al. showed that tethered TGF-β on PEG hydrogels, with a concentration higher than 10 nmol.L^{-1}, promoted human MSCs chondrogenic differentiation to a similar extent than chondrogenic culture medium containing soluble TGF-β[86]. Finally, Ding et al. recently evaluated human MSCs differentiation into vascular smooth muscle cells (vSMCs) on PEG hydrogels functionalized with RGD peptides or with both RGD and TGF-β1.[254] They demonstrated that all hydrogels led to higher gene expression compared to undifferentiated MSCs or primary vSMCs cultured on plastic, showing that the expression of vSMCs markers was predominantly regulated by soft matrix environment (stiffness of 5 kPa) regardless of the presence of soluble or tethered TGF-β1. However, cells

on hydrogels with tethered TGF-β1 exhibited greater calcium intake and higher levels of intracellular calcium signaling, as well as greater cell contractility, which are typical features of vSMCs. These results suggested that tethered TGF-β1 is more performant in directing MSCs differentiation towards functional vSMCs compared to soluble TGF-β1 that is generally used.[254]

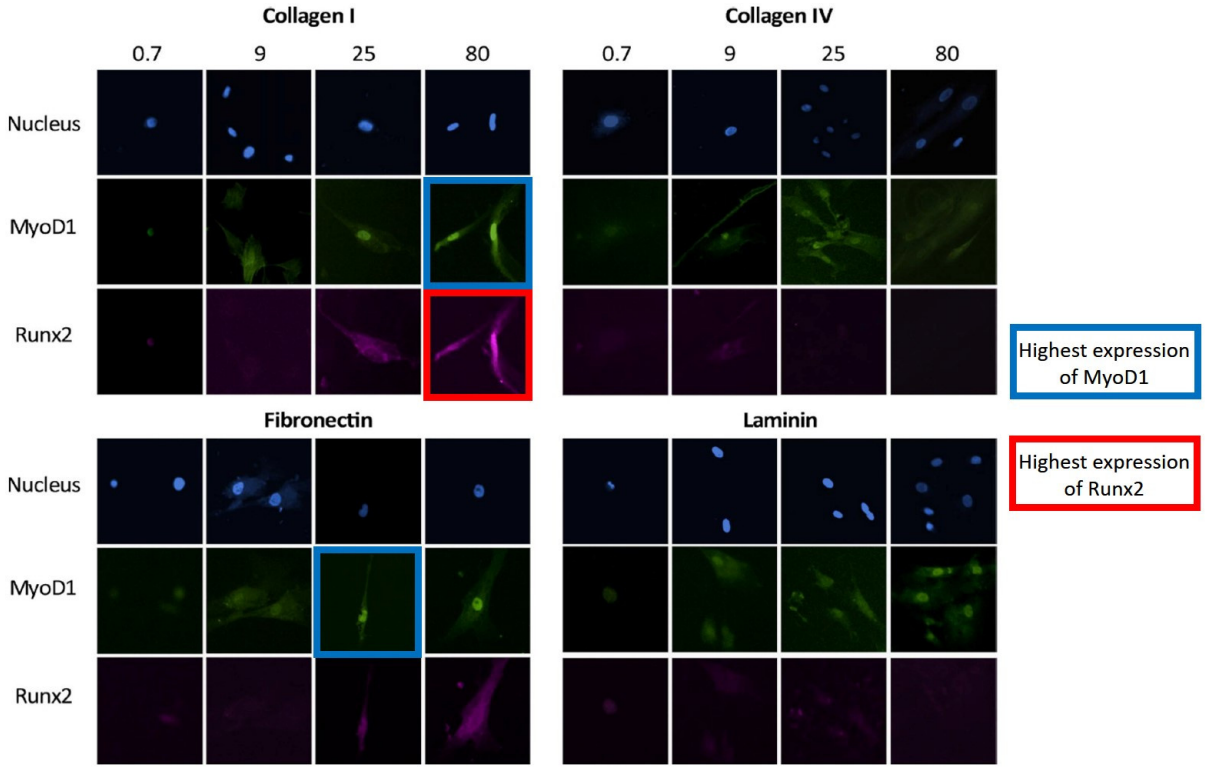

FIGURE 3.8 – Representative images of human MSCs stained for MyoD1 (myogenic marker) and Runx2 (osteogenic marker) cultured on gels of various stiffness and protein coating. Runx2 expression was higher on stiff gels coated in collagen I, whereas MyoD1 was expressed in varying amounts on substrates with a stiffness higher than 9 kPa, regardless of protein coating. Adapted from [69]

Synthetic peptides derived from ECM proteins represent a good alternative to the use of full-length proteins for materials biofunctionalization as they are readily available by synthetic methodologies, with tunable structure and high purity, and their use is exempt of immunogenic risks.[71] One of the first peptidic sequences used for biomaterials functionalization, which is still among the most widely used, is the cell adhesion sequence Arg-Gly-Asp (RGD), isolated from fibronectin.[239] Various studies have tethered RGD peptides on hydrogels, showing that peptides length, structure, and concentration could impact MSCs adhesion and differentiation. For example, Shin et al. showed that MSCs adhesion was not enhanced on hydrogels surface if the molecular weight of the peptide was smaller than the molecular weight between hydrogel crosslinks, as the peptide was buried inside the network and no receptor-

ligand complex was formed.[255] The structure of the peptide is also likely to influence cell behavior as human MSCs osteogenic differentiation was enhanced when encapsulated in alginate hydrogels presenting cyclic RGD peptides over linear RGD peptides, as cyclic peptides might promote more stable cell-ligand bonds.[256] Finally, peptide concentration is another parameter to consider to direct cell fate. It has been evidenced that the production of osteocalcin and ALP of goat MSCs, encapsulated in PEG hydrogels functionalized with RGD peptides, increased with the RGD concentration (from 0.025 to 2.5 mmol.L^{-1}), suggesting greater osteogenesis for the highest RGD concentration.[257] However, no influence of RGD concentration (from 0.1 to 2.5 mmol.L^{-1}) was observed on the osteogenic differentiation of human ASCs cultured on 2D polyacrylamide gels.[56] Peptides derived from other proteins or designed to bind to specific molecules were also investigated. For example, MSCs encapsulated within alginate hydrogels functionalized with RGD or DGEA (Asp-Gly-Glu-Ala) peptides (derived from the $\alpha 2\beta 1$ integrin-binding domain of collagen I) expressed the highest level of osteogenic markers for hydrogels presenting the DGEA peptide.[258] Parmar et al. showed that the incorporation of HA-bound and CS-bound peptides, designed to bind hyaluronic acid (HA) and chondroitin sulfate (CS) respectively, into collagen based hydrogels significantly enhanced the chondrogenic differentiation of human MSCs.[259] Specifically, the HA-bind hydrogels directed the highest increase in chondrogenic genes expression, leading to the greatest total collagen and glycosaminoglycans accumulation as compared to CS-bound hydrogels, RGD hydrogels or hydrogels without surface conjugated peptides.[259] Similarly, hyaluronic acid hydrogels functionalized with a collagen mimetic peptide ($(GPO)_8$-CG-RGDS) promoted greater chondrogenic differentiation of rabbit bone marrow MSCs as compared to gels without surface conjugated peptides.[260] On the contrary, Connelly et al. reported that agarose hydrogels functionalized with three different peptides (a RGD peptide, a collagen mimetic peptide containing the GFOGER motif [Gly-Phe-hydroxy Pro-Gly-Glu-Arg], or a fragment of fibronectin FnIII7-10) led to inhibition of cartilage matrix synthesis and chondrogenic gene expression of calf bone marrow MSCs.[261] These results support their previous observations that RGD peptides inhibited chondrogenic differentiation of calf MSCs encapsulated in alginate gels. In addition, this inhibition increased with increasing bulk densities of RGD in the gel.[262] Vega et al. observed the same trend of chondrogenic differentiation inhibition of human MSCs in hyaluronic acid hydrogels when increasing RGD concentration (from 0 to 5 mmol.L^{-1}).[263] However, they highlighted that a peptide containing the HAV (His-Ala-Val) motif extracted from N-cadherin, a transmembrane protein that mediates cell-cell adhesion and that is important for chondrogenesis, enhanced MSCs chondrogenic differentiation in a dose dependent manner (Figure 3.9a, b, and c).[263] These findings corroborate with the study of Kwon et al. as they evidenced that the inclusion of a HAV peptide into hyaluronic acid hydrogels enhanced human MSCs chondrogenesis in a dose dependent manner. In addition, this effect was lost when the peptide was not permanently linked to the substrate.[264] Similarly, Bian et al. reported that conjugating a HAV peptide to hyaluronic acid hydrogels promoted chondrogenesis of MSCs

and cartilage-specific matrix production as compared to unmodified gels or gels modified with a scrambled peptide.[265] Subcutaneous implantation of MSC-seeded hydrogels in mice also led to superior neocartilage formation in implants functionalized with the N-cadherin mimetic peptide compared with controls.[265] As N-cadherin would also be involved in the early stage of osteogenesis, Zhu et al. investigated the impact of a HAV peptide on human MSCs osteogenic differentiation.[266] It has been demonstrated that hyaluronic acid hydrogels functionalized with the combination of HAV and RGD peptides upregulated the expression of osteogenic markers, including type I collagen, osteocalcin, ALP and Runx2, and led to higher calcium content, as compared to hydrogels with RGD peptide or without peptide. The opposite effect was observed when the N-cadherin peptide was supplemented in the culture medium.[266]

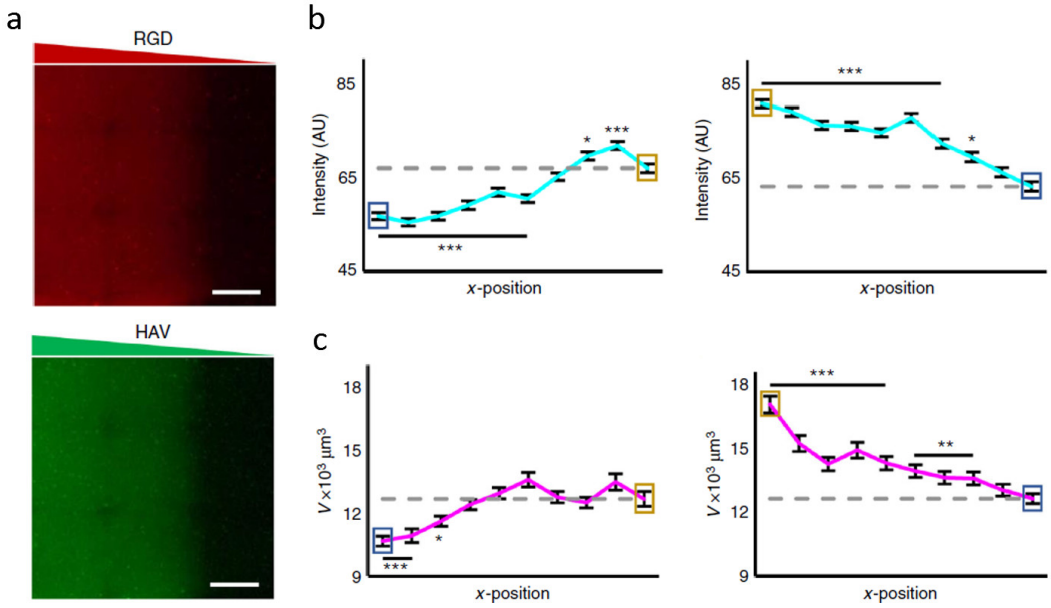

FIGURE 3.9 – a) Rhodamine-labeled RGD (GCGYGRGDSPG) or fluorescein-labeled HAV (HAVDIGGGC) peptide gradients on hyaluronic acid hydrogels. b) Effects of HAV and RGD gradients on transcription factor Sox9 expression (chondrogenic marker). c) Effects of HAV and RGD gradients on aggrecan synthesis. Generally, higher nuclear Sox9 and aggrecan content were observed with decreasing RGD and for increasing HAV. *, **, and *** indicate $p < 0.05$, 0.01, and 0.001, respectively, compared to lowest peptide region (gray dashed line). Adapted from [263]

Bone morphogenetic proteins (BMPs) are a group of bioactive proteins that constitute important inducing factors during embryonic development and are closely related to osteoinduction.[15] Among them, BMP-2 plays a significant role in stimulating the differentiation of MSCs into osteoblasts by regulating the transcription of osteogenesis-related genes such as ALP, type-I collagen, osteocalcin, and bone sialoprotein genes.[15] Consequently, several studies have used peptide sequences derived from the BMP-2 protein to promote MSCs osteogenic differentiation. Particularly, the peptide sequence corresponding to residues 73-92

of the knuckle epitope of recombinant human BMP-2 is mainly used as it would be implicated in osteogenic differentiation of bone marrow MSCs.[267] Alginate hydrogels functionalized with this peptide have been shown to promote higher MSCs ALP activity, as well as calcium and phosphate deposition, than hydrogels functionalized with RGD or DWIVA (Asp-Trp-Ile-Val-Ala, also extracted from BMP-2 protein) peptides, although the use of full-length BMP-2 protein led to the highest ALP activity, and calcium and phosphate deposition.[72] On polyacrylamide-based hydrogels, it has been found that surface modification with BMP-2 mimetic peptides engaged the commitment of human MSCs into osteogenic lineage regardless of the mechanical properties of the substrate (for stiffnesses of 15 and 47 kPa), except for very soft gels (stiffness of 0.76 kPa).[268] In addition, synergistic effects have also been found between the BMP-2 mimetic peptide and other peptides. For example, He et al. showed that the functionalization of poly(lactide-co-ethylene oxide-co-fumarate) hydrogels with both RGD and BMP-2 peptides led to significantly higher ALP activity and calcium production than RGD conjugated or BMP grafted hydrogels.[73] Later, using the same hydrogels, this group confirmed that ALP activity of BMP-2 peptide grafted gels was significantly higher than RGD grafted gels.[269] In addition, they found that gels grafted with a combination of RGD, BMP-2, and OPD (isolated from osteopontin) peptides presented the highest ALP activity and calcium deposition of rat MSCs. This combination has also proven to induce the strongest expression of vasculogenic markers (Figure 3.10).[269] Osteopontin (OPN) is one of the non-collagenous proteins present in bone matrix. OPN is expressed in cells of the osteoblastic lineage and plays a critical role in the maintenance of bone.[270] Another peptide sequence isolated from osteopontin (ODP peptide) and containing the RGD motif has been grafted onto oligo(poly(ethylene glycol) fumarate) hydrogels to investigate the effect of the biomimetic surface on MSCs differentiation into osteoblasts.[271, 272] It has been found that the presence of signaling peptides (RGD and ODP) was favorable for MSCs osteogenic differentiation, although the differentiation and mineralization of the MSCs was not dependent on the peptide sequences used.[271, 272] Identifying proteins sequences responsible for a defined cell response is a key to control cell fate, as Lee et al. showed that the peptide corresponding to the residues 150-177 of human osteopontin allowed for higher ALP activity and mineralization of human MSCs when immobilized on alginate gels as compared to the peptide corresponding to the 53-80 sequence of osteopontin.[273] Finally, as the peptides sequences and the combination of peptides used are susceptible to influence cell fate, the development of microarrays might be an interesting tool for high-throughput screening of cellular behavior in multivariate microenvironments.[274]

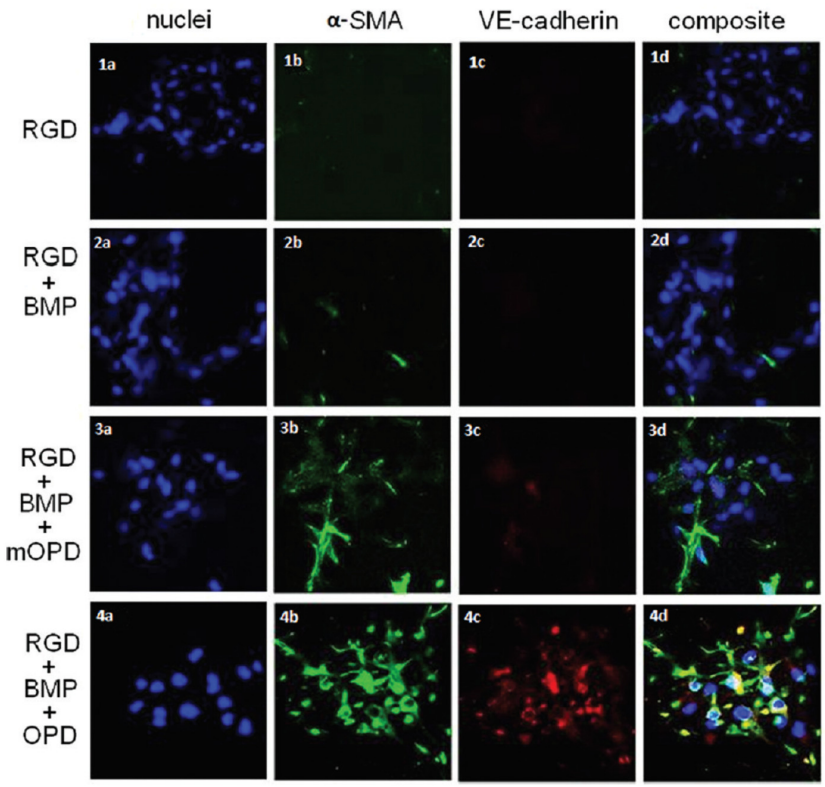

FIGURE 3.10 – Effect of BMP-2 (BMP) and osteopontin (OPD) mimetic peptides grafting on RGD-conjugated hydrogels on the expression of vasculogenic markers of rat MSCs after 28 days of incubation. Hydrogels presenting the combination of RGD, BMP and OPD peptides promoted higher expression of vasculogenic markers. (mOPD = mutant OPD peptide)[269]

In addition to the composition and density of adhesion ligands on a substrate, the spatial distribution of these ligands has also been shown to influence MSCs behavior. For example, Kasten et al. designed adhesive lines of fibronectin with varying width (between 10 μm and 80 μm) and spacings (between 5 μm and 20 μm) onto NCO-sP(EO-stat-PO) cell-repellent hydrogels.[275] This study revealed that human MSCs presented highly aligned actin filaments with decreasing the size of fibronectin lines and a directed migration of cells was observed along the lines as opposed to homogeneous surface coating, with a higher migration rate with decreasing line width. These constructs enabled to direct stem cells migration which would be important for tissue formation and regeneration. In addition, fabricating substrates with line patterns that allow cell bridging over non-adhesive gaps would mimic the ECM architecture as it is comprised of a fibrous network to which cells adhere and form bridges to cross the micron-sized gaps inside the filamentous network.[275] Patterning the adhesive ligands to form different shapes has also proven to be useful for directing MSCs differentiation. Micro-islands of RGD peptide, with different sizes (from 177 to 5652 μm^2) and containing single cells, were made on PEG hydrogels to study the impact of cell size on MSCs differentiation (Figure 3.11a and b).[74] It has been found that small cells preferred adipogenic commitment (from 177 to 1413 μm^2), while large cells preferably underwent osteogenic differentiation (from 2826 to

5652 μm^2).[74] Nano-sized patterns might also influence cell fate as RGD nanopatterns with different spacing (37, 53, 77, 87 and 124 nm) made on PEG hydrogels showed a decreased cell density and spreading area with the increase of nanospacing, unexpectedly related to a higher MSCs osteogenic and adipogenic differentiations, under differentiation culture media, with the increase of RGD nanospacing.[276] These results indicate that micro- and nanopatterns both allow to direct stem cells differentiation, although the effects are different. By varying the patterns shape of several proteins immobilized on polyacrylamide gels, Lee et al. demonstrated that smaller circular features promoted a higher expression of adipogenesis markers (1000 μm^2 > 3000 μm^2 > 5000 μm^2), while cells in anisotropic features such as 4-branched stars and ovals preferred neurogenic differentiation (Figure 3.11c).[75] In addition, MSCs cultured on fibronectin tended to express elevated adipogenic markers while MSCs on collagen tended to express elevated neurogenic markers.[75] In another study, this research team cultured MSCs on unpatterned soft or stiff polyacrylamide gels for 10 days, and then transferred the cells to different stiffness substrates containing patterns of fibronectin (circle, oval, star, or unpatterned ; 5000 μm^2).[62] They highlighted that transferred cells (from soft to stiff) in oval and star shapes showed a higher expression of osteogenic markers compared to cells in other shapes, presumably because these shapes increase cytoskeleton tension which is known to promote osteogenesis. Then, MSCs that were transferred from stiff gels to oval and star shapes on soft gels showed an increased expression of neurogenic markers, demonstrating the importance of anisotropic geometries in guiding the extension of neuron-like processes.[62] These findings corroborated with a third study in which patterned MSCs in circular shapes displayed a disordered cytoskeleton without expression of osteogenic markers, while MSCs cultured in geometries that promoted an increased cytoskeletal tension (elongated oval shape and concave shape) showed a higher expression of osteogenic markers, particularly for a stiffness of 30 kPa.[76]

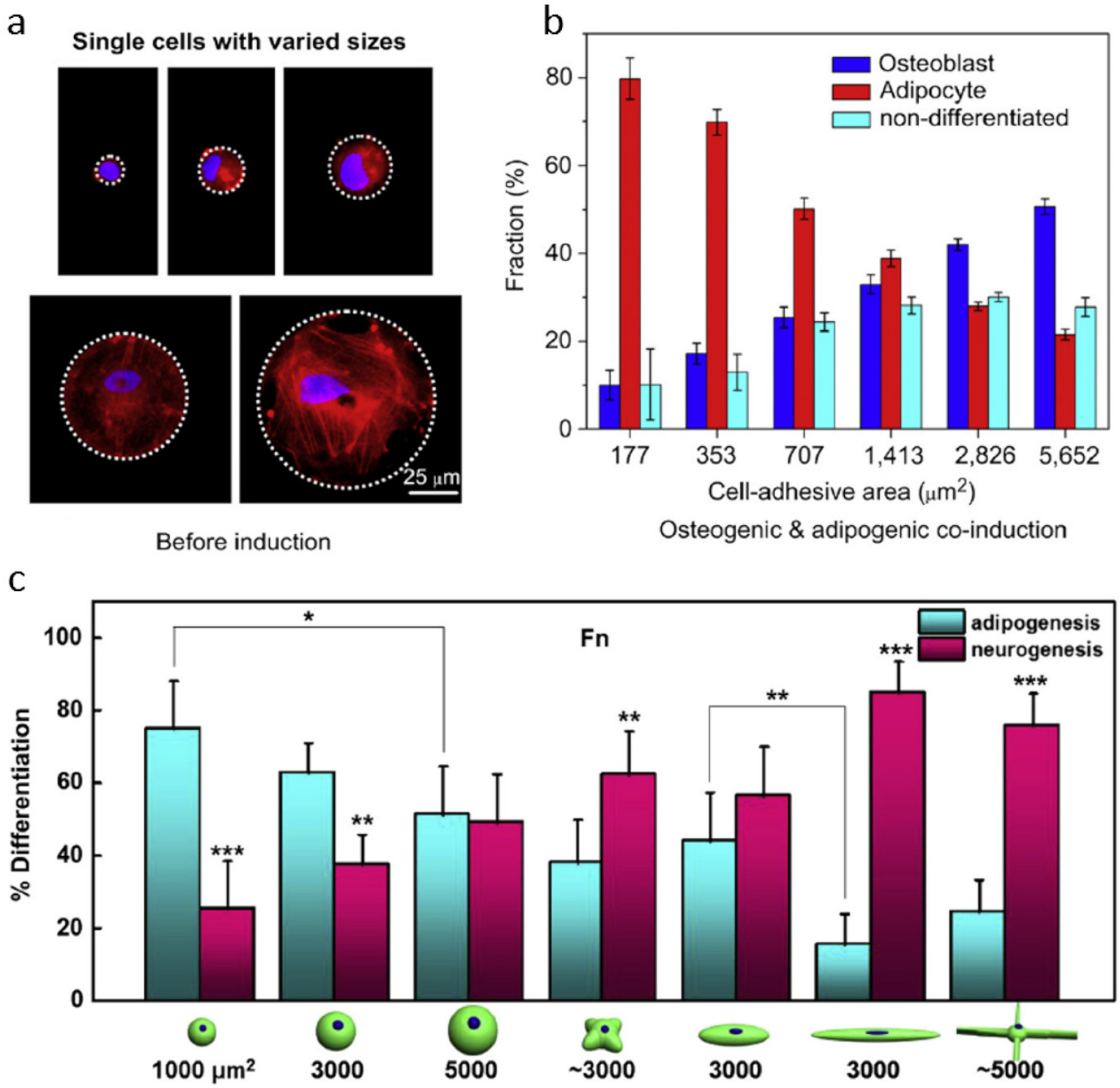

FIGURE 3.11 – Differentiation of single MSCs on microislands of a series of sizes. a) Fluorescent micrographs of single MSCs on microislands of varying size. Red : F-actin, blue : nuclei. b) Percentages of adipogenesis, osteogenesis, and undifferentiation of single MSCs in mixed induction medium for 7 days. Small and large cells preferred to adipogenic and osteogenic commitments, respectively. Adapted from [74] c) Percentage of human MSCs undergoing adipogenesis and neurogenesis on fibronectin patterns on polyacrylamide hydrogels (circular, oval, and star patterns). Smaller circular features promoted adipogenesis, while cells in anisotropic features preferred neurogenic differentiation. *, **, and *** indicate $p < 0.05$, 0.005, and 0.0005 respectively. Adapted from [75]

3.5 Conclusions

It has become clear that biomimetic approaches to modulate cell-material interactions are essential to understand and further control cell behavior, which constitutes invaluable knowledge for the use of stem cells for regenerative medicine purposes. In this context, hydrogels have proven to be good candidates to mimic the in vivo extracellular matrix and to provide a suitable environment for cell growth, whether they are made of synthetic or natural polymers. Indeed, owing to their ability to absorb large amounts of fluids and allow nutrients and growth factors circulation, as well as their capacity to encapsulate cells, hydrogels have shown to maintain cell viability and promote cell growth. In addition, they can be tuned to mimic the properties of the ECM known to affect stem cell behavior and fate, such as physical properties including stiffness, viscoelasticity, pore size, and porosity. Spatial properties are also considered including dimensionality (2D or 3D) of the scaffold, degradation, micro- and nanoscale topography of the surface with varying size, shape, and level of disorder. Finally, biochemical properties are also regarded through the presence of diverse proteins, growth factors or peptides and their spatial distribution. However, experimental studies often focus on some of these aspects, neglecting other important parameters, while the synergy between different cues from ECM is still little studied but is essential to provide long-term robust cell function. Furthermore, the variety of conditions used for cell culture might complicate the interpretations and comparisons between studies using different cell types (MSCs from bone marrow or adipose tissue, and from different animals) and different cell culture media (growth medium or differentiation media, addition of various supplements and growth factors). Although some clues and promising conditions have been identified to control stem cells fate, the differentiation of a population of cells is still not homogeneous and often requires the presence of differentiation culture medium. Nevertheless, the understanding of the influence of these physical, spatial, and biochemical properties on cell fate will enable the development of scaffolds with tailored properties adapted for specific regenerative medicine applications.

RESEARCH PROJECT AND OBJECTIVES

Chapter 4

Research project and objectives

As highlighted in the litterature review, the use of MSCs for clinical applications, including bone regeneration, is still hindered by the lack of control of their in vitro differentiation. This control goes through fundamental studies in order to try to understand MSCs behavior and response to many different features and stimuli. In addition, optimizing cell-material interactions in order to guide cell behavior and obtain the desired cell response for bone reconstruction constitutes an important step for the development of efficient materials for bone replacement. This project therefore rather falls in a fundamental approach as the aim of the project is to use hydrogels as two dimensional cell culture substrates to study the impact of the mechanical properties and the surface functionalization on human bone marrow mesenchymal stem cells osteogenic differentiation. Although this project does not directly aim at developing an implantable material for bone regeneration, the outcomes of this research might be of significant importance for the future development of efficient biomaterials that will interact with the cells.

The 3BIO's research team (Bordeaux) and the LIS laboratory (Québec) have expertise in studying the impact of the surface properties of materials on MSCs behavior, including the presence and distribution of various biomolecules[84, 85, 102, 103, 104], as well as nanotopographies[105, 106, 107, 108, 109]. However, these studies were always conducted on hard materials such as titanium, glass, silicon, and PET (polyethylene terephthalate), that do not mimic the in vivo environment of cells. Therefore, transfering this expertise of surface properties from hard materials to hydrogels that better mimic the natural cell growth environment appeared as a promising approach to further control MSCs differentiation. Indeed, this allows notably to work with materials that better match the mechanical properties of the cells extracellular matrix, which might be favorable for their differentiation. As such, the project is divided into four main objectives.

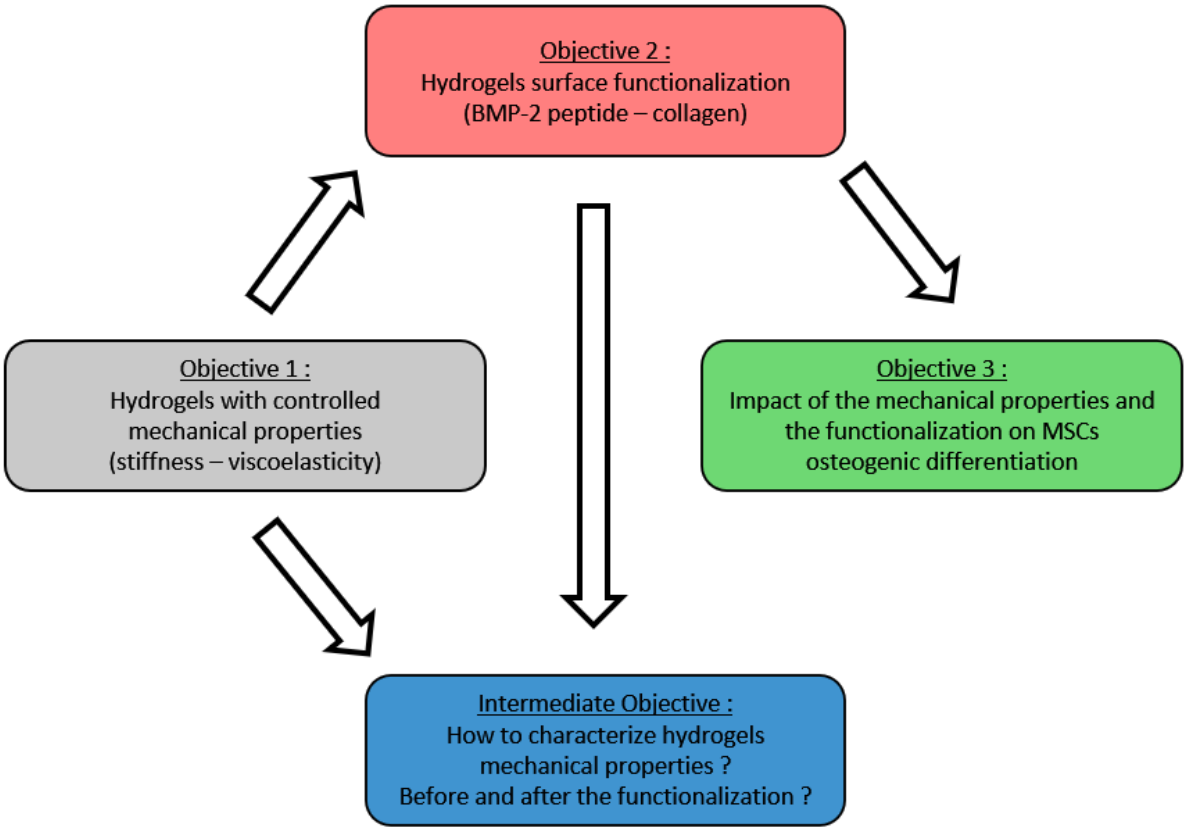

FIGURE 4.1 – Scheme describing the main objectives of the PhD project.

4.1 Objective 1

The first objective consists in synthesizing hydrogels with different and controlled mechanical properties, in terms of stiffness and viscoelastic properties, to further assess their impact on MSCs osteogenic differentiation. Although many studies have reported the impact of hydrogels stiffness on MSCs differentiation, it is now acknowledged that the mechanical properties of hydrogels and living tissues are not limited to elasticity, but include viscoelastic properties. Viscoelasticity is defined as the combination of both solid (elastic) behavior, as the material stores energy and returns to its original state after the deformation, and liquid (viscous)-like behavior, as the material dissipates energy.[277] As shown in the chapter 3, only few studies investigated the impact of hydrogels viscoelastic properties on MSCs differentiation.

As presented in the chapter 2, many different polymers can be used for the synthesis of hydrogels. Considering their ease of synthesis and their highly tunable mechanical properties[35, 36], polyacrylamide based hydrogels have been chosen for this project (Figure 4.2). These properties made them very popular to study the impact of hydrogel stiffness on cells behavior as highlighted in the chapter 3. However, polyacrylamide hydrogels being considered mainly as elastic materials[68], acrylamide has been combined to acrylic acid to

create copolymer hydrogels (Figure 4.2) with distinct viscoelastic properties. As shown in chapter 3, providing hydrogels with controlled stiffness and viscoelastic behavior allows to go further than the literature in the assessment of the impact of the mechanical properties on MSCs differentiation by including the viscoelastic dimension.

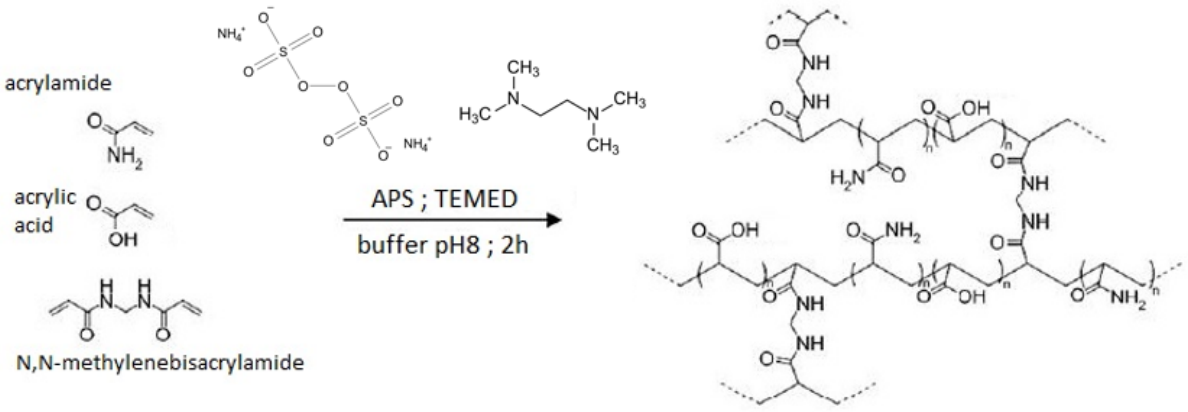

FIGURE 4.2 – Synthesis and structure of poly(acrylamide-co-acrylic acid) hydrogels. Acrylamide and acrylic acid are the monomers that form the polymer chains, while N,N-methylenebisacrylamide is the crosslinker. The radicalar polymerization is initiated by APS (ammonium persulfate) and catalyzed by TEMED (tetramethylethylenediamine). The pH of the reaction mixture is adjusted to 8 for the initiator to be active. The gelation reaction is performed under inert atmosphere (argon) during 2 hours.

4.2 Objective 2

Considering that polyacrylamide based hydrogels do not allow cell adhesion[36], the second objective consists in functionalizing the surface of these hydrogels with proteins or peptides to circumvent the lack of adhesion. In order to avoid any release of the biomolecule during cell culture and to provide a lasting bioactivity to the material, covalent binding of the biomolecule to the surface of the gel appeared as a consistent strategy. Polyacrylamide hydrogels are traditionally functionalized by using the linker Sulfo-SANPAH[55, 56, 69], that can be activated under UV light to react with the amide groups of the gel, and then subsequently reacts with amine groups carried by the protein or the peptide (Figure 4.3). The protocol using Sulfo-SANPAH has been chosen as it is well-established and described in the literature, and reproducible.[55, 56, 69]

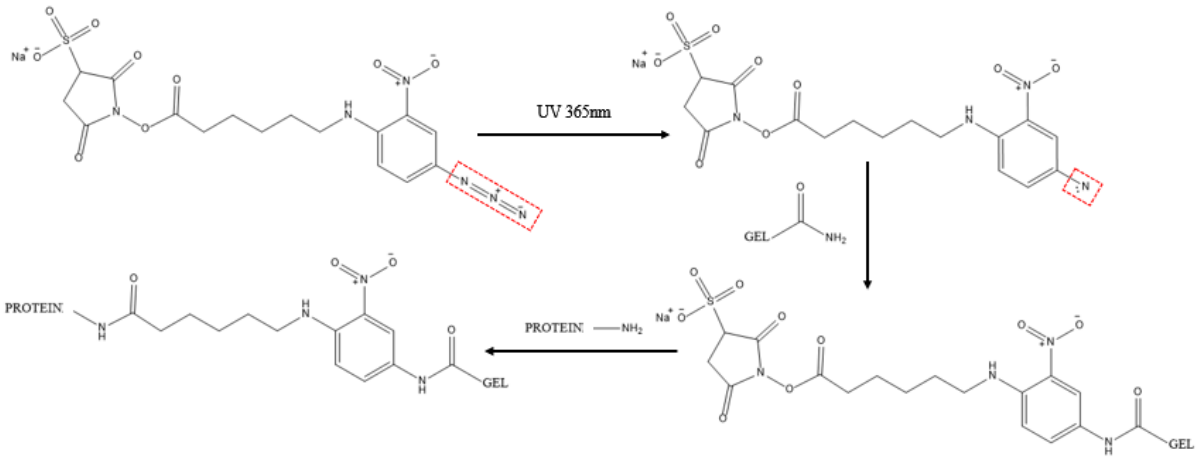

FIGURE 4.3 – Reaction scheme of hydrogels surface functionalization using Sulfo-SANPAH. The azide function of Sulfo-SANPAH is first activated under UV light to react with the amide groups of the hydrogel. Then, the succinimide group of Sulfo-SANPAH is replaced by the protein (or peptide) that reacts via an amine function.

As presented in the chapter 3, many different biomolecules can be used for hydrogels functionalization and to trigger specific cellular responses. Being a part of the cells extracellular matrix, various proteins can be immobilized on the hydrogels, such as collagen I, collagen IV, fibronectin, laminin, osteocalcin, heparin, and others. Type I collagen being the principal component of bone ECM, it is traditionally used for the functionalization of polyacrylamide hydrogels to enable cell adhesion in studies assessing the impact of hydrogels mechanical properties on MSCs differentiation.[52, 55, 56, 57, 58, 61, 63, 69, 231] However, the majority of proteins are produced by recombinant methods using living organisms such as bacteria, or are isolated from tissues. The extraction and purification of proteins is costly and the methods used can result in batch-to-batch variation and differences in biological activity depending on the method used. In addition, the presence of bacterial endotoxins or remnants of immunogenic donor material can lead to safety issues if the proteins are introduced in the body. Full-length proteins may have low solubility and high sensitivity to changes of pH, temperature, and solvents, which can make them difficult to handle.[71] Synthetic peptides, that are short amino acid sequences generally derived from ECM proteins[195], represent a good alternative to proteins for the biofunctionalization of materials.[71] Peptides are readily available by synthetic methodologies and can be produced in large quantities at low cost. In addition, they can be produced with high purity and reproducibility, eliminating variability in biological results, and their use does not present any infection or immunogenic risks. They are more stable to pH and temperature changes, and they can be easily modified to introduce anchoring units to tune their binding to the surfaces.[71] Many different peptides have been studied and applied on various materials for their potential to enhance the adhesion, spreading, proliferation, and osteogenic differentiation of MSCs or osteoprogenitor cells, and are summarized in Table 4.1.

Peptide sequence	Firstly isolated from	Impact on cell behavior	Reference
RGD	Fibronectin	Enhancement of adhesion and spreading of MSCs, osteoprogenitor cells, and osteoblasts	[278, 279]
PHSRN	Fibronectin	Enhancement of adhesion and spreading of MSCs and osteoprogenitor cells	[279]
FN-derived peptides	Fibronectin	Enhancement of adhesion and spreading of osteoblasts	[278, 280]
KRSR	Bone sialoprotein	Enhancement of adhesion and spreading of MSCs and osteoblasts	[278, 279]
FHRRIKA	Bone sialoprotein	Enhancement of adhesion and spreading of MSCs and osteoblasts	[278, 279]
SVVYGLR	Osteopontin	Enhancement of adhesion and proliferation of MSCs	[278, 280]
GFOGER	Collagen I	Enhancement of adhesion, spreading, and osteogenic differentiation of MSCs	[278, 279]
DGEA	Collagen I	Enhancement of adhesion, spreading, and osteogenic differentiation of MSCs	[278, 280]
P15	Collagen I	Enhancement of adhesion, spreading, and osteogenic differentiation of MSCs	[279, 280]
P24	BMP-2	Enhancement of adhesion and osteogenic differentiation of MSCs	[278, 279]
OGP	Blood serum	Enhancement of proliferation and osteogenic differentiation of MSCs and osteoprogenitor cells	[278, 280]

TABLE 4.1 – Examples of peptides used for the functionalization of various materials for their potential to enhance the adhesion, spreading, proliferation, and osteogenic differentiation of MSCs or osteoprogenitor cells. FN-derived peptides can be FNIII9-10/12-14 or FNIII7-10 for example, P15 sequence = GTPGPQGIAGQRGVV, P24 sequence = SKIPKASSVPTELSAISTLYLDDD, OGP (Osteogenic Growth Peptide) sequence = ALKRQGRTLYGFGG.

Among these peptides, the RGD peptide, which corresponds to the minimal binding domain of fibronectin to the integrin receptor, is the most abundantly utilized peptide to induce cell adhesion in synthetic systems.[195] A great number of different RGD peptide sequences have been used in the litterature considering that the nature of the residues surrounding the RGD tripeptide could influence cell receptor affinity and selectivity, and that the distance of

the presented RGD sequence from a surface can also modulate cell adhesion.[281, 282] In addition, varying the structure of the peptide might facilitate the grafting of the peptide on the materials using different chemical reactions.[282] The peptide sequence GRGDSP has been identified as a bioactive sequence and has been widely used in the litterature.[282] Cyclic RGD peptides would also present improved binding properties as compared to linear peptides due to their structural rigidity. Indeed, the structural rigidity conferred by cyclization would prevent the chemical degradation of the peptide and, consequently, increase the stability of cyclic RGD peptides.[281, 283] However, RGD peptides alone do not increase the osteogenic differentiation of MSCs. It has been demonstrated that associating several peptides on the materials surface could provide synergistic effects. For example, the combination of RGD and a mimetic peptide of the BMP-2 protein[84], or RGD and OGP[85] might enhance MSCs osteogenic differentiation as compared to the single peptides.
In this project, a mimetic peptide of the BMP-2 protein (KRKIPKASSVPTELSAISMLYLC), developed and pattented by the 3BIO's team[83], has been used for functionalizing the surface of the hydrogels. This peptide has been shown to induce human bone marrow MSCs osteoblast differentiation when grafted onto different materials (glass, polyethylene terephthalate, poly(acrylamide-co-acrylic acid) hydrogel).[83, 84, 85, 86, 268] Therefore, synthesizing hydrogels that combine controlled mechanical properties, that mimic the mechanical properties of the ECM, and this BMP-2 mimetic peptide, that favors MSCs osteogenic differentiation, might provide a higher MSCs osteogenic commitment compared to what is done in the literature by using collagen.

4.3 Intermediate Objective

This intermediate objective is about the choice of the method(s) used for the measurement of hydrogels mechanical properties, including the stiffness and the viscoelastic properties, and about the impact of hydrogels surface funtionalization on the mechanical properties.

Indeed, several methods are used in the literature to evaluate hydrogels stiffness, and particularly hydrogels Young's modulus, including compression, traction, rheology, and AFM (Atomic Force Microscopy).[284] The compression test is a well-established method for hydrogel elasticity measurement, in which hydrogel discs are compressed (either confined or unconfined) with a controlled force while their deformation is measured.[284] This method also enables to determine hydrogels viscoelastic properties through stress relaxation or creep tests[285, 286], which can give information about hydrogels relaxation time for example.[68, 286] Traction tests are widely used for measuring the Young's modulus of various materials, including hydrogels. However, because hydrogel specimens are hydrated and usually soft, it is not easy to grip them properly in the jaws of the machine for traction testing.[284] Rheology

consists in casting a hydrogel specimen between the top and base plates of the rheometer, and oscillating the top plate at desired frequency and shear strain. As the specimen is twisted and undergoes shear deformation, it exerts resistant shear force on the oscillating plate that is measured by the rheometer to calculate the shear modulus of the gel.[284] The storage modulus and the loss modulus of the hydrogels can be obtained with rheology, and represent the elastic and viscous behavior of hydrogels, respectively.[94] Indentation tests using AFM have been widely used to measure the elastic modulus of various hydrogels. Typically, a hydrogel specimen is indented in a liquid by a pyramidal or spherical tip of an AFM probe, with a predetermined trigger force and probe speed.[284]

Considering that compression and AFM are the most widely used methods to measure hydrogels stiffness in studies evaluating the impact of the stiffness on MSCs differentiation (summarized in chapter 3 Table 3.1), these two methods have been chosen in this project to characterize hydrogels mechanical properties. Indeed, it would be particularly interesting to compare the results obtained with the two techniques, and to evaluate if studies using compression and AFM could be compared.

Compression tests enable to measure hydrogels viscoelastic properties through stress relaxation experiments, which is useful in this project to provide hydrogels with varying viscoelastic behavior. In addition, AFM also enables to perform stress relaxation experiments on hydrogels[97], although this kind of measurements is mainly performed on cells. Indeed, the low number of papers about hydrogels stress relaxation measurements with AFM (only one to our knowledge) might suggest that it is a complex topic, but also a new topic that deserves to be investigated.

These two methods are similar as they are both based on compression, but they are also complementary since compression is used to measure hydrogels bulk properties (hundreds of μm to several mm), while AFM is used to measure hydrogels surface properties (hundreds of nm). Using these two techniques would therefore allow to assess if hydrogels bulk mechanical properties match their surface properties. AFM would also allow to evaluate the homogeneity of the surface properties of the hydrogel samples. Finally, it would be particularly interesting to evaluate hydrogels mechanical properties before and after the surface functionalization, by using these two techniques, to determine whether the surface functionalization could modify hydrogels mechanical properties, which might subsequently affect MSCs behavior.

4.4 Objective 3

The last objective of this project consists in assessing the impact of hydrogels mechanical properties, including stiffness and viscoelastic properties, on human bone marrow MSCs osteogenic differentiation. This has been achieved with hydrogels functionalized with the BMP-2 mimetic peptide. In addition, considering that polyacrylamide hydrogels are generally functionalized with type I collagen to evaluate the impact of hydrogels stiffness on MSCs differentiation, it might also be interesting to compare MSCs differentiation in response to hydrogels mechanical properties depending on hydrogels biofunctionalization (BMP-2 mimetic peptide versus type I collagen).
Finally, as mentioned in chapter 2, MSCs differentiation is influenced by the culture medium used. In this project, all the experiments have been conducted with Osteogenic differentiation culture medium in order to favor and accelerate MSCs osteogenic differentiation, and to be able to obtain an osteogenic commitment over relatively shorter time periods (2 weeks) as compared to classic growth medium (4 weeks or more).

RESULTS AND DISCUSSION

Chapter 5

Study 1 : Evaluating poly(acrylamide-co-acrylic acid) hydrogels stress relaxation to direct the osteogenic differentiation of mesenchymal stem cells

Emilie Prouvé[a,b,c,d,e], Bernard Drouin[b], Pascale Chevallier[a,b], Murielle Rémy[c,d,e], Marie-Christine Durrieu[c,d,e*†] and Gaétan Laroche[a,b*†]

[a]Laboratoire d'Ingénierie de Surface, Centre de Recherche sur les Matériaux Avancés, Département de Génie des Mines, de la Métallurgie et des Matériaux, Université Laval, 1065 Avenue de la médecine, Québec G1V 0A6, Canada
[b]Axe Médecine Régénératrice, Centre de Recherche du Centre Hospitalier Universitaire de Québec, Hôpital St-François d'Assise, 10 rue de l'Espinay, Québec G1L 3L5, Canada
[c]Université de Bordeaux, Chimie et Biologie des Membranes et Nano-Objets (UMR5248 CBMN), Allée Geoffroy Saint Hilaire - Bât B14, 33600 Pessac, France
[d]CNRS, CBMN UMR5248, Allée Geoffroy Saint Hilaire - Bât B14, 33600 Pessac, France
[e]Bordeaux INP, CBMN UMR5248, Allée Geoffroy Saint Hilaire - Bât B14, 33600 Pessac, France

†These authors contributed equally.

*Corresponding authors :
Gaetan.Laroche@gmn.ulaval.ca Phone : +1 (418) 656-7983 Fax : (418) 656-5343
marie-christine.durrieu@inserm.fr Phone : +33 5 40 00 30 37 Fax : +33 5 40 00 30 68

This work has been published in the journal : *Macromolecular Bioscience, 2021*

5.1 Résumé

Cette étude vise à mesurer la relaxation de contrainte d'hydrogels et d'évaluer son impact sur la différenciation ostéogénique de cellules souches mésenchymateuses humaines (hMSCs). Différents hydrogels ont été synthétisés en variant la quantité d'agent réticulant et le ratio entre les deux monomères (acrylamide et acide acrylique). Les hydrogels contenant 18% d'acide acrylique ont montré une relaxation moyenne de 70%, alors que les gels sans acide acrylique ont montré une relaxation moyenne de 15%. Par la suite, des hMSCs ont été mises en culture sur deux hydrogels, fonctionnalisés avec un peptide mimétique de la protéine BMP-2. Un marquage du cytosquelette des cellules a montré que pour une rigidité constante à 55 kPa, un hydrogel avec une faible relaxation (15%) mène à l'obtention de cellules de forme étoilée, qui est la forme typique des ostéocytes, tandis qu'un hydrogel avec une relaxation élevée (70%) conduit les cellules vers une forme polygonale caractéristique des ostéoblastes.

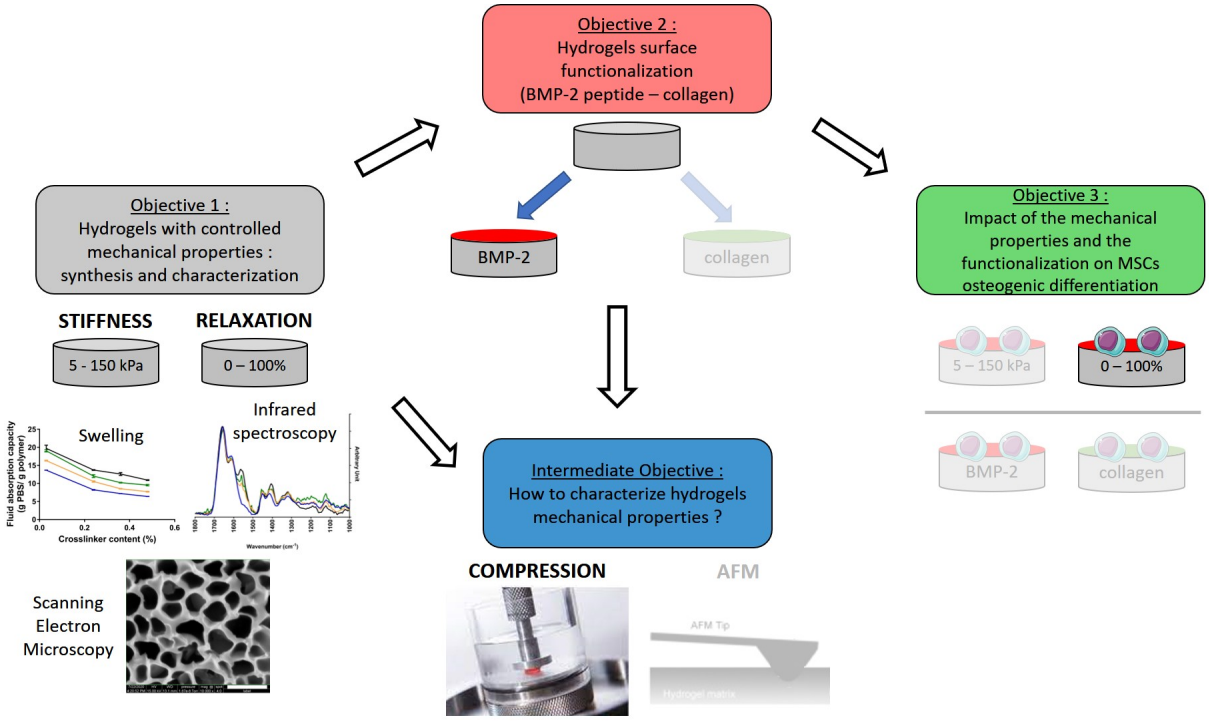

NB : The parts in transparency are not covered in this chapter.

5.2 Abstract

The aim of this study is to investigate polyacrylamide based hydrogels stress relaxation and the subsequent impact on the osteogenic differentiation of human mesenchymal stem cells (hMSCs). Different hydrogels were synthesized by varying the amount of crosslinker and the ratio between the monomers (acrylamide and acrylic acid), and characterized by compression tests. It has been found that hydrogels containing 18% of acrylic acid exhibit an average relaxation of 70%, while pure polyacrylamide gels show an average relaxation of 15%. Subsequently, hMSCs were cultured on two different hydrogels functionalized with a mimetic peptide of the BMP-2 protein to enable cell adhesion and favor their osteogenic differentiation. Phalloidin staining showed that for a constant stiffness of 55 kPa, a hydrogel with a low relaxation (15%) leads to star-shape cells, which is typical of osteocytes, while a hydrogel with a high relaxation (70%) presents cells with a polygonal shape characteristic of osteoblasts. Immunofluorescence labelling of E11, strongly expressed in early osteocytes, also showed a dramatically higher expression for cells cultured on the hydrogel with a low relaxation (15%). These results clearly demonstrated that, by fine-tuning hydrogels stress relaxation, hMSCs differentiation can be directed towards osteoblasts, and even osteocytes, which is particularly rare in vitro.

Keywords : Poly(acrylamide-co-acrylic acid) - hydrogels stress relaxation - human Mesenchymal Stem Cells - osteogenic differentiation - BMP-2 surface functionalization - osteocytes

Graphical Abstract

Poly(acrylamide-co-acrylic acid) hydrogels are synthesized with controlled stiffness, ranging between 5 and 145 kPa. Hydrogels containing 0% or 18% of acrylic acid exhibit an average relaxation of 15% and 70%, respectively. Hydrogels with the same stiffness (55 kPa), and different stress relaxation (70% and 15%) induce mesenchymal stem cells differentiation into osteoblasts and osteocytes, respectively.

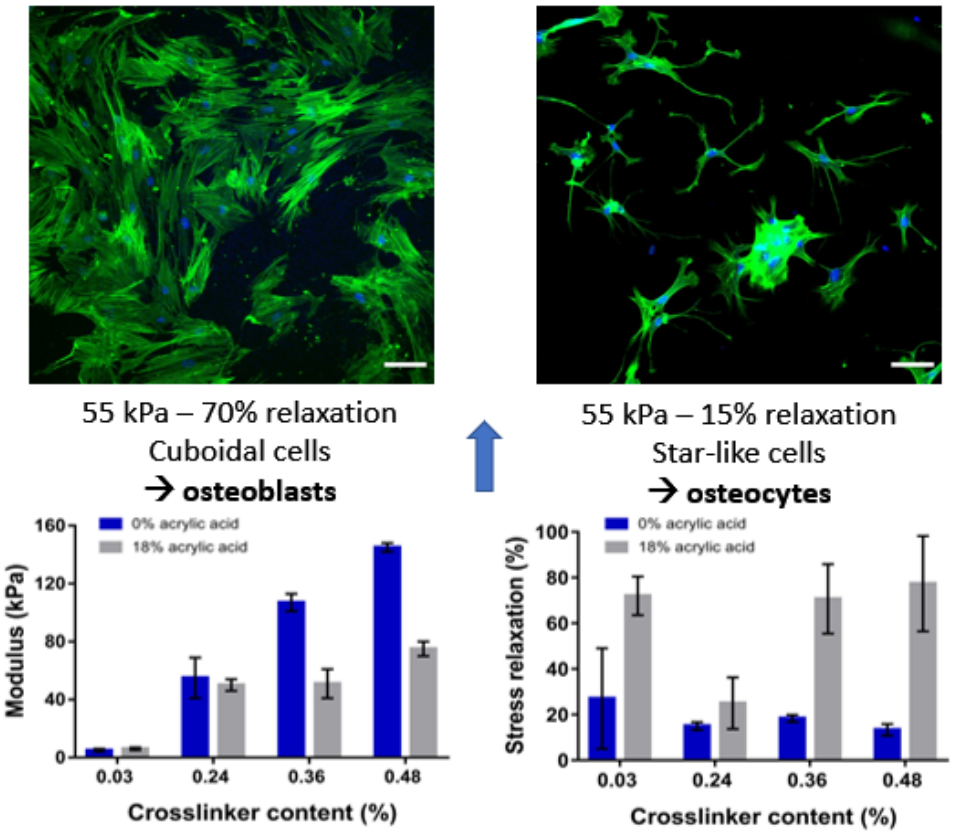

5.3 Introduction

Mesenchymal stem cells are multipotent adult stem cells that have gained high interest in tissue engineering and clinics due to their self-renewal, their ease of access in various tissues, such as adipose tissue, bone marrow, or dental pulp, and their capacity to differentiate into mesoderm-type cells such as adipocytes, chondrocytes and osteoblasts.[101, 287, 288] However, the clinical use of hMSCs is currently limited as it can be associated with complications, such as tumor formation, due to their tendency to uncontrollably proliferate and differentiate.[32] Consequently, tools to control hMSCs fate and allow their use in clinical applications are still highly needed. In this context, hydrogels have been widely used to study different cell behaviors and to identify parameters enabling to control the expansion and differentiation of various cell types.

Hydrogels are three-dimensional networks formed by the crosslinking of hydrophilic polymers, which provide them the ability to absorb large amount of water without dissolving.[196, 289] The crosslinking can be covalent, when the polymer chains are linked together through chemical bonds, and/or physical, when the crosslinking points are created by weaker interactions such as hydrogen bonds or ionic interactions.[194] Chemically crosslinked hydrogels are often used due to their good mechanical strength[194], their homogeneity at the microscale and the ease to control their physical and chemical properties, such as matrix elasticity and porosity.[68] In addition, hydrogels present a great potential for controlled drug release and tissue engineering due to their water content which closely matches that of biological tissues.[196, 289] They can also be used as bio-inks for the 3D printing of cell-laden hydrogel arrays, with various shapes and sizes, which can enable the control of cell alignment and differentiation[290, 291], as well as cell aggregation to create spheroids[292], or they can be transplanted to reconstruct damaged tissues.[293, 294] Hydrogels being multi-phase materials composed of a solid phase together with a liquid phase, their mechanical behavior cannot be simply determined by using the conventional methods and equations established for solid polymers.[289] Consequently, a detailed characterization of hydrogels mechanical properties is essential, especially in the context of tissue engineering, as it has been shown that cells are sensitive to their mechanical environment.

Several studies have focused on measuring and tuning hydrogel stiffness, which characterizes their elasticity, by varying their formulation[206, 295, 296], by using different copolymers[297, 298] and interpenetrating networks[299, 300, 301], or by adding reinforcements.[302, 303, 304] The possibility of controlling these mechanical properties opened the door to several studies on the impact of hydrogel stiffness on cell behavior (adhesion, proliferation, cell differentiation) for regenerative medicine purposes.[228, 296, 298, 299, 300, 305, 306, 307] In particular, polyacrylamide hydrogels have been extensively investigated for such studies[40, 52, 55, 56, 308], as they offer the possibility to simply modulate hydrogel stiffness and adhesive ligand presentation which lead to more complete understanding of cell responses to these stimuli.[35]

For example, Engler and co-workers showed that human mesenchymal stem cells (hMSCs) differentiation depends on hydrogel matrix stiffness, with neurogenic differentiation occurring on soft gels mimicking brain mechanical behavior (0.1-1 kPa), myogenic differentiation dominating on gels with mechanical properties close to that of muscle tissues (8-17 kPa), and osteogenic differentiation being favored on stiffer matrices (25-40 kPa).[52] Similarly, Wen et al. observed that human adipose stem cells adipogenic differentiation was higher on soft polyacrylamide gels (4 kPa), while osteogenic differentiation was predominant on stiffer gels (30 kPa).[56]

However, it is now acknowledged that hydrogels, as well as biological tissues, are intrinsically viscoelastic.[68, 309] Viscoelasticity is defined as the combination of both solid (elastic) behavior, as the material stores energy and returns to its original state after the deformation, and liquid (viscous)-like behavior, as the material dissipates energy.[277] Consequently, several studies investigated hydrogels behavior under mechanical solicitation by performing stress relaxation experiments.[68, 310, 311, 312] During these experiments, a strain is applied to the material and maintained constant, and the resulting stress is measured over time.[311, 312] These measurements enable to define the degree of viscoelastic nature of a material and to assess the time needed by the material to relax.[277] In hydrogels, elastic behavior is due to strong covalent intramolecular bonds, and covalent intermolecular bonds for chemically crosslinked hydrogels, while viscous behavior is due to rearrangements of polymer chains and reversible crosslinks.[277, 313] In addition to viscoelasticity, another property, called poroelasticity, has been identified in hydrogels and is related to the migration of water in the pores of the gel.[277, 313] Viscoelasticity and poroelasticity generally coexist in hydrogels, which means that they both contribute to these materials stress relaxation behavior.[285, 313, 314, 315] Consequently, some studies have been conducted on measuring both viscoelasticity and poroelasticity of hydrogels.[206, 315, 316] This might be of great interest, especially within the scope of tissue engineering, as it has been demonstrated that hydrogel stress relaxation can influence cell behavior in terms of cell adhesion and differentiation. For example, by entrapping linear polyacrylamide into polyacrylamide hydrogels, Charrier et al.[94] obtained three hydrogels with the same stiffness (5 kPa) but with varying viscous modulus. They showed that fibroblasts cell area and hepatic stellate cells differentiation into myofibroblasts were significantly lower with increasing the hydrogel viscous modulus.[94] Cameron and coworkers[67] prepared polyacrylamide hydrogels with different ratios of acrylamide and bis-acrylamide to obtain different viscous modulus with the same elastic modulus. In this case, they observed an increased spreading area of human mesenchymal stem cells and a higher expression of adipogenic and osteogenic differentiation markers as the viscous modulus increased.[67] Finally, Chaudhuri and coworkers[68] developed alginate hydrogels with the same stiffness but with varying relaxation time, and showed that mouse MSCs spreading was higher on gels with a faster stress relaxation. In addition, they found a higher adipogenic differentiation of MSCs for gels with a high relaxation time and a higher osteogenic differentiation for gels with a low

relaxation time.[68] Hydrogel stiffness and viscoelastic properties would therefore play a key role in regulating cell behavior, including MSCs differentiation.[277, 317, 318, 319] However, the number of studies on the impact of the stress relaxation properties of hydrogels on MSCs differentiation is still limited (15 research articles over the past five years from PubMed, key words hydrogel stress relaxation mesenchymal stem cells differentiation). Consequently, it is of particular interest to get a deeper understanding of hydrogels mechanical behavior and to supply hydrogels with different controllable stress relaxation properties, to further assess the impact of these properties on hMSCs differentiation, which constitutes the aim of this study.
The present work investigates polyacrylamide hydrogels stress relaxation, considering their extensive use to study the impact of hydrogel stiffness on cells behavior. Polyacrylamide hydrogels were therefore synthesized with constant monomer content and varying crosslinker amount in order to control hydrogel stiffness. Moreover, as polyacrylamide gels are considered mainly as elastic materials[68], we have designed copolymer hydrogels of acrylamide and acrylic acid, with 5, 10 and 18 mol% of acrylic acid, to modulate hydrogels stress relaxation. The idea is to combine high and tunable stiffness, brought by covalent crosslinks, and increased viscoelasticity, by making a copolymer hydrogel. Subsequently, the compressive stress relaxation properties of different hydrogel formulations have been measured by applying five steps of 3% compression and recording the stress as a function of time between the steps. The generalized Maxwell model was used to identify and isolate three phenomena contributing to these hydrogels stress relaxation, which are the movement of free water in the pores of the gel, viscoelasticity and poroelasticity. Finally, a preliminary study about human mesenchymal stem cells (hMSCs) osteogenic differentiation in response to hydrogel stress relaxation was conducted, and revealed that for a constant stiffness of 55 kPa, a hydrogel with a relaxation of 15% promotes faster osteogenic differentiation as compared to a hydrogel with a relaxation of 70%. hMSCs cultured on the hydrogel with a relaxation of 15% even differentiated into osteocytes, the last stage of differentiation, which represents a major achievement for tissue engineering and regenerative medicine.

5.4 Results and Discussion

5.4.1 Infrared spectroscopy

The absorption infrared spectra of polyacrylamide and poly(acrylamide-co-acrylic acid) hydrogels containing 0.48% of crosslinker and 0 or 10 mol% of acrylic acid are shown in Figure 5.1a. These spectra exhibit similar features with a broad band in the range of 3500 - 3000 cm^{-1} overlapped with more defined peaks near 3300 and 3200 cm^{-1} corresponding to asymmetric and symmetric -NH_2 stretching mode vibrations, respectively[78]. Furthermore, in this region, the -NH stretching mode features are overlapping with the broad feature assigned

to stretching modes of hydrogen bonded hydroxyl groups from acrylic acid in the copolymer hydrogel.[78, 79] Asymmetric and symmetric -CH_2 stretching mode vibrations are observed at 2940 and 2870 cm^{-1}, respectively.[79, 80] This region also includes -CH stretching usually found around 2890 cm^{-1}. The strongest peak at 1660 cm^{-1} corresponds to the stretching of the carbonyl (C=O) of acrylamide units[78, 79, 80], while the band at 1613 cm^{-1} is assigned to the bending of -NH groups.[78] Finally, the addition of acrylic acid to the reactive mixture leads to an increase of the 1560 cm^{-1} feature as compared to a pure polyacrylamide hydrogel (Figure 5.1a). This is due to the stretching of the carbonyl group in carboxylate functionalities (-COO^-), as previously reported in the literature.[79, 80] In addition, increasing the amount of acrylic acid leads to a rise of the 1560 cm^{-1} feature as shown by Figure 5.1.

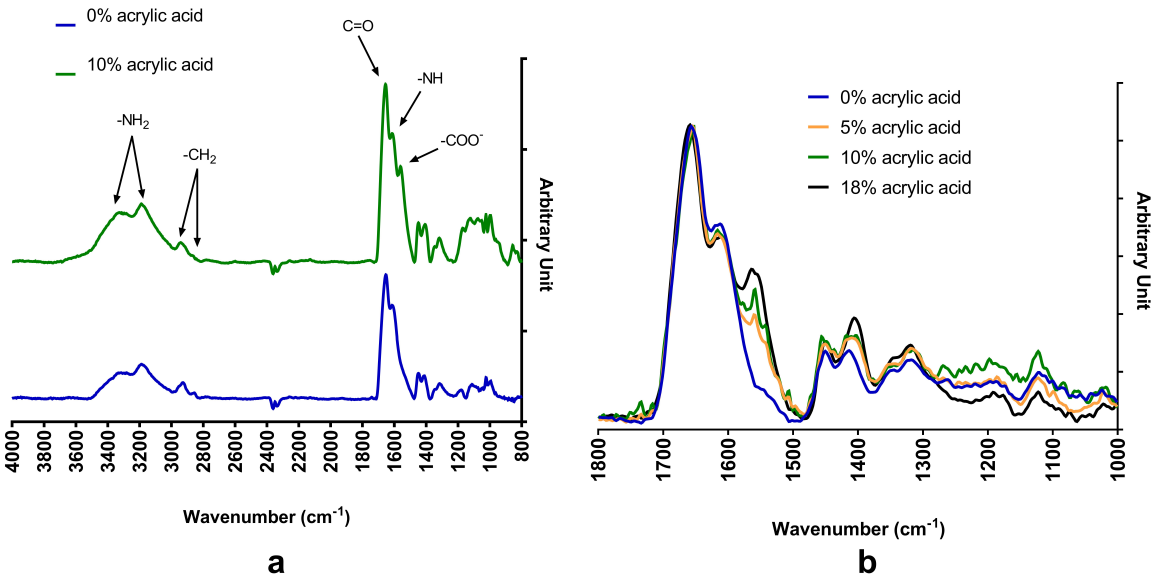

FIGURE 5.1 – a) FTIR spectra of polyacrylamide and poly(acrylamide-co-acrylic acid) hydrogels with the same amount of crosslinking agent and 0 or 10% acrylic acid. b) FTIR spectra of hydrogels with the same amount of crosslinking agent and varying acrylic acid content. The spectra were normalized according to the strongest peak at 1660 cm^{-1}. The addition of acrylic acid to the reactive mixture leads to the appearance of the 1560 cm^{-1} feature as compared to a pure polyacrylamide gel. This feature rises when increasing the acrylic acid content.

5.4.2 Swelling behavior

Figure 5.2 shows the hydrogels fluid absorption capacity as a function of the amount of crosslinker (Figure 5.2a) and acrylic acid (Figure 5.2b) (the statistical analysis is presented in Supplementary Figure 5.14a). These hydrogels are capable of absorbing 6 to 20 times their own dry weight which is consistent with the data reported in the literature.[79, 80] Hydrogels are polymer networks exhibiting the ability to contain a large fraction of aqueous solvent within their structure.[320, 321] This characteristic made them popular for various applications such as the design of superabsorbent materials, drug delivery systems, cell encapsulation and tissue repair[321] to name only a few. Hydrogel swelling mainly depends on the polymer composition because the constituents are responsible for interactions with the fluid, the degree of crosslinking and the porosity which influences the diffusion rate of fluid inside the material.[81] These general rules apply to poly(acrylamide-co-acrylic acid) hydrogels since the swelling decreases as the amount of crosslinker is higher, while it increases with the quantity of acrylic acid. The increase of the amount of crosslinker leads to a higher degree of crosslinking, and to a denser and less flexible hydrogel, therefore limiting the penetration of solvent and reducing the swelling.[80, 81] While introducing acrylic acid into the hydrogel generates negative charges which increase the swelling as a result of electrostatic repulsion between polymer chains.[81, 82]

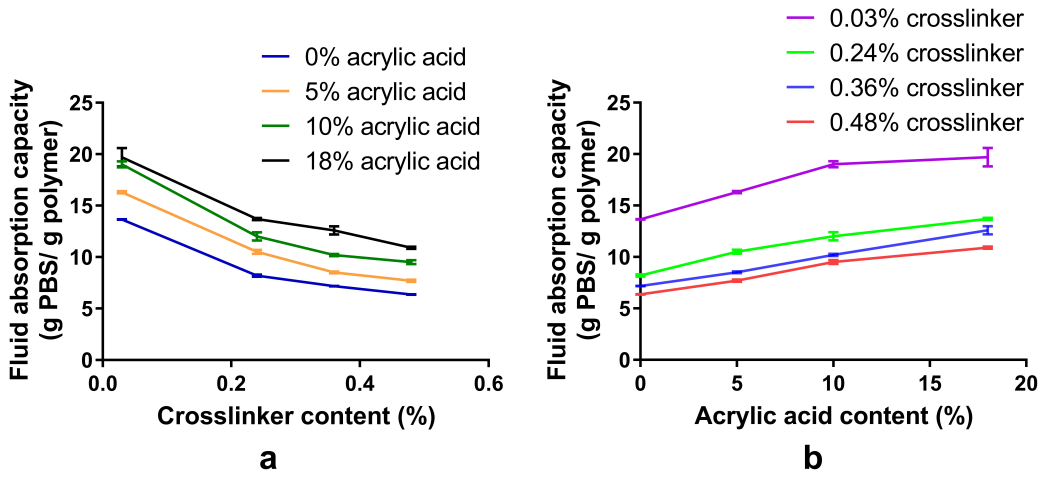

FIGURE 5.2 – Fluid absorption capacity of polyacrylamide and poly(acrylamide-co-acrylic acid) hydrogels. a) As a function of crosslinker content. b) As a function of acrylic acid content. The fluid absorption capacity decreases for higher amounts of crosslinker and increases with the amount of acrylic acid. (n=3)

With a pKa value close to 5, poly(acrylic acid) is likely to release protons and extend polymer chains under alkaline pH values.[82, 322] Therefore, these hydrogels are known to be pH-sensitive[79, 82, 322] which makes them good candidates for biomedical applications, like drug delivery, or applications requiring water permeation control for example.[82] As shown by Figure 5.3, the fluid absorption capacity of a pure polyacrylamide hydrogel does not change for pH values ranging from 3 to 10, while it decreases at pH 3 for hydrogels containing acrylic acid. This decrease is more pronounced for the hydrogels containing the highest acrylic acid content, confirming that the absence of negative charges of acrylic acid at low pH dramatically reduces poly(acrylamide-co-acrylic acid) hydrogels swelling.

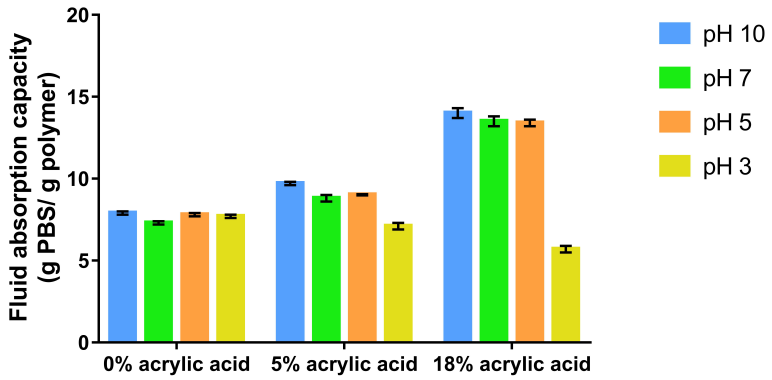

FIGURE 5.3 – Fluid absorption capacity of polyacrylamide and poly(acrylamide-co-acrylic acid) hydrogels with the same amount of crosslinking agent and varying content of acrylic acid in PBS with different pH values. The fluid absorption capacity decreases at pH 3 for hydrogels containing acrylic acid, while it is stable for pure polyacrylamide hydrogels for all the tested pH values. (n=3)

5.4.3 Hydrogels stiffness

The modulus has been evaluated for each of the sixteen hydrogel formulations as shown in Figure 5.4 (the statistical analysis is presented in Supplementary Figure 5.14b). As expected, the modulus increases with the amount of crosslinker, going from 5 $\pm$ 1 kPa to 145 $\pm$ 3 kPa for pure polyacrylamide hydrogels (Figure 5.4a). Moreover, there is a linear relationship between hydrogel stiffness and crosslinker content (Supplementary Figure 5.13). This tendency is observed for any content of acrylic acid. This behavior has already been observed by Rowlands et al.[69] The addition of acrylic acid in the gel causes a decrease in the modulus, which is more pronounced for a high amount of crosslinker, e.g. 0.36 and 0.48% (Figure 5.4b). Several studies have investigated the impact of crosslinker content in polyacrylamide hydrogels on their mechanical properties and more particularly their stiffness, and it has been shown that increasing the amount of crosslinker leads to a rise of the stiffness[69, 206], as this is the case

for the hydrogels in this study. Increasing the amount of crosslinker results in a higher number of crosslinking points, therefore leading to a denser network which is accompanied by a higher stiffness and a lower swelling capacity. Then, as acrylic acid is added, the content of ionic charges is increased, as well as the electrostatic repulsion between the polymer chains.[322] This leads to a less dense network allowing the swelling to rise while decreasing the stiffness.

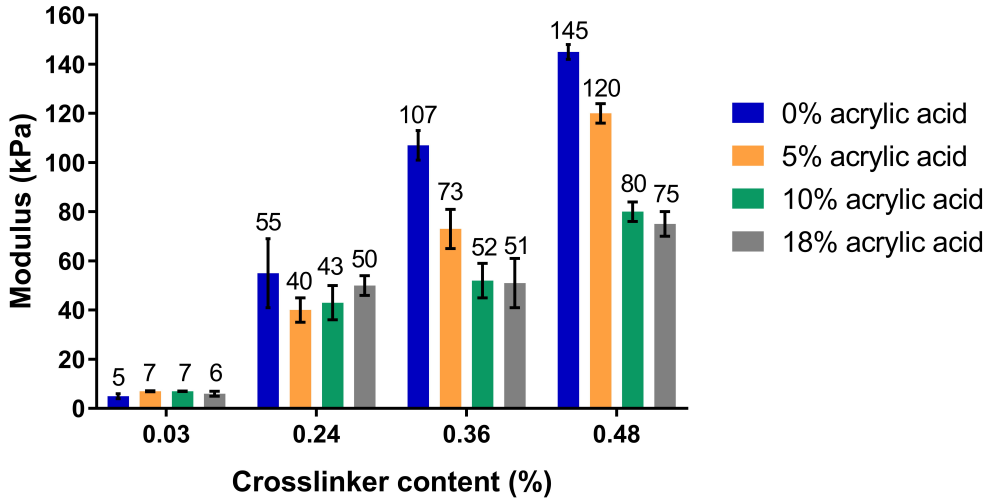

FIGURE 5.4 – Equilibrium modulus measured for the different hydrogel formulations as a function of the crosslinker content. The equilibrium modulus increases with the amount of crosslinker and decreases for higher amounts of acrylic acid. (n=3)

5.4.4 Hydrogels stress relaxation

The relaxation was first modelled with one or two Maxwell elements leading to a correlation coefficient over 0.9. However, the whole experimental curve needed to be fitted using three Maxwell elements, especially between 0 and 50 s, as the rapid decrease of the stress during the first 30 s impedes fitting with a lower number of Maxwell elements (Supplementary Figure 5.15). These results are consistent with the findings of Xin et al. who found that one relaxation time was not suitable to fit their data as they observed a rapid decrease of the stress over 25 s followed by a slower relaxation over 530 s for hybrid ionic-covalent hydrogels of polyacrylamide and alginate.[323] However, their model does not represent the relaxation found at long timescales in chemically crosslinked hydrogels.[312]

The relaxation of the hydrogels described in this study is therefore characterized by three time constants and is the result of the contribution of three different physical phenomena, each of them being the source of rearrangements in the gel leading to a decrease of the stress over time. For modelling the stress relaxation experiments, it was necessary to set limits for the relaxation times as they must happen in a chronological order, they cannot overlap

with each other, and they cannot go further than the time of the experiment, i.e. 6480 s. The first relaxation time was set between 0 and 30 s to represent the rapid initial drop of the stress. It is postulated that it is related to short range reorganization of free water in the gel.[324] The second relaxation phenomenon occurs over hundreds of seconds and is caused by the reorganization of polymer chains following the mechanical solicitation, which corresponds to hydrogel viscoelasticity.[325] The third relaxation phenomenon is measured at longer timescales and was previously found to result from water migration through the pores of the gel and is called poroelasticity.[312, 325]

Modeling of the experimental data showed that the extent of stress relaxation differs depending on the hydrogel composition. As shown in Figure 5.5, a hydrogel with 0.48% of crosslinker and 18% of acrylic acid relaxes more than a pure polyacrylamide hydrogel with the same amount of crosslinker. Of note, the compression steps are consecutive and therefore have to be considered separately. The relaxation extent appears to be lower at higher compression (Figure 5.5, Supplementary Figure 5.16), which might be due to the fact that plastic deformations occur at each compression step, with water leaving the gel, giving less possibilities to reorganization, therefore reducing the relaxation extent when increasing the compression.

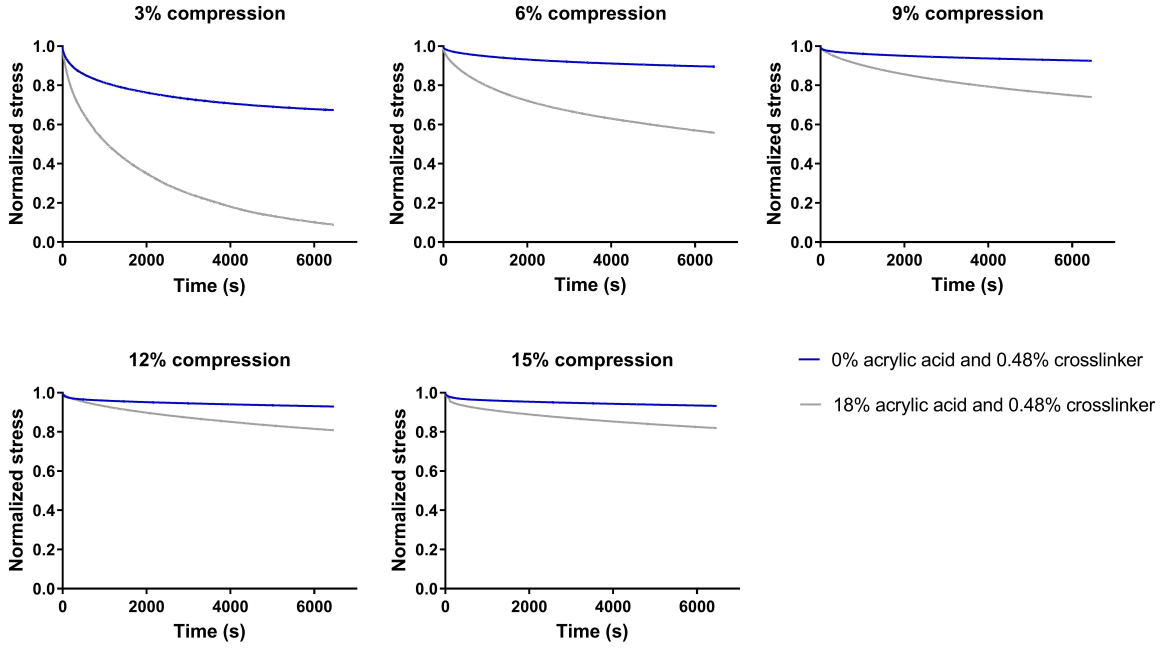

FIGURE 5.5 – Normalized stress relaxation of two hydrogels with 0.48% of crosslinker and 0 or 18% of acrylic acid as a function of time (6480 s) at different compression stages. The relaxation extent is higher for a gel with 18% acrylic acid compared to a pure polyacrylamide gel.

To further assess the impact of the mechanical properties of these hydrogels on cell behavior, the study of low compression (such as 6%), is more relevant as cells typically exert strains ranging between 3 and 5% in 2D culture on polyacrylamide hydrogels.[65]
The total relaxation is given by the percent of the maximum stress that is lost during the relaxation. It can be seen in Figure 5.6 that pure polyacrylamide hydrogels exhibit a low relaxation, which is expected as these gels are chemically crosslinked[68, 95] (the statistical analysis is presented in Supplementary Figure 5.18). The relaxation increases with the addition of acrylic acid to the hydrogel at constant crosslinker amount. In particular, the relaxation increases dramatically, up to 90%, with 18% of acrylic acid as compared to the other formulations. Pure polyacrylamide hydrogels show an average relaxation of 15%, which is consistent with the observations of Charrier et al.[94], while hydrogels with 18% of acrylic acid exhibit an average relaxation of 70%. This can be explained by the presence of negative charges brought by acrylic acid which extend the swelling by increasing the space between polymer chains and therefore facilitate polymer chain rearrangements and fluid migration in the gel. In addition, the relaxation does not change significantly when varying the crosslinker content. Finally, no significant difference has been found between the three relaxation times depending on the hydrogel formulation (data not shown). The relaxation times were found to be in the order of minutes (500 s) for viscoelasticity and in the order of hundreds of minutes for poroelasticity, which is consistent with the observations of Gentile et al. for alginate hydrogels.[326]

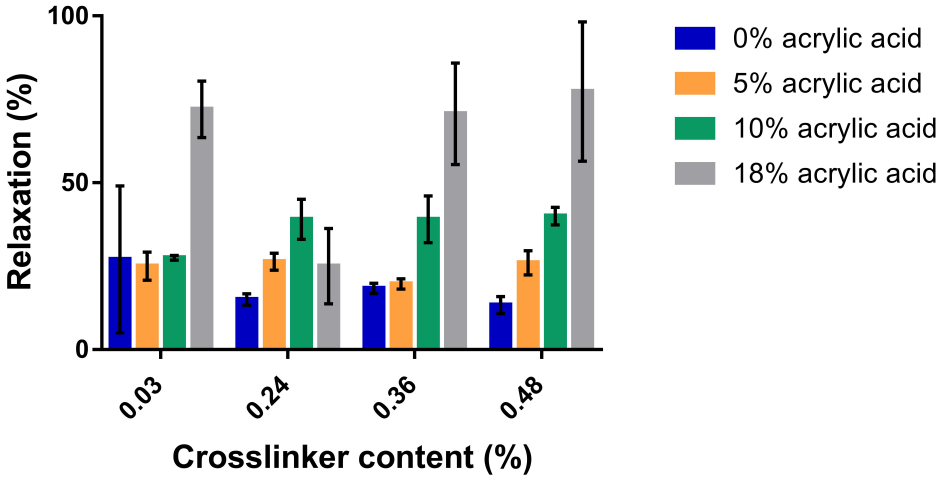

FIGURE 5.6 – Total stress relaxation for the different hydrogel formulations as a function of the crosslinker content at 6% compression. The relaxation increases with the amount of acrylic acid. (n=3)

To further confirm that the higher relaxation of hydrogels containing acrylic acid is effectively related to the negative charges brought by acrylic acid, the relaxation of a pure polyacrylamide hydrogel (Figure 5.7a) and a hydrogel containing 18% of acrylic acid (Figure 5.7b) were measured at different pH values. It has been found that the relaxation of the pure polyacrylamide hydrogel is not affected by the pH, whereas the relaxation of the copolymer hydrogel decreases dramatically at pH 3, reaching a similar level to that of the polyacrylamide gel. The relaxation of the copolymer hydrogel slightly decreases at pH 10 as compared to pH 7, although the difference is very small and often not significant. This is consistent with the finding that the fluid absorption capacity of copolymer hydrogels does not change between pH 7 and 10. The relaxation of poly(acrylamide-co-acrylic acid) hydrogels is therefore highly related to their swelling and therefore to the presence or the absence of the negative charges of acrylic acid. These results show that the presence of acrylic acid in the hydrogels increases their stress relaxation degree, as compared to pure polyacrylamide hydrogels, particularly at physiological pH (7.2-7.4). Associating acrylic acid to acrylamide to create copolymer hydrogels is therefore particularly interesting to provide hydrogels with different and controlled viscoelastic responses at physiological pH, to further study their impact on cell behavior.

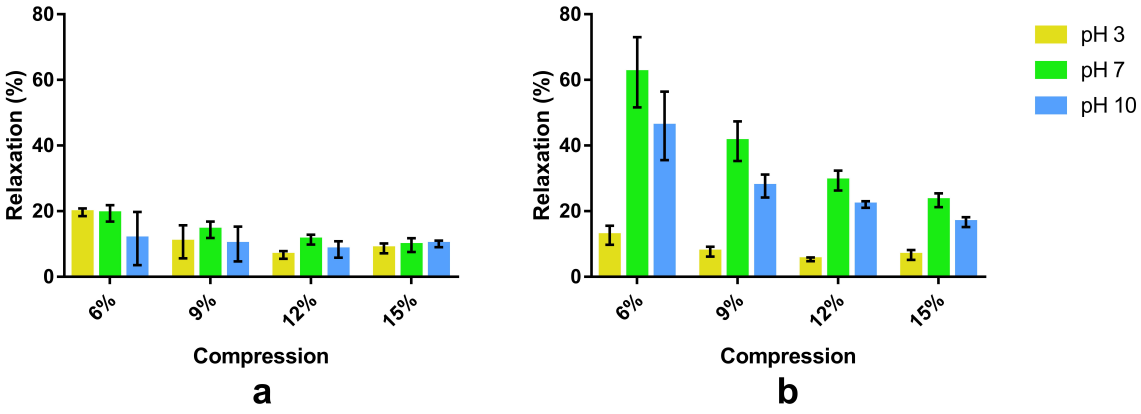

FIGURE 5.7 – Stress relaxation of hydrogels with a) 0% of acrylic acid and b) 18% of acrylic acid for different pH values at different compression. The relaxation is not affected by the pH for a pure polyacrylamide hydrogel, while the relaxation dramatically decreases at pH 3 for a hydrogel containing 18% of acrylic acid. (n=3)

Although three phenomena have been identified as contributing to these hydrogels stress relaxation behavior, viscoelasticity and poroelasticity cannot be completely separated as these two mechanisms arise concomitantly. As shown by Gentile et al., they both start at the beginning of the stress relaxation process, and, while the viscoelasticity stops after a few minutes, poroelasticity continues to be observed over longer periods of time.[326] However, this study allows a deeper understanding of polyacrylamide-based hydrogels mechanical behavior by identifying the mechanisms responsible for their stress relaxation behavior and by quantifying the extent of stress relaxation, which might influence cell behavior in terms of adhesion, spreading, and differentiation. In addition, these mechanical characterizations and stress relaxation modelling, enable to measure the timescale of stress relaxation in general and the timescale of viscoelasticity and poroelasticity, whereas this cannot be determined with rheology experiments, for example.

Finally, although the presence of acrylic acid, and therefore the presence of negative charges on the polymer chains, has been identified as a critical element impacting these hydrogels stress relaxation, it is likely that varying hydrogels formulation will also influence their porosity. Figure 5.8 shows Scanning Electron Microscopy images of four hydrogels with varying contents of crosslinker and acrylic acid, as well as a frequency distribution of the pore area in these hydrogels. Although the pore area is heterogeneous in the different hydrogels, it can be seen that the pore size decreases when increasing the crosslinker content, as already shown in the literature.[55] In addition, for the same crosslinker content, adding acrylic acid to the gel leads to a greater pore size. These results are consistent with the swelling behavior of the gels, as a higher crosslinker content results in a lower pore size and a decrease in swelling, whereas a higher acrylic acid content is related to a greater pore size and an increase in swelling. The porosity of these hydrogels has been evaluated to 40 $\pm$ 3% and 44 $\pm$ 8% for the hydrogels with 0.03% and 0.24% crosslinker, respectively, while a higher porosity of 60 $\pm$ 6% and 63 $\pm$ 2% has been found for the two hydrogels with 0.36% crosslinker, without or with acrylic acid, respectively. In addition, hydrogels without acrylic acid present a round or oval pore structure with polymer walls distinctly separating the pores, while the hydrogel with 18% acrylic acid present pores with more random shapes that seem less distinctly separated, which might suggest a higher degree of pore interconnection as compared to the hydrogels without acrylic acid. This observation might also explain the higher relaxation of the gel containing acrylic acid, as a higher degree of pore interconnection could facilitate water flowing through the pores during the stress relaxation experiment. However, the pore size and porosity of these hydrogels are not sufficient to fully explain their stress relaxation behavior, as the two hydrogels with 0% acrylic acid and 0.24% or 0.36% crosslinker present the same relaxation degree despite a different pore size and degree of porosity.

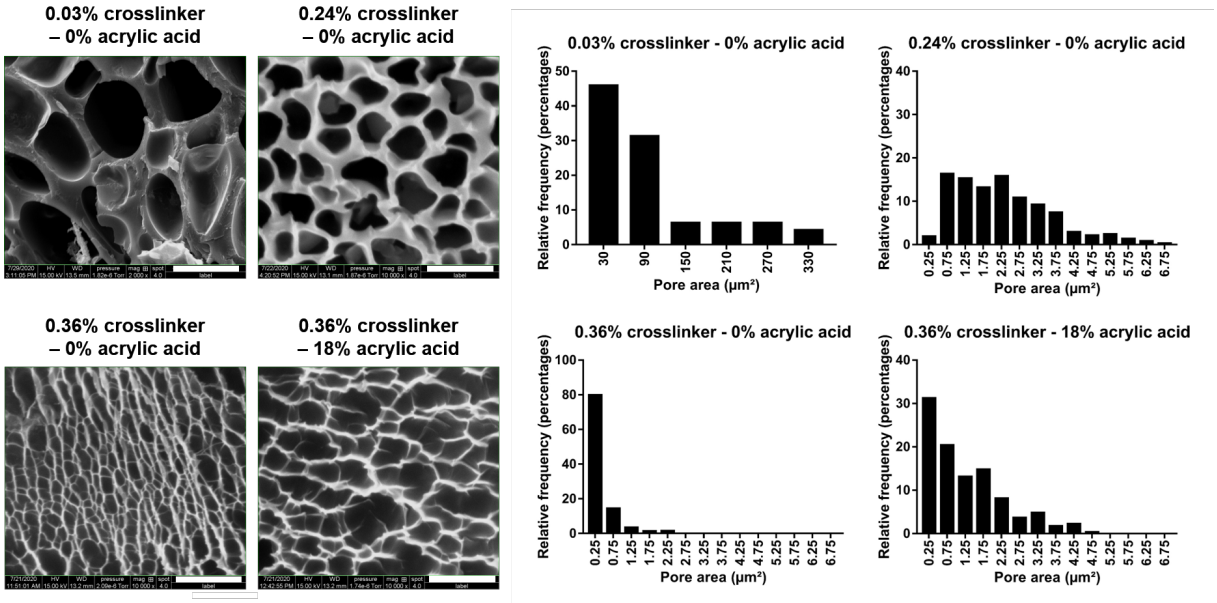

FIGURE 5.8 – Left : SEM images of hydrogels with different amount of crosslinker and acrylic acid. For the hydrogel with 0.03% crosslinker and 0% acrylic acid, scale bar = 20 μm, for the three other hydrogels, scale bar = 4 μm. Right : frequency distribution of the pore area for hydrogels with different amount of crosslinker and acrylic acid. The pore size decreases when increasing the crosslinker content and increases with the acrylic acid content.

5.4.5 Preliminary cell culture experiment

As a preliminary study, two hydrogels have been selected to assess the impact of the relaxation on human bone marrow MSCs osteogenic differentiation. A fixed stiffness of 55 kPa has been selected as this value lies within the range of stiffnesses that have been found to promote osteogenic commitment.[52, 55, 57, 63, 69, 232, 233] A pure polyacrylamide hydrogel with a low relaxation (15%) has been chosen, as polyacrylamide hydrogels are widely used in the literature to study the impact of stiffness on hMSCs differentiation, and has been compared to a hydrogel with 18% of acrylic acid exhibiting a high relaxation (70%). As polyacrylamide based materials do not support cell adhesion[52, 55], these hydrogels have been functionalized with a mimetic peptide of the Bone Morphogenetic Protein-2 (BMP-2), which corresponds to residues 73-92 of BMP-2 and has been shown to induce hMSCs osteoblast differentiation when grafted onto different materials (glass, polyethylene terephthalate, poly(acrylamide-co-acrylic acid) hydrogel).[83, 84, 85, 86, 268] Hydrogels functionalization has been assessed by using fluorescently labelled BMP-2 peptide and by following previously described protocols.[84, 85, 86, 268] It has been found that the fluorescence intensity on the surface of the two hydrogels with low and high relaxation is similar (data not shown), indicating that there is no difference in peptide density between the two hydrogels.

First, the morphology of the cells was considered after 2 weeks of culture in osteogenic culture medium by visualizing cell cytoskeleton with phalloidin. As shown in Figure 5.9, hydrogels stress relaxation has an impact on cell adhesion as a lower amount of cells can be observed on the gel with 15% relaxation (Figure 5.9c), while the hydrogel with 70% relaxation shows a higher number of cells (Figure 5.9b), comparable to hMSCs on glass (Figure 5.9a). This result has also been observed for 24 hours of cell culture (data not shown), which confirms that, for a constant stiffness and cell seeding density, a low relaxation restricts cell adhesion. These preliminary results also highlight that cells on the hydrogel with high relaxation (Figure 5.9b) are large, highly spread, and exhibit a cuboidal morphology typical of osteoblast[23, 98, 99], while cells on the hydrogel with low relaxation (Figure 5.9c) present a smaller cell body and a dendritic morphology characteristic of osteocytes.[5, 6, 98, 327] Immunofluorescence labelling of E11/podoplanin, strongly expressed in early osteocytes[5, 6, 328], is shown in Figure 5.9d-o for cells cultured for two weeks in Osteogenic Differentiation Medium on glass (control d-f) and on the hydrogels with high and low relaxation (j-l and m-o respectively), as well as for osteoblasts cultured for 24h on glass (control g-i). Quantification of E11 marker (Figure 5.9p) shows a dramatically higher expression on the hydrogel with low relaxation, as compared to controls and to hydrogel with high relaxation. E11 is strongly upregulated in osteocytes, but it can also be found in lesser amount in osteoblasts[328, 329], and especially in embedding osteoblasts[5, 330], e.g. osteoblasts that become embedded within the extracellular matrix they produce before undergoing their transition to osteocytes. This can explain the expression of E11 on the hydrogel with 70% relaxation, which is higher than hMSCs on glass, but lower than osteoblasts on glass. The higher expression of E11 on the hydrogels relative to the hMSCs on glass, and the dramatic increase on the hydrogel with low relaxation suggest that the BMP-2 mimetic peptide acts together with the mechanical properties of the hydrogel to direct hMSCs osteogenic differentiation, and that the Osteogenic Differentiation Medium alone is not sufficient to induce a differentiation towards osteocytes. Furthermore, these observations highlight that hydrogels stress relaxation has a significant impact on cell behavior and must be considered. These findings are extremely promising considering that collagen, traditionally used on polyacrylamide hydrogels in the literature[52, 55, 56], has not been found to promote the dendritic morphology observed in this study. In addition, the differentiation towards osteocytes is scarcely described[331] and it is still not clear to what extent the differentiation into osteocytes can be modulated by biomaterials.[155] Therefore, this study paves the way for the understanding of hMSCs interaction with biomaterials which will further lead to the control of their osteogenic differentiation, even reaching the last stage of differentiation. Although, at this stage, it is not clear whether the differentiation into osteocytes observed on Figure 8c is due to the fact that a low relaxation enhances the osteogenic differentiation, or that a low relaxation limits cell adhesion which favors the differentiation, as intercellular separation has been found to promote the transition from pre-osteoblasts to osteocytes.[332]

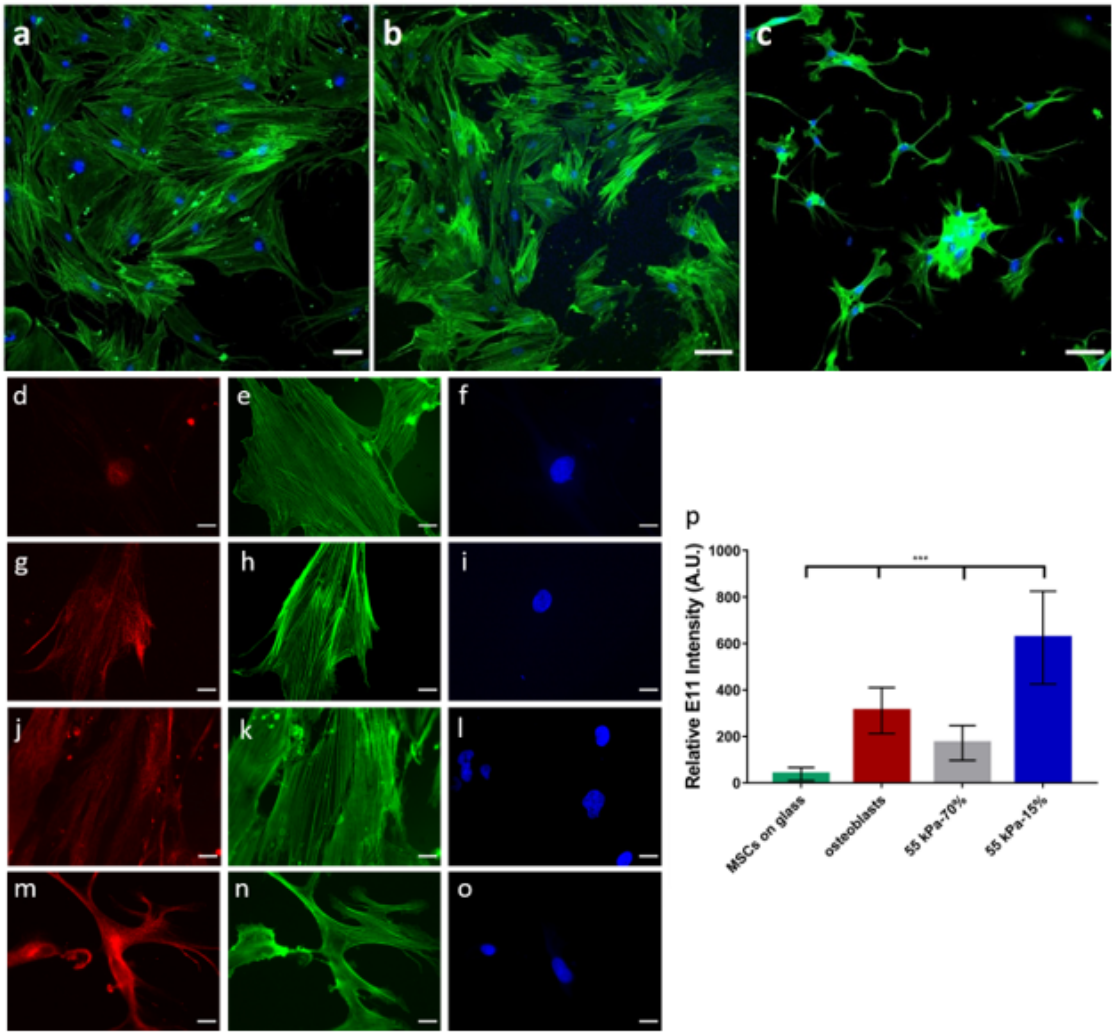

FIGURE 5.9 – Cytoskeleton and cell morphology. Phalloidin staining of the cytoskeletal fibers of human bone marrow MSCs cultured for two weeks on a) a glass slide (control), b) a poly(acrylamide-co-acrylic acid) hydrogel with a stiffness of 55 kPa and a high relaxation of 70%, and c) a pure polyacrylamide hydrogel with a stiffness of 55 kPa and a low relaxation of 15%. Both hydrogels were functionalized with a mimetic peptide of the protein BMP-2. The hydrogel with low relaxation promotes faster osteogenic differentiation as the cells present a star-like shape typical of osteocytes, while they exhibit the polygonal shape of osteoblasts on the hydrogel with high relaxation and on the control. Magnification 10x, scale bar = 100 μm. Osteogenic commitment of (d, e, f) hMSCs and (g, h, i) osteoblasts cultured on a glass slide (controls), of (j, k, l) hMSCs cultured on a poly(acrylamide-co-acrylic acid) hydrogel with a stiffness of 55 kPa and a high relaxation of 70%, and of (m, n, o) hMSCs cultured on a pure polyacrylamide hydrogel with a stiffness of 55 kPa and a low relaxation of 15%. Cells were stained for E11/podoplanin (d, g, j, m) in red, for F-actin in green (e, h, k, n) and cell nucleus in blue (f, i, l, o). Magnification 40x, scale bar = 20 μm. (p) Quantitative analysis of the total cellular E11 immunofluorescence intensity in hMSCs and osteoblasts cultured on glass (controls), and in hMSCs cultured on the two different hydrogels. (n=2) The expression of E11, an early osteocyte marker, is dramatically higher for cells on the hydrogel with low relaxation. (*** $P < 0.001$)

Finally, as E11 has been found to play a role in dendrite formation in osteocytes[147, 154], the association of the dendritic morphology of the cells together with a higher expression of E11 on the hydrogel with low stress relaxation constitutes a solid evidence of a more advanced osteogenic differentiation on this material, and even of osteocytic differentiation. However, in order to confirm that the cells were engaged towards the osteogenic commitment, the expression of osteopontin has been assessed for the same conditions (Supplementary Figure 5.17). Osteopontin is expressed at a similar level for the cells on the two hydrogels (with high and low relaxation), which is consistent with the fact that both osteoblasts and osteocytes express osteopontin at high level.[329, 333] Finally, the expression of osteopontin is higher for the cells on the two hydrogels as compared to osteoblasts or MSCs on glass in osteogenic differentiation medium, showing an osteogenic commitment of the cells.

The use of osteocytes is limited as isolating osteocytes from bone is still challenging, leading to very low yields and high cell heterogeneity.[5, 155, 156] Furthermore, although different cell lines have been developed for the study of osteocytes, they also have limitations such as absence of SOST/sclerostin expression, normally found in late osteocytes, and absence of a mineralized matrix.[155, 156] Osteocytes can also be obtained from the differentiation of pre-osteoblastic cells, however this requires several steps and takes between 3 and 6 weeks.[98] To the best of our knowledge, this study represents the first in vitro differentiation of hMSCs into osteocytes, which therefore constitutes a major step forward for the study of hMSCs osteogenic differentiation and osteocyte function, and for bone reconstruction.

5.5 Conclusions

To date, many studies have focused on investigating the impact of hydrogel stiffness on hMSCs differentiation. However, it is now acknowledged that both hydrogels and biological tissues are intrinsically viscoelastic. In this context, some studies have been conducted on tuning hydrogels viscoelasticity and evaluating the effect on stem cell differentiation, but these studies are still not numerous and led to contradictory results. By studying polyacrylamide hydrogels stress relaxation, it has been shown that these gels are mainly elastic materials, due to covalent crosslinks. It was also demonstrated that adding acrylic acid during the gel formation led to a copolymer hydrogel with increased swelling and relaxation explained by the negative charges of carboxylate functions creating electrostatic repulsion between the polymer chains. In addition, viscoelasticity and poroelasticity both contribute to these hydrogels stress relaxation, on timescales of minutes and hundreds of minutes, respectively, with a larger contribution of the poroelasticity mechanism. Finally, tuning the crosslinker content and the ratio between the two monomers leads to hydrogels with defined mechanical properties, in terms of stiffness and relaxation, which is of great interest to further investigate the impact of hydrogels mechanical properties on cell adhesion, spreading and differentiation. For instance, it has been shown that a hydrogel exhibiting a low relaxation of 15% promotes faster osteogenic differentiation of hMSCs, as compared to a hydrogel with a high relaxation of 70%. hMSCs on low relaxing gel even differentiated into osteocytes and therefore reached the final stage of differentiation, which is unprecedented in vitro. Future works will aim at functionalizing these materials with different bioactive molecules, such as proteins and peptides, and providing a deeper assessment of the impact of both hydrogel functionalization and mechanical properties, including stiffness and viscoelastic behavior, on mesenchymal stem cells differentiation. This will provide a multiparametric study which will significantly improve our knowledge of cell interaction with biomaterials which is still lacking today.

5.6 Materials & Methods

5.6.1 Materials

N,N-methylenebisacrylamide, acrylic acid, ammonium persulfate (APS), sodium phosphate dibasic and sodium phosphate monobasic, Phosphate Buffered Saline (PBS) buffer, sulfo-SANPAH (sulfosuccinimidyl 6-(4'-azido-2'-nitrophenylamino)hexanoate), HEPES (4-(2-hydroxyethyl)-1-piperazineethanesulfonic acid), paraformaldehyde, Triton X-100, Tween 20, Bovine Serum Albumine (BSA), and Fluoroshield^{TM} with Dapi were obtained from Sigma-Aldrich (Canada). Acrylamide (40% in water) was purchased from VWR Alfa Aesar (Canada). KRKIPKASSVPTELSAISMLYLC peptide, which is a BMP-2 mimetic peptide previously identified by our group, and KRKIPKASSVPTELSAISMLYLCK-TAMRA peptide were synthesized by GeneCust (France). Bone marrow hMSCs, MSCs growth medium 2 (MSC-GM2), MSC Osteogenic Differentiation medium, human osteoblasts, and Osteoblast Growth Medium were purchased from Promocell (Germany). Tetramethylethylenediamine (TEMED), Alpha Modified Eagle Medium (α-MEM), sterile PBS, trypsin/EDTA (Ethylenediaminetetraacetic acid), penicillin/streptomycin, Fetal Bovine Serum (FBS) were obtained from Thermo Fisher Scientific (Canada). Alexa Fluor^{TM} 488 phalloidin and Alexa Fluor^{TM} 647 goat anti-mouse IgG (H+L) were bought from Invitrogen (France). Mouse monoclonal anti podoplanin antibody was purchased from Abcam (UK).

5.6.2 Methods

Preparation of hydrogels

The gel precursor solutions were prepared by mixing appropriate amounts of N,N-methylene-bis-acrylamide, acrylamide, and acrylic acid in a buffered solution at pH 8 (Supplementary Table 5.1). Hydrogels with sixteen different compositions were synthesized by varying the amount of crosslinker and acrylic acid, for a total volume of solution of 25 mL. The pH of the solutions containing acrylic acid had to be adjusted to 8 by adding 1 to 5 mL of a sodium hydroxide solution (2 mol.L^{-1}). This, in turn, led to a slight increase of the volume of the reactive medium that was compensated by adding buffer solution to reach a final volume of 31 mL to keep the methylene-bis-acrylamide concentration constant from a hydrogel formulation to the other.

Two parameters are generally defined as references to compare hydrogel formulations. These two parameters are the total polymer content (T) and crosslinker concentration (C), which are calculated as follows[206] :

$$T(w/v\%) = \frac{acrylamide(g) + bis.acrylamide(g) + acide.acrylique(g)}{volume.total.de.la.solution(ml)} \times 100$$

$$C(w\%) = \frac{bis.acrylamide(g)}{acrylamide(g) + bis.acrylamide(g) + acide.acrylique(g)} \times 100$$

In this study, the total polymer content was kept constant to 16.2%, while the crosslinker concentration was varied to 0.03, 0.24, 0.36 and 0.48%.
After the solutions were prepared, they were outgassed by argon bubbling for 10 minutes. Then 12.5 μL of TEMED (tetramethylethylenediamine) and 125 μL of APS (ammonium persulfate, 10 w/v% in ultrapure water) were added simultaneously to the reaction mixture. The solutions were then quickly poured into a round petri dish of 10 cm diameter and maintained under a flow of argon into a sealed container for 2 hours, to avoid the presence of oxygen which acts as an inhibitor of the radical polymerization. Hydrogels were then put in PBS (Phosphate Buffered Saline) at room temperature and allowed to swell at equilibrium for at least 4 days before cutting disks of 10 mm diameter using a metallic punch.

FTIR (Fourier Transform Infrared Spectroscopy)

Hydrogel disks were frozen in liquid nitrogen before being freeze-dried for 24 h. The Fourier Transform Infrared (FTIR) spectra of dried samples were recorded on a Cary 660 (Agilent Technologies, USA) FTIR spectrometer in the ATR mode (Attenuated Total Reflectance) using a SplitPea attachment (Harrick Scientific) in the 500 cm-1 to 4000 cm-1 spectral range. FTIR spectra were recorded at a resolution of 4 cm-1 by co-adding 64 scans. All measurements were made at room temperature.

Swelling

Hydrogel disks of 10 mm diameter were weighed and put in 3 mL of PBS (pH 7.4). They were then weighed every day, for seven days, to assess the time needed to reach swelling equilibrium. Their weight was shown to be stable after 3 days. After seven days of swelling, samples were frozen at -20 °C overnight before being freeze-dried for 24 h. Dry samples were then weighed to obtain the initial mass of the sample. The fluid absorption capacity (FAC) was calculated using the following equation :

$$FAC(gPBS/gpolymer) = \frac{(m1 - m0)}{m1}$$

Where m1 is the weight of the sample with absorbed fluid (after seven days), and m0 is the weight of the dry sample. Measurements were performed in triplicate.
A similar procedure was used to measure the fluid absorption capacity of the hydrogels as a function of pH. The hydrogels were incubated for three weeks in PBS buffer with pH adjusted to

3 or 10, with weighing the hydrogels and changing the buffer every four days until the swelling equilibrium was reached. Samples were then frozen at -20 °C overnight before being freeze-dried for 24 h. Dry samples were then weighed to obtain the initial mass of the sample and to calculate the fluid absorption capacity. Measurements were performed in triplicate.

Mechanical testing

The modulus and stress relaxation properties of polyacrylamide and poly(acrylamide-co-acrylic acid) gels were measured from unconfined compression tests of the gel disks (10 mm in diameter, 2 mm thick, equilibrated in PBS pH 7.4 for 4 days) using a Mach-1 V500CS (Biomomentum, Canada) apparatus equipped with a 1.5 N single-axis load cell. Gel disks were compressed between two flat platens, with a flat indenter of 3 cm diameter, and were free to expand in the radial direction. Tests were performed at room temperature in a PBS bath to avoid the drying of the samples. The gel disks were compressed to 5 consecutive steps of 3% strain with a deformation rate of 1 mm.min^{-1}. The strain was held constant between two steps, while the load was recorded as a function of time for 1 hour and 50 minutes. Of note, the samples were left to swell in PBS for four days at pH 7.4, and three weeks at pH 3 and 10, before performing the mechanical tests to make sure that the swelling equilibrium was achieved and to avoid a change in swelling during the test. Measurements were performed in triplicate.

Stress relaxation curves analysis

Different models have been developed to describe the viscoelastic behavior of materials. These models are composed of springs and dashpots combined in many different ways[334]. Springs represent ideal solids and account for the elastic behavior of materials[334, 335], while dashpots correspond to ideal fluids and are responsible for the dissipation of the stress during stress relaxation experiments.[334, 335, 336, 337]
One standard approach used to describe a viscoelastic behavior involves using the Maxwell model (Supplementary Figure 5.10), which consists in one spring associated in series with a dashpot. This model can be used to describe the behavior of a viscoelastic material submitted to a stress relaxation experiment.[334, 335, 336, 337, 338] During the relaxation, the stress decreases exponentially with time. The stress as a function of time during relaxation is therefore given by the following equation :

$$\sigma(t) = \sigma 0.exp(\frac{-t}{\tau})$$

Where σ 0 is the maximal stress and τ the relaxation time.
However, the existence of a single relaxation time in the Maxwell model is considered a limitation in depicting viscoelastic materials which generally have more than one relaxation mechanism.[338] Consequently, more complex models are constructed, as the generalized

Maxwell model (Supplementary Figure 5.11), which consists in combining several Maxwell units in parallel, where each unit has different parameter values and accordingly, a different relaxation time. In general, the more elements are used, the more accurate the model will be in describing the response of materials.[336] However, the more complex the model, the more parameters need to be determined. Consequently, the selected model is usually the model comprising the minimum number of elements required to fit the experimental data. Finally, for some materials, the stress does not decrease to zero during the relaxation but reaches an equilibrium stress (Supplementary Figure 5.11). It is therefore necessary to add an isolated spring in parallel with the Maxwell elements which represents the final stress.[339]
In this study, a standard linear solid model with three Maxwell elements was used to analyze the relaxation curves and is described by the following equation :

$$\sigma(t) = a.exp(\frac{-t}{\tau 1}) + b.exp(\frac{-t}{\tau 2}) + c.exp(\frac{-t}{\tau 3}) + d$$

Where $\tau 1$, $\tau 2$ and $\tau 3$ are the three relaxation times of the three Maxwell elements and d is the equilibrium stress in the isolated spring in accordance with Supplementary Figure 5.10. The 7 parameters a, b, c, d and $\tau 1$, $\tau 2$ and $\tau 3$ were computed using Matlab® (version R2017b).
Limits for the coefficients a, b, c and d were fixed between 0 and $+\infty$, and between 0 and 30 s for $\tau 1$, 30 and 2000 s for $\tau 2$, and 2000 and 6480 s for $\tau 3$. Correlation coefficients greater than 0.97 were obtained for all relaxation tests. The first relaxation time was set between 0 and 30 s to represent the rapid initial drop of the stress observed on the experimental curves. The second relaxation time was limited to hundreds of seconds which corresponds to hydrogel viscoelasticity.[325] The third relaxation time was set to thousands of seconds to represent the relaxation at long timescales, which has been observed for covalently crosslinked hydrogels.[312] In this study, the stiffness of the hydrogels, or their equilibrium modulus, is obtained by calculating the residual force at the end of the relaxation for each of the five compression steps, and by measuring the slope of the line connecting these five points. Then, the relaxation degree (%) of the different hydrogel formulations is calculated as the proportion of the maximum stress that is lost during the stress relaxation (Supplementary Figure 5.12).

Scanning Electron Microscopy

Hydrogel porosity was assessed with a FEI Quanta 250 microscope (FEI Company Inc. Thermo-Fisher Scientific, OR), operated with an acceleration voltage of 15 kV. Prior to analyses, the hydrogels were immersed in liquid nitrogen to maintain their 3D structure, before being freeze dried and coated with a thin gold-palladium film. SEM images were recorded at 2000X and 10000X magnifications. The pore size and porosity degree were evaluated on three different regions for each hydrogel using ImageJ software.

Hydrogels functionalization

For cell seeding experiments, a BMP-2 mimetic peptide was conjugated to hydrogels surface by using the linker Sulfo-SANPAH following previously described protocols.[55, 56, 69] Briefly, 200 μL of a 1 mmol.L^{-1} solution of Sulfo-SANPAH in HEPES buffer (50 mmol.L^{-1}, pH 8.5) were pipetted onto the gel surface in a 48-well plate which was placed under ultraviolet light (365 nm) in a UV chamber (Uvitec, UK). The gels were exposed to UV light for 30 min and rinsed with 500 μL HEPES for each side of the gel disks. The gels were then incubated with a solution of BMP-2 mimetic peptide (10^{-3} mol.L^{-1}) in 50 mM HEPES overnight at 4°C. The gels were then rinsed in 5 mL HEPES for one week, with changing the rinsing solution twice a day.

Cell culture and cytofluorescent staining

Bone marrow hMSCs were thawed and cultured in MSCs growth medium 2 (MSC-GM2), in a humidified atmosphere containing 5% CO2 at 37°C as recommended by the supplier. They were subcultured twice a week using trypsin/EDTA 1x detachment and used at passage 5. For differentiation experiments, hMSCs were seeded at a density of 3,000 cells/cm^2 in α-MEM medium on glass slides or on functionalized hydrogels previously sterilized with 70% ethanol overnight. All cell seedings were carried out without any serum for the first 4 h of culture. This enabled the interaction of cells with the surface conjugated biomolecules and not with adsorbed serum proteins. After 4 h, the culture medium was supplemented with 10% FBS. After 24 h, the medium was replaced by MSC Osteogenic Differentiation medium supplemented with 1% penicillin/streptomycin. The cells were then cultured for 2 weeks and the Osteogenic Differentiation medium was changed twice a week. Human osteoblasts were thawed and cultured in Osteoblast growth medium in a humidified atmosphere containing 5% CO_2 at 37°C. They were subcultured once a week using trypsin/EDTA 1x detachment and used at passage 2. Osteoblasts were seeded at a density of 20,000 cells/cm^2 in Osteoblast Growth Medium on glass slides previously sterilized with 70% ethanol overnight.
After 24 h for osteoblasts and 2 weeks for hMSCs, cells were fixed in 4% paraformaldehyde at 4°C for 20 min, permeabilized with 0.5% Triton X-100 in PBS for 15 min at 4°C and blocked with 1% BSA in PBS for 30 min at 37°C. The cell morphology and cytoskeleton organization were evaluated by labeling filamentous actin (F-actin) with Alexa Fluor^{TM} 488 phalloidin (1 :40 dilution) for 1 h at 37°C. The expression of the early osteocyte marker E11/podoplanin was assessed by incubating cells for 1h at 37°C with 2 μg/mL mouse monoclonal anti-podoplanin primary antibody, then with the secondary antibody Alexa Fluor^{TM} 647 goat anti-mouse IgG (H+L) (1 :400 dilution) for 1 h at 37°C. Samples were then stained for nuclei using Fluoroshield^{TM} with Dapi. Fluorescently stained cells were examined using a Leica DM5500B epifluorescence microscope (Leica Biosystems) equipped with a CoolSnap HQ camera and controlled by Metamorph 7.6 software. The expression of the osteocyte marker E11 was

quantified using ImageJ software by measuring the fluorescence intensity on 40 to 50 cells per sample, with two samples per condition.

Statistical analysis

Data are expressed as the mean $\pm$ standard deviation (SD). For the data of fluid absorption capacity, hydrogels stiffness and stress relaxation extent, a F-test was used to determine the equality or inequality of the variance. Then, a t-test was used to determine the significant difference between two conditions, with Welch's correction in the case of inequal variance, using GraphPad Prism version 7 for Windows. For the data of E11 expression, the statistical analysis was performed by one-way analysis of variance (ANOVA) and Tukey's test for multiple comparisons using GraphPad Prism version 7 for Windows. Significant differences were determined for P values ≤ 0.05 (* represents $P < 0.05$, ** $P < 0.01$, and *** $P < 0.001$).

Acknowledgements

The authors thank Dr. Delphine Maurel (Laboratory for the Bioengineering of Tissues, Bordeaux University, France) for sharing her knowledge about osteocytes and osteocytes markers. This work was supported by the University of Bordeaux [Emilie Prouvé's PhD grant] and the National Sciences and Engineering Research Council of Canada (NSERC), as well as the Centre Québécois sur les Matériaux Fonctionnels (CQMF). The financial support of the ANR EchoCell (ANR-17-CE11-0020) is also acknowledged.

5.7 Supplementary information

T(%)	C(%)	Ratio acrylamide / acrylic acid (mol%)	N,N-methylene bisacrylamide (mg)	Acrylamide - 40% in water (mL)	Acrylic acid (μL)	Buffer solution pH 8 (mL)
16.2	0.03	100 / 0	10	12.5	0	12.4
16.2	0.24	100 / 0	75	12.3	0	12.6
16.2	0.36	100 / 0	112.5	12.2	0	12.4
16.2	0.48	100 / 0	150	12.1	0	12.4
16.2	0.03	95 / 5	10	11.9	242	12.7
16.2	0.24	95 / 5	75	11.7	238	12.9
16.2	0.36	95 / 5	112.5	11.6	236	13.0
16.2	0.48	95 / 5	150	11.5	234	13.1
16.2	0.03	90 / 10	10	11.3	483	13.1
16.2	0.24	90 / 10	75	11.1	476	13.3
16.2	0.36	90 / 10	112.5	11.0	472	13.4
16.2	0.48	90 / 10	150	10.9	469	13.5
16.2	0.03	82 / 18	10	10.3	869	13.7
16.2	0.24	82 / 18	75	10.1	856	13.9
16.2	0.36	82 / 18	112.5	10.0	850	14.0
16.2	0.48	82 / 18	150	9.9	843	14.1

TABLE 5.1 – Composition of gel precursor solutions, where T represents the total polymer content and C represents the crosslinker concentration.

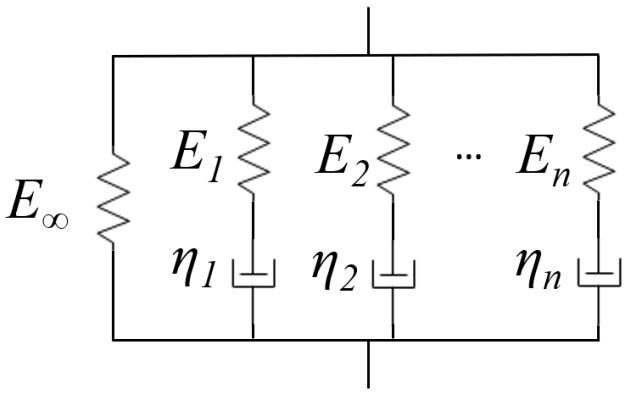

FIGURE 5.10 – Schematic of a generalized Maxwell model consisting of n Maxwell elements in parallel. A Maxwell element is composed of one spring (E) and one dashpot (η) in series. An extra isolated spring (E_∞) is added in parallel to represent the final stress.[339]

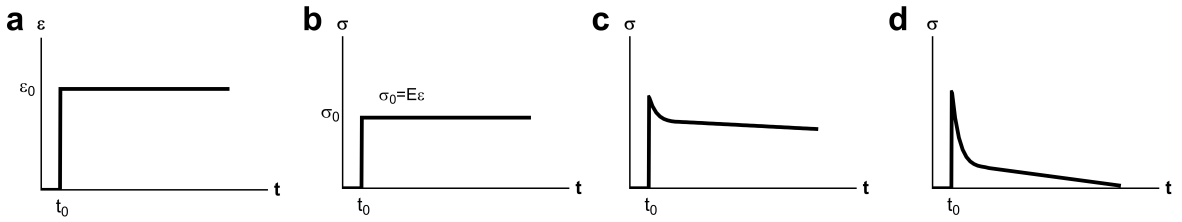

FIGURE 5.11 – a) A stress relaxation experiment is performed by applying and maintaining a constant level of strain and observing the response of the material over time. b) The stress developed in a purely elastic material remains constant as long as the strain is maintained. A viscoelastic material responds with an initial high stress that will decrease over time. c) If the material is a viscoelastic solid, the stress level does not reduce to zero. d) The stress reduces to zero for a viscoelastic fluid. Adapted from [334]

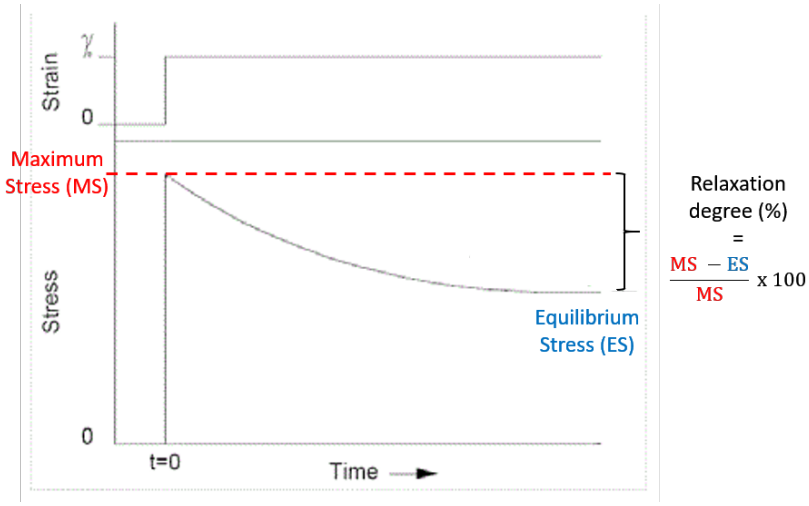

FIGURE 5.12 – Calculation of the relaxation degree of hydrogels from the stress relaxation experiments.

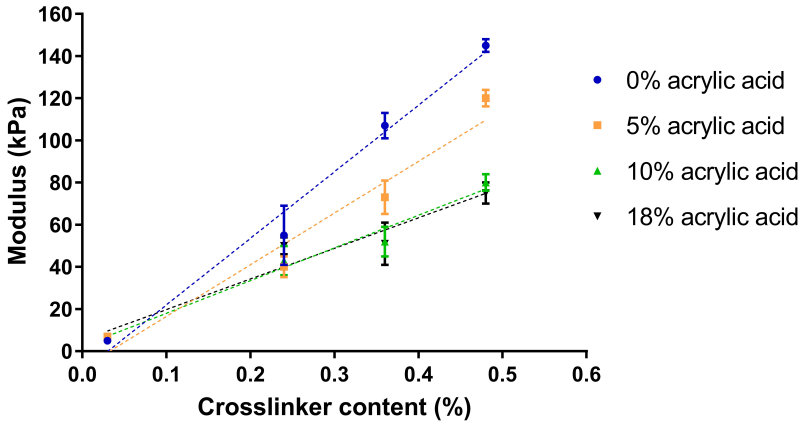

FIGURE 5.13 – Linear relation between the Modulus and the amount of crosslinker for different contents of acrylic acid. (n=3)

Swelling behavior

a	0.03% BIS-0% AAC	0.24% BIS-0% AAC	0.36% BIS-0% AAC	0.48% BIS-0% AAC	0.03% BIS-5% AAC	0.24% BIS-5% AAC	0.36% BIS-5% AAC	0.48% BIS-5% AAC	0.03% BIS-10% AAC	0.24% BIS-10% AAC	0.36% BIS-10% AAC	0.48% BIS-10% AAC	0.03% BIS-18% AAC	0.24% BIS-18% AAC	0.36% BIS-18% AAC	0.48% BIS-18% AAC
0.03% BIS-0% AAC		****	****	****	****	****	****	****	***	*	****	****	**			****
0.24% BIS-0% AAC			**	****	****	****		**	****	****	****	***	**	****	****	****
0.36% BIS-0% AAC				***	****	**	**	*	***	**	***	**	**	***	**	***
0.48% BIS-0% AAC					****	****	****	***	***	**	****	****	**	****	**	****
0.03% BIS-5% AAC						****	****	****	***	****	****	****	*	****	***	****
0.24% BIS-5% AAC							***	****	****	**		**	****	****	**	
0.36% BIS-5% AAC								**	****	***	***	**	**	****	****	****
0.48% BIS-5% AAC									****	****	****	***	**	****	****	****
0.03% BIS-10% AAC										****	****	****		****	****	****
0.24% BIS-10% AAC											**	***	***	**		**
0.36% BIS-10% AAC												**	**	****	***	**
0.48% BIS-10% AAC													**	****	***	***
0.03% BIS-18% AAC														**	***	**
0.24% BIS-18% AAC															*	****
0.36% BIS-18% AAC																*
0.48% BIS-18% AAC																

Hydrogels stiffness

b	0.03% BIS-0% AAC	0.24% BIS-0% AAC	0.36% BIS-0% AAC	0.48% BIS-0% AAC	0.03% BIS-5% AAC	0.24% BIS-5% AAC	0.36% BIS-5% AAC	0.48% BIS-5% AAC	0.03% BIS-10% AAC	0.24% BIS-10% AAC	0.36% BIS-10% AAC	0.48% BIS-10% AAC	0.03% BIS-18% AAC	0.24% BIS-18% AAC	0.36% BIS-18% AAC	0.48% BIS-18% AAC
0.03% BIS-0% AAC		*	**	***	***	**	**	***	**	**	**	***		**	*	**
0.24% BIS-0% AAC			**	***	*			**	*				*			
0.36% BIS-0% AAC				**	**	***	**		**	***	***	**	**	***	**	**
0.48% BIS-0% AAC					***	****	***	**	***	****	****	****	***	****	***	****
0.03% BIS-5% AAC						**	**	***		*	**	**	**	**	*	**
0.24% BIS-5% AAC							**	****	**			***	**			**
0.36% BIS-5% AAC								**	**	*	*		**	*		
0.48% BIS-5% AAC									***	***	***	***	***	****	***	***
0.03% BIS-10% AAC										*	**	**	*	**	*	**
0.24% BIS-10% AAC												**	*			**
0.36% BIS-10% AAC												**	**			*
0.48% BIS-10% AAC													***	***	*	
0.03% BIS-18% AAC														**	*	**
0.24% BIS-18% AAC																**
0.36% BIS-18% AAC																*
0.48% BIS-18% AAC																

BIS = crosslinker
AAC = acrylic acid

FIGURE 5.14 – Statistical analysis of a) hydrogels fluid absorption capacity and b) hydrogels stiffness. The statistical analysis was done by a F-test followed by a T-test. Grey boxes represent the absence of statistic difference. P values are represented as following * $\leq$ 0.05, ** $\leq$ 0.01, *** $\leq$ 0.001, **** $\leq$ 0.0001.)

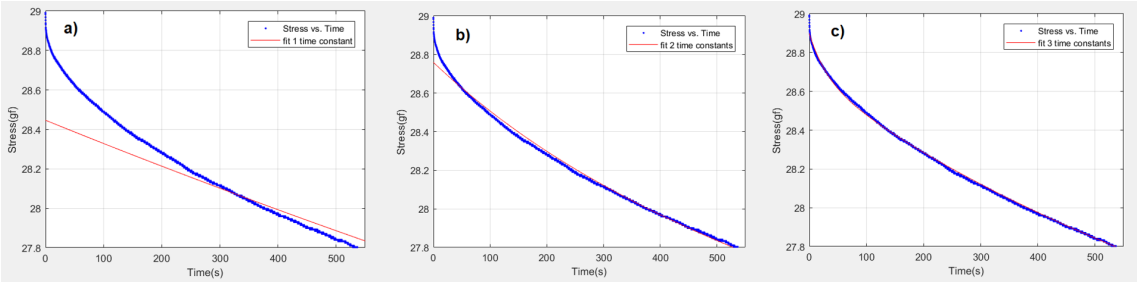

FIGURE 5.15 – Example of stress relaxation modeling with generalized Maxwell model with one (a), two (b) or three (c) time constants in red versus experimental data in blue. Between 0 and 500 s, the experimental curve could be well fitted using three time constants.

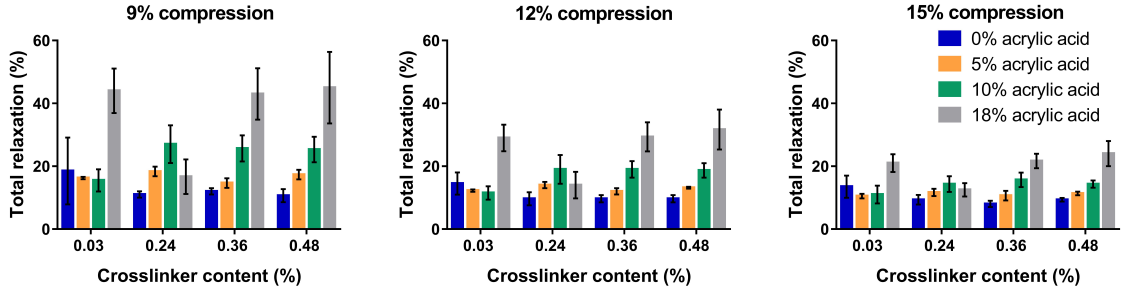

FIGURE 5.16 – Total stress relaxation for the different hydrogel formulations as a function of the crosslinker content at different compression steps. The relaxation generally increases with the amount of acrylic acid and decreases when increasing the compression. (n=3)

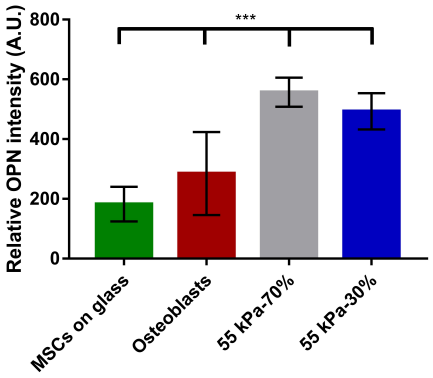

FIGURE 5.17 – Quantitative analysis of the nuclear osteopontin immunofluorescence intensity in hMSCs and osteoblasts cultured on glass (controls), and in hMSCs cultured on a poly(acrylamide-co-acrylic acid) hydrogel with a stiffness of 55 kPa and a high relaxation of 70%, or a pure polyacrylamide hydrogel with a stiffness of 55 kPa and a low relaxation of 15%. (n=2) The expression of OPN, expressed by both osteoblasts and osteocytes, is higher on the two hydrogels as compared to the controls. (*** $P < 0.001$)

Total relaxation

	0.03% BIS-0% AAC	0.24% BIS-0% AAC	0.36% BIS-0% AAC	0.48% BIS-0% AAC	0.03% BIS-5% AAC	0.24% BIS-5% AAC	0.36% BIS-5% AAC	0.48% BIS-5% AAC	0.03% BIS-10% AAC	0.24% BIS-10% AAC	0.36% BIS-10% AAC	0.48% BIS-10% AAC	0.03% BIS-18% AAC	0.24% BIS-18% AAC	0.36% BIS-18% AAC	0.48% BIS-18% AAC
0.03% BIS-0% AAC													*		*	*
0.24% BIS-0% AAC					**	**	*	**	***	*	*	***	****		*	*
0.36% BIS-0% AAC				*	*	**		*	***	*	*	***	****		*	*
0.48% BIS-0% AAC					**	**	*	**	**	**	*	***	****		*	*
0.03% BIS-5% AAC										*	*	**	***		*	*
0.24% BIS-5% AAC							*					**	***		*	*
0.36% BIS-5% AAC								*	***	*	*	***	****		*	*
0.48% BIS-5% AAC										*	*	**	***		**	*
0.03% BIS-10% AAC												**	**		*	*
0.24% BIS-10% AAC													**		*	*
0.36% BIS-10% AAC													**		*	*
0.48% BIS-10% AAC													***	*	*	*
0.03% BIS-18% AAC														***		
0.24% BIS-18% AAC															**	*
0.36% BIS-18% AAC																
0.48% BIS-18% AAC																

FIGURE 5.18 – Statistical analysis of hydrogels total relaxation for 6% compression. The statistical analysis was done by a F-test followed by a T-test. Grey boxes represent the absence of statistic difference. P values are represented as following * $\leq$ 0.05, ** $\leq$ 0.01, *** $\leq$ 0.001, **** $\leq$ 0.0001.)

Chapter 6

Study 2 : Interplay of matrix stiffness and stress relaxation in directing Mesenchymal Stem Cells osteogenic differentiation

Emilie Prouvé[a,b,c,d,e], Murielle Rémy[c,d,e], Cécile Feuillie[c,d,e], Michael Molinari[c,d,e], Pascale Chevallier[a,b], Bernard Drouin[b], Gaétan Laroche[a,b*†], and Marie-Christine Durrieu[c,d,e*†]

[a]Laboratoire d'Ingénierie de Surface, Centre de Recherche sur les Matériaux Avancés, Département de Génie des Mines, de la Métallurgie et des Matériaux, Université Laval, 1065 Avenue de la médecine, Québec G1V 0A6, Canada
[b]Axe Médecine Régénératrice, Centre de Recherche du Centre Hospitalier Universitaire de Québec, Hôpital St-François d'Assise, 10 rue de l'Espinay, Québec G1L 3L5, Canada
[c]Université de Bordeaux, Chimie et Biologie des Membranes et Nano-Objets (UMR5248 CBMN), Allée Geoffroy Saint Hilaire - Bât B14, 33600 Pessac, France
[d]CNRS, CBMN UMR5248, Allée Geoffroy Saint Hilaire - Bât B14, 33600 Pessac, France
[e]Bordeaux INP, CBMN UMR5248, Allée Geoffroy Saint Hilaire - Bât B14, 33600 Pessac, France

†These authors contributed equally.

*Corresponding authors :
Gaetan.Laroche@gmn.ulaval.ca Phone : +1 (418) 656-7983 Fax : (418) 656-5343
marie-christine.durrieu@inserm.fr Phone : +33 5 40 00 30 37 Fax : +33 5 40 00 30 68

This work is in preparation for a submission to the journal *Biomaterials* in October 2021

6.1 Résumé

Cette étude vise à évaluer l'impact de la rigidité et de la relaxation de contrainte d'hydrogels sur la différenciation ostéogénique de cellules souches mésenchymateuses humaines (hMSCs). Des hydrogels de poly(acrylamide-co-acide acrylique) ont été synthétisés en variant la formulation des gels pour obtenir des propriétés mécaniques contrôlées, mesurées par compression et par Microscopie à Force Atomique (AFM). Les hydrogels ont ensuite été fonctionnalisés avec un peptide mimétique de la protéine BMP-2 avant de mettre en culture des hMSCs sur les différents hydrogels. Des rigidités allant de 60 à 140 kPa ont mené à l'obtention de cellules étoilées, forme caractéristique des ostéocytes. Une rigidité de 60 kPa a mené à une plus forte expression de marqueurs ostéocytaires par rapport à des rigidités de 15 et 140 kPa, pour une même relaxation (15%). La plus forte expression de marqueurs de différenciation a été observée pour un gel avec une rigidité de 140 kPa et une relaxation de 70%.

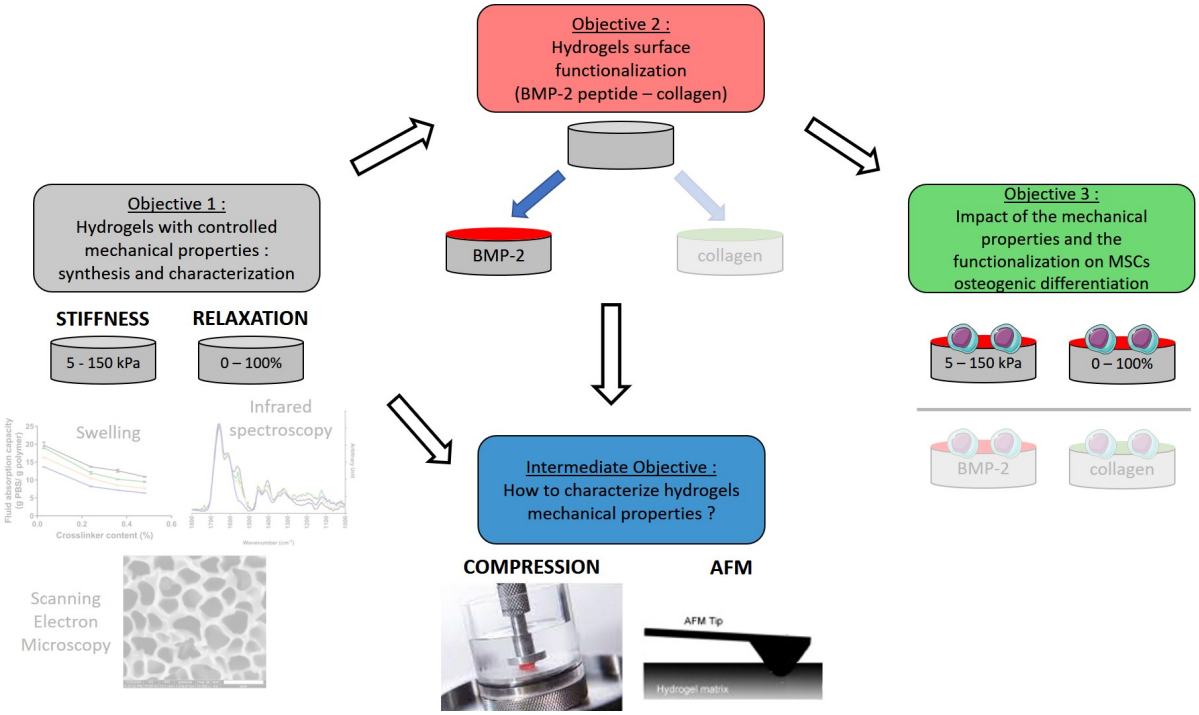

NB : The parts in transparency are not covered in this chapter.

6.2 Abstract

The aim of this study is to investigate the impact of poly(acrylamide-co-acrylic acid) hydrogels stiffness and stress relaxation on the osteogenic differentiation of human mesenchymal stem cells (hMSCs). Varying the amount of crosslinker and the ratio between the monomers enabled to obtain hydrogels with controlled mechanical properties, as characterized using unconfined compression and Atomic Force Microscopy (AFM). Subsequently, the surface of the hydrogels has been homogeneously functionalized with a mimetic peptide of the BMP-2 protein, in order to favor hMSCs osteogenic differentiation. AFM measurements revealed that the functionalization of hydrogels containing acrylic acid led to an increase in their surface stiffness, but did not affect hydrogels stress relaxation. Finally, hMSCs were cultured on the hydrogels with different stiffness and stress relaxation : 15 kPa-15%, 60 kPa-15%, 140 kPa-15%, 100 kPa-30%, and 140 kPa-70%. The cells on hydrogels with stiffnesses from 60 kPa to 140 kPa presented a star-like shape with dendritic connections between the cells, regardless of hydrogels relaxation. This shape is characteristic of osteocytes, the last stage of osteogenic differentiation. The obtention of osteocytes from MSCs differentiation on two-dimensional substrates has only been reported by our group. Then, the extent of hMSCs osteogenic differentiation has been evaluated by using immunofluorescence and by quantifying both the expression of osteoblast markers (Runx-2, osteopontin) and osteocyte markers (E11, DMP1, sclerostin), which has not been performed elsewhere. It has been found that a stiffness of 60 kPa led to a higher expression of osteocyte markers as compared to stiffnesses of 15 and 140 kPa, for a constant low relaxation of 15%. Finally, the strongest expression of osteoblast and osteocyte differentiation markers has been observed for the hydrogel with a high relaxation of 70% and a stiffness of 140 kPa. Thus, the viscoelastic properties of the matrix would have a significant impact on MSCs differentiation and should be considered in the future.

Keywords : Poly(acrylamide-co-acrylic acid) hydrogels - stiffness and stress relaxation - unconfined compression and AFM - human Mesenchymal Stem Cells - osteogenic differentiation - BMP-2 surface functionalization - osteocytes

6.3 Introduction

Mesenchymal Stem Cells (MSCs) are multipotent adult stem cells which have gained high interest in tissue engineering and regenerative medicine considering their self-renewal ability, multipotency, ease of access with few ethical issues, and high proliferative rate.[101, 287] MSCs are capable of differentiating into mesoderm-type cells such as osteoblasts (bone cells), chondrocytes (cartilage cells), and adipocytes (fat cells).[101, 287, 340, 341] In addition, some studies reported a successful differentiation into other cell types such as neurons[52], smooth muscle cells[342], and hepatocytes[343]. These observations have raised hopes for the application of MSCs in regenerative therapies through cell transplantation by intravenous or direct intra-tissue injection.[344] However, it is now accepted that MSCs need to differentiate before being introduced into patients, as the clinical use of undifferentiated stem cells may lead to uncontrolled proliferation and differentiation resulting in serious complications such as tumor formation.[32] Consequently, the use of MSCs in clinical applications requires a better understanding of their biological behavior to provide the ability to control their differentiation into a specific lineage needed for therapy. MSCs being adherent cells, many studies have evaluated the impact of materials surface properties on their differentiation, such as surface charge[189], surface chemistry[345], roughness[191], topography[105], stiffness[52], and the conjugation, organization, and conformation of biomolecules[84]. In general, the main strategy consists in trying to mimic the properties of the native extracellular matrix (ECM) of cells to induce the desired cell response.

It is now acknowledged that MSCs sense and respond to the mechanical properties of the ECM and synthetic substrates such as hydrogels, by exerting contractile forces through adhesion complexes.[64] Hydrogels are three-dimensional networks formed by the crosslinking of hydrophilic polymer chains. They have gained a huge interest in biomedical research because of their tunable chemical properties, elasticity, porosity, and their capability to absorb large amounts of fluids, providing them with the ability of mimicking the ECM.[36] Regarding the impact of the matrix stiffness on MSCs differentiation, the hypothesis is that a material mimicking the stiffness of a given natural tissue will induce a differentiation towards cells of this same tissue. Considering the case of bone, the osteoid, a collagen matrix secreted by osteoblasts, would constitute the matrix from which MSCs differentiate into preosteoblasts.[52] Engler at al. evaluated the stiffness of osteoid to 27 ± 10 kPa.[52] This value is in accordance with the range of stiffnesses identified in the literature as promoting a higher MSCs osteogenic differentiation (from 20 to 60 kPa)[52, 55, 56, 57, 58, 62, 63, 231, 232, 233, 308], using polyacrylamide hydrogels as a carrier material for cell culture. Nevertheless, this range of stiffnesses is still not very precise, and most of these papers are limited to the study of a maximal stiffness comprised between 40 and 60 kPa.[52, 56, 58, 62, 63, 231, 232, 233, 308] While a few papers investigated the impact of higher stiffnesses on MSCs osteogenic differentiation, the results are sometimes contradictory. Some studies using polyacrylamide hydrogels showed that a stiffness higher than

60 kPa (80, 90, 190 kPa) was more favorable for MSCs osteogenic differentiation[57, 60, 69], while another study found that stiffnesses of 20 and 115 kPa promoted a similar extent of MSCs osteogenic differentiation[55]. Finally, a study demonstrated that stiffnesses of 12 and 20 kPa promoted a higher MSCS osteogenic differentiation than lower stiffnesses of 2.5 and 5 kPa, and than a higher stiffness of 110 kPa, when the cells were encapsulated within alginate hydrogels.[54] Consequently, we are still lacking knowledge about the impact of high hydrogel stiffness (> 60 kPa) on MSCs osteogenic differentiation, and we are still lacking precision on the best stiffness for MSCs osteogenic differentiation. In addition to elasticity, hydrogels, as well as biological tissues, must also be characterized through their viscoelastic properties. Indeed, considering that each strain applied by a cell is first resisted by the material with a certain stiffness, which represents the elasticity, and then followed by a decrease in resistance over time due to the viscoelastic response of the material, it is of prime importance to consider hydrogels viscoelastic properties and their impact on cell behavior.[66] To date, only a few studies investigated MSCs differentiation in response to hydrogel viscoelastic properties. For example, Cameron et al. observed a higher expression of adipogenic, myogenic, and osteogenic differentiation markers of MSCs as the hydrogel viscous modulus increased.[67] Chaudhuri et al. found a higher adipogenic differentiation of MSCs for gels with a high relaxation time, and a higher osteogenic differentiation for gels with a low relaxation time.[68] Thus, despite the consensus that MSCs differentiation is affected by hydrogels mechanical properties, the knowledge of the impact of the viscoelastic properties remains limited.

Besides the mechanical properties, the presence and distribution of different proteins within the ECM are also likely to affect stem cell fate. In bone tissue, the ECM is composed by various proteins such as collagens and bone morphogenetic proteins (BMPs). BMPs are a group of proteins that can be found in bone matrix and that can induce MSCs differentiation into osteoblasts through activating cell membrane receptors.[15] Among them, it has been demonstrated that BMP-2, BMP-6, and BMP-9 play a major role in the induction of MSCs osteogenic differentiation[15], while BMP-2 is currently approved by the FDA as an osteoinductive growth factor and used as a bone graft substitute.[17] However, BMP-2 injection has also been associated with severe side effects as poor bone mineral quality, inflammation, ectopic bone formation, and osteolysis[17], which might suggest that BMP-2 immobilization on a bone implant would be preferable to injection. Nevertheless, functionalization of large areas of materials would demand high quantities of molecules, which, in the case of full-length proteins, would be very complex and costly.[71] The use of short synthetic peptides containing only the active amino acid sequence necessary to support a given biological response is therefore an alternative, as they can be produced at large scale with high purity and at low costs.[71] In this context, several peptide sequences derived from the BMP-2 protein have been synthesized and used to promote MSCs osteogenic differentiation[72, 346], including a mimetic peptide identified by Durrieu et al.[83]. This peptide has been shown to promote MSCs osteogenic differentiation when covalently attached to glass, with a decrease in the expression

of a MSC marker, STRO-1, and an increase in the expression of an early osteogenic marker, Runx-2, after 4 weeks of cell culture, as compared with bare glass or glass functionalized with a cell adhesion peptide RGD.[84] Similar results have been obtained by functionalizing PET (polyethylene terephtalate) materials using this same peptide, with a higher expression of early and late osteogenic markers, Runx-2 and OPN (osteopontin), respectively, after 2 weeks of cell culture, in comparison with oxidized PET or PET functionalized with RGD peptide.[85] However, although the use of peptides can bring to these materials a similar bioactivity to the ECM, the mechanical properties of glass or PET are far from being representative of the in vivo cell growth environment. Therefore, combining this BMP-2 mimetic peptide to hydrogels that better mimic the natural cell growth environment appears as a promising approach to further control MSCs differentiation.

Driven by such considerations, this publication proposes a study on the effect of hydrogels mechanical properties, including stiffness and viscoelasticity, on human bone marrow MSCs osteogenic differentiation. To this end, poly(acrylamide-co-acrylic acid) hydrogels with varying stiffness (from 5 to 140 kPa) and viscoelastic properties (relaxation from 15% to 70%), developed in a previous study[77], have been synthesized and characterized using uniaxial unconfined compression and AFM. Indeed, compression and AFM are the most widely used methods to measure hydrogels stiffness in studies evaluating the impact of the stiffness on MSCs differentiation. Therefore, it would be particularly interesting to compare the results obtained with the two techniques, in order to evaluate if studies using compression and AFM could be compared, and to determine which technique is the most suitable for mechanobiology studies in 2 dimensions. Subsequently, the hydrogels have been functionalized with a mimetic peptide of the BMP-2 protein to promote and accelerate MSCs osteogenic differentiation, considering that this peptide has already proven its ability to drive MSCs osteogenic differentiation.[33, 72, 73, 84, 85, 268, 269, 346, 347] Because polyacrylamide based materials do not support cell adhesion[52, 55], this peptide also enables the cells to adhere to the substrates. Then, the impact of hydrogels functionalization on the hydrogels mechanical properties has been assessed using compression and AFM. Considering the response of MSCs to hydrogels stiffness and viscoelasticity, the cell spread area has been evaluated after 24 hours of cell culture. In addition, the osteogenic differentiation of human bone marrow MSCs has been characterized by fluorescent staining of several markers after 24 hours and 2 weeks of cell culture. Early and late MSCs osteogenic differentiation were ascertained by measuring the expression of Runx-2 and OPN (osteopontin), respectively. In addition, E11 (podoplanin), DMP1 (Dentin matrix acidic phosphoprotein 1), and SOST (sclerostin) expressions were investigated as osteocyte markers.

6.4 Results and Discussion

6.4.1 Hydrogels mechanical properties

Polyacrylamide and poly(acrylamide-co-acrylic acid) hydrogels were synthesized by varying the amount of crosslinker and the ratio between the two monomers, acrylamide and acrylic acid, in order to control their stiffness and their viscoelastic properties. The mechanical properties of the hydrogels were characterized using unconfined compression and AFM, and are summarized in Figure 6.1. The statistical analysis is presented in Supplementary Figure 6.13.

Figure 6.1a shows the elastic modulus and Figure 6.1b shows the relaxation of the hydrogels as determined by stress relaxation experiments performed using unconfined compression. Increasing the amount of crosslinker within pure polyacrylamide hydrogels leads to hydrogels with increasing modulus of 5 $\pm$ 1 kPa, 55 $\pm$ 14 kPa, and 145 $\pm$ 3 kPa, but with similar low relaxation around 15-20%. The relaxation (%) of the hydrogels has been calculated as the proportion of the maximum stress that is lost during the stress relaxation. These results are consistent with the fact that polyacrylamide gels are considered mainly as elastic materials[68], and are in agreement with other studies which showed that increasing the amount of crosslinker leads to a rise of the stiffness[69, 206]. Then, increasing the amount of acrylic acid in the hydrogels leads to a rise of hydrogels stress relaxation as a result of the presence of negative charges brought by acrylic acid, which create electrostatic repulsion between the polymer chains, as demonstrated in chapter 5.[77] The hydrogels presented in this study would therefore allow to evaluate the impact of both hydrogels stiffness and stress relaxation on hMSCs osteogenic differentiation, as three hydrogels present very distinct stiffnesses of 5, 55, and 145 kPa, with a low relaxation around 15%, and three hydrogels present a similar stiffness around 55 kPa, with a very distinct relaxation of 15, 30, and 70%.

Figure 6.1c shows the elastic modulus of the hydrogels measured using AFM. It can be seen that the parameters used for the AFM measurements led to the obtention of similar modulus compared to compression. This is consistent with previous studies which obtained similar moduli for hydrogels characterized with bulk compression and AFM[348, 349, 350], although one study observed some discrepancies due to the inhomogeneity of hydrogels surface which can cause a large regional variation of the modulus measured with AFM[349]. However, it can be seen in Supplementary Figure 6.9 that the hydrogels in our study present a high surface homogeneity, as the surface modulus measured with AFM shows very little variation over large zones of 40 x 40 μm. Therefore, the bulk stiffness of these hydrogels would be comparable to their surface stiffness. It has to be noted that the modulus of the softest gel has been evaluated to 15 kPa using AFM and 5 kPa using compression. This difference might be explained by the fact that cutting discs of this hydrogel leads to highly conical samples. Therefore, the modulus of this soft gel measured using compression might be underestimated.

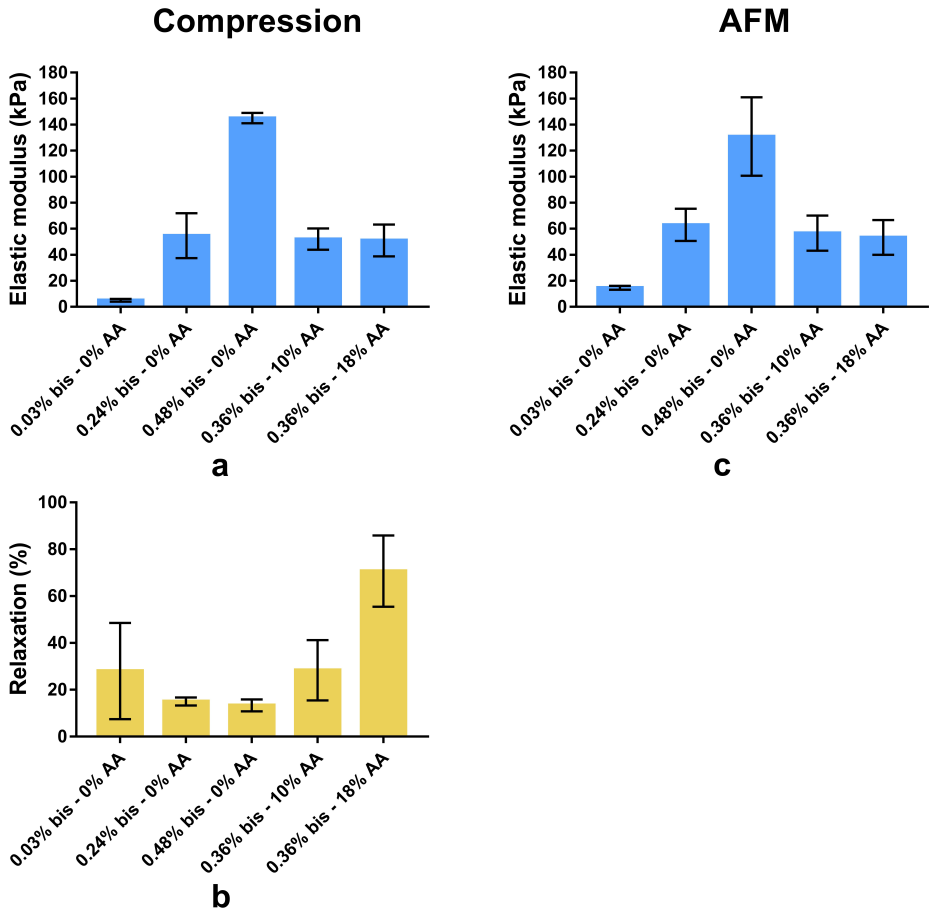

FIGURE 6.1 – Mechanical properties of the virgin hydrogels, including a) the elastic modulus and b) the relaxation mesured using unconfined compression, and c) the elastic modulus measured using AFM.

6.4.2 Homogeneous grafting of a BMP-2 mimetic peptide

After characterizing their mechanical properties, the hydrogels were functionalized with a mimetic peptide of the BMP-2 protein, which corresponds to residues 73-92 of BMP-2[83], in order to promote and accelerate MSCs osteogenic differentiation. Considering that the goal of this study is to direct MSCs differentiation towards the osteogenic lineage, this BMP-2 mimetic peptide constitutes a good candidate as it has been found to promote MSCs osteogenic differentiation on many different materials, including hydrogels[72, 73, 268, 269] and hard materials such as glass and PET[33, 84, 85, 346, 347]. These studies showed that an enhanced osteogenic differentiation could be obtained with materials that present the BMP-2 peptide through covalent immobilization. It has also been demonstrated that the immobilization of the BMP-2 protein preserves essential pathways for MSCs osteogenic differentiation, and could be even more efficient to trigger these pathways than soluble BMP-2.[351] In addition, it has been showed that MSCs exert a mechanical force on substrate-bound proteins and gauge the feedback to make cell-fate decisions.[55] As such, the covalent immobilization of the biomolecule on the

substrate is crucial for cells to feel the mechanical properties of the underlying substrate.[55] The BMP-2 peptide has therefore been covalently attached to the hydrogels to favor MSCs osteogenic differentiation, to avoid any release of the peptide during cell culture, and to allow the cells to feel the mechanical properties of the hydrogels.

In order to confirm the covalent grafting of the peptide, the hydrogels have been functionalized via Sulfo-SANPAH with a BMP-2 peptide carrying a fluorescent group, or have been immersed in the fluorescent peptide solution without prior activation with Sulfo-SANPAH. Then, the hydrogels have been washed for 15 days by changing the washing solution once a day, and the fluorescence intensity of the hydrogels has been evaluated regularly for 15 days. It has been found that the fluorescence intensity of the hydrogels is stable after 5 days of rinsing and remains stable up to 15 days of rinsing (Supplementary Figure 6.12). Consequently, the hydrogels have been rinsed during 5 days after the functionalization for all the other experiments. In addition, it has been found that the fluorescence intensity of the hydrogels activated with Sulfo-SANPAH is ten times higher than the fluorescence intensity of the non-activated hydrogels (Supplementary Figures 6.11a and 6.12). These results show that the activation with Sulfo-SANPAH leads to the covalent grafting of the peptide, while the absence of activation leads to the adsorption of the peptide on the gels, which is eliminated by rinsing the gels, although it seems that a residual amount of peptide remains adsorbed on the gels.

As previously reported[84, 85], the peptide surface density was estimated by conjugating TAMRA-coupled peptides to hydrogels and subsequently imaging the hydrogels by confocal fluorescence microscopy. Figure 6.2b shows that the functionalization has been achieved on the surface of the gels, over approximately 25 μm. This might be explained by the fact that the activation of Sulfo-SANPAH is carried out by UV irradiation and that UV light has been reported to have limited light penetration depth in biological tissues such as skin[352], as well as in hydrogels[353, 354, 355]. The BMP-2 peptide has been grafted onto the various hydrogel formulations in a controlled manner, leading to a homogeneous peptide layer, as shown by the cross-sectional view of the hydrogel (Figure 6.2b). By considering the fluorescence intensity of the top layer of the gel, i.e., the first slice of the z-stack (over 4.29 μm), and the calibration curve in Supplementary Figure 6.11b, the peptide density in the hydrogels with varying formulations has been estimated around 2 nmol.mm^{-3}. However, as the peptide grafting density is mainly reported per surface unit in the literature, we also tried to report the peptide grafting per unit of surface area. As the fluorescence intensity is homogeneous on the first ten microns of the gel, the fluorescence intensity and the peptide density can be estimated for a thickness of 1 μm, which can be considered as a surface density. The estimated peptide surface density varies between 1.5 $\pm$ 0.7 and 2.0 $\pm$ 0.5 pmol.mm^{-2} (1 molecule per nm^2), depending on hydrogels formulation, although no significant difference has been found

(Figure 6.2a). The peptide density on these hydrogels is very similar to the peptide density on glass[84] (2.2 pmol.mm^{-2}) and PET[85] (1.3 pmol/mm^{-2}), previously found by our group. The peptide density on our hydrogels (2 pmol.mm^{-2} or 500 ng.cm^{-2}) is also consistent with other studies which immobilized different peptides on materials such as hydrogels (from 2 to 9 pmol.mm^{-2})[356], gold (2 pmol.mm^{-2})[357], glass (from 100 to 600 ng.cm^{-2})[358], and titanium (from 500 to 900 ng.cm^{-2})[359]. In addition, it has been shown that a minimal BMP-2 peptide density of 0.8 pmol.mm^{-2} on glass was required to up-regulate Runx-2 gene expression in human bone marrow MSCs.[346] Moreover, the BMP-2 peptide concentration used in our study is similar to the BMP-2 peptide concentration usually used to functionalize hydrogels (1 to 5mM).[73, 268, 269] Consequently, the peptide density evaluated in our study would be sufficient to direct MSCs differentiation towards the osteogenic commitment. Finally, considering that the BMP-2 peptide has been grafted onto the various hydrogel formulations with a similar peptide density on the different hydrogels (Figure 6.2a), it is unlikely that differences in cell behavior on the different hydrogels could be attributed to differences in surface peptide density.

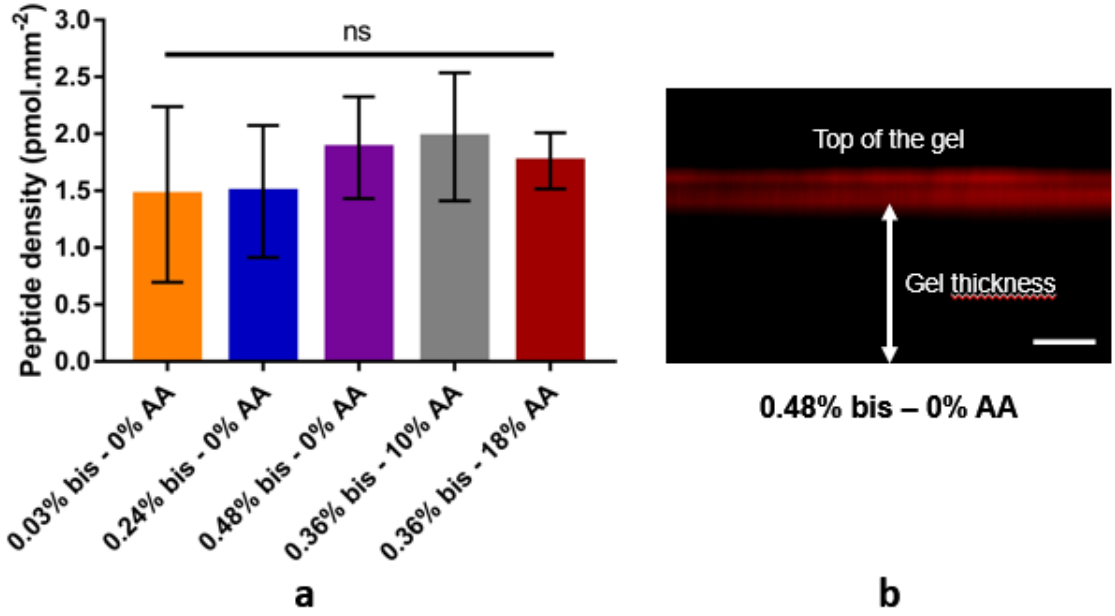

FIGURE 6.2 – a) Estimation of the BMP-2 mimetic peptide surface density on the hydrogels with different formulations. The peptide surface density has been evaluated between 1.5 and 2.0 pmol.mm^{-2}, with no significant difference depending on hydrogels formulation. (n=2) b) Cross-sectional view of a hydrogel functionalized with a fluorescent BMP-2-TAMRA peptide obtained using confocal microscopy. Scale bar = 50 μm. The peptide is located at the surface of the gel and the functionalization is homogeneous.

6.4.3 Impact of the functionalization on hydrogels mechanical properties

As shown in the previous section, the functionalization of the hydrogels via Sulfo-SANPAH and UV light leads to a peptide grafting that is located on the surface of the hydrogels. In addition, considering that the cells are cultured on the surface of the gels, it is important to evaluate the impact of the functionalization on hydrogels mechanical properties, and especially on the surface mechanical properties.

Figure 6.3 shows the mechanical properties of the different hydrogels measured before (empty bars) and after (hatched bars) the functionalization using unconfined compression (Figure 6.3a,b) or AFM (Figure 6.3c). As an illustration, it can be seen in Figure 6.3a and b, that no difference in hydrogels stiffness and relaxation are observed, before and after the functionalization, from the unconfined compression measurements for the sample containing the highest amount of acrylic acid. This was expected as it is unlikely that the surface functionalization of the gels over 25 μm could have an impact on the bulk mechanical properties of the gels that are measured at 6% deformation (0.3 mm).

Regarding the AFM measurements, Supplementary Figure 6.10 shows that the functionalized hydrogels present a high surface homogeneity of the modulus over large zones of 40 x 40 μm.
The AFM measurements presented in Figure 6.3c demonstrate that the surface stiffness of pure polyacrylamide hydrogels is not affected by the functionalization, while the surface stiffness of hydrogels containing acrylic acid significantly increases after the functionalization. In addition, this effect is more pronounced for the hydrogel containing the highest amount of acrylic acid, as the hydrogels containing 10% and 18% acrylic acid exhibit a similar stiffness around 55-60 kPa before the functionalization, and a stiffness of 100 kPa and 145 kPa, respectively, after the functionalization. The results presented in Figure 6.3 can be explained by the fact that poly(acrylic acid) is known to crosslink under UV light, even without the addition of a photo-initiator.[87, 88, 89] The crosslinking of poly(acrylic acid) under UV irradiation is thought to result from the cleavage of carboxylic acid groups, leaving radicals on the polymer chains that can subsequently react with another polymer chain to form crosslinks.[87] Therefore, the increase in crosslinking results in an increase in hydrogels stiffness. UV irradiation is also known to degrade the polymers, including polyacrylamide[360] and poly(acrylic acid)[87], which could result in a decrease in hydrogels stiffness. However, no decrease in hydrogels stiffness has been measured, either through compression or AFM. The degradation of polymers under UV irradiation is thought to be related to the presence of oxygen that reacts with the radicals created on the polymer chains, further leading to polymer chain scission.[87] Nevertheless, a degradation of only 14% has been observed when polyacrylamide was exposed to UV irradiation during 64 hours[360], so it is unlikely that an irradiation for 30 minutes

could lead to significant damage of the hydrogels. In addition, the functionalization has been performed in an aqueous environment, which might prevent the oxygen from degrading the polymer chains.

These results highlight that AFM is sensitive to variations in the surface mechanical properties of the hydrogels, while unconfined compression is not suitable to detect these variations. This is consistent with the findings of Chang et al.[350] who synthesized hydrogel beads (1.5 mm diameter) and additionally crosslinked the surface region of the beads (over 100 μm), producing a core-shell structure in order to improve the mechanical properties of the beads. They showed that the Young's Modulus of the beads measured with compression did not change with the additional crosslinking of the surface of the beads, while the surface Young's Modulus measured with AFM significantly increased when increasing the crosslinking of the surface of the beads.[350]

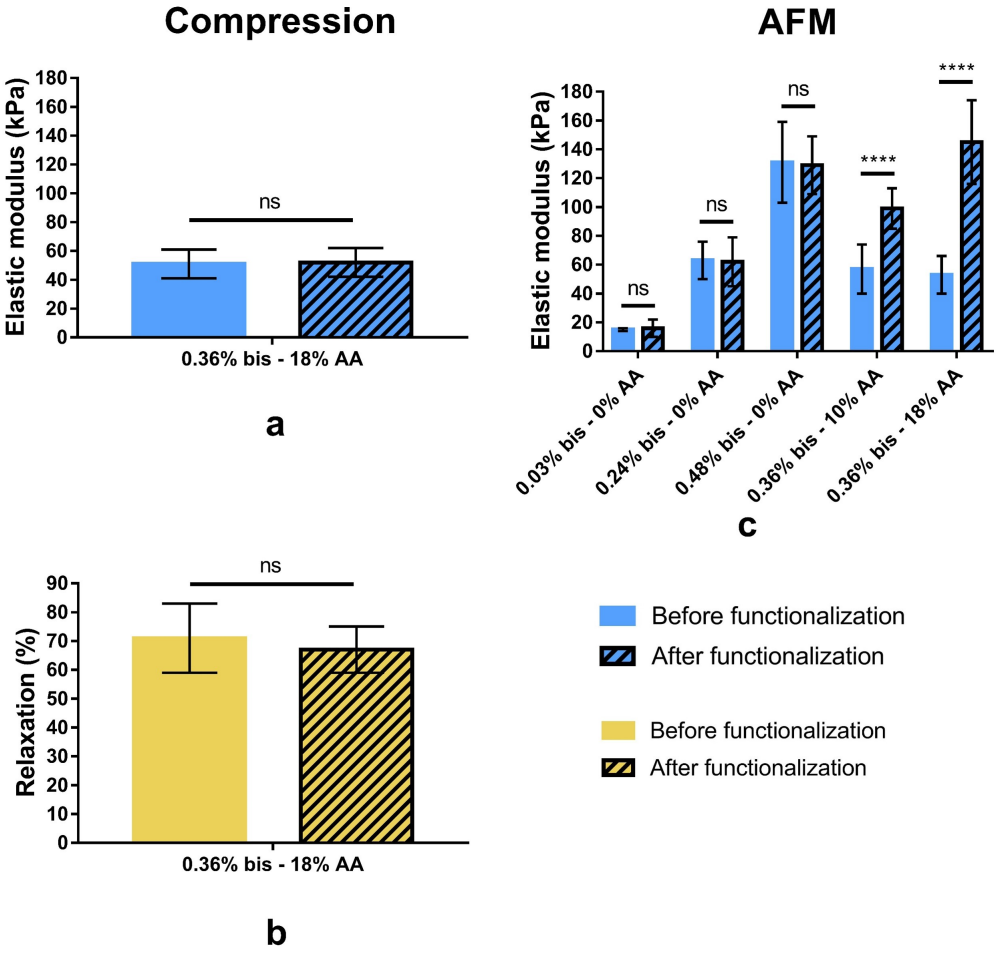

FIGURE 6.3 – Mechanical properties of the different hydrogels measured before (empty bars) and after (hatched bars) the functionalization with a BMP-2 mimetic peptide, using unconfined compression or AFM. a) Elastic modulus and b) relaxation measured using compression. c) Elastic modulus measured using AFM. (**** $P < 0.0001$)

Several studies have investigated the impact of polyacrylamide hydrogels thickness on cell behavior, and particularly cell spread area, by attaching the hydrogels to a glass slide and varying the thickness of the gel in order to evaluate if the cells could feel the higher stiffness of the glass slide beneath the hydrogel. These studies were conducted with different cell types, including smooth muscle cells[90], fibroblasts[91], and MSCs[52, 92, 93], and revealed that the cell spread area was higher for a gel thickness of the order of a few microns (generally less than 5 μm) compared to thick gels (10 to 100 μm), suggesting that cells could feel the rigid glass surface less than 5 μm beneath them. Therefore it appears that measuring hydrogels stiffness using unconfined compression is not suitable to evaluate the stiffness that the cells will actually sense. This study provides a clear comparison between compression and AFM, which is still lacking in the literature, and seems to show that the characterization of the surface mechanical properties using AFM appears to be crucial to assess the impact of the functionalization on hydrogels mechanical properties and to further evaluate the impact of these mechanical properties on cell behavior for studies in 2 dimensions. Consequently, the elastic moduli selected for the next section of the paper are the elastic moduli of the functionalized hydrogels measured using AFM.

Finally, the evaluation of hydrogels viscoelastic properties for cell behavior studies is traditionally performed using macroscopic techniques, such as compression and rheology.[67, 94, 95, 96, 100, 361, 362] However, the surface of the hydrogels is usually functionalized with biomolecules, in order to allow cell adhesion, which could alter the viscoelastic properties of the surface of the hydrogel, especially in the case of big proteins such as collagen and fibronectin for example, and therefore alter the viscoelastic properties sensed by the cells. Nevertheless, this issue has never been addressed in the literature, to our knowledge. Therefore, evaluating hydrogels viscoelastic properties at the microscopic scale seems particularly interesting and relevant to assess the impact of the surface functionalization on hydrogels viscoelastic properties and to evaluate mechanical properties closer to those actually felt by cells. Consequently, we measured the stress relaxation response of two hydrogel formulations, before and after the functionalization, by using AFM. As shown in Figure 6.4, the two hydrogels, that present a relaxation of 15% and 70% in compression, also show a very different behavior in AFM. For the pure polyacrylamide hydrogel (Figure 6.4a), the stress remains constant over time, which reflects the elasticity of the material and which was expected as polyacrylamide gels are known as elastic materials[68], while the behavior of the hydrogel containing 18% acrylic acid (Figure 6.4b) is drastically different. It can also be noticed from Figure 6.4 that the stress relaxation of the two hydrogel formulations is not affected by the surface functionalization with the BMP-2 mimetic peptide. Although these results are still preliminary, they provide, for the first time, important confirmation that the viscoelastic properties measured in our study by using compression can be considered for cell behavior studies as we found no effect of the surface functionalization with the peptide on the microscopic viscoelastic properties.

Finally, this topic is very promising and deserves further investigation in order to better understand hydrogels response to micro-scale mechanical sollicitations, which would pave the way for the understanding of hydrogels response to the mechanical sollicitations exerted by the cells and therefore provide major knowledge about cell-material interactions and cell mechanotransduction.

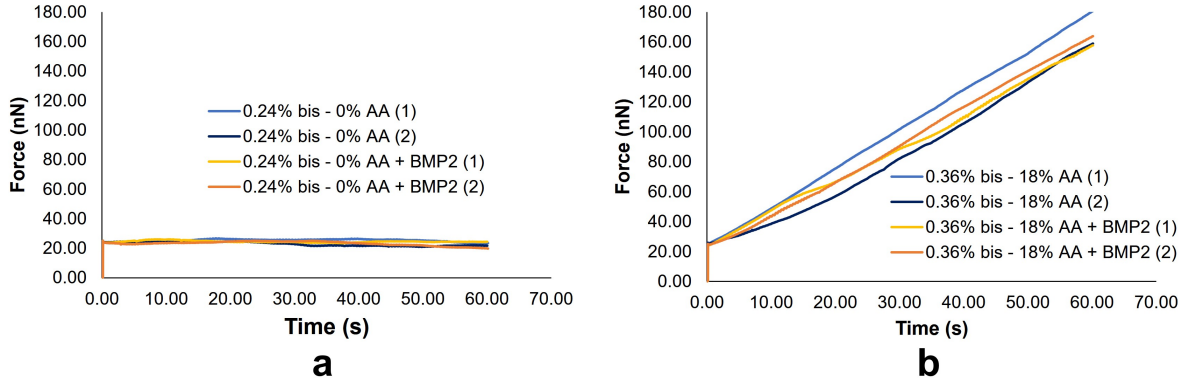

FIGURE 6.4 – Examples of stress relaxation curves of a) a pure polyacrylamide gel (15% relaxation in compression) and b) a gel containing 18% acrylic acid (70% relaxation in compression), with and without surface functionalization, measured at different locations on the sample using AFM. The behavior of the two hydrogel formulations is drastically different, and the stress relaxation is not affected by the surface functionalization with the BMP-2 mimetic peptide. (bis = bis-acrylamide, i.e., the crosslinker, AA = acrylic acid)

6.4.4 Impact of hydrogels mechanical properties on hMSCs osteogenic differentiation

First, the effect of hydrogels stiffness and stress relaxation on the spreading of human bone marrow MSCs was assessed by quantifying the area of individual MSCs cultured for 24 hours on the five hydrogels with varying elastic modulus and stress relaxation, and functionalized with the BMP-2 mimetic peptide.

Figure 6.5 demonstrates that the cell spreading area increases with hydrogels stiffness, as observed in previous studies working with polyacrylamide hydrogels (from 0.5 kPa to 80 kPa).[52, 56, 58, 62, 69] Nevertheless, the increase in the cell spreading area with hydrogels stiffness is not infinite, as Trappmann et al. showed that MSCs spreading area increases with polyacrylamide hydrogels stiffness from 0.5 to 115 kPa, but remains constant for higher stiffnesses from 115 to 740 kPa.[55] The results obtained in our study are consistent with the hypothesis that cells on soft gels need to be less contractile than on stiff gels to adhere to the matrix. Indeed, cells on stiff gels are generally highly spread and present an organized actin

cytoskeleton with stable focal adhesions, which allows the cells to maintain their contractility, while the cells are more round and present dynamic adhesions and no cytoskeleton organization on soft substrates.[65]
Figure 6.5 shows that increasing hydrogels stress relaxation leads to a decrease in the cell spreading area. Indeed, cells on hydrogels with 30% and 70% relaxation exhibit smaller spread area than on the hydrogel with a stiffness of 60 kPa and with low relaxation, although they present higher stiffnesses of 100 and 140 kPa. In addition, it can be observed that the cell spread area is similar on the hydrogels with 30% and 70% relaxation (Figure 6.5a). This might be explained by the fact that the effect of stiffer material (140 kPa vs 100 kPa) is somewhat counterbalanced by a higher relaxation (70%), therefore leading to a decrease of the cell area. In other words, the effects of hydrogels stiffness and stress relaxation would compensate each other and lead to a similar cell spread area on these two hydrogels. These observations are consistent with previous studies which showed, with different cell types including mouse fibroblasts, mouse myoblasts, and human hepatic stellate cells, that increasing hydrogels viscoelasticity resulted in a decrease in the cell spread area after 24 hours.[94, 95, 96, 97] Charrier et al. observed that cells present smaller focal adhesion on viscoelastic substrates as compared to elastic gels, which is in agreement with the hypothesis that low traction forces develop at the cell substrate interface due to the relaxation of the forces exerted by the cell on the substrate.[94] Consequently, the viscous dissipation of the cell-generated forces into the matrix would prevent cell spreading.[94, 97] However, this effect might be stiffness dependent. Indeed, Chaudhuri et al. showed that increasing hydrogels stress relaxation leads to an increase in the cell spread area for hydrogels with a low stiffness (1.4 kPa), while increasing hydrogels stress relaxation leads to a decrease in the cell spread area for higher stiffnesses (3.4 and 9 kPa).[95] Similarly, Bauer et al. observed that for stiffnesses of 3 and 12 kPa, the cell spread area is higher when increasing hydrogels stress relaxation, while it is the contrary for a high stiffness of 50 kPa.[96] It has been hypothesized that the dissipation of energy by the matrix, resulting in a decrease in stored energy, would allow cells to generate more work on soft viscoelastic substrates relative to purely elastic substrates with the same stiffness, which may facilitate cell spreading.[95] Nevertheless, other studies showed that increasing hydrogels viscoelasticity leads to a decrease in the cell spread area even for low stiffnesses of 0.5 and 5 kPa.[94, 97] The results in Figure 6.5 clearly demonstrate that increasing hydrogels stress relaxation leads to a decrease in the cell spread area for hydrogels with high stiffnesses, which supports the literature results.

Finally, it can be seen in Figure 6.5b that the cell density appears to be similar on the different materials. This is particularly important as the initial cell seeding density is known to play a role in MSCs differentiation.[175, 176, 177, 178] Therefore, in this study, it is unlikely that differences in cell behavior on the different hydrogels could be attributed to differences in initial cell seeding density.

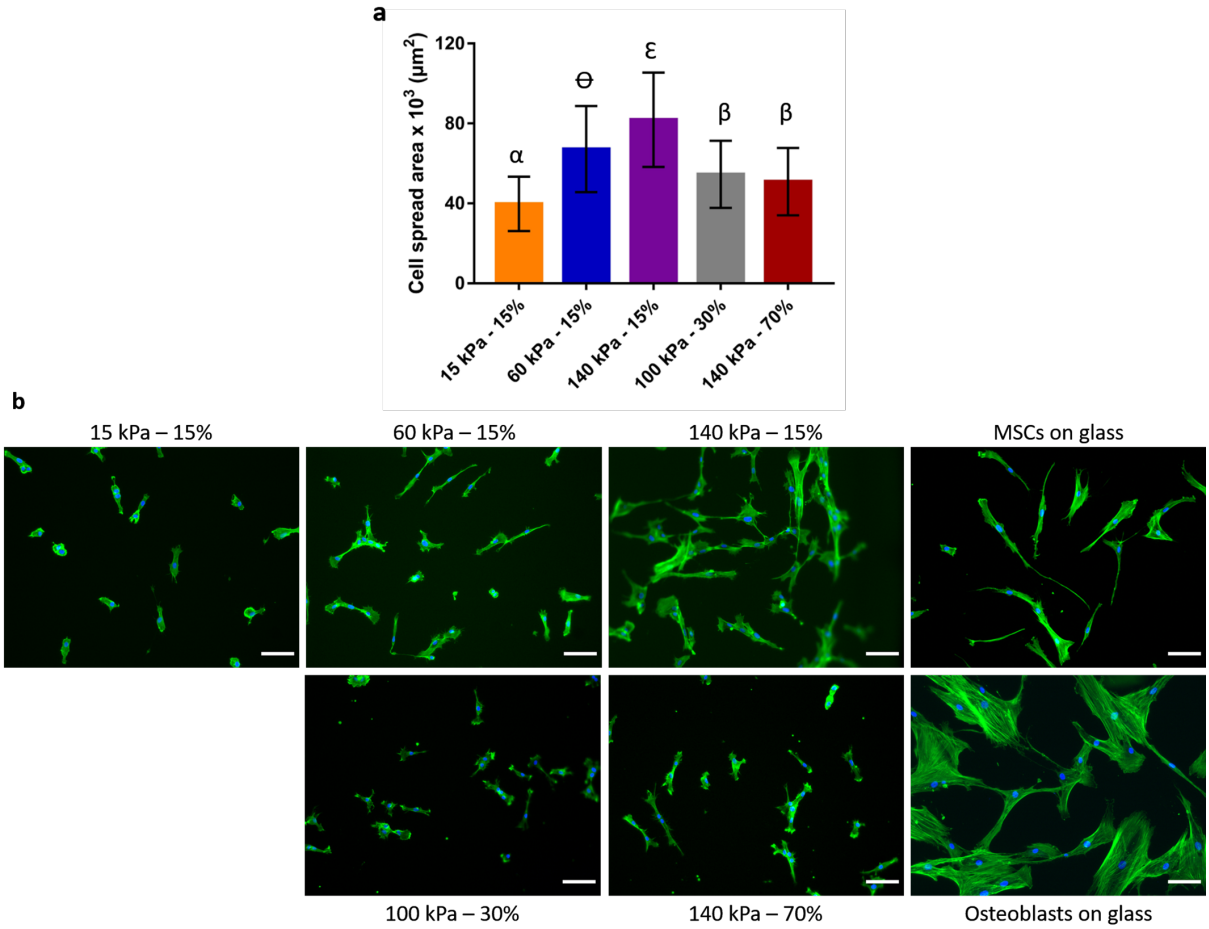

FIGURE 6.5 – Evaluation of hMSCs spreading after 24 hours depending on hydrogels mechanical properties. a) Quantification of the cell spreading area depending on hydrogels mechanical properties. The data were obtained from two identical experiments, with two samples per condition, and 25-50 cells per sample. Different greek letters represent a statistical difference while identical greek letters represent no statistical difference. ($P < 0.01$) b) Epifluorescence microscopy images of phalloidin staining of the cytoskeletal fibers of hMSCs cultured for 24 hours on hydrogels with varying mechanical properties, and staining of hMSCs and osteoblasts cultured for 24 hours on glass. Magnification 10x, scale bar = 100 μm. The cell spreading area increases with hydrogels stiffness for a low relaxation around 15%, while it is lower for the hydrogels presenting 30% and 70% stress relaxation. The cell density appears to be similar on the different materials after 24 hours.

Subsequently, the immunofluorescence labelling of early (Runx-2) and late (osteopontin) osteoblast markers, as well as early (E11, DMP1) and late (sclerostin) osteocyte markers has been performed, and the quantification of their expression after 24 hours is shown in Figure 6.6. The statistical analysis is presented in Supplementary Figure 6.14.

E11, also called podoplanin, is the earliest osteocyte-selective protein to be expressed as osteoblasts differentiate into osteocytes[147, 148], and it has been found to play a role in dendrite formation in osteocytes[147, 154]. DMP1 has been found to be highly expressed in osteocytes, with only a very low level of expression in osteoblasts.[327, 329, 363] In

bone, DMP1 would maintain the osteocyte lacunocanalicular system, by maintaining the number of canaliculi and the quality of the lacunar walls, and it would play a role in osteocyte maturation and normal bone mineralization.[363] In addition, it would suppress MSCs osteogenic differentiation[364], downregulate osteoblast-specific genes, such as osterix and collagen I, as well as upregulate the osteocyte-specific gene sclerostin[363]. Sclerostin is a marker of mature osteocytes and its expression progressively increases as osteocytes mature, while it is not expressed in osteoblasts.[365] Sclerostin has been found to inhibit osteoblast differentiation, proliferation, and activity, resulting in reduced osteoblastic bone formation.[366] The quantification of these three osteocyte markers, in addition to the quantification of the osteoblast markers Runx-2 and osteopontin, traditionally performed in the literature, is therefore particularly interesting to follow MSCs osteogenic differentiation and potentially determine the differentiation stage of the cells. Indeed, it combines the evaluation of early and late osteoblast and osteocyte markers, which has never been performed in vitro by using immunofluorescence, to the best of our knowledge. Finally, considering that the understanding of the transition of MSCs or osteoblasts towards osteocytes is mainly based on in vivo observations from the staining of histological sections[367], this study could provide a deeper knowledge about the evolution of the expression of these markers during MSCs osteogenic differentiation in vitro.

As shown in Figure 6.6, after 24 hours, the expression of Runx-2 is the highest for osteoblasts (HOB) and cells on the hydrogel 140 kPa-70%, while it is lower and similar for MSCs on the other hydrogels and on glass. This tendency is confirmed by the class distribution of Runx-2 fluorescence intensity (Supplementary Figure 6.16), although it also seems to show that the expression of Runx-2 is higher for the hydrogel 100 kPa-30% than for the hydrogels 5 kPa, 60 kPa, and 140 kPa with 15% relaxation, that cannot be seen in Figure 6.6. Then, the expression of osteopontin is upregulated for the hydrogels 60 kPa-15% and 140 kPa-15% as compared to all the other conditions (Figure 6.6). This can also be clearly observed in Supplementary Figure 6.17, as the osteopontin expression is shifted towards higher intensities for the hydrogels 60 kPa-15% and 140 kPa-15%. This is consistent with the fact that the cell spread area is higher on these two hydrogels, and that a higher cell spread area is known to favor MSCs osteogenic differentiation.[62, 69, 74, 76]
It can be noticed that the expression of the three osteocyte markers is systematically higher for cells on the different hydrogels as compared to cells on glass. The expression of E11 is the strongest for the cells on the hydrogels 60 kPa-15%, 100 kPa-30%, and 140 kPa-70%, followed by the hydrogels 15 kPa-15% and 140 kPa-15%. The expression of DMP1 is dramatically higher for MSCs on the hydrogels 100 kPa-30% and 140 kPa-70%. Then, DMP1 is expressed more significantly for cells on the hydrogel 60 kPa-15%, as compared to osteoblasts and MSCs on the hydrogels 15 kPa-15% and 140 kPa-15%. Finally, the expression of sclerostin is higher for MSCs on the hydrogels 100 kPa-30% and 140 kPa-70%, followed by MSCs on the hydrogels

15 kPa-15% and 60 kPa-15%, and followed by osteoblasts and MSCs on the hydrogel 140 kPa-15%. Supplementary Figures 6.18, 6.19, and 6.20 also clearly demonstrate the shift towards higher intensities for the expression of the three osteocyte markers for the hydrogels 100 kPa-30% and 140 kPa-70%. Taken together, these results indicate that a stiffness of 60 kPa would be more favorable for the expression of osteocyte markers than stiffnesses of 15 and 140 kPa, for the same low relaxation. Then, it appears that the hydrogels 100 kPa-30% and 140 kPa-70%, presenting a higher stress relaxation than the other conditions, promote the highest expression of osteocyte markers at a short culture time of 24 hours. This finding is particularly interesting as the impact of hydrogels mechanical properties on MSCs differentiation towards osteocytes is still unknown. These results might suggest that a high cell spread area, inducing a high cytoskeleton tension, is required for MSCs differentiation towards osteoblasts, while a lower cell spread area may favor a differentiation towards osteocytes. However, if the osteocyte differentiation was only related to the cell spread area, the expression of osteocyte markers should be comparable on the hydrogel with the lowest stiffness and the two hydrogels with a higher stress relaxation, which is not the case. Therefore, hydrogels stress relaxation might play an important role in MSCs differentiation towards osteocytes.

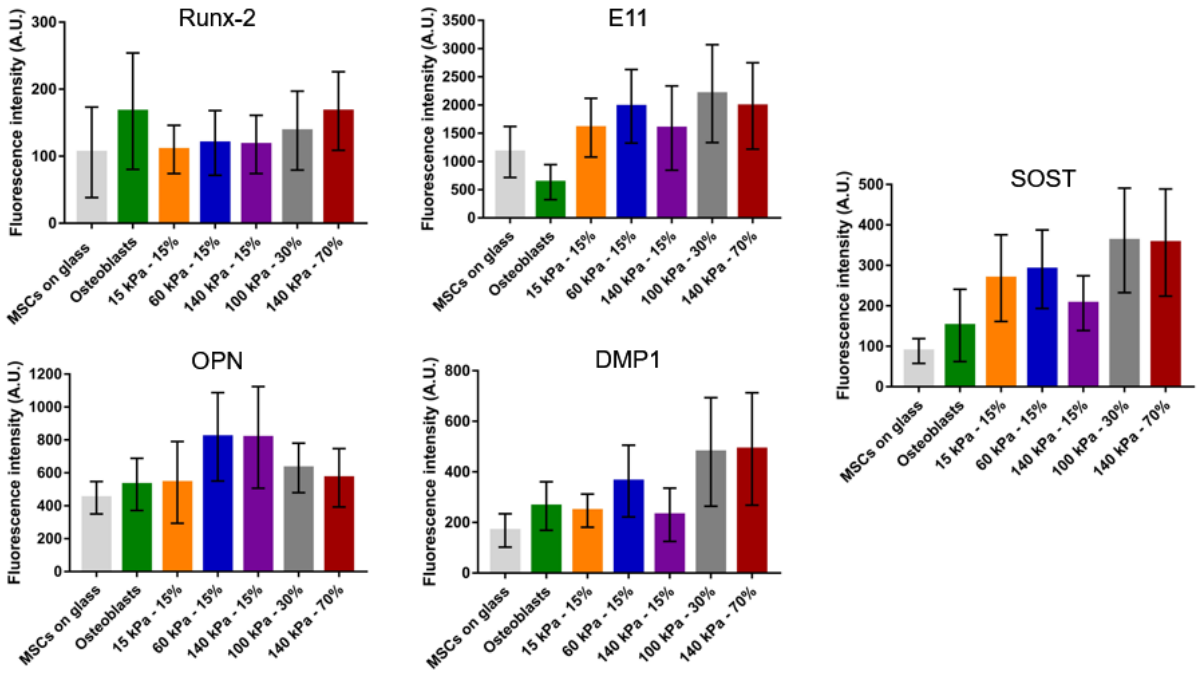

FIGURE 6.6 – Quantitative analysis of the nuclear expression of Runx-2 and OPN (osteopontin), and the total cellular E11 (podoplanin), DMP1 (Dentin Matrix Protein 1), and SOST (sclerostin) immunofluorescence intensity in hMSCs and osteoblasts cultured on glass (controls), and in hMSCs cultured on hydrogels with varying mechanical properties (stiffness - kPa, and stress relaxation - %), after 24 hours. (n=2)

The morphology of the cells on the different materials has been considered after 2 weeks of culture in osteogenic culture medium by visualizing cell cytoskeleton with phalloidin. As shown in Figure 6.7, MSCs in osteogenic culture medium on glass are large, highly spread, and exhibit a cuboidal morphology typical of osteoblasts[23, 98, 99], while cells on the hydrogels present a smaller cell body and a dendritic morphology characteristic of osteocytes[5, 6, 98, 327], except on the hydrogel with the lowest stiffness.

These results suggest that the combination of our polyacrylamide based hydrogels, together with a surface functionalization with a BMP-2 mimetic peptide, and with osteogenic culture medium, may lead to hMSCs differentiation towards osteocytes. This finding is particularly interesting considering that this BMP-2 mimetic peptide has not been found to promote this cell dentritic morphology when immobilized on glass[84] or PET[85], or even on hydrogels[73, 268, 269]. In addition, other biomolecules such as collagen I, collagen IV, fibronectin, and laminin, typically used to functionalize polyacrylamide hydrogels in the literature[52, 55, 56, 69], have not been found to promote the dendritic morphology observed in this study either. The observation of osteocyte-like cells is also probably related to the low seeding density used in our study (3,000 cells/cm^2), as it has been shown that the transition from osteoblasts to osteocytes was promoted for a low seeding density of 1,000 cells/cm^2, but not for a high seeding density of 10,000 cells/cm^2.[332] Therefore, it is possible that our unique combination of hydrogels with a stiffness between 60 and 140 kPa and a relaxation between 15% and 70%, the BMP-2 mimetic peptide, osteogenic culture medium, and low cell seeding density, led to the major achievement of obtaining a dentritic morphology on 2D substrates, while it is generally admitted that the transition from osteoblasts to osteocytes requires a 3D environment.[5, 98, 368, 369]

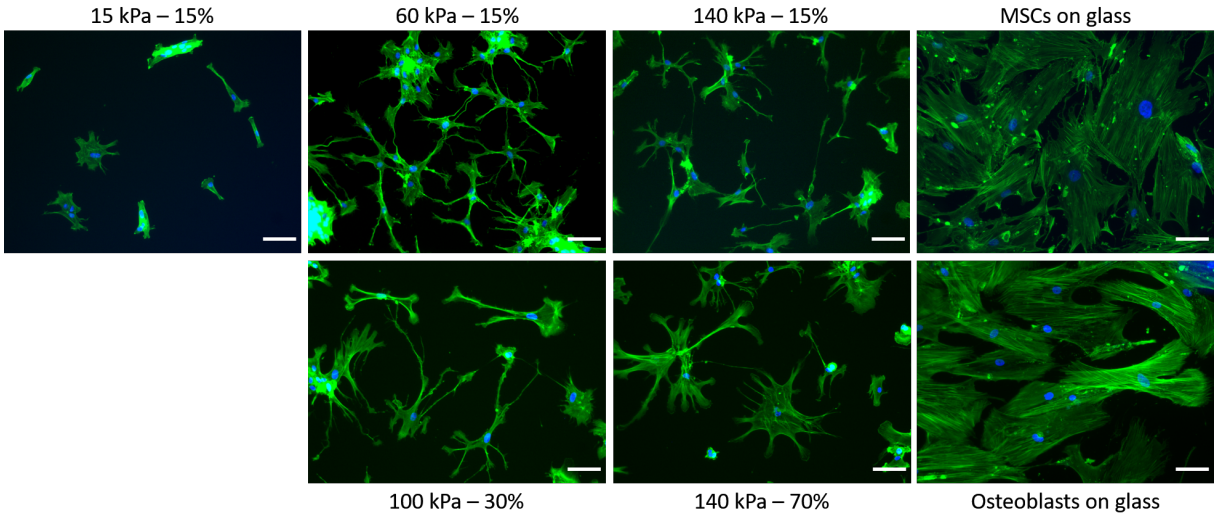

FIGURE 6.7 – Epifluorescence microscopy images of phalloidin staining of the cytoskeletal fibers of hMSCs cultured for 2 weeks in osteogenic culture medium on hydrogels with varying mechanical properties or on glass, and staining of osteoblasts cultured for 2 weeks on glass. Magnification 10x, scale bar = 100 μm. The cells present a star like shape on all the hydrogels except on the hydrogel with the lowest stiffness.

Finally, the immunofluorescence labelling of early (Runx-2) and late (osteopontin) osteoblasts markers, as well as early (E11, DMP1) and late (sclerostin) osteocytes markers has been performed after 2 weeks of culture in osteogenic culture medium, and the quantification of their expression is shown in Figure 6.8. The statistical analysis is presented in Supplementary Figure 6.15.

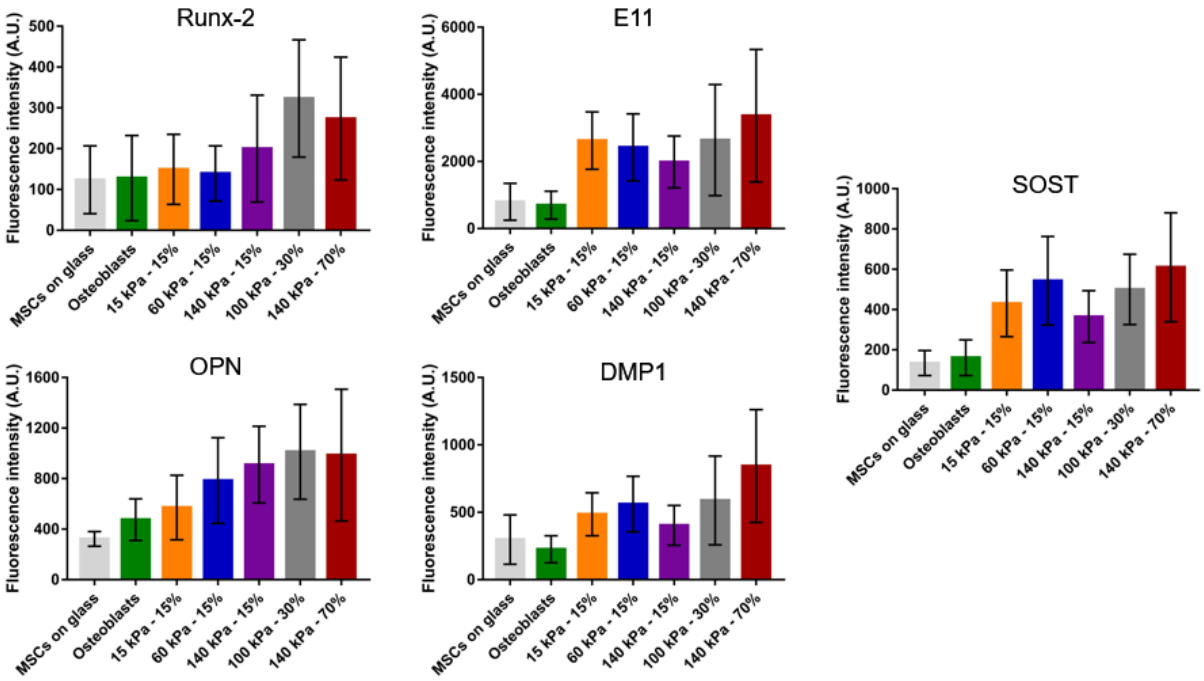

FIGURE 6.8 – Quantitative analysis of the nuclear expression of Runx-2 and OPN (osteopontin), and the total cellular E11 (podoplanin), DMP1 (Dentin Matrix Protein 1), and SOST (sclerostin) immunofluorescence intensity in hMSCs and osteoblasts cultured on glass (controls), and in hMSCs cultured on hydrogels with varying mechanical properties (stiffness - kPa, and stress relaxation - %), after 2 weeks in osteogenic culture medium. (n=2)

It can be seen in Figure 6.8 that the expression of the five differentiation markers is similar between MSCs on glass and osteoblasts, which is consistent with the morphological observations that suggest that MSCs on glass undergo a transition towards osteoblasts. The expression of Runx-2 is higher for cells on the hydrogels 140 kPa-70% and 100 kPa-30%, followed by the hydrogel 140 kPa-15%, and followed by the hydrogels 15 kPa-15% and 60 kPa-15%. The expression of osteopontin is upregulated for cells on the hydrogels with high stiffnesses (100 and 140 kPa), and gradually decreases when decreasing hydrogels stiffness. Regarding the osteocyte markers, it can be seen that their expression is systematically higher for cells on the different hydrogels as compared to MSCs and osteoblasts on glass. The expression of E11, DMP1, and sclerostin is the highest for the hydrogel with the highest stress relaxation. Then, cells on the hydrogels 60 kPa-15% and 100 kPa-30% present a similar level of expression of the three markers, generally higher than the expression on the hydrogel 15 kPa-15%. Finally,

cells on the hydrogel 140 kPa-15% show the lowest expression of the three osteocyte markers as compared to the other hydrogels.

Regarding the impact of hydrogels stiffness for a constant relaxation (around 15%), these results show that a high stiffness of 140 kPa promotes a higher expression of Runx-2 and osteopontin as compared to stiffnesses of 15 and 60 kPa. Supplementary Figures 6.21 and 6.22 undoubtedly confirm these observations as the expression of Runx-2 and osteopontin is shifted towards higher intensities for the hydrogel 140 kPa-15% as compared to the hydrogels 15 kPa-15% and 60 kPa-15%. This result is consistent with the fact that the stiffness of 140 kPa has been found to promote a higher cell spread area, which is favorable for MSCs osteogenic differentiation.[62, 69, 74, 76] This might be surprising as it has been showed that MSCs osteogenic differentiation is generally favored for stiffnesses between 20 and 60 kPa[52, 55, 56, 57, 58, 62, 63, 231, 232, 233, 308], as it corresponds to the stiffness of osteoid, the extracellular matrix secreted by osteoblasts[52]. Nevertheless, it can be seen in Figure 6.8 that a stiffness of 60 kPa leads to a higher expression of E11, DMP1, and sclerostin, as compared to stiffnesses of 15 and 140 kPa for a constant relaxation (around 15%), which is also supported by Supplementary Figures 6.23, 6.24, and 6.25. This might suggest that, after two weeks, the cells on the hydrogel 60 kPa-15% have committed into more mature osteocytes, related to a higher expression of osteocyte markers and a lower expression of osteoblast markers, while cells on the hydrogel 140 kPa-15% are less mature osteocytes as they present a lower expression of osteocyte markers and a higher expression of osteoblast markers. Therefore, the stiffness of 60 kPa might be the most favorable to direct MSCs osteogenic differentiation. This is consistent with the fact that the stiffness of 60 kPa already promoted a higher expression of the osteocyte markers after 24 hours of cell culture. Finally, our results have shed light on the impact of high hydrogel stiffness on MSCs osteogenic differentiation by showing that a stiffness of 140 kPa was less favorable than a stiffness of 60 kPa to induce MSCs differentiation towards osteocytes. In addition, while a range of stiffnesses between 20 and 60 kPa has been identified in the literature as enhancing MSCs osteogenic differentiation, our study suggests that a stiffness closest to 60 kPa is more favorable than a stiffness closest to 20 kPa.

Regarding the impact of hydrogels stress relaxation on MSCs differentiation, a high relaxation of 70% promotes the highest expression of the three osteocyte markers, which is dramatically higher than for a relaxation of 15% with the same stiffness (140 kPa). In addition, the hydrogel 140 kPa-70% also leads to a higher expression of E11, DMP1, and sclerostin, than the hydrogel 60 kPa-15%, although the stiffness of 60 kPa has been identified as the most favorable stiffness for MSCs osteogenic differentiation. Supplementary Figures 6.23, 6.24, and 6.25 also clearly demonstrate that the expression of E11, DMP1, and sclerostin is shifted towards higher intensities for the hydrogel 140 kPa-70%. These results might suggest that hydrogels stress relaxation has a major impact on MSCs differentiation towards osteocytes, and that this impact may be stronger than the impact of the stiffness. In addition, the similar level of expression of E11, DMP1, and sclerostin on the hydrogels 60 kPa-15% and 100 kPa-30% might indicate

that the higher stiffness of 100 kPa, which would be less favorable for MSCs differentiation than the stiffness of 60 kPa, is compensated by the higher relaxation of 30%, which would be more favorable for MSCs differentiation than the relaxation of 15%. Finally, considering that the hydrogels 100 kPa-30% and 140 kPa-70% lead to a high expression of osteocyte markers, which might be correlated with the obtention of more mature osteocytes, a lower expression of Runx-2 and osteopontin would have been expected for these two hydrogels, as they have been identified as early and late osteoblast markers, respectively.[111, 113] The high expression of Runx-2 and osteopontin for these two hydrogels might indicate that, although MSCs osteogenic differentiation is more advanced on these hydrogels, the differentiation is heterogeneous. Indeed, Supplementary Figures 6.16 and 6.22, reveal that the expression of Runx-2 and osteopontin is shifted towards higher intensities for the hydrogels with 30% and 70% relaxation, but they also present a larger distribution.
The results presented in our study are in agreement with previous studies which showed that increasing hydrogels viscoelasticity, i.e., loss modulus or stress relaxation, leads to a higher MSCs osteogenic differentiation whether in 2D[67] or 3D culture[100, 361, 362]. The main hypothesis to explain this phenomenon is that increasing hydrogels viscoelasticity leads to more possibilities for the cells to remodel the matrix, which enhances MSCs osteogenic differentiation.[100]

To the best of our knowledge, the in vitro differentiation of MSCs into osteocytes in 2 dimensions has only been reported by our group. Osteocyte function is difficult to study because osteocytes are embedded in a mineralized matrix.[156] In addition, only a few osteocyte models are available, and none of the available osteocyte models have completely replicated the normal in vivo differentiation process.[156] Therefore, this study is particularly promising for the study of hMSCs osteogenic differentiation and osteocyte function. This study suggests that hydrogels stress relaxation has a great impact on MSCs differentiation towards osteocytes. This is consistent with the fact that osteocytes are particularly sensitive to the deformation of the bone matrix.[5, 6] Therefore, it is possible that increasing hydrogels stress relaxation allows to better mimic the behavior of bone extracellular matrix, in which osteoblasts embed to become osteocytes.[5, 330] In addition, MSCs differentiation towards osteocytes has been achieved in a greater extent on the hydrogel with the highest stress relaxation, although this hydrogel led to a smaller cell spread area as compared to an elastic gel with the same stiffness. This might indicate that a high cell spreading is not necessary for MSCs commitment towards osteocytes.
Finally, this study also highlights that MSCs mechanotransduction does not only involve the integrin receptors. Indeed, it has been well documented that MSCs exert traction forces on two dimension substrates to gauge surrounding matrix resistance and that these MSCs-substrate interactions involve the cells integrin receptors.[370] Bone morphogenetic proteins are extracellular cytokines, which can also be found sequestered in the extracellular matrix, which would be a similar configuration to the immobilized BMP-2 peptide on our hydrogels.

It has been shown that BMPs, including BMP-2, interact with transmembrane receptors known as Type I and Type II receptors. Ligand binding induces the formation of receptor complexes, involving two Type I and two Type II receptors. These receptor complexes can subsequently interact with co-receptors, such as integrins, therefore affecting integrin and BMP-signaling, and cell adhesion and differentiation.[371] The peptide sequence proposed in our study and patented by our team has been designed to preserve this interaction with the Type II receptor.[83] In addition, BMPs receptors interact with multiple proteins, including proteins acting as signal transducers that allow stem cells to sense and respond to extracellular stiffness cues.[371] This BMP-2 mimetic peptide would therefore allow cell adhesion and cell mechanosensing, although it would not be by direct interaction with integrin receptors.

6.5 Conclusions

This study showed that varying the amount of crosslinker and the ratio between the two monomers of poly(acrylamide-co-acrylic acid) hydrogels enabled to obtain hydrogels with controlled stiffness and stress relaxation as measured using unconfined compression and AFM. Subsequently, it has been demonstrated that the functionalization of the hydrogels with a mimetic peptide of the BMP-2 protein via Sulfo-SANPAH led to a homogeneous functionalization of the surface of the hydrogels over approximately a 25 μm depth, with no difference in peptide density depending on hydrogels formulation. However, it has been found that the UV irradiation performed during hydrogels functionalization was responsible for an increase in the surface stiffness of hydrogels containing acrylic acid as measured using AFM, while this variation was not detected using unconfined compression. Considering that the cells are able to sense the stiffness of the substrate up to 5 μm deep, it is likely that the cells will sense the increase in stiffness caused by the functionalization. Therefore, this study provides a clear comparison between unconfined compression and AFM for mechanobiology studies, which is still lacking today, and highlights that the characterization of the surface mechanical properties using AFM appears to be crucial to assess the impact of the mechanical properties of 2 dimensions substrates on cell behavior. The stress relaxation measurements carried out using AFM also provided, for the first time, important confirmation that the viscoelastic properties measured using compression could be considered for cell behavior studies as we found no effect of the surface functionalization with the peptide on the microscopic viscoelastic properties. The immunofluorescence results demonstrated that the BMP-2 mimetic peptide at a density around 1.5-2 pmol.mm^{-2} effectively induced human bone marrow MSCs commitment towards the osteogenic lineage, and even towards osteocytes as the cells presented a small cell body and a dendritic morphology for hydrogels stiffnesses between 60 and 140 kPa, which has only been reported by our group. It has been shown that for a constant relaxation around 15%, a stiffness of 60 kPa promoted a higher expression of osteocyte markers after 24 hours and 2 weeks, as compared to stiffnesses of 15 kPa and 140 kPa. Then, the hydrogel with a stiffness of 140 kPa and the highest relaxation (70%) promoted the highest expression of osteocyte markers after 2 weeks. These results suggest that hydrogels stress relaxation has a major impact on MSCs differentiation towards osteocytes, which may be stronger than that of the stiffness, as a high viscoelasticity would favor MSCs osteogenic differentiation even if it is associated with a stiffness that is not the most favorable. Therefore, this study provides a new insight about the effect of hydrogels viscoelastic properties on MSCs osteogenic differentiation, and highlights the importance of considering these properties for the design of effective materials to promote bone regeneration. In addition, the results presented herein are particularly promising for the study of MSCs differentiation towards osteocytes, which is still a relatively unknown process, and to investigate osteocyte function, which is a difficult task as these cells are particularly difficult to extract.

6.6 Materials & Methods

6.6.1 Materials

Acrylamide (40% in water), acrylic acid, ammonium persulfate (APS), sodium phosphate dibasic, sodium phosphate monobasic, Tetramethylethylenediamine (TEMED), sulfo-SANPAH (sulfosuccinimidyl 6-(4'-azido-2'-nitrophenylamino)hexanoate), HEPES (4-(2-hydroxyethyl)-1-piperazineethanesulfonic acid), paraformaldehyde, N,N-methylene-bis-acrylamide, Triton X-100, Tween 20, Bovine Serum Albumine (BSA), and FluoroshieldTM with Dapi were obtained from Sigma-Aldrich (France). KRKIPKASSVPTELSAISMLYLC peptide, which is a BMP-2 mimetic peptide previously identified by our group[83], and the fluorescent peptide KRKIPKASSVPTELSAISMLYLCK-TAMRA were synthesized by GeneCust (France). Bone marrow hMSCs, MSCs growth medium 2 (MSC-GM2), MSC Osteogenic Differentiation medium, human osteoblasts, and Osteoblast Growth Medium were purchased from Promocell (Germany). Alpha Modified Eagle Medium (α-MEM), sterile Phosphate Buffered Saline (PBS), trypsin/EDTA (Ethylenediaminetetraacetic acid), penicillin/streptomycin, Fetal Bovine Serum (FBS) were obtained from Thermo Fisher Scientific (France). Alexa Fluor^{TM} 488 phalloidin, Alexa Fluor^{TM} 568 phalloidin, Alexa Fluor^{TM} 647 goat anti-mouse IgG (H+L), and Alexa Fluor^{TM} 488 goat anti-rabbit IgG (H+L) were bought from Invitrogen (France). Rabbit monoclonal anti-Runx-2 antibody was obtained from Cell Signaling Technology (USA) and mouse monoclonal anti-osteopontin antibody was obtained from Santa Cruz Biotechnology (USA). Mouse monoclonal anti-podoplanin, rabbit polyclonal anti DMP1, and rabbit polyclonal anti-sclerostin antibodies were purchased from Abcam (UK).

6.6.2 Methods

Preparation of hydrogels

Poly(acrylamide-co-acrylic acid) hydrogels have been synthesized according to a previously established protocol.[77] Briefly, the gel precursor solutions were made by mixing appropriate amounts of N,N-methylene-bis-acrylamide, acrylamide, and acrylic acid in a buffered solution at pH 8. The total polymer content was kept constant while the crosslinker content and the ratio between the monomers were varied to tune the mechanical properties of the resulting hydrogels. After the solutions were prepared, they were outgassed by argon bubbling for 10 minutes. Then TEMED and APS were added simultaneously to the reaction mixture. The solutions were then quickly poured into a round petri dish of 10 cm diameter and maintained under a flow of argon into a sealed container for 2 hours. Hydrogels were then put in PBS (Phosphate Buffered Saline)

at room temperature and allowed to swell at equilibrium for at least 4 days before cutting disks of 10 mm diameter using a metallic punch.

Unconfined compression for bulk mechanical properties measurements

The modulus and stress relaxation properties of the hydrogels were first measured from unconfined compression tests of the gel disks (10mm in diameter, 4 mm thick, equilibrated in PBS pH 7.4 for 4 days) using a Mach-1 V500CS (Biomomentum, Canada) apparatus equipped with a 1.5 N single-axis load cell as described elsewhere.[77] Gel disks were compressed between two flat platens, with a flat indenter of 3 cm diameter, and were free to expand in the radial direction. Tests were performed at room temperature in a PBS bath to avoid the drying of the samples. The gel disks were compressed to 5 consecutive steps of 3% strain with a deformation rate of 1 mm.min^{-1}. The strain was held constant between two steps, while the load was recorded as a function of time for 1 hour and 50 minutes. Measurements were performed in triplicate.
A standard linear solid model with three Maxwell elements was used to analyze the relaxation curves and is described by the following equation :

$$\sigma(t) = a.exp(\frac{-t}{\tau 1}) + b.exp(\frac{-t}{\tau 2}) + c.exp(\frac{-t}{\tau 3}) + d$$

Where $\tau 1$, $\tau 2$ and $\tau 3$ are the three relaxation times of the three Maxwell elements and d is the equilibrium stress in the isolated spring. The 7 parameters a, b, c, d, and $\tau 1$, $\tau 2$, and $\tau 3$ were computed using Matlab® (version R2017b). Limits for the coefficients a, b, c, and d were fixed between 0 and $+\infty$, and between 0 and 30 s for $\tau 1$, 30 and 2000 s for $\tau 2$, and 2000 and 6480 s for $\tau 3$. Correlation coefficients greater than 0.97 were obtained for all relaxation tests. The stiffness of the hydrogels, or their equilibrium modulus, is obtained by calculating the residual force at the end of the relaxation for each of the five compression steps, and by measuring the slope of the line connecting these five points. The relaxation degree (%) of the different hydrogel formulations is calculated as the proportion of the maximum stress that is lost during the stress relaxation.[77]

Homogeneous surface functionalization of hydrogels

For cell seeding experiments, a BMP-2 mimetic peptide was conjugated to hydrogels surface by using the linker Sulfo-SANPAH following previously described protocols.[55, 56, 69] Briefly, 200 μL of a 1 mmol.L^{-1} solution of Sulfo-SANPAH in HEPES buffer (50 mmol.L^{-1}, pH 8.5) were pipetted onto the gel surface in a 48-well plate which was placed under ultraviolet light (365 nm) in a UV chamber (Uvitec, UK). The gels were exposed to UV light for 30 min and rinsed in HEPES overnight. The gels were then incubated with a solution of BMP-2 mimetic peptide (5.10^{-4} - 10^{-3} mol.L^{-1}) in 50 mM HEPES overnight at 4°C. The gels were then rinsed

in 5 mL HEPES for one week, with changing the rinsing solution once a day.

Characterization of the functionalization

The functionalized surfaces were characterized using fluorescence microscopy. The gels were functionalized with a BMP-2 mimetic peptide linked to TAMRA fluorochrome (BMP-2-TAMRA) at the C terminal. A Leica SP8 confocal microscope was used to confirm a uniform grafting on the surface of the gel and to observe the repartition of the molecules in the thickness of the gel. Images were collected with identical microscope and laser settings for each sample (objective HC PL Fluotar 10x/0.3, 4096 x 4096, 16 bits per pixel). Z-stacks were created over 100 μm with a slice-thickness of 4.29 μm. In parallel, a series of droplets of BMP-2-TAMRA peptide were deposited on PET surfaces with calibrated concentrations (from 1 mM to 1 μM) and imaged under identical conditions to obtain a calibration curve, which was then used to measure the peptide density on the hydrogels. Image J software was used to quantify the relative fluorescent intensity of the grafted molecules as a function of hydrogels mechanical properties.

AFM imaging and nanomechanical analyses

The gel samples were deposited on glass bottom petri dishes (Willco wells, ref HBST 5040) and immobilized by casting agarose (1% w/v) around it. Caution was applied in order to keep the surface of the gels free of any contamination during the immobilization process.
A Bioscope Resolve^{TM} (Bruker, USA) AFM coupled to a Zeiss Axio Observer inverted microscope (Zeiss, Germany) was used in this study. After localizing the borders of the gel by optical microscopy, we studied several areas of each gel sample. The AFM tip was approached towards the area to be analyzed. We used two types of probes depending on the range of expected Young's moduli, following the PFQNM protocol allowing the Young's Modulus to be measured : MLCT-A probes (Bruker, Billerica, USA) with pyramidal shape, having a nominal spring constant of 0.07 N/m and a resonance frequency of $\approx$22 kHz were used for the softest sample (15 kPa-15%) and MLCT-F probes (Bruker, USA) with nominal spring constants of 0.6 N/m, and resonance frequencies of 125 kHz were used for the other samples. Prior to each experiment, the AFM probe has been calibrated following the PF-QNM advanced calibration process, which involves engaging the tip on a hard sample (glass) and acquiring representative force curves to measure the deflection sensitivity and using a thermal tune to calculate the spring constant. Images were captured in PBS buffer on 40 μm x 40 μm zones with a resolution of 128 pixels per line, and with a PeakForce frequency of 0.25 kHz and a PeakForce amplitude of 250 nm for stiffer gels to 1 μm for the softest one. The force setpoint was kept between 1 and 2 nN. In complement to PFT imaging, we performed force volume measurements on 40 μm x 40 μm zones, with 16x16 grids of 0.5 to 1.5 μm ramps performed with a force setpoint of 1 nN and an approach and retract speed of 1 μm/s. This small approach velocity minimized the potential contribution of the gel's viscosity to the mechanical response, resulting in the suppression

of the hydrodynamic damping hysteresis observed in PFT. Indeed, a small approach velocity allowed to minimize the impact of the viscosity in the mechanical response of the tip.[372, 373] Regarding the relative Young's modulus calculation and the topographical measurements, for each gel, at least two different samples were studied with at least 3 different areas studied on each sample. The indentation depth never exceeded 100 - 200 nm, for gels that were ≈5 mm thick ; therefore we consider that the substrate is not contributing to the measured relative Young's modulus. Images and force curves were treated using Nanoscope Analysis v2.0. For the determination of the relative Young's modulus, force curves were extracted from force volumes and processed with the indentation feature of the Nanoscope analysis software. We applied the classical Hertz model to fit the force curves :

$$F(\delta) = \frac{4}{3}\frac{E}{1-\nu^2}\sqrt{R}\delta^{3/2}$$

where E is the relative Young's modulus, ν is the Poisson ratio of the sample (0.3 for our samples), R is the nominal radius of the tip. Curves where the Hertz model fit with a $r^2 < 0.9$ were discarded from the analysis.

AFM relaxation experiments

In order to perform relaxation experiments by AFM, we prepared colloidal probes in order to increase the diameter of the area probed. Single silica microbeads of 7.75 μm diameter (Cospheric) were immobilized at the extremity of MLCT-F tipless cantilevers, with similar spring constants as the pyramidal MLCT-F probes, using UV-curable glue (NOA 63, Norland Edmund Optics) and a Bioscope Resolve AFM coupled to a Zeiss Axio Observer inverted microscope. Each relaxation experiment was performed as follows : the cantilever was engaged on the surface of the gel at an approach speed of 10 μm/s until reaching a force setpoint of 25 nN, then the z height was kept constant for 60 seconds while measuring the mechanical response of the gel through the evolution of cantilever deflection as a function of time. This ramp script was applied to several areas of each gel in order to check the reproducibility of our measurements, as well as the homogeneity of the gels. Regular force curves were acquired with 10 μm/s approach speed and 25 nN setpoint in order to check the indentation depth reached during our relaxation experiments. Indentation reached at most 200 nm.

Cell culture

Bone marrow hMSCs were thawed and cultured in MSCs growth medium 2 (MSC-GM2), in a humidified atmosphere containing 5% CO_2 at 37°C as recommended by the supplier. They were subcultured twice a week using trypsin/EDTA 1x detachment and used at passage 4. For differentiation experiments, hMSCs were seeded at a density of 3,000 cells/cm^2 in α-MEM medium on glass slides or on functionalized hydrogels previously sterilized with 70% ethanol

for 48 hours. All cell seedings were carried out without any serum for the first 4 h of culture. This enabled the interaction of cells with the surface conjugated biomolecules and not with adsorbed serum proteins. After 4 h, the culture medium was supplemented with 10% FBS. After 24 h, the medium was replaced by MSC Osteogenic Differentiation medium supplemented with 0.1% penicillin/streptomycin. The cells were then cultured for 2 weeks and the Osteogenic Differentiation medium was changed twice a week. Human osteoblasts (HOB) were thawed and cultured in Osteoblast growth medium in a humidified atmosphere containing 5% CO_2 at 37°C. They were subcultured once a week using trypsin/EDTA 1x detachment and used at passage 4. Osteoblasts were seeded at a density of 20,000 cells/cm^2 in Osteoblast Growth Medium on glass slides previously sterilized with 70% ethanol overnight.

Evaluation of the cell spread area

After 24 hours of cell culture, the cells on the different hydrogels were fixed in 4% paraformaldehyde at 4°C for 20 min, permeabilized with 0.5% Triton X-100 in PBS for 15 min at 4°C, and blocked with 1% Bovine Serum Albumin (BSA) in PBS for 30 min at 37°C. Subsequently, cells were incubated with Alexa fluor 488 phalloidin (1 :40 dilution) or Alexa fluor 568 phalloidin (1 :40 dilution) for 1 h at 37°C in order to visualize the cell cytoskeleton. After the fluorescent staining, single cells were examined using a Leica DM5500B epifluorescence microscope (Leica Biosystems) equipped with a CoolSnap HQ camera and controlled by Metamorph 7.6 software (magnification 40x). The cell area was then quantified using ImageJ software by automatic detection of the cell cytoskeleton and measurement of the area. The data were obtained from two identical experiments, with two samples per hydrogel formulation for each experiment, and 25 to 50 cells analyzed per sample.

Lineage-specific differentiation assays

The extent of hMSCs osteogenic differentiation was evaluated using specific markers of osteoblasts (Runx-2, Osteopontin (OPN)) and osteocytes (Podoplanin (E11), Dentin matrix acidic phosphoprotein 1 (DMP1), and Sclerostin (SOST)). The expression of Runx-2, OPN, E11, DMP1, and SOST was assessed by immunofluorescence staining after 24 hours or 2 weeks of cell differentiation. Cells were fixed in 4% paraformaldehyde at 4°C for 20 min, permeabilized with 0.5% Triton X-100 in PBS for 15 min at 4°C, and blocked with 1% Bovine Serum Albumin (BSA) in PBS for 30 min at 37°C. Subsequently, cells were incubated with the primary antibodies for 1 h at 37°C : Rabbit monoclonal anti-Runx-2 (1 :1600 dilution), Mouse monoclonal anti-OPN (1 :200 dilution), Mouse monoclonal anti-E11 (2 μg/mL), Rabbit monoclonal anti-DMP1 (1 :250 dilution), and Rabbit monoclonal anti-Sclerostin (5 μg/mL). Cells were washed in PBS containing 0.05% Tween 20, before and after incubation with the secondary antibodies, Alexa Fluor 488 goat anti-rabbit IgG (H+L) and Alexa Fluor 647 goat anti-mouse IgG (H+L) (1 :400 dilution) for 1 h at 37°C. The cell morphology and

cytoskeleton organization were evaluated by labeling filamentous actin (F-actin) with Alexa Fluor 488 phalloidin or Alexa Fluor 568 phalloidin (Invitrogen, France) (1 :40 dilution) for 1 h at 37°C. Samples were then stained for nuclei using Fluoroshield^{TM} with Dapi. Fluorescently stained cells were examined using a Leica DM5500B epifluorescence microscope (Leica Biosystems) equipped with a CoolSnap HQ camera and controlled by Metamorph 7.6 software (magnification 40x). The expression of the differentiation markers was quantified using ImageJ software by measuring the fluorescence intensity on 40 to 50 cells per sample, with two samples per condition. The expression of Runx-2 and osteopontin was measured in the nucleus, while the expression of E11, DMP1, and sclerostin was measured in the whole cell. After quantifying the expression of the differentiation markers by measuring the fluorescence intensity in the cells, a frequency distribution has been calculated using GraphPad Prism version 7 for Windows, in order to display the number of observations within a given interval of fluorescence intensities for the different hydrogel formulations (Supplementary Figures 6.16 to 6.25). The cell morphology has been observed from two identical experiments, with two samples per hydrogel formulation for each experiment, except for the hydrogel 60 kPa-15% for which the cell morphology has been observed from four identical experiments, with two samples per hydrogel formulation for each experiment.

Statistical analysis

Data are expressed as the mean $\pm$ standard deviation (SD). For the data of hydrogels mechanical properties, peptide surface density, cell spread area, and expression of differentiation markers, the statistical analysis was performed by one-way analysis of variance (ANOVA) and Tukey's test for multiple comparisons using GraphPad Prism version 7 for Windows. Significant differences were determined for P values ≤ 0.05 (* represents $P < 0.05$, ** $P < 0.01$, *** $P < 0.001$, and **** $P < 0.0001$).

Acknowledgements

The authors thank Dr. Delphine Maurel (Laboratory for the Bioengineering of Tissues, Bordeaux University, France) for sharing her knowledge about osteocytes and osteocytes markers. This work was supported by the University of Bordeaux [Emilie Prouvé's PhD grant] and the National Sciences and Engineering Research Council of Canada (NSERC), as well as the Centre Québécois sur les Matériaux Fonctionnels (CQMF). The financial support of the ANR EchoCell (ANR-17-CE11-0020) is also acknowledged.

The microscopy for the evaluation of peptide density and distribution was done in the Bordeaux Imaging Center a service unit of the CNRS-INSERM and Bordeaux University, member of the national infrastructure France BioImaging supported by the French National Research Agency (ANR-10-INBS-04). The help of Fabrice Cordelières and Magali Mondin is acknowledged.

6.7 Supplementary information

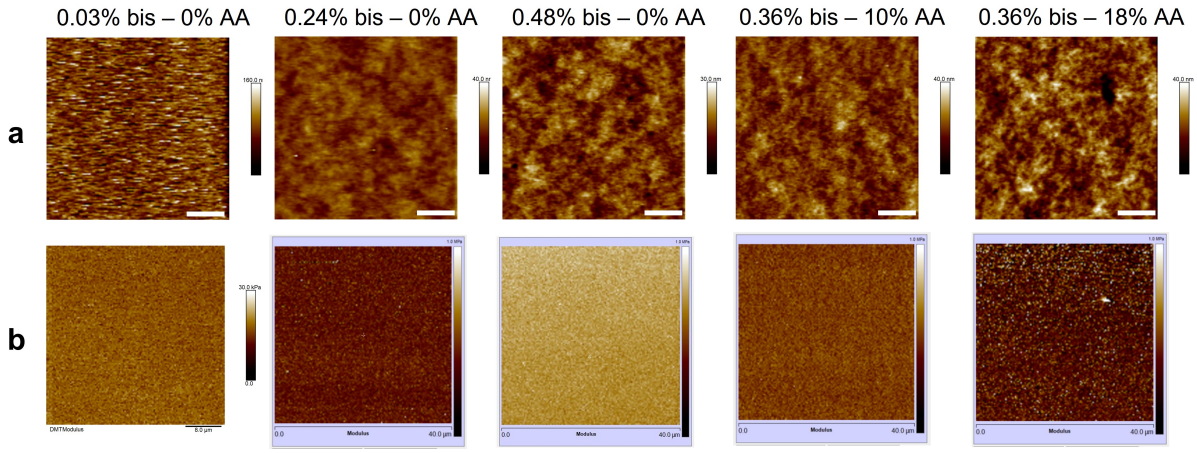

FIGURE 6.9 – a) AFM images of the surface topography on different hydrogel formulations. Scale bar = 8 μm. b)AFM indentation map on a 40 μm x 40 μm area of five polyacrylamide based hydrogels with varying formulation. The color bar represents the elastic modulus (Young's modulus). The surface topography is similar between the different hydrogel formulations. The surface elastic modulus is highly homogeneous for all the hydrogel formulations. (bis = bis-acrylamide, i.e., the crosslinker, AA = acrylic acid)

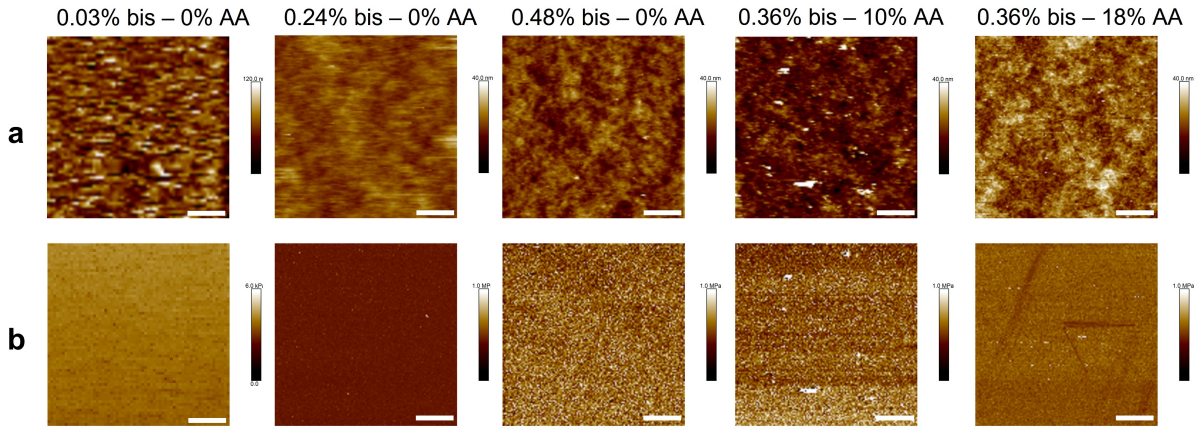

FIGURE 6.10 – a) AFM images of the surface topography on different hydrogel formulations after surface functionalization with a BMP-2 mimetic peptide. Scale bar = 8 μm. b) AFM indentation map on a 40 μm x 40 μm area of five polyacrylamide based hydrogels with varying formulation after surface functionalization with a BMP-2 mimetic peptide. The color bar represents the elastic modulus (Young's modulus). The surface topography is similar between the different hydrogel formulations. The surface elastic modulus is highly homogeneous for all the hydrogel formulations. In addition, the surface roughness (arithmetic mean roughness Ra) of the hydrogels after the functionalization has been evaluated between 2.1 $\pm$ 0.5 nm and 3.4 $\pm$ 0.6 nm. Therefore, the roughness of the functionalized hydrogels is similar, which excludes that differences in cell behavior on the different hydrogels could be attributed to differences in surface roughness. (bis = bis-acrylamide, i.e., the crosslinker, AA = acrylic acid)

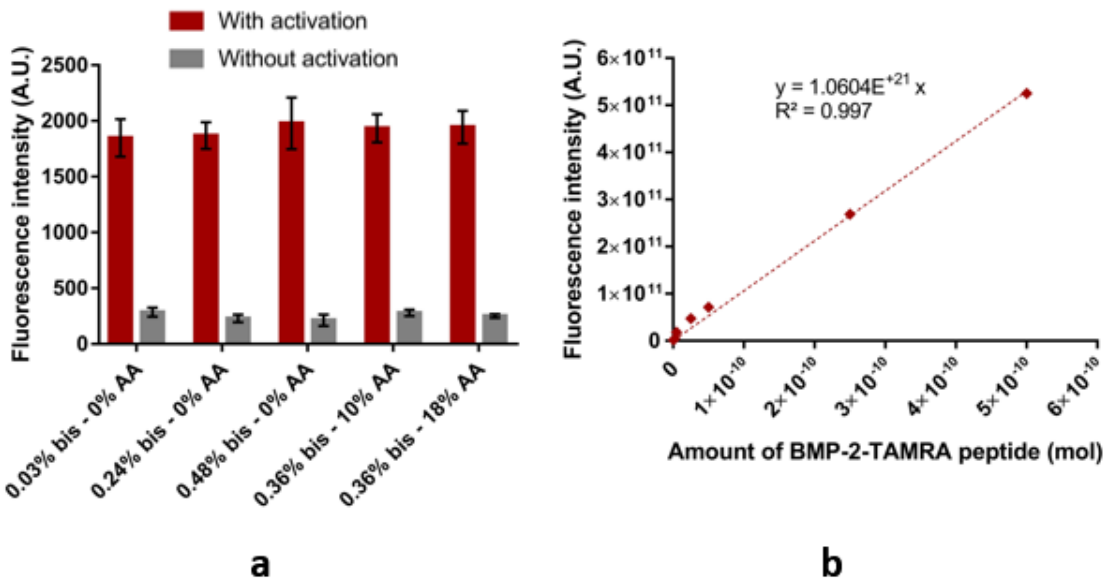

FIGURE 6.11 – a) Fluorescence intensity of hydrogels functionalized with a fluorescently labelled BMP-2 peptide with Sulfo-SANPAH activation (red) or without activation (grey) after 5 days of rinsing. The fluorescence intensity of the hydrogels activated with Sulfo-SANPAH is approximately ten times higher than the fluorescence intensity of the non-activated hydrogels. b) Standard curve of the total fluorescent intensity as a function of the amount of fluorescently labelled BMP-2 peptide. There is a linear relationship between the fluorescence intensity and the amount of BMP-2-TAMRA peptide. This enables to estimate the density of peptide on the hydrogels. (bis = bis-acrylamide, i.e., the crosslinker, AA = acrylic acid)

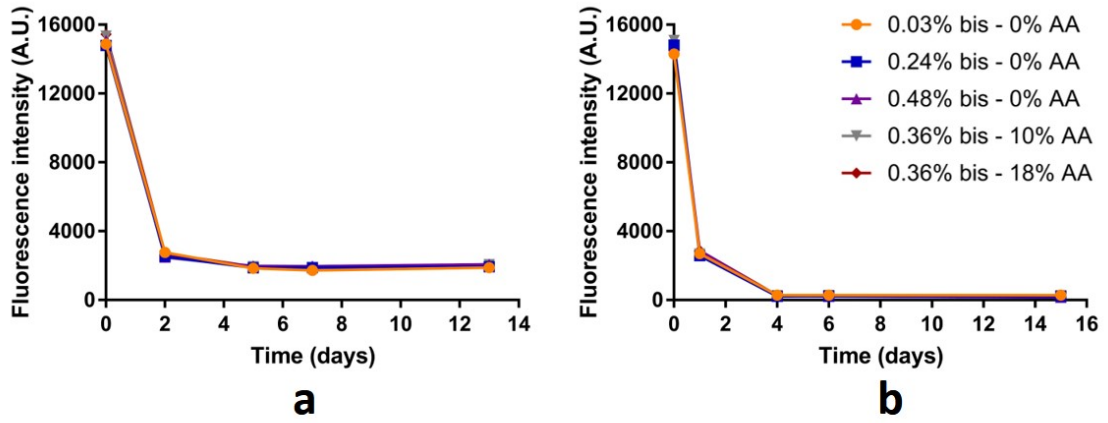

FIGURE 6.12 – Fluorescence intensity of a) hydrogels functionalized with a fluorescently labelled BMP-2 peptide with Sulfo-SANPAH activation or b) without activation, as a function of the number of days of rinsing. The fluorescence intensity is stable after 5 days of rinsing and remains stable up to at least 15 days of rinsing. The fluorescence intensity of the hydrogels activated with Sulfo-SANPAH is higher than the fluorescence intensity of the non-activated hydrogels. (bis = bis-acrylamide, i.e., the crosslinker, AA = acrylic acid)

Elastic modulus (compression)

a	0.03% bis 0% AA	0.24% bis 0% AA	0.48% bis 0% AA	0.36% bis 10% AA	0.36% bis 18% AA
0.03% bis - 0% AA		*	***	**	*
0.24% bis - 0% AA			***		
0.48% bis - 0% AA				****	***
0.36% bis - 10% AA					
0.36% bis - 18% AA					

Stress relaxation (compression)

b	0.03% bis 0% AA	0.24% bis 0% AA	0.48% bis 0% AA	0.36% bis 10% AA	0.36% bis 18% AA
0.03% bis - 0% AA					*
0.24% bis - 0% AA				*	*
0.48% bis - 0% AA				*	*
0.36% bis - 10% AA					*
0.36% bis - 18% AA					

Elastic modulus (AFM)

c	0.03% bis 0% AA	0.24% bis 0% AA	0.48% bis 0% AA	0.36% bis 10% AA	0.36% bis 18% AA
0.03% bis - 0% AA		*	*	*	*
0.24% bis - 0% AA			*	*	*
0.48% bis - 0% AA				*	*
0.36% bis - 10% AA					*
0.36% bis - 18% AA					

FIGURE 6.13 – Statistical analysis of the virgin hydrogels mechanical properties a) elastic modulus and b) stress relaxation measured using unconfined compression, c) elastic modulus measured using AFM. The statistical analysis was done by one-way analysis of variance (ANOVA) and Tukey's test for multiple comparisons. Grey boxes represent the absence of statistic difference. P values are represented as following * $\leq$ 0.05, ** $\leq$ 0.01, *** $\leq$ 0.001, **** $\leq$ 0.0001.)

Runx-2 / 24 hours

a	MSCs on glass	Osteoblasts	15 kPa - 15%	60 kPa - 15%	140 kPa - 15%	100 kPa - 30%	140 kPa - 70%
MSCs on glass		****				*	****
Osteoblasts			****	****	****	*	
15 kPa - 15%							****
60 kPa - 15%							****
140 kPa - 15%							****
100 kPa - 30%							*
140 kPa - 70%							

OPN / 24 hours

b	MSCs on glass	Osteoblasts	15 kPa - 15%	60 kPa - 15%	140 kPa - 15%	100 kPa - 30%	140 kPa - 70%
MSCs on glass				****	****	****	**
Osteoblasts				****	****	*	
15 kPa - 15%				****	****		
60 kPa - 15%						****	****
140 kPa - 15%						****	****
100 kPa - 30%							
140 kPa - 70%							

E11 / 24 hours

c	MSCs on glass	Osteoblasts	15 kPa - 15%	60 kPa - 15%	140 kPa - 15%	100 kPa - 30%	140 kPa - 70%
MSCs on glass		****	****	****	****	****	****
Osteoblasts			****	****	****	****	****
15 kPa - 15%				***		****	***
60 kPa - 15%					****	*	
140 kPa - 15%						****	****
100 kPa - 30%							
140 kPa - 70%							

DMP1 / 24 hours

d	MSCs on glass	Osteoblasts	15 kPa - 15%	60 kPa - 15%	140 kPa - 15%	100 kPa - 30%	140 kPa - 70%
MSCs on glass		****	****	****	***	****	****
Osteoblasts				****		****	****
15 kPa - 15%				****		****	****
60 kPa - 15%					****	****	****
140 kPa - 15%						****	****
100 kPa - 30%							
140 kPa - 70%							

SOST / 24 hours

e	MSCs on glass	Osteoblasts	15 kPa - 15%	60 kPa - 15%	140 kPa - 15%	100 kPa - 30%	140 kPa - 70%
MSCs on glass		****	****	****	****	****	****
Osteoblasts			****	****		****	****
15 kPa - 15%					****	****	****
60 kPa - 15%					****	****	****
140 kPa - 15%						****	****
100 kPa - 30%							
140 kPa - 70%							

FIGURE 6.14 – Statistical analysis of several differentiation markers a) Runx-2, b) Osteopontin, c) E11, d) DMP1, and e) Sclerostin, after 24 hours. The statistical analysis was done by one-way analysis of variance (ANOVA) and Tukey's test for multiple comparisons. Grey boxes represent the absence of statistic difference. P values are represented as following * ≤ 0.05, ** ≤ 0.01, *** ≤ 0.001, **** ≤ 0.0001.)

Runx-2 / 2 weeks

a	MSCs on glass	Osteoblasts	15 kPa - 15%	60 kPa - 15%	140 kPa - 15%	100 kPa - 30%	140 kPa - 70%
MSCs on glass					***	****	****
Osteoblasts					***	****	****
15 kPa - 15%						****	****
60 kPa - 15%					*	****	****
140 kPa - 15%						****	**
100 kPa - 30%							
140 kPa - 70%							

OPN / 2 weeks

b	MSCs on glass	Osteoblasts	15 kPa - 15%	60 kPa - 15%	140 kPa - 15%	100 kPa - 30%	140 kPa - 70%
MSCs on glass		*	***	****	****	****	****
Osteoblasts				****	****	****	****
15 kPa - 15%				**	****	****	****
60 kPa - 15%						***	**
140 kPa - 15%							
100 kPa - 30%							
140 kPa - 70%							

E11 / 2 weeks

c	MSCs on glass	Osteoblasts	15 kPa - 15%	60 kPa - 15%	140 kPa - 15%	100 kPa - 30%	140 kPa - 70%
MSCs on glass			****	****	****	****	****
Osteoblasts			****	****	****	****	****
15 kPa - 15%					****		****
60 kPa - 15%					***		****
140 kPa - 15%						****	****
100 kPa - 30%							****
140 kPa - 70%							

DMP1 / 2 weeks

d	MSCs on glass	Osteoblasts	15 kPa - 15%	60 kPa - 15%	140 kPa - 15%	100 kPa - 30%	140 kPa - 70%
MSCs on glass		*	****	****	***	****	****
Osteoblasts			****	****	****	****	****
15 kPa - 15%				*	**	***	****
60 kPa - 15%					****		****
140 kPa - 15%						****	****
100 kPa - 30%							****
140 kPa - 70%							

SOST / 2 weeks

e	MSCs on glass	Osteoblasts	15 kPa - 15%	60 kPa - 15%	140 kPa - 15%	100 kPa - 30%	140 kPa - 70%
MSCs on glass			****	****	****	****	****
Osteoblasts			****	****	****	****	****
15 kPa - 15%				****	**	**	****
60 kPa - 15%					****		***
140 kPa - 15%						****	****
100 kPa - 30%							****
140 kPa - 70%							

FIGURE 6.15 – Statistical analysis of several differentiation markers a) Runx-2, b) Osteopontin, c) E11, d) DMP1, and e) Sclerostin, after 2 weeks. The statistical analysis was done by one-way analysis of variance (ANOVA) and Tukey's test for multiple comparisons. Grey boxes represent the absence of statistic difference. P values are represented as following * ≤ 0.05, ** ≤ 0.01, *** ≤ 0.001, **** ≤ 0.0001.)

Runx-2 - 24h

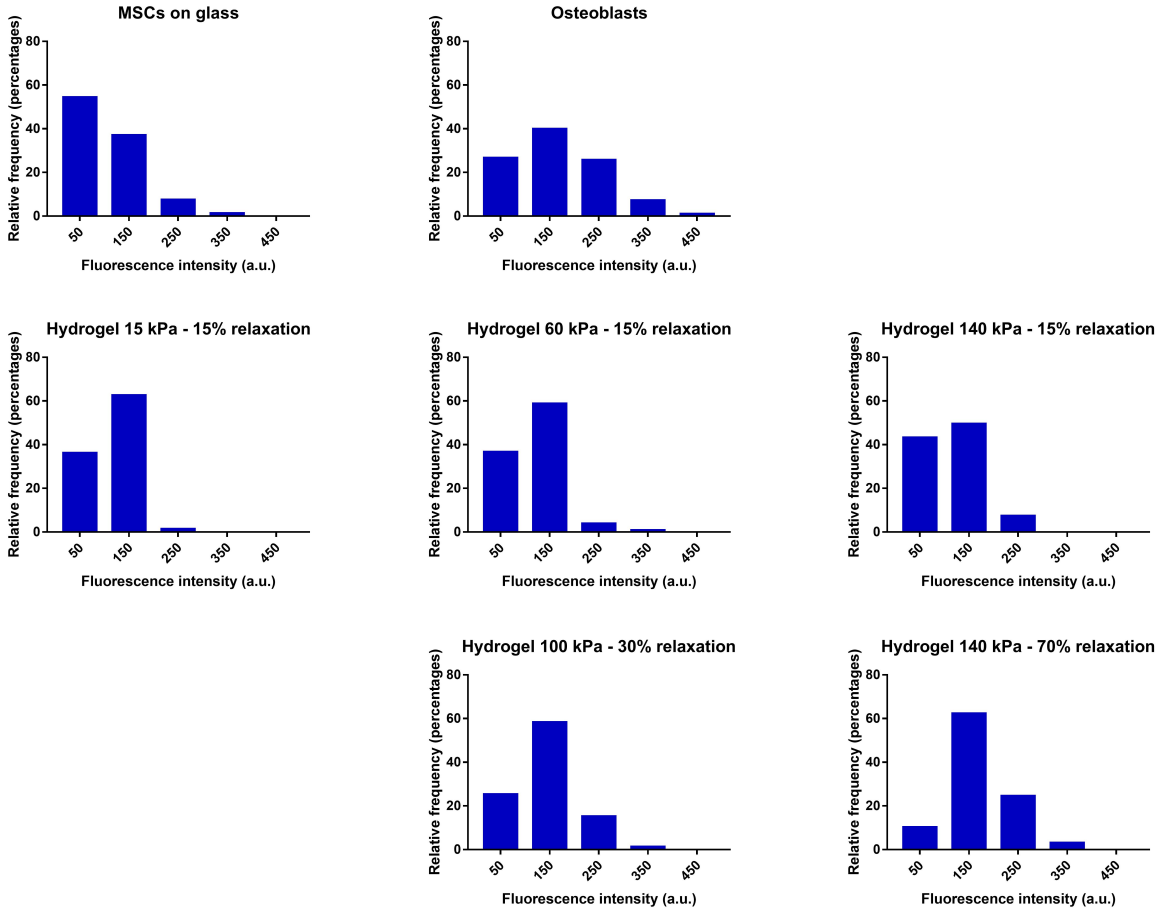

FIGURE 6.16 – Class distribution of the immunofluorescence expression of Runx-2 after 24 hours for MSCs and osteoblasts cultured on glass (controls), and for MSCs cultured on poly(acrylamide-co-acrylic acid) hydrogels with varying mechanical properties. (n=2) Considering these distributions, the conditions can be ranked from the strongest expression to the lowest : osteoblasts > 140 kPa-70% > 100 kPa-30% > 15 kPa-15% = 60 kPa-15% > 140 kPa-15% > MSCs on glass.

Osteopontin - 24h

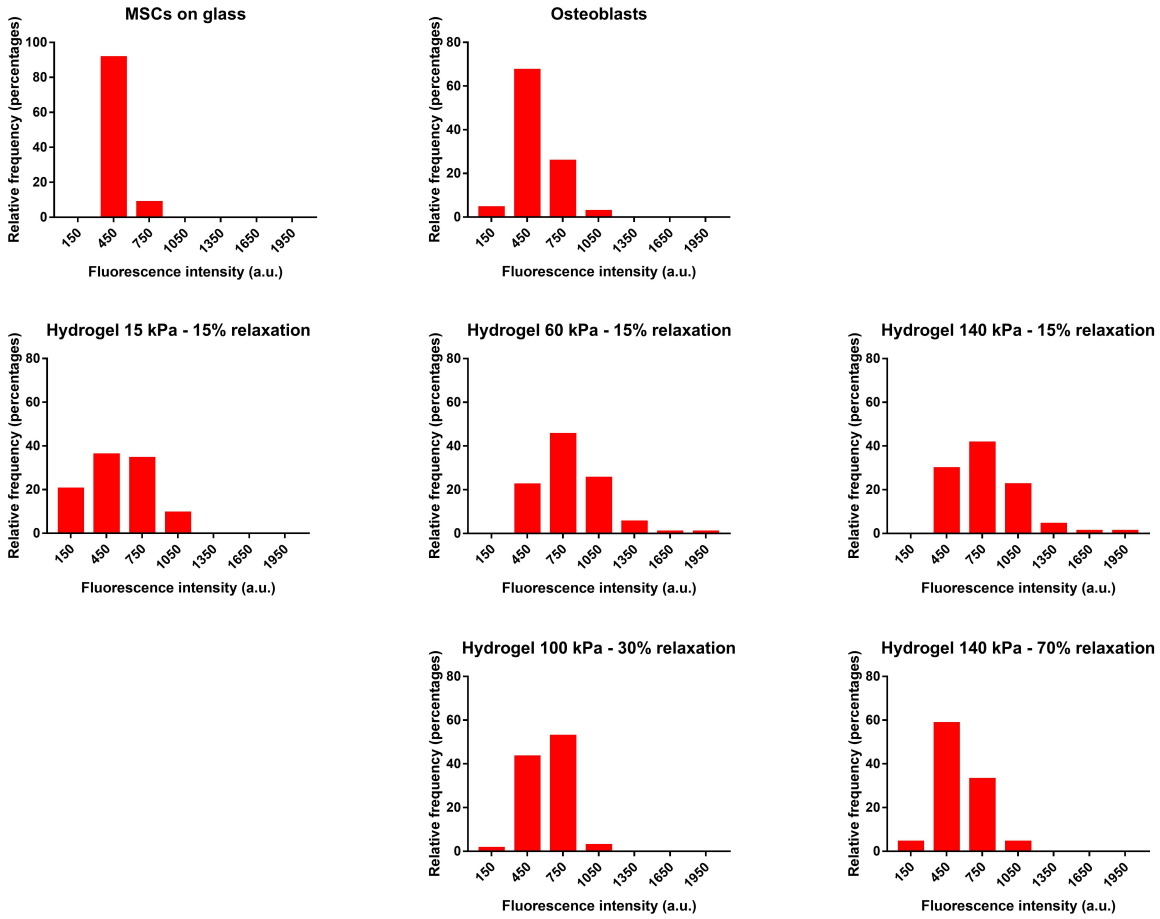

FIGURE 6.17 – Class distribution of the immunofluorescence expression of osteopontin after 24 hours for MSCs and osteoblasts cultured on glass (controls), and for MSCs cultured on poly(acrylamide-co-acrylic acid) hydrogels with varying mechanical properties. (n=2) Considering these distributions, the conditions can be ranked from the strongest expression to the lowest : 60 kPa-15% = 140 kPa-15% > 100 kPa-30% > 140 kPa-70% > osteoblasts > 15 kPa-15% > MSCs on glass.

E11 - 24h

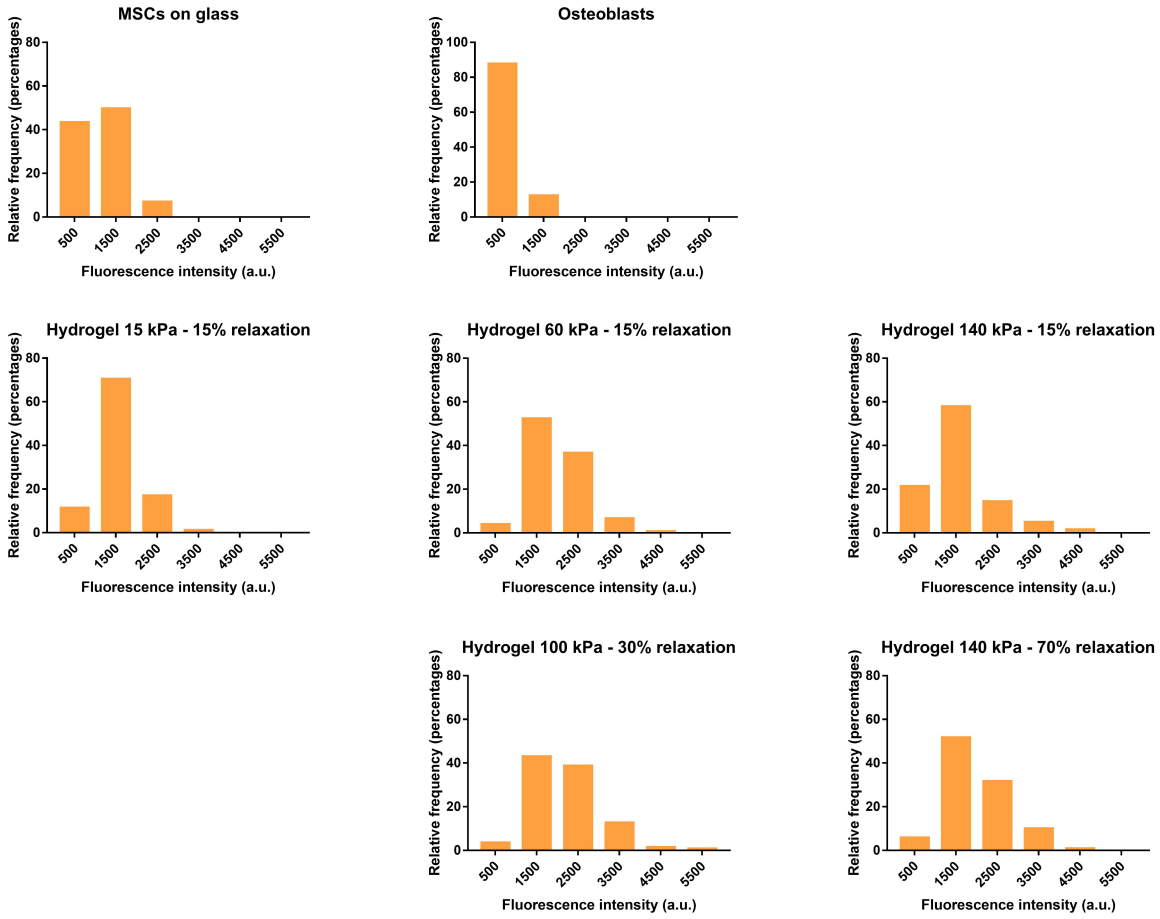

FIGURE 6.18 – Class distribution of the immunofluorescence expression of E11 after 24 hours for MSCs and osteoblasts cultured on glass (controls), and for MSCs cultured on poly(acrylamide-co-acrylic acid) hydrogels with varying mechanical properties. (n=2) Considering these distributions, the conditions can be ranked from the strongest expression to the lowest : 100 kPa-30% > 60 kPa-15% = 140 kPa-70% > 15 kPa-15% > 140 kPa-15% > MSCs on glass > osteoblasts.

DMP1 - 24h

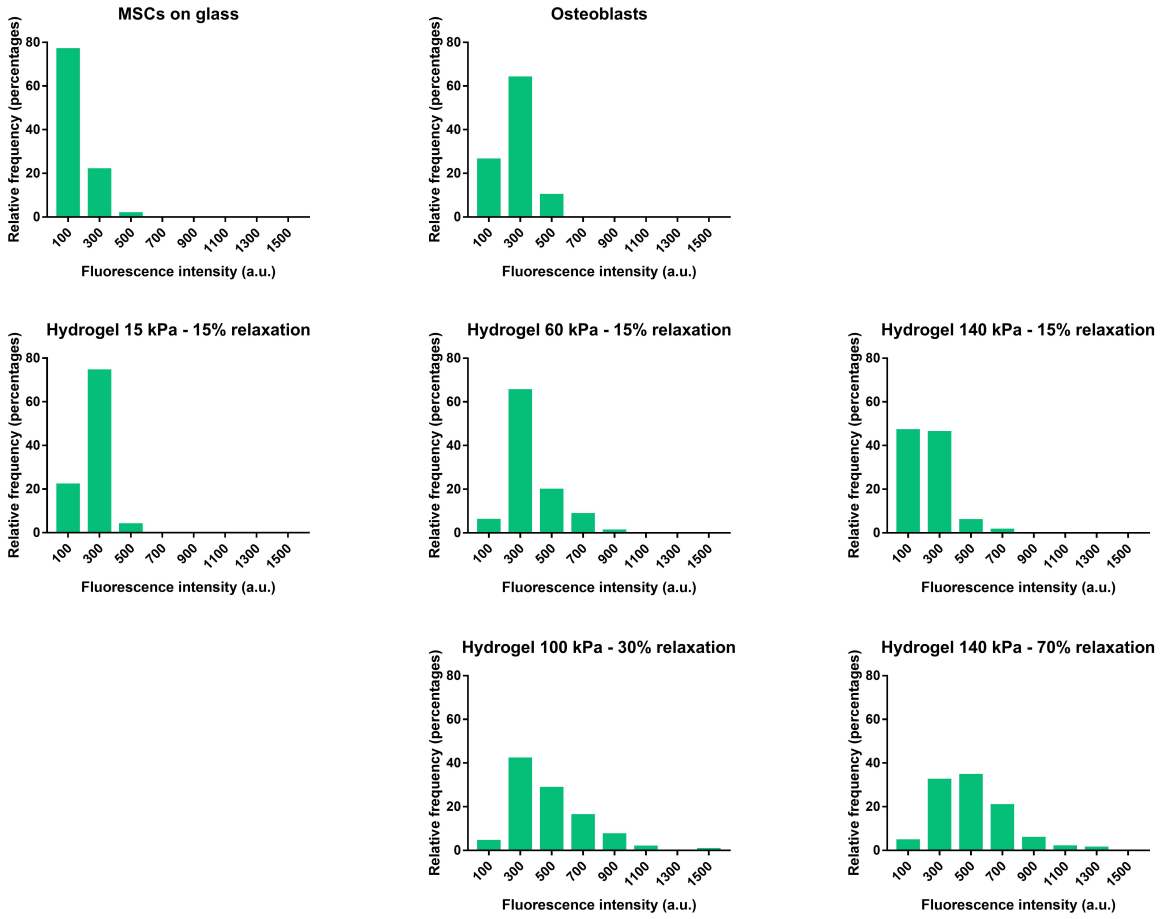

FIGURE 6.19 – Class distribution of the immunofluorescence expression of DMP1 after 24 hours for MSCs and osteoblasts cultured on glass (controls), and for MSCs cultured on poly(acrylamide-co-acrylic acid) hydrogels with varying mechanical properties. (n=2) Considering these distributions, the conditions can be ranked from the strongest expression to the lowest : 140 kPa-70% > 100 kPa-30% > 60 kPa-15% > 15 kPa-15% = osteoblasts > 140 kPa-15% > MSCs on glass.

Sclerostin - 24h

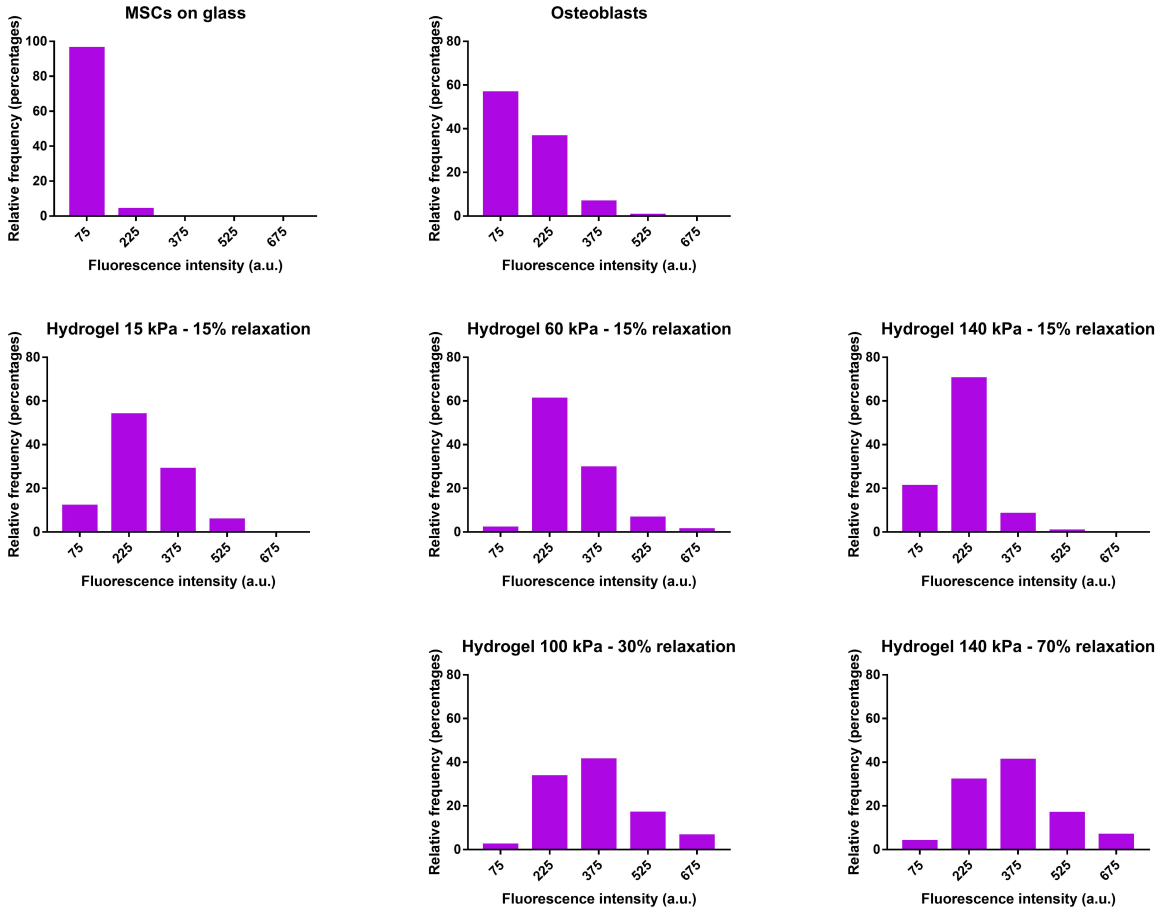

FIGURE 6.20 – Class distribution of the immunofluorescence expression of sclerostin after 24 hours for MSCs and osteoblasts cultured on glass (controls), and for MSCs cultured on poly(acrylamide-co-acrylic acid) hydrogels with varying mechanical properties. (n=2) Considering these distributions, the conditions can be ranked from the strongest expression to the lowest : 140 kPa-70% = 100 kPa-30% > 60 kPa-15% > 15 kPa-15% > 140 kPa-15% > osteoblasts > MSCs on glass.

Runx-2 - 2 weeks

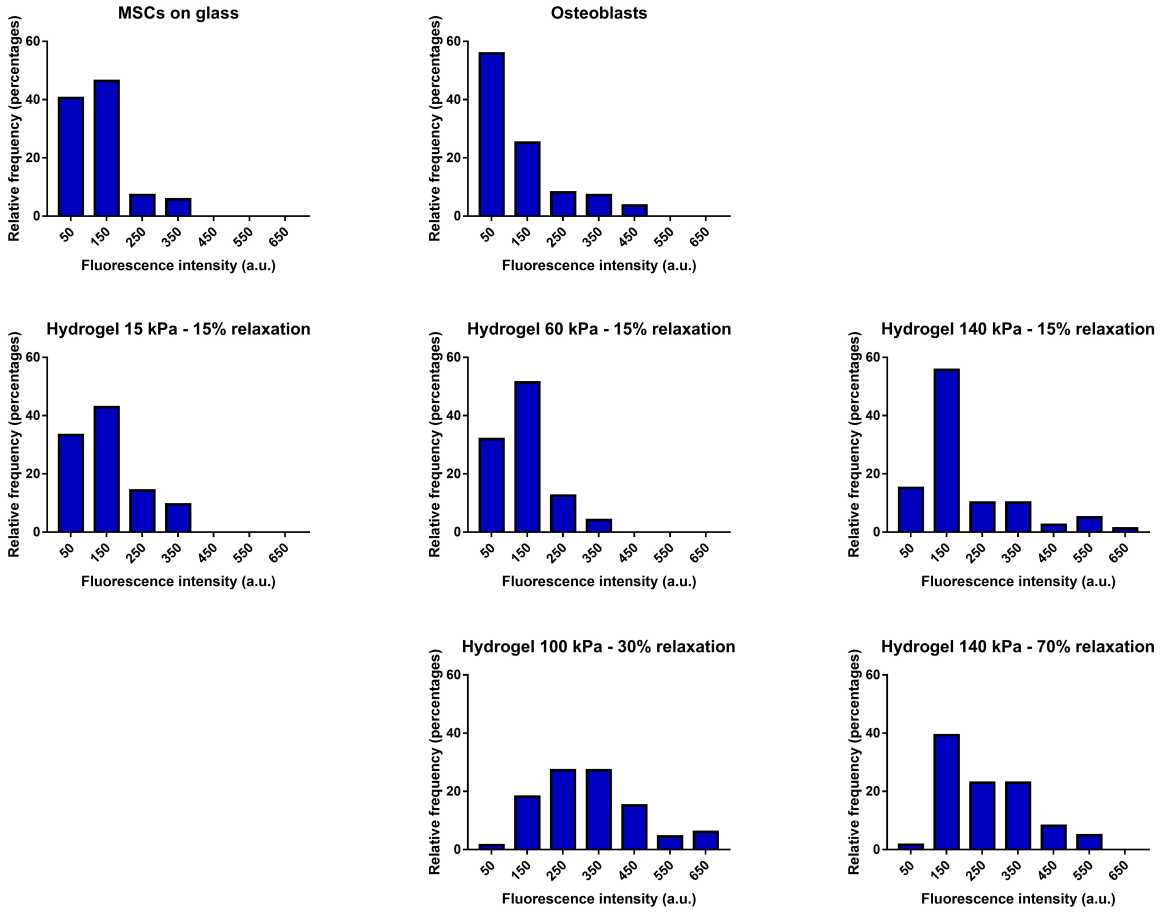

FIGURE 6.21 – Class distribution of the immunofluorescence expression of Runx-2 after 2 weeks for MSCs and osteoblasts cultured on glass (controls), and for MSCs cultured on poly(acrylamide-co-acrylic acid) hydrogels with varying mechanical properties. (n=2) Considering these distributions, the conditions can be ranked from the strongest expression to the lowest : 100 kPa-30% > 140 kPa-70% > 140 kPa-15% > 15 kPa-15% > 60 kPa-15% > MSCs on glass > osteoblasts.

Osteopontin - 2 weeks

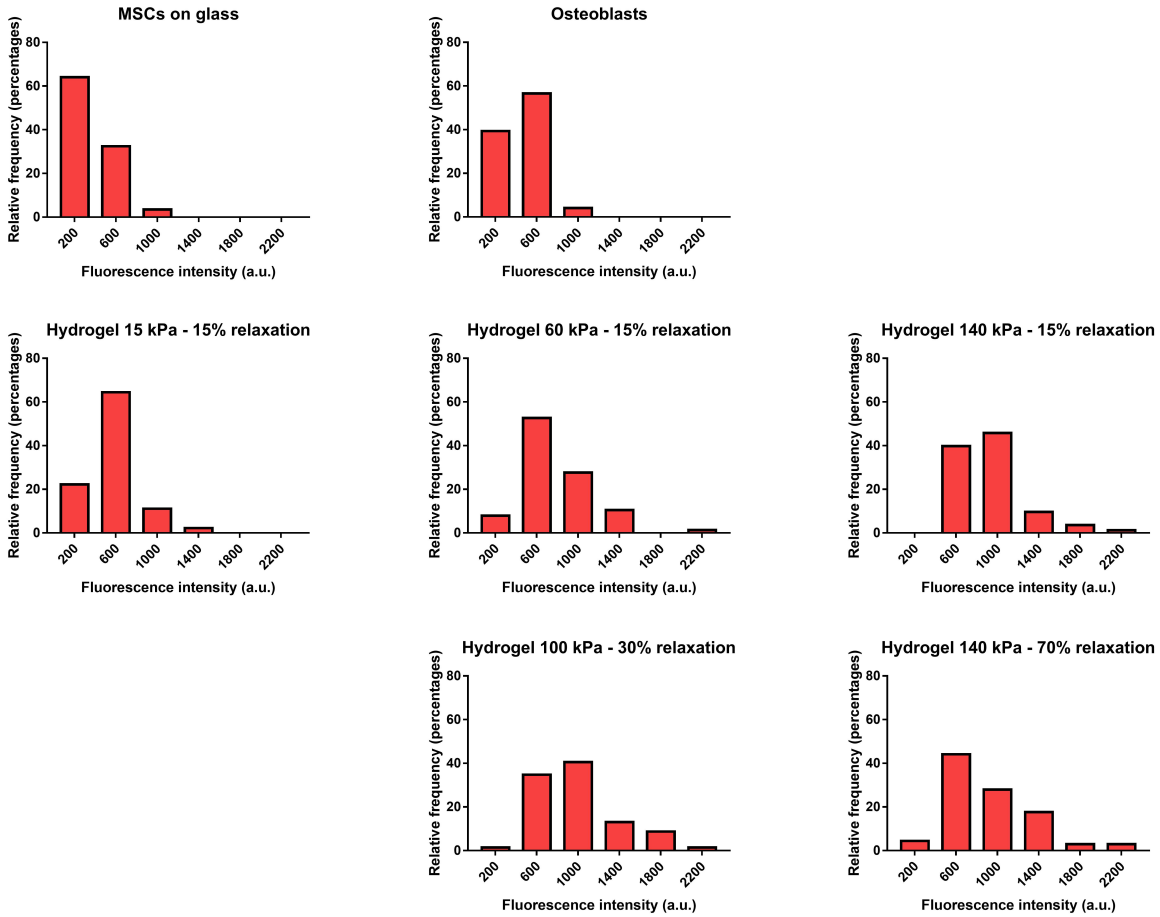

FIGURE 6.22 – Class distribution of the immunofluorescence expression of OPN after 2 weeks for MSCs and osteoblasts cultured on glass (controls), and for MSCs cultured on poly(acrylamide-co-acrylic acid) hydrogels with varying mechanical properties. (n=2) Considering these distributions, the conditions can be ranked from the strongest expression to the lowest : 100 kPa-30% > 140 kPa-15% > 140 kPa-70% > 60 kPa-15% > 15 kPa-15% > osteoblasts > MSCs on glass.

E11 - 2 weeks

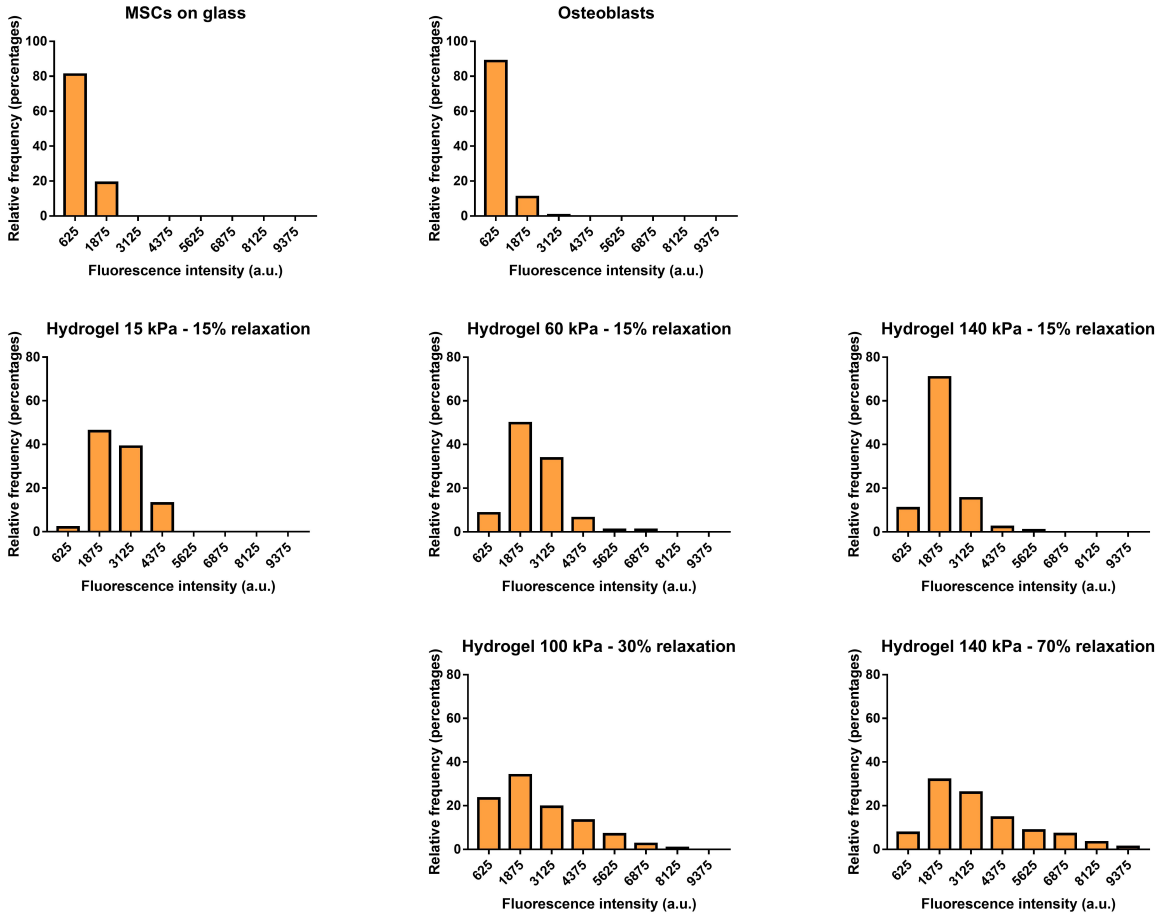

FIGURE 6.23 – Class distribution of the immunofluorescence expression of E11 after 2 weeks for MSCs and osteoblasts cultured on glass (controls), and for MSCs cultured on poly(acrylamide-co-acrylic acid) hydrogels with varying mechanical properties. (n=2) Considering these distributions, the conditions can be ranked from the strongest expression to the lowest : 140 kPa-70% > 100 kPa-30% > 15 kPa-15% > 60 kPa-15% > 140 kPa-15% > MSCs on glass > osteoblasts.

DMP1 - 2 weeks

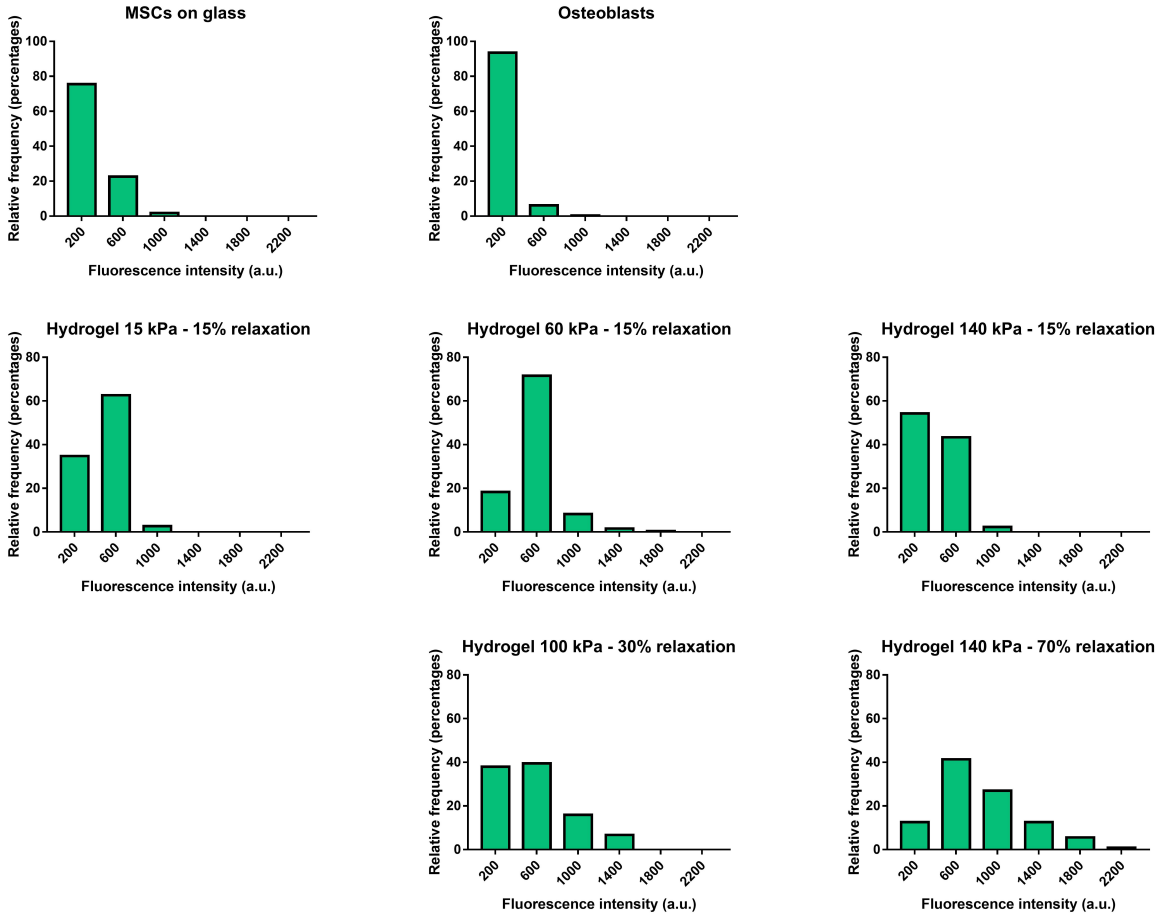

FIGURE 6.24 – Class distribution of the immunofluorescence expression of DMP1 after 2 weeks for MSCs and osteoblasts cultured on glass (controls), and for MSCs cultured on poly(acrylamide-co-acrylic acid) hydrogels with varying mechanical properties. (n=2) Considering these distributions, the conditions can be ranked from the strongest expression to the lowest : 140 kPa-70% > 60 kPa-15% > 100 kPa-30% > 15 kPa-15% > 140 kPa-15% > MSCs on glass > osteoblasts.

Sclerostin - 2 weeks

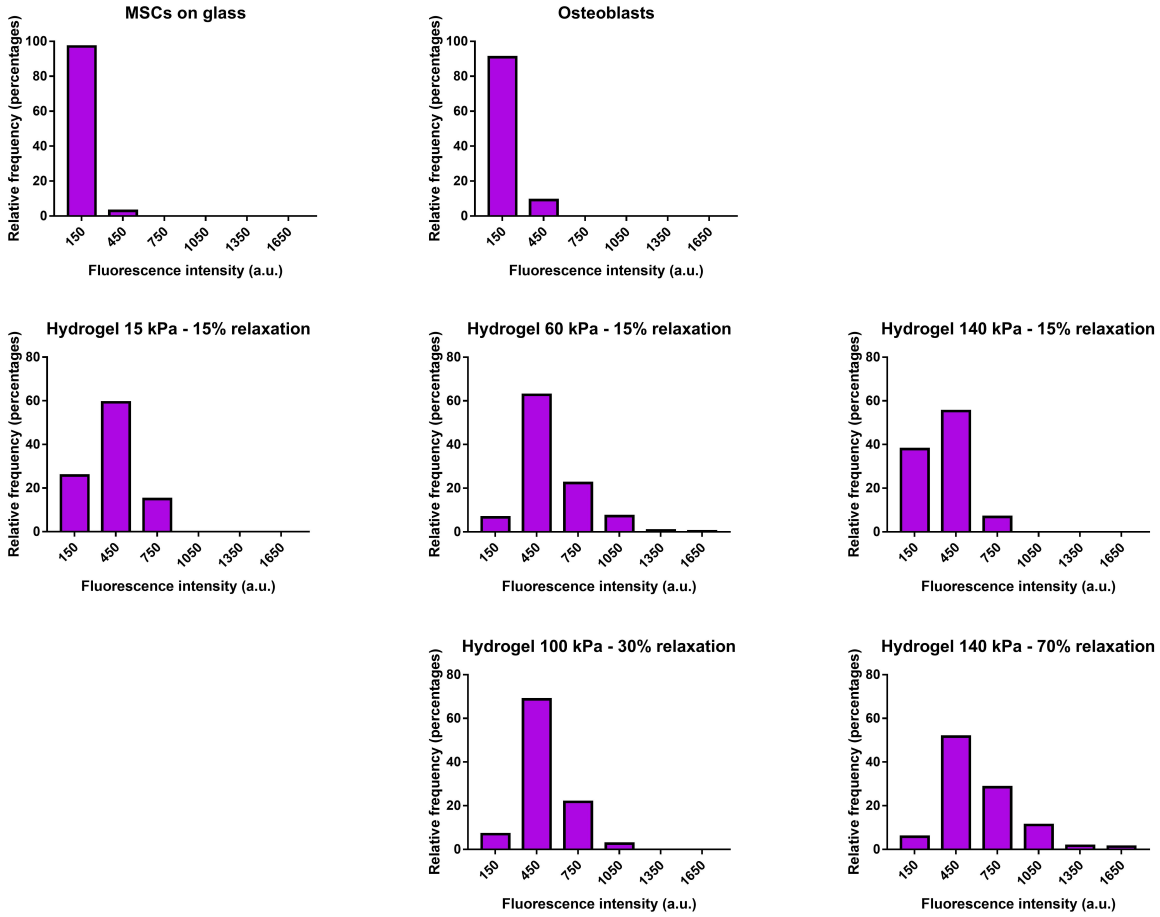

FIGURE 6.25 – Class distribution of the immunofluorescence expression of sclerostin after 2 weeks for MSCs and osteoblasts cultured on glass (controls), and for MSCs cultured on poly(acrylamide-co-acrylic acid) hydrogels with varying mechanical properties. (n=2) Considering these distributions, the conditions can be ranked from the strongest expression to the lowest : 140 kPa-70% > 60 kPa-15% > 100 kPa-30% > 15 kPa-15% > 140 kPa-15% > osteoblasts > MSCs on glass.

Chapter 7

Supplementary studies

This chapter presents experiments that have been conducted during the PhD but that have not been published. The first section describes the evaluation of hydrogels cytotoxicity to ensure that there were no residues of toxic unreacted monomers or ethanol, used for hydrogels sterilization, that could release during cell culture. The second section presents the functionalization of hydrogels with type I collagen in order to compare MSCs differentiation in response to the BMP-2 mimetic peptide or collagen.

7.1 Evaluation of hydrogels cytotoxicity

As mentioned in the chapter 2, one disadvantage of polyacrylamide based hydrogels is the toxicity of the monomers which prevents their use to encapsulate cells in 3D and which might cause cytotoxicty issues if unreacted monomers are trapped in the gel and are released during cell culture. To prevent this effect, the hydrogels are left to swell in PBS for one week after their synthesis to enable the release of the unreacted monomers, initiator, and catalyst.

In addition, prior to any cell culture experiment, the hydrogels need to be sterilized. The different methods that can be used to sterilize hydrogels, as well as their advantages and drawbacks, are presented in Table 7.1. Various methods are effective against many different micro-organisms, such as bacteria, molds, yeasts, and viruses. These methods include sterilization by dry heat, steam heat, gamma irradiation, ethylene oxide, and peracetic acid. However, these methods often result in significant damage of the polymer chains and might leave toxic residues within the hydrogel.[374, 375] Besides causing polymer crosslinking or degradation, sterilization with plasma leaves reactive species within the scaffolds even long after sterilization, resulting in potential side effects if the residual reactive species are not properly removed before in vitro or in vivo studies.[374, 375] The penetration depth of electron beam irradiation or UV irradiation might be increased by increasing the intensity and the time of irradiation respectively, but this can lead to further polymer damage.[374] Although the ability

of ethanol disinfection to eliminate all types of pathogenic components might be a concern for in vivo studies[374, 375, 376], its bactericidal and fungicidal potential is generally sufficient for in vitro studies.[375] In addition, ethanol sterilization presents many advantages as it is fast and simple, it does not require any particular installation, it is performed at low temperature and with low cost[374, 375], which is why this method has been selected in this project. Nevertheless, the side effects of ethanol on hydrogels properties remain controversial in the literature.[374]

Sterilization method	**Mode of action**	**Advantages**	**Drawbacks**
Dry Heat	Oxidation of cell components	Effective, fast, simple, no toxic residues, high penetration	Melting, degradation of the polymer
Steam Heat	Denaturation of enzymes and structural proteins	Effective, fast, simple, no toxic residues, high penetration	Hydrolytic degradation of the polymer
Gamma irradiation	Scission of DNA and RNA strands	Effective, no toxic residues, high penetration, low temperature	Expensive, polymer chain scission or crosslinking
Electron beam irradiation	Scission of DNA and RNA strands	Fast, no toxic residues, low temperature	Polymer chain scission or crosslinking, low penetration
UV irradiation	Damages DNA and prevents DNA replication	Fast, low temperature, low cost, no toxic residues	Not effective, polymer and biomolecules damage
Plasma	Oxidation that damages proteins and nucleic acids	Fast, low temperature, improve cell-material interaction due to surface modification	Leave reactive species, polymer damage
Ethylene oxide	Alkylation of cellular molecules	Effective, low temperature	Toxic residues, explosive, flammable, carcinogenic
Peracetic acid	Oxidation of enzymes	Effective, low temperature	Polymer and biomolecules damage, acidic residues
Ethanol	Cell dehydration, membranes disruption	Fast, simple, low cost, low temperature	Limited efficiency, potential material damage

TABLE 7.1 – Hydrogels sterilization methods with their advantages and drawbacks.[374, 375]

Some of the above mentioned methods are used for the sterilization of healthcare products and the sterilization process must follow a standard. For example, sterilization using gamma radiation from Cobalt-60 requires an irradiation dose of 25 kGy to be validated by the ISO-11137 standard. The sterilization with ethylene oxide, moist heat, and dry heat are described by the ISO standards 11135, 17665, and 20857, respectively. Finally, although UV irradiation, and ethanol sterilization are commonly used for the sterilization of materials for in vitro studies, these methods are not suitable for the sterilization of materials that are implanted in vivo because of their limited efficiency and their potential to cause degradation of the materials. Considering that ethanol sterilization may leave ethanol residues within the hydrogels, hydrogels cytotoxicity has been evaluated at the beginning of the project to ensure that there were no residues of toxic unreacted monomers or ethanol that could be released during cell culture and damage the cells.

7.1.1 Methods

Preparation of the cells Human bone marrow MSCs (PromoCell, Germany) were cultured in Mesenchymal Stem Cell Growth Medium 2 (PromoCell) and incubated in a humidified atmosphere containing 5% CO_2 at 37°C. All cells were used at passage number 5, were subconfluently cultured, and were seeded at 6,000 cells/cm^2 in a 48 well-plate. Cells were grown to 80% confluency in the 48 well-plate before initiating the assay.

Preparation of the extract tests Following ISO standards 10993-5 and 10993-12, that deal with the in vitro evaluation of materials toxicity, extract tests have been performed to evaluate whether there was a cytotoxic response to the materials. The extract test evaluates the cytotoxicity of any leachable by-products from the material.
Cells cultured under normal, or blank, conditions and without any material were used as negative control. A solution of culture medium containing 64 g/L of phenol was used as a cytotoxic (positive) control. Two hydrogels were selected for this study (0.24% crosslinker - 0% acrylic acid and 0.36% crosslinker - 18% acrylic acid) and functionalized with the BMP-2 peptide following the procedure described in chapter 5. After five days of rinsing, the hydrogels were sterilized in ethanol 70% for 2.5 hours. Then, the ethanol was changed and the gels were left to sterilize overnight. After sterilization, the gels were rinsed in PBS three times for 10 minutes (Figure 7.1a) or three times for 1 hour (Figure 7.1b). The gels were then incubated in Mesenchymal Stem Cell Growth Medium 2 culture medium at a concentration of 5 cm^2/ml at 37°C for 72 hours, as indicated by the ISO standard 10993-5.

Extract tests After 72 hours, the culture medium of the cells in the 48 well-plate was removed and replaced with the extract medium (medium in contact with the gels). Cells were incubated with the extract medium at 37°C and 5% CO_2 for 24 hours before cytotoxic evaluation with 2,3-bis-(2-methoxy-4-nitro-5-sulfophenyl)-2H-tetrazolium-5-carboxanilide (XTT) cell metabolic activity assay. The cytotoxic control was performed in a separate well-plate to avoid phenol evaporation and interaction with the cells in the surrounding wells. For this cytotoxic control, the culture medium was removed and replaced by culture medium containing 64 g/L of phenol for 24 hours.

Evaluation of cell metabolic activity The Cell Proliferation Kit II (XTT ; Roche, Mannheim, Germany) was used to quantitatively evaluate the cell metabolic activity. XTT was used according to the manufacturer's protocols. The electron coupling and XTT labeling reagents were thawed and immediately combined in a 1 :50 μl ratio. Then the XTT solution was added to the cell culture wells, 250 μl for a 48 well-plate. After 18 hours of incubation, absorbance was measured at 450 and 630 nm at 37°C with a ELx808 Absorbance Microplate Reader (BioTek Instruments). Net absorbance was calculated (A450 - A630) for each sample of the five biological replicates. The relative cell metabolic activity was normalized to the mean of the blank culture media.

7.1.2 Results

Figure 7.1a shows that the cell metabolic activity of the cells in contact with the extract medium was below the limitation for acceptable cytotoxicity (dashed line) and was much lower than that of cells in the fresh culture medium (blank), indicating a cytotoxicity of the gels. It has been hypothesized that washing the gels three times for 10 minutes after ethanol sterilization was not sufficient to remove the ethanol from the gels. Figure 7.1b clearly demonstrates the non-alteration of the cell metabolic activity when the cells were cultured in extracts issued from the two hydrogels rinsed three times for 1 hour, while the cell metabolic activity dropped to around 10% with the cytotoxic control (phenol). Although the evaluation of the cell metabolic activity might be controversial to assess cytotoxicity effects, as it does not consider the number of dead or living cells, we were able to see an effect of the rinsing time after ethanol sterilization on cell metabolic activity. Therefore, it can be concluded that with three washes for 1 hour after sterilization, there was no leaching of toxic compounds from the hydrogels, such as unreacted monomers or ethanol.

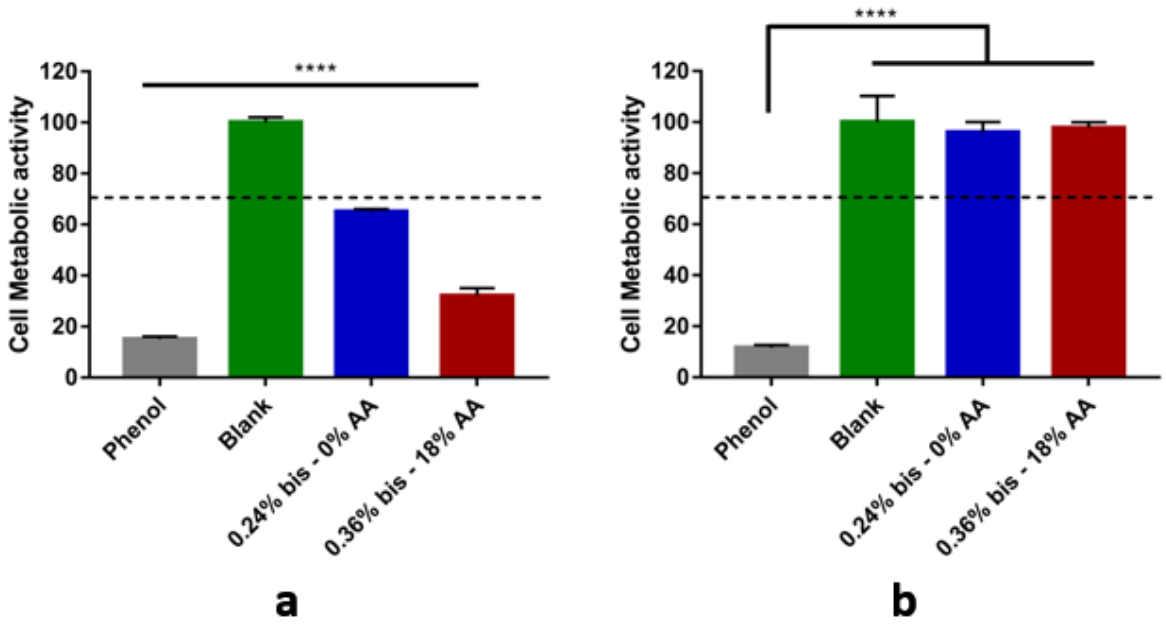

FIGURE 7.1 – Cell metabolic activity for human mesenchymal stem cells cultured with extracts collected from two hydrogels functionalized with a BMP-2 mimetic peptide and sterilized with ethanol 70%. a) The hydrogels were rinsed in PBS three times for 10 minutes after ethanol sterilization. The cell metabolic activity of the cells in contact with the extract medium is higher than the cytotoxic control (phenol) but lower than the fresh culture medium (blank). b) The hydrogels were rinsed in PBS three times for 1 hour after ethanol sterilization. No difference was found between the culture medium (blank) and the extracts of the gels. A statistical difference was found between phenol and all other groups. The dashed line represents the ISO 10993-5 limitation for acceptable cytotoxicity. (**** $p < 0.0001$).

7.2 Hydrogels functionalization with type I collagen

As mentioned in chapter 4, type I collagen has been highly used for the functionalization of polyacrylamide hydrogels to enable cell adhesion in studies assessing the impact of hydrogels mechanical properties on MSCs differentiation. [52, 55, 56, 57, 58, 61, 63, 69, 231] Therefore, it might be interesting to study MSCs osteogenic differentiation in response to hydrogels stiffness and stress relaxation on hydrogels functionalized with type I collagen. This would allow to compare the results with the literature and to assess the impact of hydrogels biofunctionalization on MSCs osteogenic differentiation (type I collagen versus BMP-2 mimetic peptide). In addition, it would be particularly interesting to see if the osteocyte-like cell shape could also be obtained with a type I collagen coating. Consequently, preliminary experiments have been conducted on hydrogels functionalization with type I collagen and on the response of MSCs to hydrogels biofunctionalization.

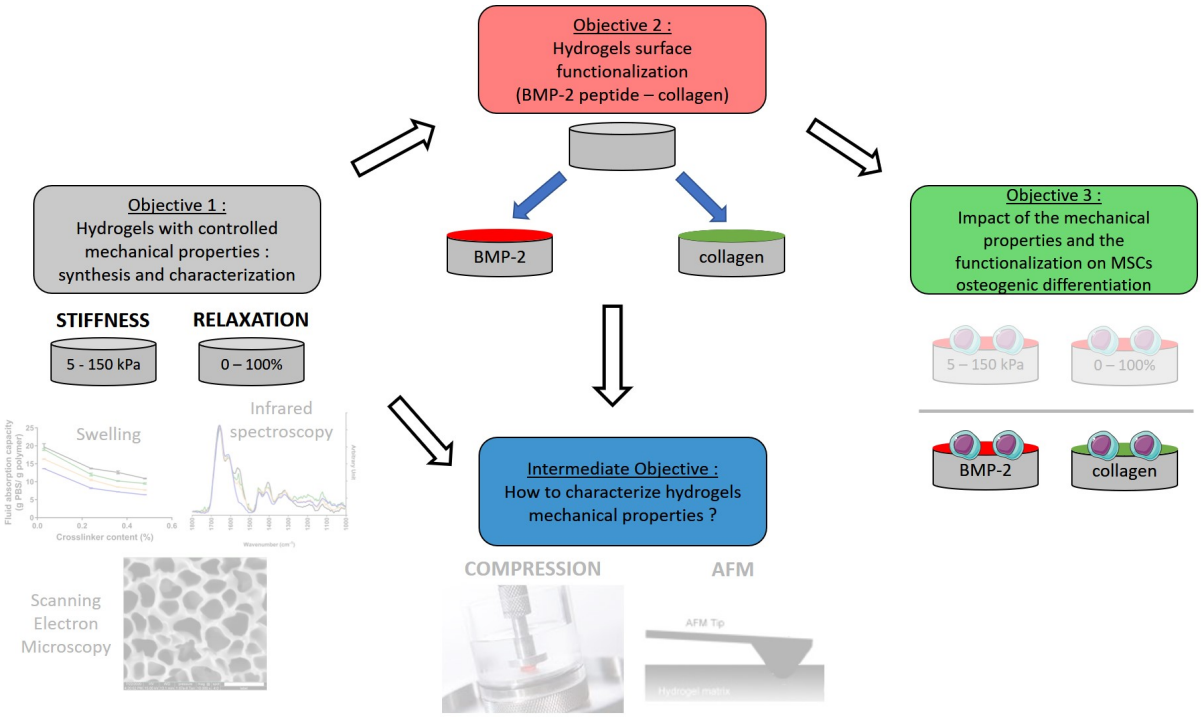

NB : The parts in transparency are not covered in this chapter.

7.2.1 Methods

Collagen grafting Type I collagen has been conjugated to the hydrogels similar to the peptide. Briefly, 200 μL of a 1 mmol.L^{-1} solution of Sulfo-SANPAH in HEPES buffer (50 mmol.L^{-1}, pH 8.5) were pipetted onto the gel surface in a 48-well plate which was placed under ultraviolet light (365 nm) in a UV chamber (Uvitec, UK). The gels were exposed to UV light for 30 min and rinsed with 500 μL HEPES for each side of the gel disks. The gels were then incubated with a solution of type I collagen (0.05 mg/mL) in 50 mM HEPES overnight at 4°C. The gels were then rinsed in 5 mL HEPES for one week, with changing the rinsing solution twice a day.

Evaluation of collagen grafting on the hydrogels Hydrogels functionalization with type I collagen was evaluated using immunofluorescence. Following previously described protocols[63, 231], the gels were washed with PBS and blocked with 1% Bovine Serum Albumin (BSA) for 30 minutes and then incubated with mouse monoclonal anti-collagen I (1 :1000; Novus Biologicals) for 1 hour at 37°C. After washing with PBS containing 0.05% Tween 20, the gels were incubated with the secondary antibody Alexa Fluor 488 goat anti-mouse IgG (1 :400; Invitrogen) for 1 hour at 37°C. A Leica SP8 confocal microscope was used to confirm a uniform grafting on the surface of the gel and to observe the repartition of collagen in the thickness of the gel. Images were collected with identical microscope and laser settings for each sample (objective HC Plan Fluotar 10x NA 0.3, 4096 x 4096, 16 bits per pixel). Z-stacks were created over 700 μm with a slice-thickness of 4.29 μm.

Calibration curve to evaluate collagen surface density A series of droplets of type I collagen were deposited on a nitrocellulose membrane with calibrated concentrations (from 0.2 mg/ml to 0.01 mg/ml). Subsequently, a western blot protocol has been followed for the immunostaining of the collagen drops. The membrane was blocked with 5% BSA in TBST (Tris-Buffered Saline-Tween) for 1 hour at room temperature, and then incubated with mouse monoclonal anti-collagen I (1 :1000; Novus Biologicals) for 1 hour at room temperature. After washing three times with TBST, the membrane was incubated with the secondary antibody Alexa Fluor 488 goat anti-mouse IgG (1 :400; Invitrogen) for 1 hour at room temperature. Finally, the membrane was washed three times with TBST and left to dry. The drops on the membrane were then imaged under identical conditions than the hydrogels in order to obtain a calibration curve of the fluorescence intensity as a function of collagen quantity, which was then used to measure the collagen density on the hydrogels. Image J software was used to quantify the relative fluorescent intensity of the grafted molecules as a function of hydrogels mechanical properties.

Cell culture on hydrogels functionalized with collagen or the BMP-2 peptide Bone marrow hMSCs were thawed and cultured in MSCs growth medium 2 (MSC-GM2), in a humidified atmosphere containing 5% CO_2 at 37°C as recommended by the supplier. They

were subcultured twice a week using trypsin/EDTA 1x detachment and used at passage 4. For differentiation experiments, hMSCs were seeded at a density of 10,000 cells/cm^2 in α-MEM medium on functionalized hydrogels (collagen 0.05 mg/mL or BMP-2 peptide 10^{-3} M) previously sterilized with 70% ethanol overnight. All cell seedings were carried out without any serum for the first 4 h of culture. This enabled the interaction of cells with the surface conjugated biomolecules and not with adsorbed serum proteins. After 4 h, the culture medium was supplemented with 10% FBS. After 24 h, the medium was replaced by MSC Osteogenic Differentiation medium. The cells were then cultured for 2 weeks and the Osteogenic Differentiation medium was changed twice a week.

Lineage-specific differentiation assays The extent of hMSCs osteogenic differentiation was evaluated using specific markers of osteoblasts (Osteopontin (OPN)) and osteocytes (Podoplanin (E11), Dentin matrix acidic phosphoprotein 1 (DMP-1) and Sclerostin (SOST)). The expression of OPN, E11, DMP-1 and SOST was assessed by immunocytochemistry staining after 2 weeks of cell differentiation. Cells were fixed in 4% paraformaldehyde at 4°C for 20 min, permeabilized with 0.5% Triton X-100 in PBS for 15 min at 4°C and blocked with 1% Bovine Serum Albumin (BSA) in PBS for 30 min at 37 °C. Subsequently, cells were incubated with the primary antibodies for 1 h at 37°C. Cells were washed in PBS containing 0.05% Tween 20, before and after incubation with the secondary antibodies, Alexa Fluor 488 goat anti-rabbit IgG (H+L) and Alexa Fluor 647 goat anti-mouse IgG (H+L) (1 :400 dilution) for 1 h at 37 °C. The cell morphology and cytoskeleton organization were evaluated by labeling filamentous actin (F-actin) with Alexa Fluor 488 phalloidin (Invitrogen, France) (1 :40 dilution) for 1 h at 37 °C. Samples were then stained for nuclei using Fluoroshield^{TM} with Dapi. Fluorescently stained cells were examined using a Leica DM5500B epifluorescence microscope (Leica Biosystems) equipped with a CoolSnap HQ camera and controlled by Metamorph 7.6 software. The expression of the differentiation markers was quantified using ImageJ software by measuring the fluorescence intensity on 20 to 30 cells per sample, with two samples per condition.

7.2.2 Results

Collagen grafting Figure 7.2a shows that there is a linear relationship between the fluorescence intensity and the amount of collagen. This shows that the method that has been developed in this project, which consists in depositing droplets of type I collagen with known concentrations on a western blot nitrocellulose membrane and subsequently performing an immunofluorescent staining of collagen on the membrane, is suitable to obtain the relationship between the fluorescence intensity and the amount of collagen. This will enable to estimate the density of collagen on the surface of the hydrogels. In parallel, the immunofluorescent staining of collagen has been performed on different hydrogel samples, as shown in Figure 7.2b, in order to validate the protocol and the specificity of the staining. Figure 7.2b shows that no fluorescence is detected after the immunofluorescent staining of a virgin hydrogel (without collagen), while a hydrogel with grafted collagen (after activation of the gel with Sulfo-SANPAH) shows a high fluorescence intensity. Finally, a hydrogel with adsorbed collagen, so without any activation of the gel, presents some spots of fluorescence, indicating that some collagen might remain on the surface after rinsing of the hydrogel, but in a lesser amount compared to the activated gel. These results confirm that the immunofluorescent staining that has been performed is specific to collagen, and that the activation of the hydrogel with Sulfo-SANPAH leads to the immobilization of collagen on the surface of the hydrogels.

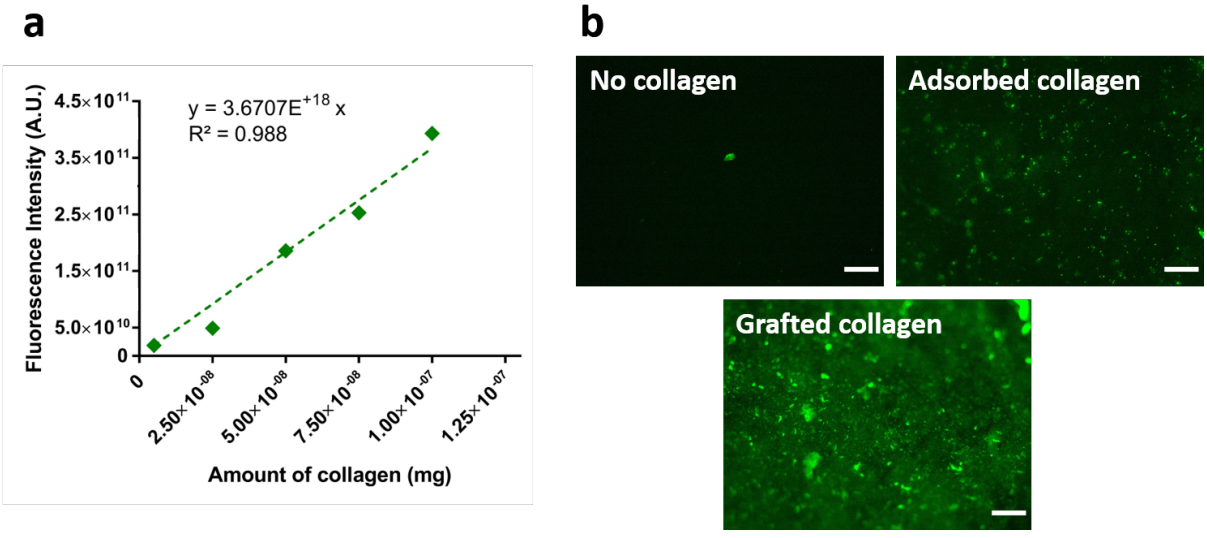

FIGURE 7.2 – a) Standard curve of the total fluorescent intensity as a function of the amount of collagen (after immunostaining). There is a linear relationship between the fluorescence intensity and the amount of collagen. This enables to estimate the density of collagen on the hydrogels. b) Epifluorescence microscopy images of the immunofluorescent staining of type I collagen for a hydrogel without collagen, with adsorbed collagen (no activation of the gel), and with grafted collagen (after activation of the gel with Sulfo-SANPAH). Scale bar = 100 μm. The fluorescence intensity of the activated gel is higher than the non-activated gel, while no fluorescence is detected for the virgin hydrogel.

Figure 7.3a-d shows the presence of type I collagen (green), as visualized with immunofluorescent staining for type I collagen bound to different polyacrylamide or poly(acrylamide-co-acrylic acid) substrates. The collagen coating appears to be homogeneous on zones of 350 x 350 μm. Semiquantification of fluorescence intensity from Figure 7.3e shows no statistical difference between the different hydrogels, although the hydrogel with 0.03% crosslinker and 0% acrylic acid seems to show a less homogeneous coating and a lower fluorescence intensity. These results are consistent with the literature as some studies showed that there were no difference in the fluorescence intensity depending on polyacrylamide hydrogels stiffness.[55, 63] Nevertheless, this preliminary study has been conducted on only one sample of each hydrogel formulation to demonstrate the feasibility of the technique, and should therefore be conducted on more samples.

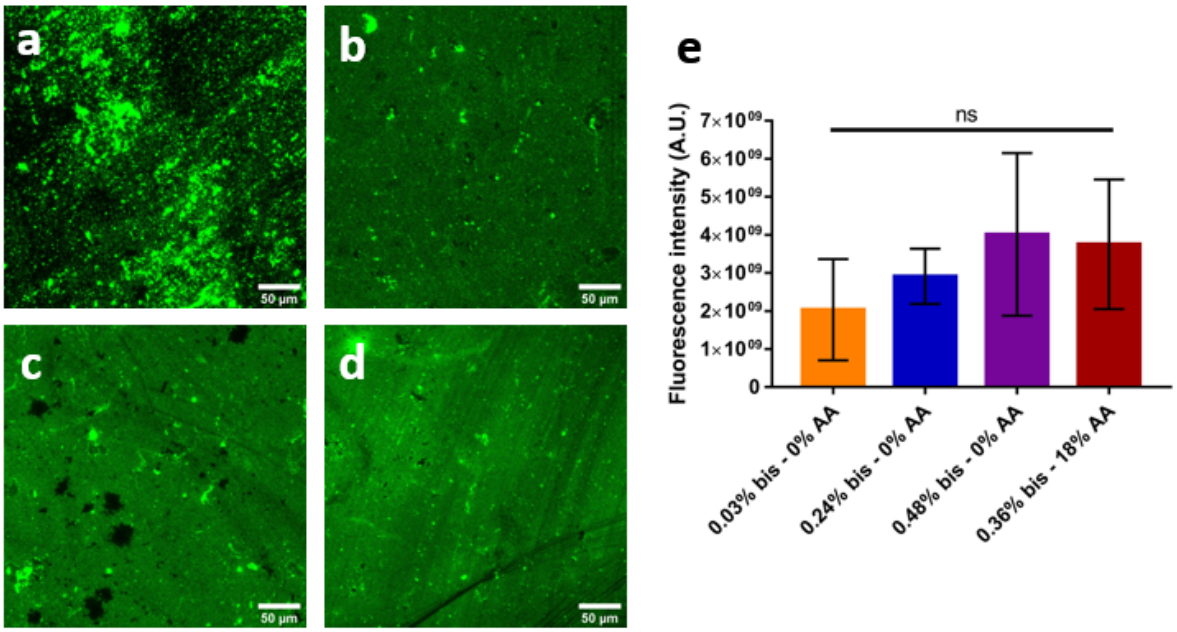

FIGURE 7.3 – Immunofluorescent staining of type I collagen conjugated to the surface of hydrogels. Confocal microscopy images of the surface of hydrogels coated with type I collagen. Hydrogel with a) 0.03% crosslinker - 0% acrylic acid, b) 0.24% crosslinker - 0% acrylic acid, c) 0.48% crosslinker - 0% acrylic acid, and d) 0.36% crosslinker - 18% acrylic acid. Scale bar = 50 μm. e) Fluorescence intensity measured on four different zones of each hydrogel. bis = N,N'-methylene-bis-acrylamide, AA = acrylic acid.

Finally, Figure 7.4, that presents cross-sectional images of a hydrogel functionalized with the BMP-2 mimetic peptide (Figure 7.4a) or with collagen (Figure 7.4b), shows that the biomolecules are located on the surface of the gel. This result is consistent with the literature, as the functionalization protocol used has already been shown to functionalize only the surface of polyacrylamide gels.[69] By using the calibration curve presented in Figure 7.2 and following the same method than for the BMP-2 peptide (presented in chapter 6), the density of collagen on the surface of the hydrogels has been estimated around 1.5 ± 0.7 μg.cm^{-2}, or 8 ± 3 pmol.cm^{-2} (5 molecules per μm^2). Given the information provided by the supplier of the collagen (Sigma), a molecular weight of 175,000 g/mol has been considered for the estimation of the collagen surface density. The collagen density found on the hydrogels (1.5 ± 0.7 μg.cm^{-2}) is consistent with the data provided by the supplier which indicates a surface coverage of 6 to 10 μg.cm^{-2} on plastic culture plates. Finally, the estimated collagen surface density (8 ± 3 pmol.cm^{-2}) is lower than the estimated BMP-2 peptide surface density (chapter 6) that was comprised between 1.5 ± 0.7 and 2.0 ± 0.5 pmol.mm^{-2}. This is probably due to the significantly higher size of collagen (175.000 g/mol) compared to the BMP-2 peptide (2.500 g/mol). Using similar protocols for collagen and fibronectin grafting on polyacrylamide hydrogels, Engler et al. reported a collagen density between 0.25 and 1 μg.cm^{-2}[52], while Sun et al. obtained a fibronectin density of 1 μg.cm^{-2}[232], which is consistent with our estimated density.

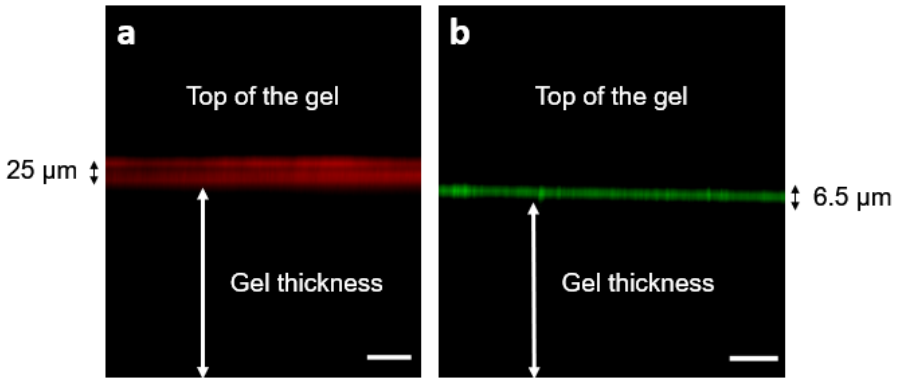

FIGURE 7.4 – Confocal microscopy images of the cross-sectional view of a hydrogel functionalized with a) a fluorescent BMP-2-TAMRA mimetic peptide or with b) type I collagen with subsequent immunofluorescent staining. Scale bar = 50 μm. The biomolecules are located at the surface of the gel.

Preliminary cell culture experiment As a preliminary study, one hydrogel has been selected, with a stiffness of 80 kPa and a relaxation of 40%, and has been functionalized with either the BMP-2 mimetic peptide (10^{-3} M) or with type I collagen (0.05 mg/mL). Then, hMSCs have been cultured on these hydrogels for two weeks in Osteogenic Differentiation medium to study the impact of hydrogel biofunctionalization on MSCs osteogenic differentiation. The cells have been stained with phalloidin to visualize cell cytoskeleton. Figure 7.5 shows that the cells on

tissue culture polystyrene (Figure 7.5a) and on a gel functionalized with the BMP-2 peptide (Figure 7.5b) are very similar. They are highly spread and present a cuboidal morphology similar to osteoblasts.[23, 98, 99] While the cells on the hydrogel functionalized with collagen (Figure 7.5c) seem to be smaller and more elongated. In addition, the cells are confluent for the BMP-2 functionalization, while they are not confluent for the collagen functionalization.

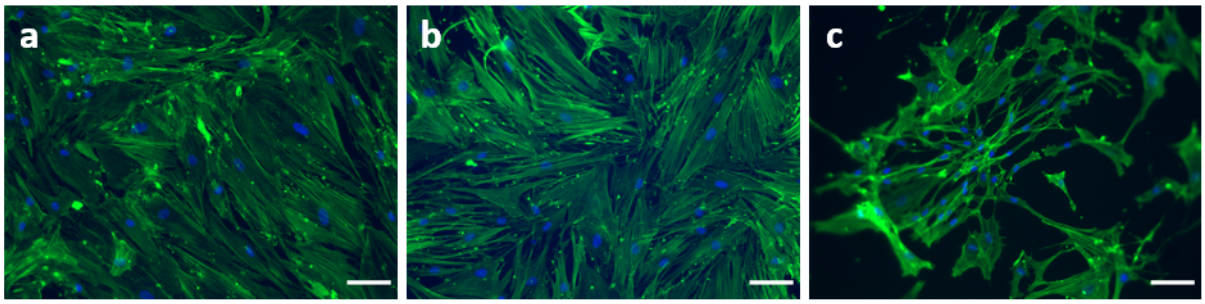

FIGURE 7.5 – Epifluorescence microscopy images of cytoskeleton and cell morphology in response to hydrogels biofunctionalization. Phalloidin staining of the cytoskeletal fibers of human bone marrow MSCs cultured for two weeks in Osteogenic Differentiation medium on a) tissue culture polystyrene, or on a poly(acrylamide-co-acrylic acid) hydrogel with a stiffness of 80 kPa and a relaxation of 40% functionalized with b) a BMP-2 mimetic peptide, or c) type I collagen. Nucleus in blue. Magnification 10x. Scale bar = 100 μm.

Considering the immunofluorescence labelling of four differentiation markers, osteopontin (OPN) expressed by both osteoblasts and osteocytes[329, 333], E11 and DMP1 expressed by early osteocytes[5], and sclerostin (SOST) expressed by late osteocytes[5], it can be seen on Figure 7.6 that the expression of these markers is dramatically higher when the gel is functionalized with the BMP-2 peptide as compared to collagen. These results are consistent with the studies conducted by previous students that demonstrated that MSCs osteogenic differentiation was higher for surfaces functionalized with the BMP-2 mimetic peptide as compared to a cell adhesion peptide GRGDS.[84, 85] It can be noticed that, although the cells are confluent on the surface of the hydrogels and do not present an osteocyte-like morphology, the cells express osteocyte markers. This is consistent with the fact that osteoblasts have been found to express E11, DMP1, and SOST, in the chapter 6. However, the results presented in Figure 7.6 should be compared with controls, such as non differentiated MSCs, MSCs in osteogenic culture medium, and osteoblasts. Nevertheless, these preliminary results clearly show that the expression of OPN, E11, DMP1, and SOST is higher for hydrogels functionalized with the BMP-2 mimetic peptide compared to type I collagen.

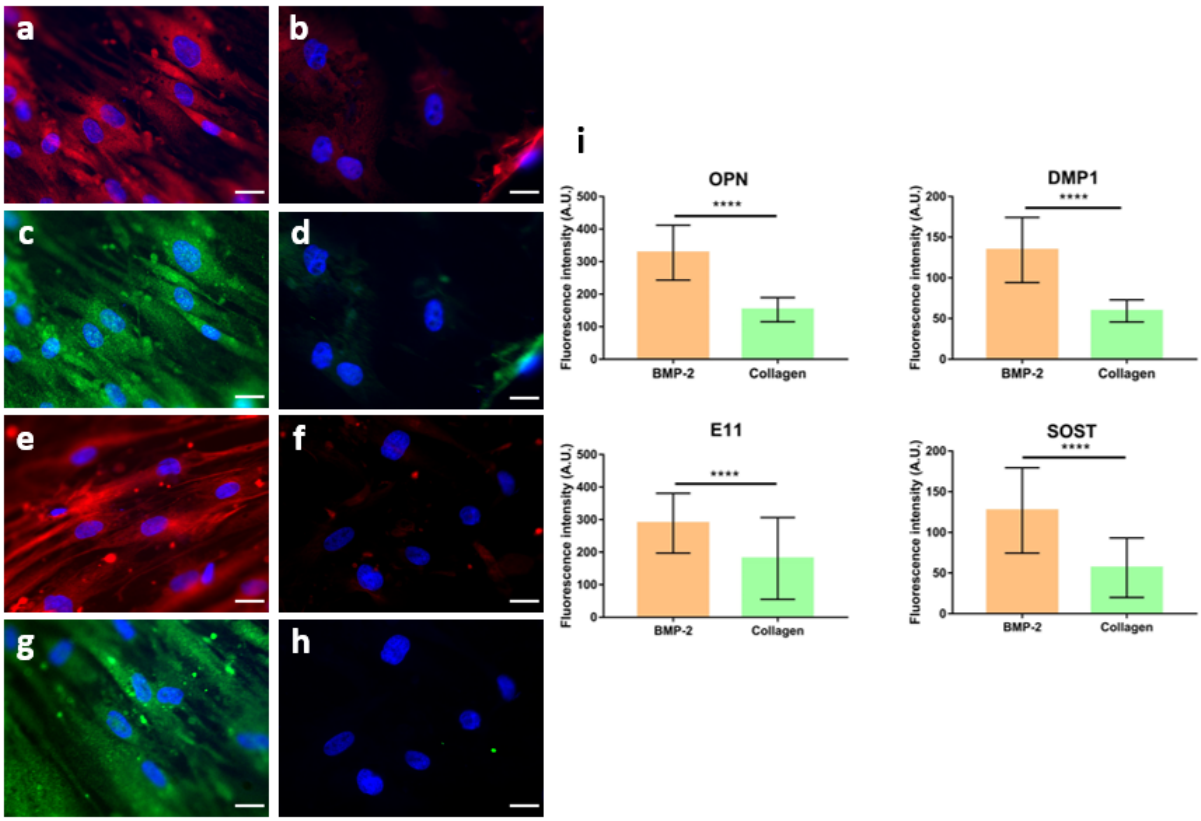

FIGURE 7.6 – Osteogenic commitment of MSCs in response to hydrogels biofunctionalization. Epifluorescence microscopy images of MSCs cultured on a poly(acrylamide-co-acrylic acid) hydrogel with a stiffness of 80 kPa and a relaxation of 40% functionalized with (a, c, e, g) a BMP-2 mimetic peptide, or (b, d, f, h) type I collagen. Cells were stained for (a, b) osteopontin, (c, d) DMP-1, (e, f) E11, and (g, h) sclerostin. Nucleus in blue. Magnification 40x. Scale bar = 25 μm. (i) Quantitative analysis of the immunofluorescence intensity of osteopontin (OPN), DMP-1, E11, and sclerostin (SOST) in hMSCs cultured on hydrogels functionalized with a BMP-2 mimetic peptide or with type I collagen. (n=2) The expression of all the markers is dramatically higher for cells on the hydrogels functionalized with the BMP-2 mimetic peptide. (**** $P < 0.0001$)

However, considering the difference in surface density which has been ascertained between the BMP-2 peptide and collagen, it is difficult to determine whether the different expression level of the osteogenic markers is related to the presence of different biomolecules, or to the difference in biomolecules density, or both. Indeed, it is acknowledged that the biomolecules density can affect cell spreading[377, 378] and differentiation[257, 263]. Moreover, comparing the surface density bewteen the BMP-2 peptide and collagen is maybe not relevant as one peptide molecule is carrying one bioactive sequence able to interact with the cells, while one collagen molecule is carrying several bioactive sequences. In addition, collagen can carry different bioactive sequences, including RGD, GFOGER, and DGEA[1, 279, 280], that could lead to different interactions with the cells and might trigger different cellular responses. As such, it might be interesting to compare the number of available bioactive sites on surfaces

functionalized with the BMP-2 peptide or with collagen, instead of comparing the biolomecules density. Finally, one peptide molecule is likely to form one covalent bond with sulfo-SANPAH on the surface of the gels, while one collagen molecule is carrying several free amine groups that are susceptible to react with Sulfo-SANPAH molecules on the surface of the gels. In other words, one peptide molecule has one anchoring point to the matrix, while one collagen molecule has multiple anchoring points to the matrix. It has been demonstrated by Trappmann et al. that varying the number of anchoring points of collagen to the matrix modifies the way that cells feel the mechanical properties of the underlying substrate.[55] Indeed, polyacrylamide substrates of the same stiffness (20 kPa), but with collagen covalently attached using different concentrations of sulfo-SANPAH, induced different responses in cells, with lower sulfo-SANPAH concentration leading to cell behavior typically found on softer gels.[55] Therefore, depending on the number of anchoring points of collagen to the matrix, the cells might feel different mechanical properties between the hydrogels functionalized with the BMP-2 peptide or with collagen. As a result, comparing the impact of two peptides with a similar molecular weight and a similar surface density on cell behavior might be more appropriate than comparing the effect of a peptide and a large protein. Nevertheless, the results presented here clearly demonstrate the higher capacity of the peptide to direct MSCs osteogenic differentiation as compared to collagen, and confirm that this peptide is a good candidate to accelerate MSCs osteogenic differentiation.

For future experiments, it might also be interesting to evaluate the surface mechanical properties of hydrogels functionalized with collagen by using AFM, as performed for the BMP-2 peptide in chapter 6, to see if collagen could alter the surface stiffness and stress relaxation of hydrogels, as it is a large molecule (around 175,000 g/mol), as compared to the BMP-2 peptide which is much smaller (around 2,500 g/mol). In addition, considering that this preliminary experiment has been conducted with a high initial cell seeding density of 10,000 cells/cm^2, it would be interesting to repeat the experiment with the same seeding density than in chapters 5 and 6 (3,000 cells/cm^2) to see if osteocyte-like cells could be obtained for hydrogels functionalized with collagen. Indeed, while it is mentioned in the chapter 2 that MSCs seeding density might influence their differentiation into osteoblasts, this parameter might also alter their differentiation into osteocytes. For example, it has been shown that the differentiation of mouse pre-osteoblasts into osteocytes was favored for a low seeding density of 1,000 cells/cm^2, compared to a high seeding density of 10,000 cells/cm^2.[332] To explain this result, it has been hypothesized that a high seeding density allows cell communication by direct contact, while a low seeding density restricts cell communication and drives the cells to develop dentrites to communicate, which favors a differentiation into osteocytes.[332]

Conclusions and perspectives

This PhD work aims at identifying some promising material surface properties, such as surface mechanical properties and surface functionalization, for the control of mesenchymal stem cells osteogenic differentiation, in order to provide some tools for the design of effective materials to promote bone regeneration. The innovative aspect of this work is based on three main points : the design of hydrogels with controlled viscoelastic properties and the evaluation of the impact of these viscoelastic properties on MSCs osteogenic differentiation, the measurement of hydrogels mechanical properties at different length scales using compression and AFM, and the combination of the BMP-2 mimetic peptide to hydrogels that better mimic the natural cell growth environment than the materials previoulsy used in the team.

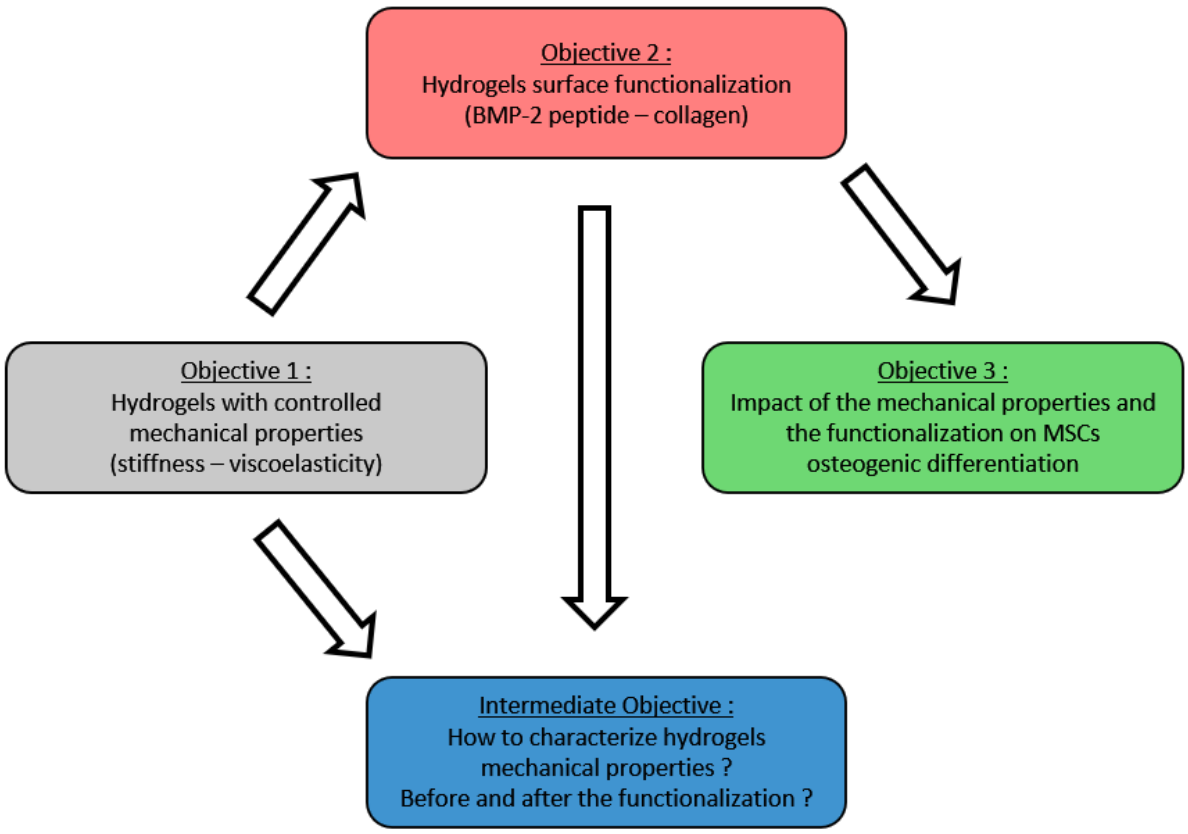

FIGURE 7.7 – Scheme describing the main objectives of the PhD project.

Regarding the design of hydrogels with controlled mechanical properties :

As previously mentioned, polyacrylamide based hydrogels have been chosen for this project considering their ease of synthesis and their highly tunable stiffness.[35, 36] Then, acrylamide has been combined to acrylic acid to create copolymer hydrogels with distinct viscoelastic properties. Indeed, it has been shown that associating acrylic acid to acrylamide to create copolymer hydrogels was a relatively easy way to provide hydrogels with different and controlled viscoelastic responses, to further study their impact on cell behavior. Nevertheless, these hydrogels also present some limitations, such as the lack of cell adhesion moieties, the covalent crosslinking that leads to hydrogels that remain highly elastic, and the inability to grow the cells in 3 dimensions.

The problem of the lack of cell adhesion moieties can be solved by functionalizing the surface of the hydrogel with varying biomolecules, including peptides and proteins, although it might affect the surface properties of the hydrogel as shown in chapter 6.

It is generally recognized that the covalent crosslinking of hydrogels leads to elastic substrates, while the ionic crosslinking of hydrogels leads to viscoelastic substrates.[68, 95, 100, 362] Indeed, the ionic crosslinking of alginate with divalent cations is often performed to obtain viscoelastic substrates, as ionic crosslinks are reversible, and can unbind and rebind when stresses are applied to the hydrogels.[95] Nevertheless, ionic crosslinking is not the only method to modulate hydrogels viscoelastic properties, as Cameron et al. entrapped linear polyacrylamide into covalently crosslinked polyacrylamide hydrogels to modulate hydrogels viscous modulus.[67] In addition, this PhD project demonstrated that stress relaxing hydrogels could be obtained from covalently crosslinked and mainly elastic polyacrylamide based hydrogels, thanks to the copolymerization of acrylamide with acrylic acid. The hydrogels used in this project are therefore particularly interesting for mechanobiology studies, as the covalent crosslinking enables to obtain a wide range of stiffnesses (1 kPa to hundreds of kPa) and to fine tune hydrogels stiffness by varying the amount of crosslinker, while the ratio between acrylamide and acrylic acid modulates hydrogels stress relaxation, although these parameters are not completely independent so that varying the ratio between the two monomers also affects the stiffness. The covalent crosslinking also provides more stability and structural integrity than ionic crosslinking, when placed in contact with biological fluids.[379] Considering that acrylic acid has been incorporated into the hydrogels with a concentration from 5 to 18 mol%, it might be interesting to further increase the acrylic acid content in the hydrogels to evaluate whether it might lead to a further increase of hydrogels stress relaxation.

Finally, because of the toxicity of the monomers, this hydrogel system does not allow cell encapsulation[35], which might be a limitation for the study of cell behavior considering that 3D cell culture is recognized as better mimicking in vivo cellular behavior[380]. Moreover, 3D bioprinting of cell laden hydrogels is also a growing research topic as it has raised hopes in regenerative medicine by enabling the design of structurally complex scaffolds for tissue regeneration.[379] Nevertheless, studying and optimizing cell-material interactions in 2 dimensions is also necessary in order to improve the performance of the existing bone implants, such as metallic and polymeric implants, whose surface is expected to interact with bone tissue. Furthermore, it has been shown in chapter 6 that MSCs seem to differentiate towards osteocytes on the surface of the hydrogels, although it is surprising as osteocytes are known to evolve within a 3D environment in vivo, as they are embedded within bone.[2, 4, 23] Indeed, osteocytes culture and differentiation from osteoblasts is generally performed in 3 dimensions.[98, 155, 369, 381, 382] Recently, Sawa et al. demonstrated that switching osteoblasts from a 2D to a 3D environment led to their differentiation towards osteocytes, while they regained osteoblast characteristics when they were switched back to a 2D environment.[368] Nevertheless, osteocyte differentiation from osteoblasts has been achieved in 2 dimensions in another study by decreasing the initial cell seeding density.[332] Therefore, it is still not clear to what extent osteoblast-to-osteocyte differentiation can be modulated by the biomaterials properties, by the dimensionality of the system, and by the culture conditions, and this is even less clear for MSC-to-osteocyte differentiation. Thus, this PhD project paves the way for a deeper understanding of MSCs commitment towards osteocytes through cell-material interactions.

Regarding hydrogels surface functionalization and the impact on MSCs osteogenic differentiation :

In this project, the hydrogels have been functionalized with a mimetic peptide of the BMP-2 protein[83] for the evaluation of the impact of hydrogels mechanical properties on MSCs osteogenic differentiation, as this peptide has been found to promote MSCs osteogenic differentiation on many different materials. In addition, considering that polyacrylamide hydrogels are generally functionalized with type I collagen to evaluate the impact of hydrogels stiffness on MSCs differentiation, preliminary experiments have been conducted with collagen to evaluate MSCs differentiation depending on hydrogels biofunctionalization (BMP-2 mimetic peptide versus type I collagen).

Type I collagen and the BMP-2 mimetic peptide have been covalently immobilized on the surface of the hydrogels via the linker Sulfo-SANPAH. This step is crucial to evaluate the impact of hydrogels mechanical properties on cell behavior as the cells will exert mechanical forces on the substrate-bound proteins or peptides, and will therefore undirectly exert forces

on the underlying matrix because of the covalent bonds between the matrix and the proteins or peptides.[55] The covalent grafting of the two biomolecules has been confirmed by using a fluorescent peptide or by performing an immunostaining of collagen, and by showing that the fluorescence intensity of hydrogels with absorbed molecules (so without activation of the gel) was much lower than the fluorescence intensity of hydrogels with grafted molecules (so with activation of the gel). In addition to these characterizations, chemical analysis have been performed on the virgin and the functionalized hydrogels, including X-ray photoelectron spectrometry (XPS) and infrared and Raman spectroscopy, in order to confirm the covalent grafting of the biomolecules. Nevertheless, the chemical composition of the biomolecules being very similar to the composition of the gel, it was impossible to assess the covalent grafting by using these techniques. In addition, this required drying the hydrogels, which can deform the hydrogel samples and affect the distribution of the biomolecules on the surface of the gels, that may no longer be detectable.

Regarding the impact of hydrogels biofunctionalization on MSCs osteogenic differentiation, it has been demonstrated in chapter 7 that the BMP-2 mimetic peptide led to a higher expression of osteoblast and osteocyte markers than type I collagen. This was expected as this peptide has been specifically chosen for its capability to enhance MSCs osteogenic differentiation. Nevertheless, it has been shown that the collagen surface density was lower than the peptide surface density, which might make it difficult to compare the effects of these two biomolecules on MSCs behavior. In addition, considering that one peptide molecule is carrying one bioactive sequence able to interact with the cells, while one collagen molecule is carrying several bioactive sequences, it might be more appropriate to compare the density of available bioactive sites instead of comparing the biomolecules density. Finally, comparing the impact of two peptides with a similar molecular weight and a similar surface density on cell behavior might be more appropriate than comparing the effect of a peptide and a large protein. This BMP-2 mimetic peptide could be compared to other osteogenic peptides, such as OGP and P15, or to cell adhesion peptides, such as RGD. Moreover, it might be interesting to combine several peptides on the surface of the hydrogels as it could provide synergistic effects, such as the combination of RGD and the BMP-2 peptide that has been found to enhance MSCs osteogenic differentiation.[84]

While the peptide[257, 263, 377] or protein[383] surface density is known to modulate MSCs adhesion and differentiation, the BMP-2 peptide concentration has been adjusted in chapter 6 in order to obtain a similar peptide density on the five different hydrogel formulations. This enables to ensure that differences in cell behavior on the different hydrogels can not be attributed to differences in peptide surface density. However, it can be noticed that MSCs differentiation in response to hydrogels mechanical properties is different between chapter 5 and chapter 6. Indeed, in chapter 5, the highly stress relaxing hydrogel did not promote the

osteocyte morphology observed in chapter 6. The peptide surface density has been evaluated in chapter 5 and it has been found that the peptide density on the high relaxing gel was the double of the peptide density on the low relaxing gel. Nevertheless, it has been considered that the peptide density obtained by fluorescence measurements was an estimation and that is was of the same order of magnitude on the two hydrogels. Indeed, it was not expected that a 2-fold difference in peptide density might affect MSCs behavior. The different results obtained in chapters 5 and 6 tend to show that the higher peptide density on the high relaxing gel in chapter 5 promoted higher cell adhesion, which resulted in a higher initial cell seeding density compared to the low relaxing gel, responsible for the different cell shape and E11 expression on the two hydrogels. This hypothesis would confirm that the lower cell adhesion on the low relaxing gel, which results in intercellular separation, would drive the cells to develop dentrites to communicate and would therefore favor MSCs differentiation towards osteocytes, while the higher cell adhesion on the high relaxing gel allows cell communication by direct contact, leading to MSCs differentiation towards osteoblasts.[332] Consequently, it might be interesting to evaluate the impact of varying peptide density and varying cell seeding density on MSCs osteogenic differentiation, and to assess whether these two parameters have similar effects.

Finally, while the BMP-2 peptide and collagen have been homogeneously distributed on the surface of the hydrogels in this project, it might be interesting to investigate the impact of the spatial distribution of these biomolecules on MSCs osteogenic differentiation. Indeed, several studies have shown that varying the micro-scale distribution of peptides by making geometric patterns with different sizes and shapes might significantly enhance MSCs osteogenic differentiation on rigid materials.[102, 103, 104] In addition, the spatial distribution of biomolecules has also been shown to influence MSCs behavior on hydrogels, as discussed in chapter 3. Nevertheless, these patterns are generally obtained by photolithography[102, 103, 104] or soft-lithography[384] (Figure 7.8) which are complex and long procedures, and which are only suitable for the patterning of 2D substrates.[385] In addition, the patterns produced using these two methods are generally very organized patterns with periodic repetition, which is not necessarily the best configuration to represent cells natural environment. Indeed, Dalby et al. showed that more randomly distributed patterns had a higher potential to direct MSCs osteogenic differentiation than organized patterns.[192] In this context, the LIS laboratory (Québec) developped a micropatterning method with aerosols.[386, 387, 388] This method enables to create circular patterns with a random distribution but with controlled diameter and surface coverage (Figure 7.8c), and it can be used on many different materials, including 3D materials. Therefore, it might be interesting to use this technique to create biomolecules patterns on the surface of the hydrogels and to evaluate the impact on MSCs osteogenic differentiation.

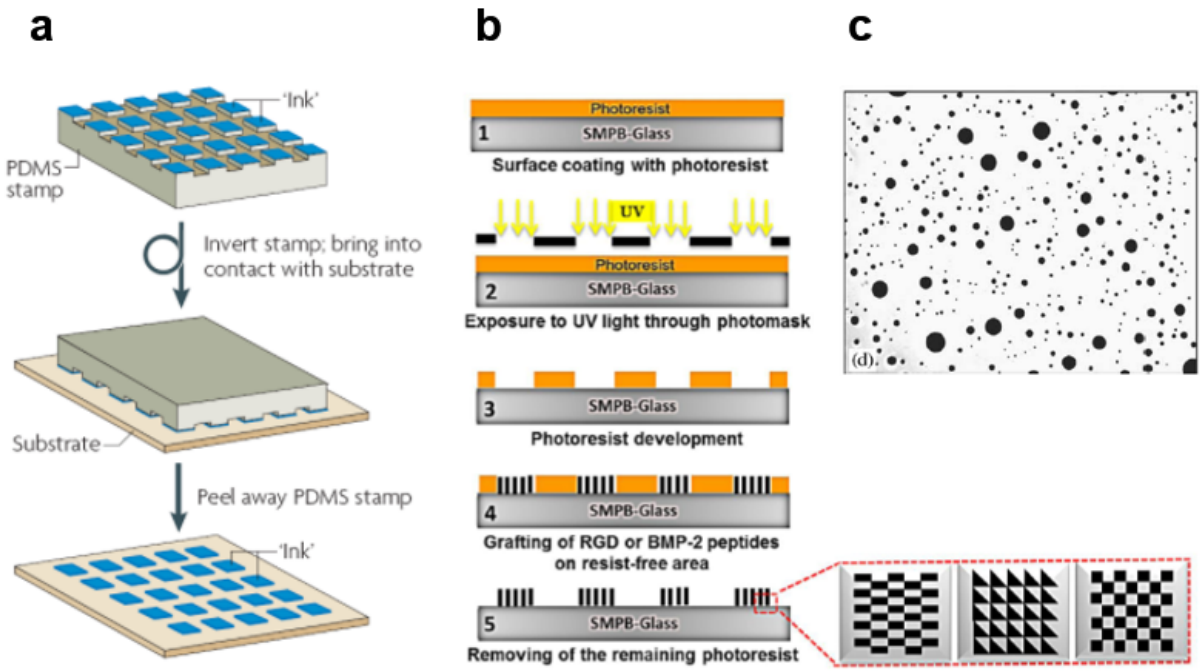

FIGURE 7.8 – a) Schematic representation of soft-lithography. b) Schematic representation of peptide micropatterning onto glass surfaces using photolithography technique. From [103]. c) Example of peptide patterning of a polytetrafluoroethylene surface using aerosols. From [387]

Regarding the characterization of hydrogels mechanical properties :

As previously mentioned, hydrogels being multi-phase materials composed of a solid phase together with a liquid phase, the characterization and modelling of their mechanical properties is still a challenging task. Considering that compression and AFM are the most widely used methods to measure hydrogels stiffness in studies evaluating the impact of the stiffness on MSCs differentiation, these two methods have been chosen in this project to characterize hydrogels mechanical properties. It has been shown that AFM was sensitive to variations in surface stiffness caused by hydrogels surface functionalization, while compression did not allow to measure these variations. In addition, it has been shown, for the first time, that there was no effect of the surface functionalization with the peptide on the microscopic viscoelastic properties of our hydrogels measured using AFM, although this still requires further investigation in order to understand hydrogels response to micro-scale sollicitations. Indeed, this would be particularly interesting as it would provide a complete study, not only about cell response to hydrogel mechanical properties, but also about hydrogels response to micro-scale sollicitations that can be exerted by cells, providing new insight on cell-material interactions. Moreover, it would be particularly interesting to perform the same study on hydrogels functionalized with type I collagen. Indeed, many studies use type I collagen for hydrogels surface functionalization but only measure the bulk mechanical properties of the

hydrogels, while collagen being a large molecule, it is susceptible to modify hydrogels surface mechanical properties, possibly because of weak interactions between the collagen molecules such as hydrogen bonding, and/or because of collagen molecules entanglement.
The results presented in this work indicate that compression does not seem to be the most suitable technique to evaluate the mechanical properties that the cells will feel on the surface of the hydrogels, although it is challenging to find the technique that will perfectly represent what the cells will feel. Indeed, considering that the cells would be able to feel hydrogels mechanical properties up to 5 μm deep, the length scale of compression measurements might be too high (hundreds of μm to several mm), while the length scale of AFM measurements might be too low (hundreds of nm). Nevertheless, there still does not seem to be a perfect answer to this problematic yet. In addition, the choice of the technique might also depend on the dimensionality of the system in the sense that it might be more relevant to measure hydrogels bulk mechanical properties using compression when the cells are cultivated in 3 dimensions and are encapsulated within the hydrogel, while it might make more sense to measure hydrogels surface mechanical properties using AFM when the cells are cultivated in 2 dimensions.

Regarding the impact of hydrogels mechanical properties on MSCs osteogenic differentiation :

This study allows to go further than the literature in the assessment of the impact of hydrogels mechanical properties on MSCs osteogenic differentiation by including both hydrogels stiffness and stress relaxation. It has been found that our combination of hydrogels with a stiffness between 60 and 140 kPa and a relaxation between 15% and 70%, the BMP-2 mimetic peptide, osteogenic culture medium, and low cell seeding density, led to the major achievement of obtaining a dentritic morphology on 2D substrates. In addition, the expression of three osteocyte markers (E11, DMP1, sclerostin) has been evaluated using immunofluorescence, which is very rare in the literature, and revealed that a stiffness of 60 kPa promoted a higher expression of these markers after 24 hours and 2 weeks, as compared to stiffnesses of 15 kPa and 140 kPa, for a constant relaxation around 15%. Then, the hydrogel with a stiffness of 140 kPa and the highest relaxation (70%) promoted the highest expression of osteocyte markers after 2 weeks, which suggests that hydrogels stress relaxation has a major impact on MSCs differentiation towards osteocytes, which may be stronger than that of the stiffness, as a high viscoelasticity seems to favor MSCs osteogenic differentiation even if it is associated with a stiffness that is not the most favorable. Considering that the hydrogel 140 kPa-15% led to a lower expression of osteocyte markers compared to the hydrogels 15 kPa-15% and 60 kPa-15%, it would be interesting to evaluate the impact of hydrogels stress relaxation on MSCs osteogenic differentiation for stiffnesses of 15 and 60 kPa, with the hypothesis that the best results would be obtained for a stiffness of 60 kPa and a high relaxation.
In addition to the evaluation of MSCs osteogenic differentiation using immunofluorescence,

other techniques could be used to confirm the results, such as qPCR, although this technique generally requires a high amount of cells, which might be an issue in our case as the cell seeding density is low. Other differentiation markers could also be investigated, such as bone sialoprotein, collagen type I, and alkaline phosphatase, as their expression is supposed to be down-regulated during the transition towards osteocytes.[327, 329] This could provide additional evidence of cell commitment towards osteocytes. Finally, comparing the level of expression of osteocyte markers for MSCs on our hydrogels to the level of expression of these markers for osteocytes would also be particularly interesting to determine whether cells are closer to early or mature osteocytes. Nevertheless, the in vitro study of osteocytes is still challenging as isolating osteocytes from bone is a complex process, leading to very low yields, high cell heterogeneity, and cells that may not express markers normally found in osteocytes, such as sclerostin.[155, 156]
Finally, it might be interesting to investigate the mechanotransduction pathways through which MSCs are capable of sensing hydrogels mechanical properties, and particularly their stress relaxation. Indeed, different pathways would be involved in MSCs response to hydrogels stiffness, such as YAP/TAZ signaling, Rho/ROCK signaling, and MAPK signaling for example.[389] As such, it would be interesting to evaluate whether these pathways are also involved in MSCs response to hydrogels stress relaxation.

The experimental conditions chosen for the cell culture experiments are important parameters to discuss as they can greatly influence MSCs differentiation. First, all the experiments have been conducted with Osteogenic differentiation medium in order to favor and accelerate MSCs osteogenic differentiation, and to be able to obtain an osteogenic commitment over relatively short time periods. It might be interesting to assess whether MSCs could differentiate towards osteocytes without osteogenic supplements, and to assess how long it would take. Regarding the cells, many parameters could be varied in order to investigate their impact on MSCs differentiation towards osteocytes. As mentioned in chapter 2, the number of cell passages is likely to affect MSCs differentiation potential. In this project, the cells have always been used from the same donor and at low number of passages (passage 4 or 5) to preserve MSCs differentiation potential and to ensure the reproducibility of the results. As previously discussed, the cell seeding density is an important parameter to consider. It is likely that the low cell seeding density used in this project (3,000 cells/cm^2) favored MSCs differentiation towards osteocytes, although it would be interesting to confirm this hypothesis. Nevertheless, although this parameter probably influenced MSCs fate, it does not mean that lowering the cell seeding density on any material would result in MSCs differentiation towards osteocytes. Indeed, the osteocyte-like shape observed in this study is probably the result of the combination of several parameters, and it might be particularly interesting to determine which of these parameters are essential to obtain these osteocyte-like cells. This would allow to gain knowledge about MSCs differentiation towards osteocytes, which is still a relatively

unknown process. Finally, as presented in chapter 2, several studies highlighted that MSCs proliferation and differentiation could be affected by the age of the donor, with MSCs losing their osteogenic differentiation potential due to increasing donor age.[172] Therefore, it might be surprising to have obtained osteocyte-like cells from a 65-years old donor, and it might be interesting to repeat the experiments with cells from another donor to assess whether osteocyte-like cells could be obtained under the same conditions. The use of MSCs from a younger donor might even reduce the inhomogeneity of the osteogenic differentiation markers expression that has been observed in chapter 6, as it has been demonstrated by our team that the population of cells from an old donor (65 years old) exhibited a more heterogeneous expression of osteogenic differentiation markers than cells from a young donor (36 years old).[105] Finally, as highlighted in chapter 2, the application of stimuli, such as hypoxia or mechanical loading, can also modulate MSCs behavior. Considering that osteocytes reside within a low oxygen microenvironment[390], it might be interesting to investigate whether hypoxia could favor MSCs differentiation towards osteocytes under the same conditions than in chapter 6. In addition, osteocytes being sensitive to mechanical stress applied on bones[2, 4, 23, 28], it might be interesting to assess the impact of a mechanical sollicitation of the hydrogel on MSCs differentiation towards osteocytes.

Regarding the impact of the system for bone regeneration :

Regarding the impact of this work for bone regeneration, it is unlikely that the hydrogels used in this project might be used as bone substitutes as their mechanical properties are far from that of bone, they do not provide a 3D environment, and they are not resorbable. Nevertheless, it could be considered to apply these hydrogels as a coating on metallic and polymeric implants. Indeed, this coating would be able to interact with bone cells and would potentially promote bone growth around the prosthesis, which would therefore be well integrated within the bone and would avoid the formation of a fibrous tissue around the implant. The formation of this capsule of fibrous tissue is particularly problematic with current implants as it can provoke interfacial micromovements that might result in the failure of the prosthesis.[8] In addition, because these hydrogels are not resorbable, the implant would not loose its coating over time.
The hydrogels developed in this work are also particularly interesting for fundamental studies about the understanding of the processes of MSCs osteogenic differentiation. Indeed, being able to control MSCs differentiation would be a major step forward for the development of effective strategies for tissue engineering and regenerative medicine. In addition, this work might provide a deeper knowledge about MSCs transition towards osteocytes, which is still lacking today. Finally, this hydrogel system might be used as an in vitro cell culture platform that would allow to obtain osteoblasts or osteocytes from MSCs differentiation in a fast and reproducible way. Subsequently, these osteoblasts or osteocytes might be used for implantation or for other in vitro and in vivo studies.

Bibliography

[1] Wenhao Wang and Kelvin W.K. Yeung. Bone grafts and biomaterials substitutes for bone defect repair : A review. *Bioactive Materials*, 2 :224–247, 2017.

[2] Stuart H Ralston. Bone structure and metabolism. *Medicine*, 41 :581–585, 2017.

[3] Marina Panek, Inga Marijanović, and Alan Ivković. Stem cells in bone regeneration. *Periodicum Biologorum*, 117 :177–184, 2015.

[4] Delphine Spruyt, Céline Gillet, and Joanne Rasschaert. Bone and Bone Marrow, Interactions. *Encyclopedia of Endocrine Diseases, 2nd Edition*, 4 :31–39, 2019.

[5] Sarah L Dallas, Matthew Prideaux, and Lynda F Bonewald. The Osteocyte : An Endocrine Cell and More. *Endocrine Reviews*, 34 :658–690, 2013.

[6] Lynda F Bonewald. The Amazing Osteocyte. *Journal of Bone and Mineral Research*, 26 :229–238, 2011.

[7] David C Lobb, Brent R Degeorge Jr, and A Bobby Chhabra. Bone Graft Substitutes : Current Concepts and Future Expectations. *Journal of Hand Surgery*, 44 :497–505, 2019.

[8] Maria Vallet-Regi and Antonio J Salinas. Ceramics as bone repair materials. In *Bone Repair Biomaterials*, pages 141–178. Woodhead Publishing, 2019.

[9] Maria-Pau Ginebra, Montserrat Espanol, Yassine Maazouz, Victor Bergez, and David Pastorino. Bioceramics and bone healing. *EFORT Open Reviews*, 3 :173–183, 2018.

[10] Shayesteh Narges Moghaddam, Taheri Mohsen Andani, Amirhesam Amerinatanzi, Christoph Haberland, Scott Huff, Michael Miller, Mohammad Elahinia, and David Dean. Metals for bone implants : safety, design, and efficacy. *Biomanufacturing Reviews*, 1 :1–16, 2016.

[11] Qizhi Chen and George A Thouas. Metallic implant biomaterials. *Materials Science & Engineering R*, 87 :1–57, 2015.

[12] Mônica Rufino Senra and Maria de Fatima Vieira Marques. Synthetic Polymeric Materials for Bone Replacement. *Journal of Composite Science*, 4 :191, 2020.

[13] Shuai Wei, Jian-Xiong Ma, Lai Xu, Xiao-Song Gu, and Xin-Long Ma. Biodegradable materials for bone defect repair. *Military Medical Research*, 7 :1–25, 2020.

[14] Valentina Devescovi, Elisa Leonardi, Gabriela Ciapetti, and Elisabetta Cenni. Growth factors in bone repair. *La Chirurgia degli organi di movimento*, 92 :161–168, 2008.

[15] Jian Yang, Pujie Shi, Maolin Tu, Yun Wang, Meng Liu, Fengjiao Fan, and Ming Du. Bone morphogenetic proteins : Relationship between molecular structure and their osteogenic activity. *Food Science and Human Wellness 3*, 3 :127–135, 2014.

[16] Gopal Shankar Krishnakumar, Alice Roffi, Davide Reale, Elizaveta Kon, and Giuseppe Filardo. Clinical application of bone morphogenetic proteins for bone healing : a systematic review. *International Orthopaedics*, 41 :1073–1083, 2017.

[17] Aaron W James, Gregory Lachaud, Jia Shen, Greg Asatrian, Vi Nguyen, Xinli Zhang, Kang Ting, and Chia Soo. A Review of the Clinical Side Effects of Bone Morphogenetic Protein-2. *Tissue Engineering Part A*, 22 :284–297, 2016.

[18] Maria Rosa Iaquinta, Elisa Mazzoni, Marco Manfrini, Antonio D'Agostino, Lorenzo Trevisiol, Riccardo Nocini, Leonardo Trombelli, Giovanni Barbanti-Brodano, Fernanda Martini, and Mauro Tognon. Innovative Biomaterials for Bone Regrowth. *International Journal of Molecular Sciences*, 20 :618, 2019.

[19] Huawei Qu, Hongya Fu, Zhenyu Han, and Yang Sun. Biomaterials for bone tissue engineering scaffolds : a review. *RSC Advances*, 9 :26252, 2019.

[20] Jose R Perez, Dimitrios Kouroupis, Deborah J Li, Thomas M Best, Lee Kaplan, and Diego Correa. Tissue Engineering and Cell-Based Therapies for Fractures and Bone Defects. *Frontiers in Bioengineering and Biotechnology*, 6 :105, 2018.

[21] Monia Orciani, Milena Fini, Roberto Di Primio, and Monica Mattioli-Belmonte. Biofabrication and Bone Tissue Regeneration : Cell Source, Approaches, and Challenges. *Frontiers in Bioengineering and Biotechnology*, 5 :17, 2017.

[22] Mojtaba Ansari. Bone tissue regeneration : biology, strategies and interface studies. *Progress in Biomaterials*, 8 :223–237, 2019.

[23] Asha Rupani, Richard Balint, and Sarah H Cartmell. Osteoblasts and their applications in bone tissue engineering. *Cell Health and Cytoskeleton*, 4 :49–61, 2012.

[24] Wasim S Khan, Faizal Rayan, Baljinder S Dhinsa, and David Marsh. An Osteoconductive, Osteinductive, and Osteogenic Tissue-Engineered Product for Trauma and Orthopaedic Surgery : How Far Are We ? *Stem Cells International*, 2012, 2012.

[25] Antonio Uccelli, Lorenzo Moretta, and Vito Pistoia. Mesenchymal stem cells in health and disease. *Nature Reviews Immunology*, 8 :726–736, 2008.

[26] Kourosch C Elahi, Gerd Klein, Meltem Avci-Adali, Karl D Sievert, Sheila MacNeil, and Wilhelm K Aicher. Human Mesenchymal Stromal Cells from Different Sources Diverge in Their Expression of Cell Surface Proteins and Display Distinct Differentiation Patterns. *Stem Cells International*, 2016 :1–9, 2016.

[27] M Noelle Knight and Kurt D Hankenson. Mesenchymal Stem Cells in Bone Regeneration. *Advances in Wound Care*, 2 :306–316, 2013.

[28] Andrea I Alford, Kenneth M Kozloff, and Kurt D Hankenson. Extracellular matrix networks in bone remodeling. *The International Journal of Biochemistry and Cell Biology*, 65 :20–31, 2015.

[29] Arantza Infante and Clara I Rodríguez. Osteogenesis and aging : lessons from mesenchymal stem cells. *Stem Cell Research & Therapy*, 2 :1–7, 2018.

[30] Shihua Wang, Pengchao Xu, Xiaoxia Li, Xiadong Su, Yunfei Chen, Wan Li, Linyuan Fan, Kan Yin, Yan Liu, and Robert Chunhua Zhao. Mesenchymal Stem Cells and Cell Therapy for Bone Repair. *Current Molecular Pharmacology*, 9 :289–299, 2016.

[31] Parisa Kangari, Tahereh Talaei-Khozani, Iman Razeghian-Jahromi, and Mahboobeh Razmkhah. Mesenchymal stem cells : amazing remedies for bone and cartilage defects. *Stem Cell Research & Therapy*, 11 :1–21, 2020.

[32] Phuc Van Pham. Mesenchymal Stem Cells in Clinical Applications. In *Stem Cell Processing*, pages 37–70. Springer, Cham, 2016.

[33] Nayoun Kim and Seok-goo Cho. Clinical applications of mesenchymal stem cells. *Korean Journal of Internal Medicine*, 28 :387–402, 2013.

[34] Yuan-zhe Jin and Jae Hyup Lee. Mesenchymal Stem Cell Therapy for Bone Regeneration. *Clinics in Orthopedic Surgery*, 10 :271–278, 2018.

[35] Steven R Caliari and Jason A Burdick. A practical guide to hydrogels for cell culture. *Nature Methods*, 13 :405–414, 2018.

[36] Yung-hao Tsou, Joe Khoneisser, Ping-chun Huang, and Xiaoyang Xu. Hydrogel as a bioactive material to regulate stem cell fate. *Bioactive Materials*, 1 :39–55, 2016.

[37] Desireé Alesa Gyles, Lorena Diniz Castro, José Otavio Carréra Jr Silva, and Roseane Maria Ribeiro-Costa. A review of the designs and prominent biomedical advances of natural and synthetic hydrogel formulations. *European Polymer Journal*, 88 :373–392, 2017.

[38] Mostafa Mahinroosta, Zohreh Jomeh Farsangi, Ali Allahverdi, and Zahra Shakoori. Hydrogels as intelligent materials : A brief review of synthesis, properties and applications. *Materials Today Chemistry*, 8 :42–55, 2018.

[39] J J Roberts and P J Martens. Engineering biosynthetic cell encapsulation systems. In *Biosynthetic Polymers for Medical Applications*, pages 205–239. Woodhead Publishing, 2016.

[40] Zhan Li, Yuanwei Gong, Shujin Sun, Yu Du, Dongyuan Lü, Xiaofeng Liu, and Mian Long. Differential regulation of stiffness, topography, and dimension of substrates in rat mesenchymal stem cells. *Biomaterials*, 34 :7616–7625, 2013.

[41] Yuhang Hu, Jin-oh You, and Joanna Aizenberg. Micropatterned Hydrogel Surface with High-Aspect-Ratio Features for Cell Guidance and Tissue Growth. *ACS Applied Materials and Interfaces*, 8 :21939–21945, 2016.

[42] Yong Hou, Leixiao Yu, Wenyan Xie, Luis Cuellar Camacho, Man Zhang, Zhiqin Chu, Qiang Wei, and Rainer Haag. Surface Roughness and Substrate Stiffness Synergize To Drive Cellular Mechanoresponse. *Nano Letters*, 20 :748–757, 2019.

[43] Christophe Merceron, Sophie Portron, Martial Masson, Julie Lesoeur, Borhane Hakim Fellah, Olivier Gauthier, Olivier Geffroy, Pierre Weiss, Jérôme Guicheux, and Claire Vinatier. The Effect of Two- and Three-Dimensional Cell Culture on the Chondrogenic Potential of Human Adipose-Derived Mesenchymal Stem Cells After Subcutaneous Transplantation With an Injectable Hydrogel. *Cell Transplantation*, 20 :1575–1588, 2011.

[44] Shyni Varghese, Nathaniel S Hwang, Adam C Canver, Parnduangji Theprungsirikul, Debora W Lin, and Jennifer Elisseeff. Chondroitin sulfate based niches for chondrogenic differentiation of mesenchymal stem cells. *Matrix Biology*, 27 :12–21, 2008.

[45] Li Zhang, Tun Yuan, Likun Guo, and Xingdong Zhang. An in vitro study of collagen hydrogel to induce the chondrogenic differentiation of mesenchymal stem cells. *Journal of Biomedical Materials Research - Part A*, 100 :2717–2725, 2012.

[46] L Zheng, H S Fan, J Sun, X N Chen, G Wang, L Zhang, Y J Fan, and X D Zhang. Chondrogenic differentiation of mesenchymal stem cells induced by collagen-based hydrogel : An in vivo study. *Journal of Biomedical Materials Research - Part A*, 93 :783–792, 2010.

[47] Sudhir Khetan, Murat Guvendiren, Wesley R Legant, Daniel M Cohen, Christopher S Chen, and Jason A Burdick. Degradation-mediated cellular traction directs stem cell fate in covalently crosslinked three-dimensional hydrogels. *Nature Materials*, 12 :1–8, 2013.

[48] Sughir Khetan, Joshua S. Katz, and Jason A. Burdick. Sequential crosslinking to control cellular spreading in 3-dimensional hydrogels. *Soft Matter*, 5 :1601–1606, 2009.

[49] Matthew G Haugh and Sarah C Heilshorn. Integrating Concepts of Material Mechanics, Ligand Chemistry, Dimensionality and Degradation to Control Differentiation of Mesenchymal Stem Cells. *Current Opinion in Solid State & Materials Science*, 20 :171–179, 2016.

[50] Ameya Phadke, YongSung Hwang, Su Hee Kim, Soo Hyun Kim, Tomonori Yamaguchi, Koichi Masuda, and Shyni Varghese. Effect of scaffold microarchitecture on osteogenic differentiation of human Mesenchymal Stem Cells. *European Cells & Materials*, 25 :114–129, 2015.

[51] Limin Wang, Steven Lu, Johnny Lam, F Kurtis Kasper, and Antonios G Mikos. Fabrication of Cell-Laden Macroporous Biodegradable Hydrogels with Tunable Porosities and Pore Sizes. *Tissue Engineering Part C*, 21 :263–273, 2015.

[52] Adam J. Engler, Shamik Sen, H. Lee Sweeney, and Dennis E. Discher. Matrix Elasticity Directs Stem Cell Lineage Specification. *Cell*, 126 :677–689, 2006.

[53] Li-shan Wang, Jérôme Boulaire, Peggy P Y Chan, Joo Eun Chung, and Motoichi Kurisawa. The role of stiffness of gelatin-hydroxyphenylpropionic acid hydrogels formed by enzyme-mediated crosslinking on the differentiation of human mesenchymal stem cell. *Biomaterials*, 31 :8608–8616, 2010.

[54] Nathaniel Huebsch, Praveen R. Arany, Angelo S. Mao, Dmitry Shvartsman, Omar A. Ali, Sidi A. Bencherif, José Rivera-Feliciano, and David J. Mooney. Harnessing traction-mediated manipulation of the cell/matrix interface to control stem-cell fate. *Nature Materials*, 9 :518–526, 2010.

[55] Britta Trappmann, Julien E. Gautrot, John T. Connelly, Daniel G. T. Strange, Yuan Li, Michelle L. Oyen, Martien A. Cohen Stuart, Heike Boehm, Bojun Li, Viola Vogel, Joachim P. Spatz, Fiona M. Watt, and Wilhelm T. S. Huck. Extracellular-matrix tethering regulates stem-cell fate. *Nature Materials*, 11 :642–649, 2012.

[56] Jessica H. Wen, Ludovic G. Vincent, Alexander Fuhrmann, Yu Suk Choi, Kolin C. Hribar, Hermes Taylor-Weiner, Shaochen Chen, and Adam J. Engler. Interplay of matrix stiffness and protein tethering in stem cell differentiation. *Nature Materials*, 13 :979–987, 2014.

[57] Ram I Sharma and Jess G Snedeker. Paracrine Interactions between Mesenchymal Stem Cells Affect Substrate Driven Differentiation toward Tendon and Bone Phenotypes. *Plos One*, 7 :1–11, 2012.

[58] Ruyue Xue, Julie Yi-Shuan Li, Yiting Yeh, Li Yang, and Shu Chien. Effects of matrix elasticity and cell density on human mesenchymal stem cells differentiation. *Journal of Orthopaedic Research*, 31 :1360–1365, 2013.

[59] Ciara M Murphy, Amos Matsiko, Matthew G Haugh, John P Gleeson, and Fergal J O'Brien. Mesenchymal stem cell fate is regulated by the composition and mechanical properties of collagen glycosaminoglycan scaffolds. *Journal of the Mechanical Behavior of Biomedical Materials*, 11 :53–62, 2012.

[60] Se Heang Oh, Dan Bi An, Tae Ho Kim, and Jin Ho Lee. Wide-range stiffness gradient PVA / HA hydrogel to investigate stem cell differentiation behavior. *Acta Biomaterialia*, 35 :23–31, 2016.

[61] Jennifer S Park, Julia S Chu, Anchi D Tsou, Rokhaya Diop, Zhenyu Tang, Aijun Wang, and Song Li. The effect of matrix stiffness on the differentiation of mesenchymal stem cells in response to TGF- b. *Biomaterials*, 32 :3921–3930, 2011.

[62] Junmin Lee, Amr A Abdeen, and Kristopher A Kilian. Rewiring mesenchymal stem cell lineage specification by switching the biophysical microenvironment. *Scientific Reports*, 4 :5188, 2014.

[63] Yu Ru V Shih, Kuo Fung Tseng, Hsiu Yu Lai, Chi Hung Lin, and Oscar K. Lee. Matrix stiffness regulation of integrin-mediated mechanotransduction during osteogenic differentiation of human mesenchymal stem cells. *Journal of Bone and Mineral Research*, 26 :730–738, 2011.

[64] Jin Hao, Yueling Zhang, Dian Jing, Yu Shen, Ge Tang, Shishu Huang, and Zhihe Zhao. Mechanobiology of Mesenchymal Stem Cells : A new perspective into the mechanically induced MSC fate. *Acta Biomaterialia*, 20 :1–9, 2015.

[65] Dennis E. Discher, Paul Janmey, and Yu-li Wang. Tissue Cells Feel and Respond to the Stiffness of Their Substrate. *Science*, 310 :1139–1143, 2005.

[66] Kyle H Vining and David J Mooney. Mechanical forces direct stem cell behaviour in development and regeneration. *Nature Reviews Molecular Cell Biology*, 18 :728–742, 2017.

[67] Andrew R. Cameron, Jessica E. Frith, and Justin J. Cooper-White. The influence of substrate creep on mesenchymal stem cell behaviour and phenotype. *Biomaterials*, 32 :5979–5993, 2011.

[68] Ovijit Chaudhuri, Luo Gu, Darinka Klumpers, Max Darnell, Sidi A. Bencherif, James C. Weaver, Nathaniel Huebsch, Hong Pyo Lee, Evi Lippens, Georg N. Duda, and David J. Mooney. Hydrogels with tunable stress relaxation regulate stem cell fate and activity. *Nature Materials*, 15 :326–334, 2016.

[69] Andrew S. Rowlands, Peter A. George, and Justin J. Cooper-White. Directing osteogenic and myogenic differentiation of MSCs : interplay of stiffness and adhesive ligand presentation. *AJP : Cell Physiology*, 295 :C1037–C1044, 2008.

[70] Alireza Dolatshahi-Pirouz, Mehdi Nikkhah, Akhilesh K Gaharwar, Basma Hashmi, Enrico Guermani, Hamed Aliabadi, Gulden Camci-Unal, Thomas Ferrante, Morten Foss, Donald E. Ingber, and Ali Khademhosseini. A combinatorial cell-laden gel microarray for inducing osteogenic differentiation of human mesenchymal stem cells. *Scientific Reports*, 4 :1–9, 2014.

[71] C. Mas-Moruno. Surface functionalization of biomaterials for bone tissue regeneration and repair. In *Peptides and Proteins as Biomaterials for Tissue Regeneration and Repair*, pages 73–100. Woodhead Publishing, 2018.

[72] Christopher M. Madl, Manav Mehta, Georg N. Duda, Sarah C. Heilshorn, and David J. Mooney. Presentation of BMP-2 Mimicking Peptides in 3D Hydrogels Directs Cell Fate Commitment in Osteoblasts and Mesenchymal Stem Cells. *Biomacromolecules*, 15 :445–455, 2014.

[73] Xuezhong He, Junyu Ma, and Esmaiel Jabbari. Effect of Grafting RGD and BMP-2 Protein-Derived Peptides to a Hydrogel Substrate on Osteogenic Differentiation of Marrow Stromal Cells. *Langmuir*, 24 :12508–12516, 2008.

[74] Rong Peng, Xiang Yao, Bin Cao, Jian Tang, and Jiandong Ding. The effect of culture conditions on the adipogenic and osteogenic inductions of mesenchymal stem cells on micropatterned surfaces. *Biomaterials*, 33 :6008–6019, 2012.

[75] Junmin Lee, Amr A Abdeen, Douglas Zhang, and Kristopher A Kilian. Directing stem cell fate on hydrogel substrates by controlling cell geometry, matrix mechanics and adhesion ligand composition. *Biomaterials*, 34 :8140–8148, 2013.

[76] Junmin Lee, Amr A Abdeen, Tiffany H Huang, and Kristopher A Kilian. Controlling cell geometry on substrates of variable stiffness can tune the degree of osteogenesis in human mesenchymal stem cells. *Journal of the Mechanical Behavior of Biomedical Materials*, 38 :209–218, 2014.

[77] Emilie Prouvé, Bernard Drouin, Pascale Chevallier, Murielle Rémy, Marie-Christine Durrieu, and Gaétan Laroche. Evaluating Poly (Acrylamide-co-Acrylic Acid) Hydrogels Stress Relaxation to Direct the Osteogenic Differentiation of Mesenchymal Stem Cells. *Macromolecular Bioscience*, 2100069 :1–12, 2021.

[78] Parisa Ghorbaniazar, Amir Sepehrianazar, Morteza Eskandani, Mohsen Nabi-Meibodi, Maryam Kouhsoltani, and Hamed Hamishehkar. Preparation of poly acrylic acid-poly acrylamide composite nanogels by radiation technique. *Advanced Pharmaceutical Bulletin*, 5 :269–275, 2015.

[79] Seddiki Nesrinne and Aliouche Djamel. Synthesis, characterization and rheological behavior of pH sensitive poly(acrylamide-co-acrylic acid) hydrogels. *Arabian Journal of Chemistry*, 10 :539–547, 2017.

[80] Rajiv Singh Tomar, Indu Gupta, Reena Singhal, and A. K. Nagpal. Synthesis of poly(acrylamide-co-acrylic acid)-based super-absorbent hydrogels by gamma radiation : Study of swelling behaviour and network parameters. *Designed Monomers and Polymers*, 10 :49–66, 2007.

[81] H. Holback, Y. Yeo, and K. Park. Hydrogel swelling behavior and its biomedical applications. In *Biomedical Hydrogels*, pages 3–24. Woodhead Publishing, 2011.

[82] Peng Fei Cao, Joey Dacula Mangadlao, and Rigoberto C. Advincula. Stimuli-Responsive Polymers and their Potential Applications in Oil-Gas Industry. *Polymer Reviews*, 55 :706–733, 2015.

[83] Marie-Christine Durrieu and Omar F. Zouani. *Substituts osseux greffés par des peptides mimétiques de la protéine humaine BMP-2*. Patent WO 2014/140504 Al, 2014.

[84] I. Bilem, P. Chevallier, L. Plawinski, E. D. Sone, M. C. Durrieu, and G. Laroche. RGD and BMP-2 mimetic peptide crosstalk enhances osteogenic commitment of human bone marrow stem cells. *Acta Biomaterialia*, 36 :132–142, 2016.

[85] Laurence Padiolleau, Christel Chanseau, Stéphanie Durrieu, Pascale Chevallier, Gaétan Laroche, and Marie-Christine Durrieu. Single or Mixed Tethered Peptides To Promote hMSC Differentiation toward Osteoblastic Lineage. *ACS Applied Biomaterials*, 1 :1800–1809, 2018.

[86] Omar F Zouani, Céline Chollet, Bertrand Guillotin, and Marie-Christine Durrieu. Differentiation of pre-osteoblast cells on poly (ethylene terephthalate) grafted with RGD and/or BMPs mimetic peptides. *Biomaterials*, 31 :8245–8253, 2010.

[87] Adrian Gestos, Philip G Whitten, Geoffrey M Spinks, and Gordon G Wallace. Crosslinking neat ultrathin films and nanofibres of pH-responsive poly (acrylic acid) by UV radiation. *Soft Matter*, 6 :1045–1052, 2010.

[88] Halina Kaczmarek and Magdalena Metzler. The Properties of Poly(Acrylic Acid) Modified with N-Phenylbenzothioamide as Potential Drug Carriers. *The Open Process Chemistry Journal*, 6 :1–7, 2014.

[89] M Y Mulla, P Seshadri, L Torsi, K Manoli, A Mallardi, N Ditaranto, M V Santacroce, C Di Franco, G Scamarcio, and M Magliulo. UV crosslinked poly(acrylic acid) : a simple method to bio-functionalize electrolyte-gated OFET biosensors. *Journal of Materials Chemistry B*, 3 :5049–5057, 2015.

[90] Adam J Engler, Ludovic Richert, Joyce Wong, Catherine Picart, and Dennis E Discher. Surface probe measurements of the elasticity of sectioned tissue, thin gels and polyelectrolyte multilayer films : correlations between substrate stiffness and cell adhesion. *Surface Science*, 570 :142–154, 2004.

[91] John M Maloney, Emily B Walton, Christopher M Bruce, and Krystyn J Van Vliet. Influence of finite thickness and stiffness on cellular adhesion-induced deformation of compliant substrata. *Physical Review E*, 78 :041923, 2008.

[92] Chandan K. Sen, Gayle M. Gordillo, Sashwati Roy, Robert Kirsner, Lynn Lambert, Thomas K. Hunt, Finn Gottrup, Geoffrey C. Gurtner, and Michael T. Longaker. Human skin wounds : A major and snowballing threat to public health and the economy : PERSPECTIVE ARTICLE. *Wound Repair and Regeneration*, 17 :763–771, 2009.

[93] Amnon Buxboim, Karthikan Rajagopal, Andre E X Brown, and Dennis E Discher. How deeply cells feel : methods for thin gels. *Journal of Physics : Condensed Matter*, 22 :194116, 2010.

[94] Elisabeth E Charrier, Katarzyna Pogoda, Rebecca G Wells, and Paul A Janmey. Control of cell morphology and differentiation by substrates with independently tunable elasticity and viscous dissipation. *Nature Communications*, 9 :1–13, 2018.

[95] Ovijit Chaudhuri, Luo Gu, Max Darnell, Darinka Klumpers, Sidi A. Bencherif, James C. Weaver, Nathaniel Huebsch, and David J. Mooney. Substrate stress relaxation regulates cell spreading. *Nature Communications*, 6 :1–7, 2015.

[96] Aline Bauer, Luo Gu, Brian Kwee, Aileen Li, Maxence Dellacherie, Celiz D Adam, and David J Mooney. Hydrogel substrate stress-relaxation proliferation of mouse myoblasts. *Acta Biomaterialia*, 62 :82–90, 2017.

[97] Erica Hui, Kathryn I Gimeno, Grant Guan, and Steven R Caliari. Spatial control of viscoelasticity in phototunable hyaluronic acid hydrogels. *BioRxiv*, 2019 :646778, 2019.

[98] Jasmin Skottke, Michael Gelinsky, and Anne Bernhardt. In Vitro Co-Culture Model of Primary Human Osteoblasts and Osteocytes in Collagen Gels. *International Journal of Molecular Sciences*, 20 :1–12, 2019.

[99] Harry C Blair, Quitterie C Larrouture, Yanan Li, Hang Lin, Donna Beer-Stoltz, Li Liu, Rocky S. Tuan, Lisa J. Robinson, Paul H Schlesinger, and Deborah J. Nelson. Osteoblast Differentiation and Bone Matrix Formation. *Tissue Engineering Part B*, 23 :268–280, 2017.

[100] Jacklyn Whitehead, Katherine H Griffin, Marissa Gionet-Gonzales, Charlotte E Vorwald, Serena E Cinque, and J Kent Leach. Hydrogel mechanics are a key driver of bone formation by mesenchymal stromal cell spheroids. *Biomaterials*, 269 :120607, 2020.

[101] Imran Ullah, Raghavendra Baregundi Subbarao, and Gyu Jin Rho. Human mesenchymal stem cells - current trends and future prospective. *Bioscience Reports*, 35 :1–18, 2015.

[102] Ibrahim Bilem. *Micro-engineered substrates as bone extracellular matrix mimics*. PhD thesis, Université de Bordeaux, Université Laval, 2017.

[103] I. Bilem, L. Plawinski, P. Chevallier, C. Ayela, E. D. Sone, G. Laroche, and M. C. Durrieu. The spatial patterning of RGD and BMP-2 mimetic peptides at the subcellular scale modulates human mesenchymal stem cells osteogenesis. *Journal of Biomedical Materials Research - Part A*, 106 :959–970, 2018.

[104] Laurence Padiolleau, Christel Chanseau, Stéphanie Durrieu, Cédric Ayela, Gaétan Laroche, and Marie-Christine Durrieu. Directing hMSCs fate through geometrical cues

and mimetics peptides. *Journal of Biomedical Materials Research Part A*, 108 :201–211, 2020.

[105] Catarina R Pedrosa, Didier Arl, Patrick Grysan, Irfan Khan, Stéphanie Durrieu, Sivashankar Krishnamoorthy, and Marie-christine Durrieu. Controlled Nanoscale Topographies for Osteogenic Differentiation of Mesenchymal Stem Cells. *ACS Applied Materials and Interfaces*, 11 :8858–8866, 2019.

[106] Alexandre Cunha, Omar Farouk Zouani, Laurent Plawinski, Ana Maria Botelho do Rego, Amélia Almeida, Rui Vilar, and Marie-Christine Durrieu. Human mesenchymal stem cell behavior on femtosecond laser-textured Ti-6Al-4V surfaces. *Nanomedicine*, 10 :725–739, 2015.

[107] Omar F Zouani, Christel Chanseau, Brigitte Brouillaud, Reine Bareille, Florent Deliane, Marie-Pierre Foulc, Ahmad Mehdi, and Marie-Christine Durrieu. Altered nanofeature size dictates stem cell differentiation. *Journal of Cell Science*, 125 :1217–1224, 2012.

[108] Rajat K Das, Omar F Zouani, Christine Labrugère, Reiko Oda, and Marie-Christine Durrieu. Influence of Nanohelical Shape and Periodicity on Stem Cell Fate. *ACS nano*, 7 :3351–3361, 2013.

[109] Zhe A Cheng, Omar F Zouani, Karine Glinel, Alain M Jonas, and Marie-Christine Durrieu. Bioactive Chemical Nanopatterns Impact Human Mesenchymal Stem Cell Fate. *Nano Letters*, 13 :3923–3929, 2013.

[110] Pierre Marie. Différenciation, fonction et contrôle de l'ostéoblaste. *Médecine Sciences*, 17 :1252–1259, 2001.

[111] Paul H Schlesinger, Harry C Blair, Donna Beer Stolz, Vladimir Riazanski, Evan C Ray, Irina L Tourkova, and Deborah J Nelson. Cellular and extracellular matrix of bone, with principles of synthesis and dependency of mineral deposition on cell membrane transport. *American Journal of Physiology Cell Physiology*, 318 :C111–C124, 2021.

[112] Xiao Lin, Suryaji Patil, Yong-guang Gao, and Airong Qian. The Bone Extracellular Matrix in Bone Formation and Regeneration. *Frontiers in Pharmacology*, 11 :1–15, 2020.

[113] Xiangli Yang and Gerard Karsenty. Transcription factors in bone : developmental and pathological aspects. *Trends in Molecular Medicine*, 8 :340–345, 2002.

[114] Elena Kozhemyakina, Andrew B Lassar, and Elazar Zelzer. A pathway to bone : signaling molecules and transcription factors involved in chondrocyte development and maturation. *Development*, 142 :817–831, 2015.

[115] R Setiawati and P Rahardjo. Bone development and growth. In *Osteogenesis and Bone Regeneration*. Haisheng Yang, IntechOpen, 2019.

[116] F Shapiro. Bone development and its relation to fracture repair. The role of mesenchymal osteoblasts and surface osteoblasts. *European Cells and Materials*, 15 :53–76, 2008.

[117] Mohamed N Rahaman, Wei Xiao, Qiang Fu, and Wenhai Huang. Review - bioactive glass implants for potential application in structural bone repair. *Biomed Glasses*, 3 :56–66, 2017.

[118] Gabriel Fernandez de Grado, Laetitia Keller, Ysia Idoux-Gillet, Quentin Wagner, Anne-marie Musset, Nadia Benkirane-Jessel, Fabien Bornert, and Damien Offner. Bone substitutes : a review of their characteristics, clinical use, and perspectives for large bone defects management. *Journal of Tissue Engineering*, 9 :1–18, 2018.

[119] V Lalzawmliana, Akrity Anand, Mangal Roy, Biswanath Kundu, and Samit Kumar Nandi. Mesoporous bioactive glasses for bone healing and biomolecules delivery. *Materials Science & Engineering C*, 106 :110180, 2020.

[120] N A P Van Gestel, J Geurts, D J W Hulsen, B Van Rietbergen, S Hofmann, and J J Arts. Clinical Applications of S53P4 Bioactive Glass in Bone Healing and Osteomyelitic Treatment : A Literature Review. *BioMed Research International*, 2015 :1–12, 2015.

[121] Li-On Lam, Karl Stoffel, Alan Kop, and Eric Swarts. Catastrophic failure of 4 cobalt-alloy Omnifit hip arthroplasty femoral components. *Acta Orthopaedica*, 79 :18–21, 2008.

[122] Raju Vaishya, Mayank Chauhan, and Abhishek Vaish. Bone cement. *Journal of Clinical Orthopaedics and Trauma*, 4 :157–163, 2013.

[123] Mrinal K Musib. A Review of the History and Role of UHMWPE as A Component in Total Joint Replacements. *International Journal of Biological Engineering*, 1 :6–10, 2011.

[124] Yujung Lee, Jeongil Kwon, Gilson Khang, and Dongwon Lee. Reduction of Inflammatory Responses and Enhancement of Extracellular Matrix Formation by Vanillin-Incorporated Poly(lactic-co-glycolic acid) Scaffolds. *Tissue Engineering Part A*, 18 :1967–1978, 2012.

[125] Hao Zhang, Li Yang, Xiong-gang Yang, Feng Wang, Jiang-tao Feng, Kun-chi Hua, Qi Li, and Yong-cheng Hu. Demineralized Bone Matrix Carriers and their Clinical Applications : An Overview. *Orthopaedic Surgery*, 11 :725–737, 2019.

[126] Ahmad Oryan, Soodeh Alidadi, and Ali Moshiri. Platelet-rich plasma for bone healing and regeneration. *Expert Opinion on Biological Therapy*, 16 :213–232, 2016.

[127] Ye-Rang Yun, Jun-Hyeog Jang, Wonmo Jeon, Sujin Lee, Jong-Eun Won, Hae-Won Kim, and Ivan Wall. Administration of growth factors for bone regeneration. *Regenerative Medicine*, 7 :369–385, 2012.

[128] Pornkawee Charoenlarp, Arun Kumar Rajendran, and Sachiko Iseki. Role of fibroblast growth factors in bone regeneration. *Inflammation and Regeneration*, 19 :1–7, 2017.

[129] Kai Hu and Bjorn R Olsen. The roles of vascular endothelial growth factor in bone repair and regeneration. *Bone*, 91 :30–38, 2016.

[130] Prasun Shah, Louise Keppler, and James Rutkowski. A Review of Platelet Derived Growth Factor Playing Pivotal Role in Bone Regeneration. *Journal of Oral Implantology*, 40 :330–340, 2014.

[131] Xiaoxuan Zhang, Helin Xing, Feng Qi, Hongchen Liu, Lizeng Gao, and Xing Wang. Local delivery of insulin/IGF-1 for bone regeneration : carriers , strategies , and effects. *Nanotheranostics*, 4 :242, 2020.

[132] Guiqian Chen, Chuxia Deng, and Yi-Ping Li. TGF-β and BMP Signaling in Osteoblast Differentiation and Bone Formation. *International Journal of Biological Sciences*, 8 :272, 2012.

[133] Ivo Dumic-Cule, Mihaela Peric, Lucija Kucko, Lovorka Grgurevic, Marko Pecina, and Slobodan Vukicevic. Bone morphogenetic proteins in fracture repair. *International Orthopaedics*, 42 :2619–2626, 2018.

[134] Bonnie Poon, Tram Kha, Sally Tran, and Crispin R Dass. Bone morphogenetic protein-2 and bone therapy : successes and pitfalls. *Journal of Pharmacy and Pharmacology*, 68 :139–147, 2016.

[135] Ami R Amini, Cato T Laurencin, and Syam P Nukavarapu. Bone Tissue Engineering : Recent Advances and Challenges. *Critical Reviews in Biomedical Engineering*, 40 :363–408, 2013.

[136] F Akter. Principles of Tissue Engineering. In *Tissue Engineering Made Easy*, pages 3–16. Academic Press, 2016.

[137] Antonio Romito and Gilda Cobellis. Pluripotent Stem Cells : Current Understanding and Future Directions. *Stem Cells International*, 2016, 2016.

[138] Azizeh-mitra Yousefi, Paul F James, Rosa Akbarzadeh, Aswati Subramanian, Conor Flavin, and Hassane Oudadesse. Prospect of Stem Cells in Bone Tissue Engineering : A Review. *Stem Cells International*, 2016, 2016.

[139] Susanne Kern, Hermann Eichler, Johannes Stoeve, Harald Klüter, and Karen Bieback. Comparative Analysis of Mesenchymal Stem Cells from Bone Marrow, Umbilical Cord Blood, or Adipose Tissue. *Stem Cells*, 24 :1294–1301, 2006.

[140] Vivian Alonso-Goulart, Lorraine Braga Ferreira, Cristiane Angélico Duarte, Isabela Lemos de Lima, Enza Rafaela Ferreira, Bárbara Candido de Oliveira, Luna Nascimento Vargas, Dayane Dotto de Moraes, Isaura Beatriz Borges Silva, Rafael de Oliveira Faria, Aline Gomes de Souza, and Leticia de Souza Castro-Filice. Mesenchymal stem cells from human adipose tissue and bone repair : a literature review. *Biotechnology Research and Innovation*, 2 :74–80, 2018.

[141] Shinya Eto, Mizuki Goto, Minami Soga, Yumi Kaneko, Yusuke Uehara, Hiroshi Mizuta, and Takumi Era. Mesenchymal stem cells derived from human iPS cells via mesoderm and neuroepithelium have different features and therapeutic potentials. *Plos One*, 13 :e0200790, 2018.

[142] Urszula Kozlowska, Agnieszka Krawczenko, Katarzyna Futoma, Tomasz Jurek, Marta Rorat, Dariusz Patrzalek, and Aleksandra Klimczak. Similarities and differences between mesenchymal stem/progenitor cells derived from various human tissues. *World Journal of Stem Cells*, 11 :347–375, 2019.

[143] Linyi Peng, Zhuqing Jia, Xinhua Yin, Xin Zhang, Yinan Liu, Ping Chen, Kangtao Ma, and Chunyan Zhou. Comparative Analysis of Mesenchymal Stem Cells from Bone Marrow, Cartilage, and Adipose Tissue. *Stem Cells and Development*, 17 :761–774, 2008.

[144] Daniel Seungyoul Han, Hee Kyung Chang, Keun Ryoung Kim, and Sang Min Woo. Consideration of Bone Regeneration Effect of Stem Cells : Comparison of Bone Regeneration Between Bone Marrow Stem Cells and Adipose-Derived Stem Cells. *The Journal of Craniofacial Surgery*, 25 :196–201, 2014.

[145] Gun-Il Im, Yong-Woon Shin, and Kee-Byung Lee. Do adipose tissue-derived mesenchymal stem cells have the same osteogenic and chondrogenic potential as bone marrow-derived cells ? *OsteoArthritis and Cartilage*, 13 :845–853, 2005.

[146] Richard J Miron and Yufeng Zhang. Osteoinduction : A Review of Old Concepts with New Standards. *Journal of Dental Research*, 91 :736–744, 2012.

[147] Sarah L Dallas and Lynda F Bonewald. Dynamics of the Transition from Osteoblast to Osteocyte. *Annals of the New York Academy of Sciences*, 1192 :437–443, 2011.

[148] Matthew Prideaux, Nigel Loveridge, Andrew A Pitsillides, and Colin Farquharson. Extracellular Matrix Mineralization Promotes E11/gp38 Glycoprotein Expression and Drives Osteocytic Differentiation. *Plos One*, 7 :e36786, 2012.

[149] Saad Mechiche Alami, Sophie C. Gangloff, Dominique Laurent-Maquin, Yu Wang, and Halima Kerdjoudj. Concise Review : In Vitro Formation of Bone - Like Nodules Sheds Light on the Application of Stem Cells for Bone Regeneration. *Stem Cells Translational Medicine*, 5 :1587–1593, 2016.

[150] Luciana D Trino, Luiz G S Albano, Erika S Bronze-uhle, Anne George, Mathew T Mathew, and Paulo N Lisboa-filho. Physicochemical, osteogenic and corrosion properties of bio-functionalized ZnO thin films : Potential material for biomedical applications. *Ceramics International*, 44 :1–11, 2018.

[151] Ellis E Golub and Kathleen Boesze-Battaglia. The role of alkaline phosphatase in mineralization. *Current Opinion in Orthopaedics*, 18 :444–448, 2007.

[152] Selvaraj Vimalraj. Alkaline phosphatase : Structure, expression and its function in bone mineralization. *Gene*, 754 :144855, 2020.

[153] Jane E Aubin. Mesenchymal Stem Cells and Osteoblast Differentiation. In *Principles of Bone Biology*, pages 59–81. Academic Press, 2002.

[154] Keqin Zhang, Cielo Barragan-Adjemian, Ling Ye, Shiva Kotha, Mark Dallas, Yongbo Lu, Shujie Zhao, Marie Harris, Stephen E Harris, Jian Q Feng, and Lynda F Bonewald. E11 / gp38 Selective Expression in Osteocytes : Regulation by Mechanical Strain and Role in Dendrite Elongation. *Molecular and Cellular Biology*, 26 :4539–4552, 2006.

[155] Kulwinder Kaur, Sanskrita Das, and Sourabh Ghosh. Regulation of Human Osteoblast-to-Osteocyte Differentiation by Direct-Write 3D Microperiodic Hydroxyapatite Scaffolds. *ACS Omega*, 4 :1504–1515, 2019.

[156] Stacey M. Woo, Jennifer Rosser, Vladimir Dusevich, Ivo Kalajzic, and Lynda F. Bonewald. Cell line IDG-SW3 replicates osteoblast-to-late-osteocyte differentiation in vitro and accelerates bone formation in vivo. *Journal of Bone and Mineral Research*, 26 :2634–2646, 2012.

[157] Aleksandra Musial-Wysocka, Marta Kot, and Marcin Majka. The Pros and Cons of Mesenchymal Stem Cell-Based Therapies. *Cell Transplantation*, 28 :801–812, 2019.

[158] Barbara Lukomska, Luiza Stanaszek, Ewa Zuba-Surma, Pawel Legosz, Sylwia Sarzynska, and Katarzyna Drela. Challenges and Controversies in Human Mesenchymal Stem Cell Therapy. *Stem Cells International*, 2019 :1–10, 2019.

[159] Yuxin Hu, Bin Lou, Xiafang Wu, Ruirui Wu, Huihui Wang, Lanyue Gao, Jingbo Pi, and Yuanyuan Xu. Comparative Study on In Vitro Culture of Mouse Bone Marrow Mesenchymal Stem Cells. *Stem Cells International*, 2018 :1–14, 2018.

[160] Christopher B Erickson and Karin A Payne. Inductive Signals and Progenitor Fates During Osteogenesis. In *Encyclopedia of Tissue Engineering and Regenerative Medicine*, pages 395–404. Academic Press, 2019.

[161] Fabian Langenbach and Jörg Handschel. Effects of dexamethasone, ascorbic acid and β-glycerophosphate on the osteogenic differentiation of stem cells in vitro. *Stem Cell Research & Therapy*, 4 :1–7, 2013.

[162] Q Chen, P Shou, C Zheng, M Jiang, G Cao, Q Yang, J Cao, N Xie, T Velletri, X Zhang, C Xu, L Zhang, H Yang, J Hou, Y Wang, and Y Shi. Fate decision of mesenchymal stem cells : adipocytes or osteoblasts ? *Cell Death and Differentiation*, 23 :1128–1139, 2016.

[163] Itsurou Nishimura, Ryuichi Hisanaga, Toru Sato, Taichi Arano, Syuntaro Nomoto, Yoshito Ikada, and Masao Yoshinari. Effect of osteogenic differentiation medium on proliferation and differentiation of human mesenchymal stem cells in three-dimensional culture with radial flow bioreactor. *Regenerative Therapy*, 2 :24–31, 2015.

[164] Yoshitomo Honda, Xianting Ding, Federico Mussano, Akira Wiberg, Chih-ming Ho, and Ichiro Nishimura. Guiding the osteogenic fate of mouse and human mesenchymal stem cells through feedback system control. *Scientific Reports*, 3 :1–9, 2013.

[165] Cornelia Hildebrandt, Heiko Büth, and Hagen Thielecke. Influence of cell culture media conditions on the osteogenic differentiation of cord blood-derived mesenchymal stem cells. *Annals of Anatomy*, 191 :23–32, 2009.

[166] Terezia Okajcekova, Jan Strnadel, Michal Pokusa, Romana Zahumenska, Maria Janickova, Erika Halasova, and Henrieta Skovierova. A Comparative In Vitro Analysis of the Osteogenic Potential of Human Dental Pulp Stem Cells Using Various Differentiation Conditions. *International Journal of Molecular Sciences*, 21 :2280, 2020.

[167] Alexander Popov, Colin Scotchford, David Grant, and Virginie Sottile. Impact of Serum Source on Human Mesenchymal Stem Cell Osteogenic Differentiation in Culture. *International Journal of Molecular Sciences*, 20 :5051, 2019.

[168] Andrea Banfi, Anita Muraglia, Beatrice Dozin, Maddalena Mastrogiacomo, Ranieri Cancedda, and Rodolfo Quarto. Proliferation kinetics and differentiation potential of ex vivo expanded human bone marrow stromal cells : Implications for their use in cell therapy. *Experimental Hematology*, 28 :707–715, 2000.

[169] Yueh-Hsun Kevin Yang, Courtney R Ogando, Carmine Wang See, Tsui-Yun Chang, and Gilda A Barabino. Changes in phenotype and differentiation potential of human mesenchymal stem cells aging in vitro. *Stem Cell Research & Therapy*, 9 :1–14, 2018.

[170] Noridzzaida Ridzuan, Akram Al Abbar, Wai Kien Yip, Maryam Maqbool, and Rajesh Ramasamy. Characterization and Expression of Senescence Marker in Prolonged Passages of Rat Bone Marrow-Derived Mesenchymal Stem Cells. *Stem Cells International*, 2016 :1–14, 2016.

[171] James D Kretlow, Yu-Qing Jin, Wei Liu, Wen Jie Zhang, Tan-Hui Hong, Guangdong Zhou, L Scott Baggett, Antonios G Mikos, and Yilin Cao. Donor age and cell passage affects differentiation potential of murine bone marrow-derived stem cells. *BMC Cell Biology*, 9 :1–13, 2008.

[172] Merve Zaim, Serap Karaman, Guven Cetin, and Sevim Isik. Donor age and long-term culture affect differentiation and proliferation of human bone marrow mesenchymal stem cells. *Annals of Hematology*, 91 :1175–1186, 2012.

[173] Hongzhi Zhou, Michael Weir, and Hockin H K Xu. Effect of Cell Seeding Density on Proliferation and Osteodifferentiation of Umbilical Cord Stem Cells on Calcium Phosphate Cement-Fiber Scaffold. *Tissue Engineering Part A*, 17 :2603–2613, 2011.

[174] Kyobum Kim, David Dean, Antonios G Mikos, and John P Fisher. Effect of Initial Cell Seeding Density on Early Osteogenic Signal Expression of Rat Bone Marrow Stromal Cells Cultured on Cross-Linked Poly(propylene fumarate) Disks. *Biomacromolecules*, 10 :1810–1817, 2009.

[175] Shulu Luo, Shuyi Wu, Jianmeng Xu, Xingcai Zhang, Leiyan Zou, Run Yao, Lin Jin, and Yan Li. Osteogenic differentiation of BMSCs on MoS2 composite nanofibers with different cell seeding densities. *Applied Nanoscience*, 10 :3703–3716, 2020.

[176] Jeroen Eyckmans, Grace L Lin, and Christopher S Chen. Adhesive and mechanical regulation of mesenchymal stem cell differentiation in human bone marrow and periosteum-derived progenitor cells. *Biology Open*, 1 :1058–1068, 2012.

[177] Rowena McBeath, Dana M Pirone, Celeste M Nelson, Kiran Bhadriraju, and Christopher S Chen. Cell Shape, Cytoskeletal Tension, and RhoA Regulate Stem Cell Lineage Commitment. *Developmental Cell*, 6 :483–495, 2004.

[178] Samatha Bhat, Pachaiyappan Viswanathan, Shashank Chandanala, S Jyothi Prasanna, and Raviraja N Seetharam. Expansion and characterization of bone marrow derived human mesenchymal stromal cells in serum-free conditions. *Scientific Reports*, 11 :1–18, 2021.

[179] Xin Yu, Qilong Wan, Xiaoling Ye, Yuet Cheng, Janak L Pathak, and Zubing Li. Cellular hypoxia promotes osteogenic differentiation of mesenchymal stem cells and bone defect healing via STAT3 signaling. *Cellular & Molecular Biology Letters*, 24 :1–17, 2019.

[180] Shun-Pei Hung, Jennifer H Ho, Yu-Ru V Shih, Ting Lo, and Oscar K Lee. Hypoxia Promotes Proliferation and Osteogenic Differentiation Potentials of Human Mesenchymal Stem Cells. *Journal of Orthopaedic Research*, 30 :260–266, 2012.

[181] Claudia Cicione, Emma Muiños-López, Tamara Hermida-Gómez, Isaac Fuentes-Boquete, Silvia Díaz-Prado, and Francisco J Blanco. Effects of Severe Hypoxia on Bone Marrow Mesenchymal Stem Cells Differentiation Potential. *Stem Cells International*, 2013 :1–11, 2013.

[182] Hao Ding, Song Chen, Jun-Hui Yin, Xue-Tao Xie, Zhen Hong Zhu, You-Shui Gao, and Chang-Qing Zhang. Continuous hypoxia regulates the osteogenic potential of mesenchymal stem cells in a time-dependent manner. *Molecular Medicine Reports*, 10 :2184–2190, 2014.

[183] Hatice Imran Gungordu, Min Bao, Sjoerd Van Helvert, John A Jansen, Sander C G Leeuwenburgh, and X Frank Walboomers. Effect of mechanical loading and substrate elasticity on the osteogenic and adipogenic differentiation of mesenchymal stem cells. *Journal of Tissue Engineering and Regenerative Medicine*, 13 :2279–2290, 2019.

[184] Runguang Li, Liang Liang, Yonggang Dou, Zeping Huang, Huiting Mo, Yaning Wang, and Bin Yu. Mechanical Strain Regulates Osteogenic and Adipogenic Differentiation of Bone Marrow Mesenchymal Stem Cells. *BioMed Research International*, 2015 :1–10, 2015.

[185] J Wang, C D Wang, N Zhang, W X Tong, Y F Zhang, S Z Shan, X L Zhang, and Q F Li. Mechanical stimulation orchestrates the osteogenic differentiation of human bone marrow stromal cells by regulating HDAC1. *Cell Death and Disease*, 7 :e2221, 2016.

[186] Xiaoyan Chen, Yuan Liu, Wanghui Ding, Jiejun Shi, Shenglai Li, Yali Liu, Mengjie Wu, and Huiming Wang. Mechanical stretch-induced osteogenic differentiation of human jaw bone marrow mesenchymal stem cells (hJBMMSCs) via inhibition of the NF-kB pathway. *Cell Death and Disease*, 9 :1–9, 2018.

[187] Asmat Ullah Khan, Rongmei Qu, Tingyu Fan, Jun Ouyang, and Jingxing Dai. A glance on the role of actin in osteogenic and adipogenic differentiation of mesenchymal stem cells. *Stem Cell Research & Therapy*, 11 :1–14, 2020.

[188] Zongliang Wang, Li Chen, Yu Wang, Xuesi Chen, and Peibiao Zhang. Improved Cell Adhesion and Osteogenesis of op-HA/PLGA Composite by Poly(dopamine)-Assisted Immobilization of Collagen Mimetic Peptide and Osteogenic Growth Peptide. *ACS Applied Materials and Interfaces*, 8 :26559–26569, 2016.

[189] Jianhua Li, Xiaoning Mou, Jichuan Qiu, Shu Wang, Dongzhou Wang, Dehui Sun, Weibo Guo, Deshuai Li, Anil Kumar, Xuebin Yang, Aixue Li, and Hong Liu. Surface Charge

Regulation of Osteogenic Differentiation of Mesenchymal Stem Cell on Polarized Ferroelectric Crystal Substrate. *Advanced Healthcare Materials*, 4 :998–1003, 2015.

[190] Ting-ting Yu, Fu-zhai Cui, Qingyuan Meng, Juan Wang, De-cheng Wu, Jin Zhang, Xiao-Xing Kou, Rui-Li Yang, Yan Liu, Yu Shrike Zhang, Fei Yang, and Yan-Heng Zhou. Influence of Surface Chemistry on Adhesion and Osteo / Odontogenic Differentiation of Dental Pulp Stem Cells. *ACS Biomaterials Science & Engineering*, 3 :1119–1128, 2017.

[191] Ana B Faia-torres, Stefanie Guimond-lischer, Markus Rottmar, Mirren Charnley, Tolga Goren, Katharina Maniura-weber, Nicholas D Spencer, Rui L Reis, Marcus Textor, and Nuno M Neves. Differential regulation of osteogenic differentiation of stem cells on surface roughness gradients. *Biomaterials*, 35 :9023–9032, 2014.

[192] Matthew J Dalby, Nikolaj Gadegaard, Rahul Tare, Abhay Andar, Mathis O Riehle, Pawel Herzyk, Chris D W Wilkinson, and Richard O C Oreffo. The control of human mesenchymal cell differentiation using nanoscale symmetry and disorder. *Nature Materials*, 6 :997, 2007.

[193] N. Gui, W. Xu, D. E. Myers, R. Shukla, H. P. Tang, and M. Qian. The effect of ordered and partially ordered surface topography on bone cell responses : a review. *Biomaterials Science*, 6 :250–264, 2017.

[194] Muhammad Faheem Akhtar, Muhammad Hanif, and Nazar Muhammad Ranjha. Methods of synthesis of hydrogels ... A review. *Saudi Pharmaceutical Journal*, 24 :554–559, 2016.

[195] Nick Huettner, Tim R Dargaville, and Aurelien Forget. Discovering Cell-Adhesion Peptides in Tissue Engineering : Beyond RGD. *Trends in Biotechnology*, 36 :372–383, 2018.

[196] Naziha Chirani, L'Hocine Yahia, Lukas Gritsch, Federico Leonardo Motta, Sounia Chirani, and Silvia Faré. History and Applications of Hydrogels. *Journal of Biomedical Sciencies*, 4 :1–23, 2015.

[197] Shih-Ching Wu, Wei-Hong Chang, Guo-Chung Dong, Kuo-Yu Chen, Yueh-Sheng Chen, and Chun-Hsu Yao. Cell adhesion and proliferation enhancement by gelatin nanofiber scaffolds. *Journal of Bioactive and Compatible Polymers*, 26 :565–577, 2011.

[198] Hongru Li, Zhiping Qi, Shuang Zheng, Yuxin Chang, Weijian Kong, Chuan Fu, Ziyuan Yu, Xiaoyu Yang, and Su Pan. The Application of Hyaluronic Acid-Based Hydrogels in Bone and Cartilage Tissue Engineering. *Advances in Materials Science and Engineering*, 2019 :1–12, 2019.

[199] Mahadevappa Hemshekhar, Ram M Thushara, Siddaiah Chandranayaka, Larry S Sherman, Kempaiah Kemparaju, and Kesturu S Girish. Emerging roles of hyaluronic acid bioscaffolds in tissue engineering and regenerative medicine. *International Journal of Biological Macromolecules*, 86 :917–928, 2016.

[200] Sayan Deb Dutta, Dinesh K Patel, and Ki-Taek Lim. Functional cellulose-based hydrogels as extracellular matrices for tissue engineering. *Journal of Biological Engineering*, 13 :1–19, 2019.

[201] Daniela Rusu, Diana Ciolacu, and Bogdan C Simionescu. Cellulose-based hydrogels in tissue engineering applications. *Cellulose Chemistry and Technology*, 53 :907–923, 2019.

[202] Christian Demitri, Marta Madaghiele, Maria Grazia Raucci, Alessandro Sannino, and Luigi Ambrosio. Investigating the Structure-Related Properties of Cellulose-Based

Superabsorbent Hydrogels. In *Hydrogels-Smart Materials for Biomedical Applications.* IntechOpen, 2018.

[203] Guoke Tang, Zhihong Tan, Wusi Zeng, Xing Wang, Changgui Shi, Yi Liu, Hailong He, Rui Chen, and Xiaojian Ye. Recent Advances of Chitosan-Based Injectable Hydrogels for Bone and Dental Tissue Regeneration. *Frontiers in Bioengineering and Biotechnology*, 8 :1084, 2020.

[204] Payam Zarrintaj, Saeed Manouchehri, Zahed Ahmadi, Mohammad Reza Saeb, Aleksandra M Urbanska, David L Kaplan, and Masoud Mozafari. Agarose-based biomaterials for tissue engineering. *Carbohydrate Polymers*, 187 :66–84, 2018.

[205] Mohammad Amin Salati, Javad Khazai, Amir Mohammad Tahmuri, Ali Samadi, Ali Taghizadeh, Mohsen Taghizadeh, Payam Zarrintaj, Josh D Ramsay, Sajjad Habibzadeh, Farzad Seidi, Mohammad Reza Saeb, and Masoud Mozafari. Agarose-Based Biomaterials : Opportunities and Challenges in Cartilage Tissue Engineering. *Polymers*, 12 :1150, 2020.

[206] Aleksandra K. Denisin and Beth L. Pruitt. Tuning the Range of Polyacrylamide Gel Stiffness for Mechanobiology Applications. *ACS Applied Materials and Interfaces*, 8 :21893–21902, 2016.

[207] Pariksha J Kondiah, Yahya E Choonara, Pierre P D Kondiah, Thashree Marimuthu, Pradeep Kumar, Lisa C du Toit, and Viness Pillay. A Review of Injectable Polymeric Hydrogel Systems for Application in Bone Tissue Engineering. *Molecules*, 21 :1580, 2016.

[208] Ananya Barui. Synthetic polymeric gel. In *Polymeric Gels*, pages 55–90. Woodhead Publishing, 2018.

[209] Anuj Kumar and Sung Soo Han. PVA-based hydrogels for tissue engineering : A review. *International Journal of Polymeric Materials and Polymeric Biomaterials*, 66 :159–182, 2017.

[210] Alireza Dolatshahi-Pirouz, Mehdi Nikkhah, Kristian Kolind, Mehmet R Dokmeci, and Ali Khademhosseini. Micro- and Nanoengineering Approaches to Control Stem Cell-Biomaterial Interactions. *Journal of Functional Biomaterials*, 2 :88–106, 2011.

[211] Shinya Watari, Kei Hayashi, Joshua A Wood, Paul Russell, Paul F Nealey, Christopher J Murphy, and Damian C Genetos. Modulation of osteogenic differentiation in hMSCs cells by submicron topographically-patterned ridges and grooves. *Biomaterials*, 33 :128–136, 2012.

[212] Gabriel Romero Liguori, Qihui Zhou, Tacia Tavares Aquinas Liguori, Guilherme Garcia Barros, Philipp Till Kühn, Luiz Felipe Pinho Moreira, Patrick Van Rijn, and Martin C Harmsen. Directional Topography Influences Adipose Mesenchymal Stromal Cell Plasticity : Prospects for Tissue Engineering and Fibrosis. *Stem Cells International*, 2019 :1–14, 2019.

[213] Yingnan Wu, Zheng Yang, Jaslyn Bee Khuan Law, Ai Yu He, Azlina A Abbas, Vinitha Denslin, Tunku Kamarul, James HP Hui, and Eng Hin Lee. The combined effect of substrate stiffness and surface topography on chondrogenic differentiation of Mesenchymal Stem Cells. *Tissue Engineering Part A*, 23 :43–54, 2017.

[214] Julin Yang, Aiming Liu, and Changren Zhou. Proliferation of Mesenchymal Stem Cell on Chitosan Films Associated with Convex Micro- topography. *Journal of Biomaterials Science, Polymer Edition*, 22 :919–929, 2011.

[215] Michael J Poellmann, Patrick A Harrell, William P King, and Amy J Wagoner Johnson. Geometric microenvironment directs cell morphology on topographically patterned hydrogel substrates. *Acta Biomaterialia*, 6 :3514–3523, 2010.

[216] Murat Guvendiren and Jason A Burdick. The control of stem cell morphology and differentiation by hydrogel surface wrinkles. *Biomaterials*, 31 :6511–6518, 2010.

[217] Rotsiniaina Randriantsilefisoa, Yong Hou, Yuanwei Pan, José Luis, Cuellar Camacho, Michaël W Kulka, Jianguang Zhang, and Rainer Haag. Interaction of Human Mesenchymal Stem Cells with Soft Nanocomposite Hydrogels Based on Polyethylene Glycol and Dendritic Polyglycerol. *Advanced Functional Materials*, 30 :1905200, 2020.

[218] YJ Bae, YR Kwon, HJ Kim, S Lee, and YJ Kim. Enhanced differentiation of mesenchymal stromal cells by three-dimensional culture and azacitidine. *Blood Research*, 52 :18–24, 2017.

[219] Nipha Chaicharoenaudomrung, Phongsakorn Kunhorm, and Parinya Noisa. Three-dimensional cell culture systems as an in vitro platform for cancer and stem cell modeling. *World Journal of Stem Cells*, 11 :1065–1084, 2019.

[220] CM Madl and SC Heilshorn. Engineering Hydrogel Microenvironments to Recapitulate the Stem Cell Niche. *Annual Review of Biomedical Engineering*, 20 :21–47, 2018.

[221] Brendan A C Harley, Hyung-do Kim, Muhammad H Zaman, Ioannis V Yannas, Douglas A Lauffenburger, and Lorna J Gibson. Microarchitecture of Three-Dimensional Scaffolds Influences Cell Migration Behavior via Junction Interactions. *Biophysical Journal*, 95 :4013–4024, 2008.

[222] Jangwook P. Jung, Meredith K Bache-Wiig, Paolo P Provenzano, and Brenda M. Ogle. Heterogeneous Differentiation of Human Mesenchymal Stem Cells in 3D Extracellular Matrix Composites. *BioResearch Open Access*, 5 :37–48, 2016.

[223] Jun Ho Song, Sun-Mi Lee, and Kyung-Hwa Yoo. Label-free and real-time monitoring of human mesenchymal stem cell differentiation in 2D and 3D cell culture systems using impedance cell sensors. *RSC Advances*, 8 :31246–31254, 2018.

[224] Mahrokh Dadsetan, Theresa E Hefferan, Jan P Szatkowski, Prasanna K Mishra, Slobodan I Macura, Lichun Lu, and Michael J Yaszemski. Effect of hydrogel porosity on marrow stromal cell phenotypic expression. *Biomaterials*, 29 :2193–2202, 2009.

[225] Jirong Yang, Yuanqi Li, Yanbo Liu, Dongxiao Li, Lei Zhang, Qiguang Wang, Yumei Xiao, and Xingdong Zhang. Influence of hydrogel network microstructures on mesenchymal stem cell chondrogenesis in vitro and in vivo. *Acta Biomaterialia*, 91 :159–172, 2019.

[226] Matsiko Amos, John P. Gleeson, and Fergal J. O'Brien. Scaffold Mean Pore Size Influences Mesenchymal Stem Cell Chondrogenic Differentiation and Matrix Deposition. *Tissue Engineering Part A*, 21 :486–497, 2014.

[227] Hongwei Lv, Heping Wang, Zhijun Zhang, Wang Yang, Wenbin Liu, Yulin Li, and Lisha Li. Biomaterial stiffness determines stem cell fate. *Life Sciences*, 178 :42–48, 2017.

[228] Wen Zhao, Xiaowei Li, Xiaoyan Liu, Ning Zhang, and Xuejun Wen. Effects of substrate stiffness on adipogenic and osteogenic differentiation of human mesenchymal stem cells. *Materials Science & Engineering C*, 40 :316–323, 2014.

[229] Michael Floren, Walter Bonani, Anirudh Dharmarajan, Antonella Motta, Claudio Migliaresi, and Wei Tan. Human mesenchymal stem cells cultured on silk hydrogels with variable stiffness and growth factor differentiate into mature smooth muscle cell phenotype. *Acta Biomaterialia*, 31 :156–166, 2015.

[230] Chun Yang, Frank W Delrio, Hao Ma, Anouk R Killaars, Lena P Basta, Kyle A Kyburz, and Kristi S. Anseth. Spatially patterned matrix elasticity directs stem cell fate. *Proceedings of the National Academy of Sciences*, 31 :4439–4445, 2016.

[231] Malgorzata Witkowska-Zimny, Katarzyna Walenko, Edyta Wrobel, Piotr Mrowka, Agnieszka Mikulska, and Jacek Przybylski. Effect of substrate stiffness on the osteogenic differentiation of bone marrow stem cells and bone-derived cells. *Cell Biology International*, 37 :608–616, 2013.

[232] Meiyu Sun, Guangfan Chi, Pengdong Li, Shuang Lv, Juanjuan Xu, Ziran Xu, Yuhan Xia, Ye Tan, Jiayi Xu, Lisha Li, and Yulin Li. Effects of Matrix Stiffness on the Morphology, Adhesion, Proliferation and Osteogenic Differentiation of Mesenchymal Stem Cells. *International Journal of Medical Sciences*, 15 :257–268, 2018.

[233] Meiyu Sun, Guangfan Chi, Juanjuan Xu, Ye Tan, Jiayi Xu, Shuang Lv, Ziran Xu, Yuhan Xia, Lisha Li, and Yulin Li. Extracellular matrix stiffness controls osteogenic differentiation of mesenchymal stem cells mediated by integrin α 5. *Stem Cell Research & Therapy*, 9 :52, 2018.

[234] Raimon Sunyer, Albert J Jin, Ralph Nossal, and Dan L Sackett. Fabrication of Hydrogels with Steep Stiffness Gradients for Studying Cell Mechanical Response. *Plos One*, 7 :e46107, 2012.

[235] Chun-min Lo, Hong-bei Wang, Micah Dembo, and Yu-li Wang. Cell Movement Is Guided by the Rigidity of the Substrate. *Biophysical Journal*, 79 :144–152, 2000.

[236] Christian Franck, Stacey A Maskarinec, David A Tirrell, and Guruswami Ravichandran. Three-Dimensional Traction Force Microscopy : A New Tool for Quantifying Cell-Matrix Interactions. *Plos One*, 6 :e17833, 2011.

[237] Jennet Toyjanova, Erin Hannen, Eyal Bar-kochba, Eric M Darling, David L Henann, and Christian Franck. 3D viscoelastic traction force microscopy. *Soft Matter*, 10 :8095–8106, 2014.

[238] Wesley R Legant, Jordan S Miller, Brandon L Blakely, Daniel M Cohen, Guy M Genin, and Christopher S Chen. Measurement of mechanical tractions exerted by cells within three-dimensional matrices. *Nature Methods*, 7 :969–971, 2010.

[239] F Raquel Maia, Sílvia J Bidarra, Pedro L Granja, and Cristina C Barrias. Functionalization of biomaterials with small osteoinductive moieties. *Acta Biomaterialia*, 9 :8773–8789, 2013.

[240] DE Discher, DJ Mooney, and PW Zandstra. Growth factors, matrices, and forces combine and control stem cells. *Science*, 324 :1673–1677, 2009.

[241] AW James. Review of Signaling Pathways Governing MSC Osteogenic and Adipogenic Differentiation. *Scientifica*, 2013, 2013.

[242] AJ Keung, S Kumar, and DV Schaffer. Presentation counts : microenvironmental regulation of stem cells by biophysical and material cues. *Annual Review of Cell and Developmental Biology*, 26 :533–556, 2010.

[243] S Tsutsumi, A Shimazu, K Miyazaki, H Pan, C Koike, E Yoshida, K Takagishi, and Y Kato. Retention of multilineage differentiation potential of mesenchymal cells during proliferation in response to FGF. *Biochemical and Biophysical Research Communications*, 288 :413–419, 2001.

[244] Danielle S W Benoit, Michael P Schwartz, Andrew R Durney, and Kristi S Anseth. Small functional groups for controlled differentiation of hydrogel-encapsulated human mesenchymal stem cells. *Nature Materials*, 7 :816–823, 2008.

[245] Dong-an Wang, Christopher G Williams, Fan Yang, Nicholas Cher, Hyukjin Lee, and Jennifer H Elisseeff. Bioresponsive Phosphoester Hydrogels for Bone Tissue Engineering. *Tissue Engineering*, 11 :201–213, 2005.

[246] Mathieu Lanniel, Ejaz Huq, Stephanie Allen, Lee Buttery, Philip M. Williams, and Morgan R. Alexander. Substrate induced differentiation of human mesenchymal stem cells on hydrogels with modified surface chemistry and controlled modulus. *Soft Matter*, 7 :6501–6514, 2011.

[247] Navakanth R Gandavarapu, Peter D Mariner, Michael P Schwartz, and Kristi S Anseth. Extracellular matrix protein adsorption to phosphate-functionalized gels from serum promotes osteogenic differentiation of human mesenchymal stem cells. *Acta Biomaterialia*, 9 :4525–4534, 2013.

[248] Ramses Ayala, Chao Zhang, Darren Yang, Yongsung Hwang, Aereas Aung, Sumeet S Shroff, Fernando T Arce, Ratnesh Lal, Gaurav Arya, and Shyni Varghese. Engineering the cell-material interface for controlling stem cell adhesion, migration, and differentiation. *Biomaterials*, 32 :3700–3711, 2011.

[249] Joshua D Mccall, Jacob E Luoma, and Kristi S Anseth. Covalently tethered transforming growth factor beta in PEG hydrogels promotes chondrogenic differentiation of encapsulated human mesenchymal stem cells. *Drug Delivery and Translational Research*, 2 :305–312, 2012.

[250] Danielle S W Benoit, Andrew R Durney, and Kristi S Anseth. The effect of heparin-functionalized PEG hydrogels on three-dimensional human mesenchymal stem cell osteogenic differentiation. *Biomaterials*, 28 :66–77, 2007.

[251] Timothy A. Petrie and Andrés J. Garcia. Extracellular Matrix-derived Ligand for Selective Integrin Binding to Control Cell Function. In *Biological Interactions on Materials Surfaces*, chapter 7, pages 133–156. New York, springer edition, 2009.

[252] Veronica Lifshitz and Dan Frenkel. TGF-β. In *Handbook of Biologically Active Peptides : Neurotrophic Peptides*, pages 1647–1653. 2013.

[253] Paul W Kopesky, Eric J Vanderploeg, John D Kisiday, David D Frisbie, John D Sandy, Alan J Grodzinsky, and D Sc. Controlled Delivery of Transforming Growth Factor b1 by Self-Assembling Peptide Hydrogels Induces Chondrogenesis of Bone Marrow Stromal Cells and Modulates Smad2/3 Signaling. *Tissue Engineering Part A*, 17 :83–92, 2011.

[254] Yonghui Ding, Richard Johnson, Sadhana Sharma, Xiaoyun Ding, Stephanie J Bryant, and Wei Tan. Tethering transforming growth factor β1 to soft hydrogels guides vascular smooth muscle commitment from human mesenchymal stem cells. *Acta Biomaterialia*, 105 :68–77, 2020.

[255] Heungsoo Shin, Seongbong Jo, and Antonios G Mikos. Modulation of marrow stromal osteoblast adhesion on biomimetic oligo [poly(ethylene glycol) fumarate] hydrogels modified with Arg-Gly-Asp peptides and a poly (ethylene glycol) spacer. In *28th Annual Meeting of the Society for Biomaterials*, 2002.

[256] Susan X Hsiong, Tanyarut Boontheekul, Nathaniel Huebsch, and David J Mooney. Cyclic Arginine-Glycine-Aspartate Peptides Enhance Three-Dimensional Stem Cell Osteogenic Differentiation. *Tissue Engineering Part A*, 15 :263–272, 2009.

[257] Fan Yang, Christopher G Williams, Dong-an Wang, Hyukjin Lee, Paul N Manson, and Jennifer Elisseeff. The effect of incorporating RGD adhesive peptide in polyethylene glycol diacrylate hydrogel on osteogenesis of bone marrow stromal cells. *Biomaterials*, 26 :5991–5998, 2005.

[258] Manav Mehta, Christopher M Madl, Shimwoo Lee, Georg N Duda, and David J Mooney. The collagen I mimetic peptide DGEA enhances an osteogenic phenotype in mesenchymal stem cells when presented from cell-encapsulating hydrogels. *Journal of Biomedical Materials Research - Part A*, 103 :3516–3525, 2015.

[259] Paresh A Parmar, Lesley W Chow, Jean-Philippe St-Pierre, Christine-Maria Horejs, Yong Y Peng, Jerome A Werkmeister, John A M Ramshaw, and Molly M Stevens. Collagen-mimetic peptide-modifiable hydrogels for articular cartilage regeneration. *Biomaterials*, 54 :213–225, 2015.

[260] Ying Ren, Han Zhang, Wenjuan Qin, Bo Du, Lingrong Liu, and Jing Yang. A collagen mimetic peptide-modified hyaluronic acid hydrogel system with enzymatically mediated degradation for mesenchymal stem cell differentiation. *Materials Science & Engineering C*, 108 :110276, 2020.

[261] J T Connelly, T A Petrie, A J García, and M E Levenston. Fibronectin- and Collagen-Mimetic Ligands Regulate BMSC Chondrogenesis in 3D Hydrogels. *European Cells & Materials*, 22 :168–177, 2016.

[262] John T. Connelly, Andrés J. Garcia, and Marc E Levenston. Inhibition of in vitro chondrogenesis in RGD-modified three-dimensional alginate gels. *Biomaterials*, 28 :1071–1083, 2007.

[263] Sebastian L. Vega, Mi Y Kwon, Kwang Hoon Song, Chao Wang, Robert L Mauck, Lin Han, and Jason A. Burdick. Combinatorial hydrogels with biochemical gradients for screening 3D cellular microenvironments. *Nature Communications*, 9 :1–10, 2018.

[264] Mi Y Kwon, Sebastián L Vega, William M Gramlich, Minwook Kim, Robert L Mauck, and Jason A Burdick. Dose and Timing of N-Cadherin Mimetic Peptides Regulate MSC Chondrogenesis within Hydrogels. *Advanced Healthcare Materials*, 7 :1701199, 2018.

[265] Liming Bian, Murat Guvendiren, Robert L Mauck, and Jason A Burdick. Hydrogels that mimic developmentally relevant matrix and N-cadherin interactions enhance MSC chondrogenesis. *Proceedings of the National Academy of Sciences*, 110 :10117–10122, 2013.

[266] Meiling Zhu, Sien Lin, Yuxin Sun, Qian Feng, Gang Li, and Liming Bian. Hydrogels functionalized with N-cadherin mimetic peptide enhance osteogenesis of hMSCs by emulating the osteogenic niche. *Biomaterials*, 77 :44–52, 2016.

[267] Atsuhiro Saito, Yoshihisa Suzuki, Shin-ichi Ogata, Chikara Ohtsuki, and Masao Tanihara. Accelerated bone repair with the use of a synthetic BMP-2- derived peptide and bone-marrow stromal cells. *Journal of Biomedical Materials Research - Part A*, 72 :77–82, 2004.

[268] Omar F. Zouani, Jérôme Kalisky, Emmanuel Ibarboure, and Marie Christine Durrieu. Effect of BMP-2 from matrices of different stiffnesses for the modulation of stem cell fate. *Biomaterials*, 34 :2157–2166, 2013.

[269] Xuezhong He, Xiaoming Yang, and Esmaiel Jabbari. Combined Effect of Osteopontin and BMP-2 Derived Peptides Grafted to an Adhesive Hydrogel on Osteogenic and Vasculogenic Differentiation of Marrow Stromal Cells. *Langmuir*, 28 :5387–5397, 2012.

[270] Masaki Noda and David T Denhardt. Osteopontin. In *Principles of Bone Biology*, pages 351–366. Academic Press, 2008.

[271] Heungsoo Shin, Kyriacos Zygourakis, Mary C Farach-carson, Michael J Yaszemski, and Antonios G Mikos. Modulation of differentiation and mineralization of marrow stromal

cells cultured on biomimetic hydrogels modified with Arg-Gly-Asp containing peptides. *Journal of Biomedical Materials Research - Part A*, 69 :535–543, 2004.

[272] Heungsoo Shin, Johnna S Temenoff, Gregory C Bowden, Kyriacos Zygourakis, Mary C Farach-carson, Michael J Yaszemski, and Antonios G Mikos. Osteogenic differentiation of rat bone marrow stromal cells cultured on Arg-Gly-Asp modified hydrogels without dexamethasone and b-glycerol phosphate. *Biomaterials*, 26 :3645–3654, 2005.

[273] Jue-yeon Lee, Jung-eun Choo, Hyun-jung Park, Jun-bum Park, Sang-chul Lee, Inho Jo, Seung-jin Lee, Chong-pyoung Chung, and Yoon-jeong Park. Injectable gel with synthetic collagen-binding peptide for enhanced osteogenesis in vitro and in vivo. *Biochemical and Biophysical Research Communications*, 357 :68–74, 2007.

[274] Sadhana Sharma, Michael Floren, Yonghui Ding, Kurt R Stenmark, Wei Tan, and Stephanie J Bryant. A photoclickable peptide microarray platform for facile and rapid screening of 3-D tissue microenvironments. *Biomaterials*, 143 :17–28, 2017.

[275] Annika Kasten, Tamara Naser, Kristina Brüllhoff, Jörg Fiedler, Petra Müller, Martin Möller, Joachim Rychly, Jürgen Groll, and Rolf E Brenner. Guidance of Mesenchymal Stem Cells on Fibronectin Structured Hydrogel Films. *Plos One*, 9 :1–10, 2014.

[276] Xuan Wang, Ce Yan, Kai Ye, Yao He, Zhenhua Li, and Jiandong Ding. Effect of RGD nanospacing on differentiation of stem cells. *Biomaterials*, 34 :2865–2874, 2013.

[277] Kamol Dey, Elena Roca, Giorgio Ramorino, and Luciana Sartore. Progress in Mechanical Modulation of Cell Function in Tissue Engineering. *Biomaterials Science*, 8 :7033–7081, 2020.

[278] Cunyang Wang, Yan Liu, Yubo Fan, and Xiaoming Li. The use of bioactive peptides to modify materials for bone tissue repair. *Regenerative Biomaterials*, 4 :191–206, 2017.

[279] George Bullock, Joss Atkinson, Piergiorgio Gentile, Paul Hatton, and Cheryl Miller. Osteogenic Peptides and Attachment Methods Determine Tissue Regeneration in Modified Bone Graft Substitutes. *Journal of Functional Biomaterials*, 12 :22, 2021.

[280] Ippokratis Pountos, Michalis Panteli, Anastasios Lampropoulos, Elena Jones, Giorgio Maria Calori, and Peter V Giannoudis. The role of peptides in bone healing and regeneration : a systematic review. *BMC Medicine*, 14 :1–15, 2016.

[281] P Schaffner and M M Dard. Structure and function of RGD peptides involved in bone biology. *Cellular and Molecular Life Sciences CMLS*, 60 :119–132, 2003.

[282] Ulrich Hersel, Claudia Dahmen, and Horst Kessler. RGD Modified Polymers : Biomaterials for Stimulated Cell Adhesion and Beyond. *Biomaterials*, 24 :4385–4415, 2003.

[283] J Park, K Singha, S Son, J Kim, R Namgung, C-o Yun, and W J Kim. A review of RGD-functionalized nonviral gene delivery vectors for cancer therapy. *Cancer Gene Therapy*, 19 :741–748, 2012.

[284] Donghee Lee, Haipeng Zhang, and Sangjin Ryu. Elastic Modulus Measurement of Hydrogels. In *Cellulose-based Superabsorbent Hydrogels*, chapter 27, pages 1–21. Springer International Publishing, 2019.

[285] Matteo Galli, Kerstyn S C Comley, Tamaryn A V Shean, and Michelle L. Oyen. Viscoelastic and poroelastic mechanical characterization of hydrated gels. *Journal of Materials Research*, 24 :973–979, 2009.

[286] D Caccavo, S Cascone, G Lamberti, and A A Barba. Hydrogels : experimental characterization and mathematical modelling of their mechanical and diffusive behavior. *Chemical Society Reviews*, 47 :2357–2373, 2018.

[287] Hilary J. Anderson, Jugal Kishore Sahoo, Rein V. Ulijn, and Matthew J. Dalby. Mesenchymal Stem Cell Fate : Applying Biomaterials for Control of Stem Cell Behavior. *Frontiers in Bioengineering and Biotechnology*, 4 :1–14, 2016.

[288] Ming Li and Susumu Ikehara. Bone-Marrow-Derived Mesenchymal Stem Cells for Organ Repair. *Stem Cells International*, 2013, 2013.

[289] M. L. Oyen. Mechanical characterisation of hydrogel materials. *International Materials Reviews*, 59 :44–59, 2014.

[290] Thomas Distler, Aditya A Solisito, Dominik Schneidereit, Oliver Friedrich, Rainer Detsch, and Aldo R Boccaccini. 3D printed oxidized alginate-gelatin bioink provides guidance for C2C12 muscle precursor cell orientation and differentiation via shear stress during bioprinting. *Biofabrication*, 12 :045005, 2020.

[291] Yufan Liu, Jianjun Li, Bin Yao, Yihui Wang, Rui Wang, Siming Yang, Zhao Li, Yijie Zhang, Sha Huang, and Xiaobing Fu. The stiffness of hydrogel-based bioink impacts mesenchymal stem cells differentiation toward sweat glands in 3D-bioprinted matrix. *Materials Science & Engineering C*, 118 :111387, 2021.

[292] Kai Ling, Guoyou Huang, Juncong Liu, Xiaohui Zhang, Yufei Ma, Tianjian Lu, and Feng Xu. Bioprinting-Based High-Throughput Fabrication of Three-dimensional MCF-7 Human Breast Cancer Cellular Spheroids. *Engineering*, 1 :269–274, 2015.

[293] Yufei Ma, Yuan Ji, Guoyou Huang, Kai Ling, Xiaohui Zhang, and Feng Xu. Bioprinting 3D cell-laden hydrogel microarray for screening human periodontal ligament stem cell response to extracellular matrix. *Biofabrication*, 7 :044105, 2015.

[294] Yufei Ma, Yuan Ji, Tianyu Zhong, Wanting Wan, Qingzhen Yang, Ang Li, Xiaohui Zhang, and Min Lin. Bioprinting-based PDLSC-ECM Screening for in vivo Repair of Alveolar Bone Defect using Cell-laden, Injectable and Photocrosslinkable Hydrogels. *ACS Biomaterials Science & Engineering*, 3 :3534–3545, 2017.

[295] Hyun Joon Kong, Emma Wong, and David J Mooney. Independent Control of Rigidity and Toughness of Polymeric Hydrogels. *Macromolecules*, 36 :4582–4588, 2003.

[296] Arn Mignon, Daniele Pezzoli, Emilie Prouvé, Lucie Lévesque, Aysu Arslan, Nele Pien, David Schaubroeck, Jasper Van Hoorick, Diego Mantovani, Sandra Van Vlierberghe, and Peter Dubruel. Combined effect of Laponite and polymer molecular weight on the cell- interactive properties of synthetic PEO-based hydrogels. *Reactive and Functional Polymers*, 136 :95–106, 2019.

[297] Xian Ming Qi, Ge Gu Chen, Xiao Dong Gong, Gen Que Fu, Ya Shuai Niu, Jing Bian, Feng Peng, and Run Cang Sun. Enhanced mechanical performance of biocompatible hemicelluloses-based hydrogel via chain extension. *Scientific Reports*, 6 :2–11, 2016.

[298] Kazutoshi Haraguchi, Huan Jun Li, Yingjia Xu, and Guang Li. Copolymer nanocomposite hydrogels : Unique tensile mechanical properties and network structures. *Polymer*, 96 :94–103, 2016.

[299] Pavlo Demianenko, Benoît Minisini, Mouad Lamrani, and Fabienne Poncin-Epaillard. Stiff IPN Hydrogels of Poly(Acrylamide) and Alginate : Influence of the Crosslinking Ion's Valence on Hydrogel's Final Properties. *Journal of Chemical Engineering & Process Technology*, 7 :1–6, 2016.

[300] Yu Zhang, Philipp Heher, Jöns Hilborn, Heinz Redl, and Dmitri A. Ossipov. Hyaluronic acid-fibrin interpenetrating double network hydrogel prepared in situ by orthogonal disulfide cross-linking reaction for biomedical applications. *Acta Biomaterialia*, 38 :23–32, 2016.

[301] Yeshun Zhang, Jia Liu, Lei Huang, Zheng Wang, and Lin Wang. Design and performance of a sericin-alginate interpenetrating network hydrogel for cell and drug delivery. *Scientific Reports*, 5 :1–13, 2015.

[302] Khaow Tonsomboon, Annabel L. Butcher, and Michelle L. Oyen. Strong and tough nanofibrous hydrogel composites based on biomimetic principles. *Materials Science and Engineering C*, 72 :220–227, 2016.

[303] Supansa Yodmuang, Stephanie L. McNamara, Adam B. Nover, Biman B. Mandal, Monica Agarwal, Terri Ann N. Kelly, Pen Hsiu Grace Chao, Clark Hung, David L. Kaplan, and Gordana Vunjak-Novakovic. Silk microfiber-reinforced silk hydrogel composites for functional cartilage tissue repair. *Acta Biomaterialia*, 11 :27–36, 2015.

[304] Miguel Castilho, Gernot Hochleitner, Wouter Wilson, Bert Van Rietbergen, Paul D. Dalton, Jürgen Groll, Jos Malda, and Keita Ito. Mechanical behavior of a soft hydrogel reinforced with three-dimensional printed microfibre scaffolds. *Scientific Reports*, 8 :1–10, 2018.

[305] Shih Jye Tan, Josephine Y. Fang, Zhi Yang, Marcel E. Nimni, and Bo Han. The synergetic effect of hydrogel stiffness and growth factor on osteogenic differentiation. *Biomaterials*, 35 :5294–5306, 2014.

[306] Se Heang Oh, Dan Bi An, Tae Ho Kim, and Jin Ho Lee. Wide-range stiffness gradient PVA/HA hydrogel to investigate stem cell differentiation behavior. *Acta Biomaterialia*, 35 :23–31, 2016.

[307] Kar Wey Yong, Yuhui Li, Fusheng Liu, Bin Gao, Tian Jian Lu, Wan Abu Bakar Wan Abas, Wan Kamarul Zaman Wan Safwani, Belinda Pingguan-Murphy, Yufei Ma, Feng Xu, and Guoyou Huang. Paracrine Effects of Adipose- Derived Stem Cells on Matrix Stiffness-Induced Cardiac Myofibroblast Differentiation via Angiotensin II Type 1 Receptor and Smad7. *Scientific Reports*, 6 :33067, 2016.

[308] Angelo S. Mao, Jae Won Shin, and David J. Mooney. Effects of substrate stiffness and cell-cell contact on mesenchymal stem cell differentiation. *Biomaterials*, 98 :184–191, 2016.

[309] Ryan K. Roeder. Mechanical Characterization of Biomaterials. In *Characterization of Biomaterials*, pages 49–104. Academic Press, 2013.

[310] Xueting Zou, Xing Kui, Rongchun Zhang, Yue Zhang, Xiaoliang Wang, Qiang Wu, Tiehong Chen, and Pingchuan Sun. Viscoelasticity and Structures in Chemically and Physically Dual-Cross-Linked Hydrogels : Insights from Rheology and Proton Multiple-Quantum NMR Spectroscopy. *Macromolecules*, 50 :9340–9352, 2017.

[311] Sengqiang Cai, Yuhang Hu, Xuanhe Zhao, and Zhigang Suo. Poroelasticity of a covalently crosslinked alginate hydrogel under compression. *Journal of Applied Physics*, 108 :113514, 2010.

[312] Xuanhe Zhao, Nathaniel Huebsch, David J. Mooney, and Zhigang Suo. Stress-relaxation behavior in gels with ionic and covalent crosslinks. *Journal of Applied Physics*, 107 :1–5, 2010.

[313] Qi-ming Wang, Anirudh C. Mohan, Michelle L. Oyen, and Xuan-He Zhao. Separating viscoelasticity and poroelasticity of gels with different length and time scales. *Acta Mechanica Sinica*, 30 :20–27, 2014.

[314] Edwin P Chan, Blessing Deeyaa, M Johnson, and Christopher M Stafford. Poroelastic relaxation of polymer-loaded hydrogels. *Soft Matter*, 8 :8234–8240, 2012.

[315] Edwin P Chan, Yuhang Hu, Peter M Johnson, Zhigang Suo, and Christopher M Stafford. Spherical indentation testing of poroelastic relaxations in thin hydrogel layers. *Soft Matter*, 8 :1492–1498, 2012.

[316] Daniel G T Strange, Timothy L Fletcher, Khaow Tonsomboon, Helen Brawn, Xuanhe Zhao, and Michelle L Oyen. Separating poroviscoelastic deformation mechanisms in hydrogels. *Applied Physics Letters*, 102 :0131913, 2013.

[317] Yufei Ma, Min Lin, Guoyou Huang, Yuhui Li, Shuqi Wang, Guiqin Bai, Tian Jian Lu, and Feng Xu. 3D Spatiotemporal Mechanical Microenvironment : A Hydrogel-Based Platform for Guiding Stem Cell Fate. *Advanced Materials*, 1705911 :1–27, 2018.

[318] Emilie Prouvé, Gaétan Laroche, and Marie-Christine Durrieu. Hydrogels for mesenchymal stem cell behavior study. In *Superabsorbent Polymers*, pages 103–142. Boston : De Gruyter, Berlin, 2021.

[319] Guoyou Huang, Fei Li, Xin Zhao, Yufei Ma, Yuhui Li, Min Lin, Guorui Jin, Tian Jian Lu, Guy M Genin, and Feng Xu. Functional and Biomimetic Materials for Engineering of the Three-Dimensional Cell Microenvironment. *Chemical Reviews*, 117 :12764–12850, 2017.

[320] Fariba Ganji, Samira Vasheghani-Farahani, and Ebrahim Vasheghani-Farahani. Theoretical Description of Hydrogel Swelling : A Review. *Iranian Polymer Journal*, 19 :375–398, 2010.

[321] Enas M. Ahmed. Hydrogel : Preparation, characterization, and applications : A review. *Journal of Advanced Research*, 6 :105–121, 2015.

[322] A Thakur, R K Wanchoo, and P Singh. Structural Parameters and Swelling Behavior of pH Sensitive Poly (acrylamide-co-acrylic acid) Hydrogels. *Chemical and Biochemical Engineering Quarterly*, 25 :181–194, 2011.

[323] Hai Xin, Hugh Ralph Brown, Sina Naficy, and Geoffrey M Spinks. Time-dependent mechanical properties of tough ionic-covalent hybrid hydrogels. *Polymer*, 65 :253–261, 2015.

[324] Vladimir M Gun'ko, Irina N Savina, and Sergey V Mikhalovsky. Properties of Water Bound in Hydrogels. *Gels*, 3 :37, 2017.

[325] Yuhang Hu and Zhigang Suo. Viscoelasticity and poroelasticity in elastomeric gels. *Acta Mechanica Solida Sinica*, 25 :441–458, 2012.

[326] Giancarmine Gentile, Francesco Greco, and Domenico Larobina. Stress-relaxation behavior of a physical gel : Evidence of co-occurrence of structural relaxation and water diffusion in ionic alginate gels. *European Polymer Journal*, 49 :3929–3936, 2013.

[327] Mattia Capulli, Riccardo Paone, and Nadia Rucci. Osteoblast and osteocyte : Games without frontiers. *Archives of Biochemistry and Biophysics*, 561 :3–12, 2014.

[328] Takashi Ariizumi, Akira Ogose, Hiroyuki Kawashima, Tetsuo Hotta, Guidong Li, Yongjun Xu, Hajime Umezu, Mika Sugai, and Naoto Endo. Expression of podoplanin in human bone and bone tumors : New marker of osteogenic and chondrogenic bone tumors. *Pathology International*, 60 :193–202, 2010.

[329] Ivo Kalajzic, Brya G Matthews, Elena Torreggiani, Marie A Harris, Paola Divieti Pajevic, and Stephen E Harris. In vitro and in vivo approaches to study osteocyte biology. *Bone*, 54 :296–306, 2013.

[330] Lora A Shiflett, Leann M Tiede-lewis, Yixia Xie, Yongbo Lu, Eleanor C Ray, and Sarah L Dallas. Collagen Dynamics During the Process of Osteocyte Embedding and Mineralization. *Frontiers in Cell and Developmental Biology*, 7 :178, 2019.

[331] Marita Westhrin, Minli Xie, Magnus Ø Olderoy, Pawel Sikorski, Berit L Strand, and Therese Standal. Osteogenic Differentiation of Human Mesenchymal Stem Cells in Mineralized Alginate Matrices. *Plos One*, 10 :1–16, 2015.

[332] C A Mullen, M G Haugh, M B Schaffler, R J Majeska, and L M McNamara. Osteocyte differentiation is regulated by extracellular matrix stiffness and intercellular separation. *Journal of the Mechanical Behavior of Biomedical Materials*, 28 :183–194, 2013.

[333] Tamara A Franz-Odendaal, Brian K Hall, and P Eckhard Witten. Buried Alive : How Osteoblasts Become Osteocytes. *Developmental Dynamics : an official publication of the American Association of Anatomists*, 235 :176–190, 2006.

[334] N Ozkaya, M Nordin, D Goldsheyder, and D Leger. Mechanical properties of Biological Tissues. In *Fundamentals of Biomechanics*, pages 361–387. Springer, Cham, 2017.

[335] M A Del Nobile, S Chillo, A Mentana, and A Baiano. Use of the generalized Maxwell model for describing the stress relaxation behavior of solid-like foods. *Journal of Food Engineering*, 78 :978–983, 2007.

[336] G C Papanicolaou and S P Zaoutsos. Viscoelastic constitutive modeling of creep and stress relaxation in polymers and polymer matrix composites. In *Creep and fatigue in polymer matrix composites*, pages 3–59. Woodhead Publishing, 2019.

[337] P Kelly. Rheological Models. In *Solid Mechanics Part I : An introduction to solid mechanics*, chapter 10, pages 292–301. A Creative Commons Attributions, Mountain View CA 94042, 2013.

[338] Enrique A López-Guerra and Santiago D Solares. Modeling viscoelasticity through spring-dashpot models in intermittent-contact atomic force microscopy. *Beilstein Journal of nanotechnology*, 5 :2149–2163, 2014.

[339] Seung-hyun Chae, Jie-hua Zhao, Darvin R Edwards, and Paul S Ho. Characterization of the Viscoelasticity of Molding Compounds in the Time Domain. *Journal of Electronic Materials*, 39 :419–425, 2010.

[340] Arnold I Caplan. Adult Mesenchymal Stem Cells for Tissue Engineering Versus Regenerative Medicine. *Journal of Cellular Physiology*, 213 :341–347, 2007.

[341] B M Abdallah and M Kassem. Human mesenchymal stem cells : from basic biology to clinical applications. *Gene Therapy*, 106 :109–116, 2008.

[342] Na Li, Hanna Sanyour, Tyler Remund, Patrick Kelly, and Zhongkui Hong. Vascular extracellular matrix and fibroblasts-coculture directed differentiation of human mesenchymal stem cells toward smooth muscle- like cells for vascular tissue engineering. *Materials Science & Engineering C*, 93 :61–69, 2018.

[343] Jun-song Ye, Xiao-san Su, J Stoltz, N De Isla, and Lei Zhang. Signalling pathways involved in the process of mesenchymal stem cells differentiating into hepatocytes. *Cell Proliferation*, 48 :157–165, 2015.

[344] Andreas Kurtz. Mesenchymal Stem Cell Delivery Routes and Fate. *International Journal of Stem Cells*, 1 :1–7, 2008.

[345] Jennifer E. Phillips, Timothy A. Petrie, Francis P. Creighton, and Andrés J. Garcia. Human mesenchymal stem cell differentiation on self-assembled monolayers presenting different surface chemistries. *Acta Biomaterialia*, 6 :12–20, 2010.

[346] Nicole M Moore, Nancy J Lin, Nathan D Gallant, and Matthew L Becker. Synergistic enhancement of human bone marrow stromal cell proliferation and osteogenic differentiation on BMP-2 derived and RGD peptide concentration gradients. *Acta Biomaterialia*, 7 :2091–2100, 2011.

[347] Yeji Kim, Julie N Renner, and Julie C Liu. Incorporating the BMP-2 peptide in genetically-engineered biomaterials accelerates osteogenic differentiation. *Biomaterials Science*, 2 :1110–1119, 2014.

[348] David C Lin, Emilios K Dimitriadis, and Ferenc Horkay. Robust Strategies for Automated AFM Force Curve Analysis - II : Adhesion-Influenced Indentation of Soft, Elastic Materials. *Journal of Biomechanical Engineering*, 129 :430–440, 2007.

[349] Giuseppe Tronci, Colin A Grant, Neil H Thomson, Stephen J Russell, and David J Wood. Multi-scale mechanical characterization of highly swollen photo-activated collagen hydrogels. *Journal of the Royal Society Interface*, 12 :20141079, 2015.

[350] Sooho Chang, Minsu Kim, Seunghee Oh, Ji Hong Min, Donyoung Kang, Changsun Han, Taebin Ahn, Won-Gun Koh, and Hyungsuk Lee. Multi-scale characterization of surface-crosslinked superabsorbent polymer hydrogel spheres. *Polymer*, 145 :174–183, 2018.

[351] Elisabeth H Schwab, Theresa L M Pohl, Tamas Haraszti, Gerburg K Schwaerzer, Christian Hiepen, Joachim P Spatz, Petra Knaus, and Elisabetta A Cavalcanti-Adam. Nanoscale Control of Surface Immobilized BMP-2 : Toward a Quantitative Assessment of BMP-Mediated Signaling Events. *Nano Letters*, 15 :1526–1534, 2014.

[352] Merve Meinhardt, Ronald Krebs, Angelika Anders, Ulrike Heinrich, and Hagen Tronnier. Wavelength-dependent penetration depths of ultraviolet radiation in human skin. *Journal of Biomedical Optics*, 13 :044030, 2008.

[353] James E Walsh, Laura V Koehler, David P Fleming, and Jan P G Bergmanson. Novel Method for Determining Hydrogel and Silicone Hydrogel Contact Lens Transmission Curves and Their Spatially Specific Ultraviolet Radiation Protection Factors. *Eye & Contact Lens*, 33 :58–64, 2007.

[354] Jui-Teng Lin, Hsia-Wei Liu, Kuo-Ti Chen, and Da-Chuan Cheng. Modeling the Kinetics, Curing Depth, and Efficacy of Radical-Mediated Photopolymerization : The Role of Oxygen Inhibition, Viscosity, and Dynamic Light Intensity. *Frontiers in Chemistry*, 7 :760, 2019.

[355] Khoon S Lim, Barbara J Klotz, Gabriella C J Lindberg, Ferry P W Melchels, Gary J Hooper, Debby Gawlitta, and Tim B F Woodfield. Visible Light Cross-Linking of Gelatin Hydrogels Offers an Enhanced Cell Microenvironment with Improved Light Penetration Depth. *Macromolecular Bioscience*, 19 :1900098, 2019.

[356] Indong Jun, Kyung Min Park, Dong Yun Lee, Ki Dong Park, and Heungsoo Shin. Control of adhesion, focal adhesion assembly, and differentiation of myoblasts by enzymatically crosslinked cell-interactive hydrogels. *Macromolecular Research*, 19 :911, 2011.

[357] Mihaela Puiu, Andrea Idili, Danila Moscone, Francesco Ricci, and Camelia Bala. A modular electrochemical peptide-based sensor for antibody detection. *Chemical Communications*, 50 :8962, 2014.

[358] Shan Yu, Xingang Zuo, Tao Shen, Yiyuan Duan, Zhengwei Mao, and Changyou Gao. A density gradient of VAPG peptides on a cell-resisting surface achieves selective adhesion and directional migration of smooth muscle cells over fibroblasts. *Acta Biomaterialia*, 72 :70–81, 2018.

[359] Junjian Chen, Yuchen Zhu, Menghua Xiong, Guansong Hu, Jiezhao Zhan, Tianjie Li, Lin Wang, and Yingjun Wang. Antimicrobial Titanium Surface via Click-Immobilization of Peptide and Its in Vitro/Vivo Activity. *ACS Biomaterials Science & Engineering*, 5 :1034–1044, 2019.

[360] Mayumi Ishizuka, Kazutoshi Fujioka, and Takayuki Shibamoto. Analysis of Acrylamide in a Complex Matrix of Polyacrylamide Solutions Treated by Heat and Ultraviolet Light. *Journal of Agricultural and Food Chemistry*, 56 :6093–6096, 2008.

[361] Sungmin Nam, Ryan Stowers, Junzhe Lou, Yan Xia, and Ovijit Chaudhuri. Varying PEG density to control stress relaxation in alginate-PEG hydrogels for 3D cell culture studies. *Biomaterials*, 200 :15–24, 2019.

[362] Ben P Hung, Tomas Gonzalez-Fernandez, Jenny B Lin, Takeyah Campbell, Yu Bin Lee, Alyssa Panitch, Eben Alsberg, and J Kent Leach. Multi-peptide presentation and hydrogel mechanics jointly enhance therapeutic duo-potential of entrapped stromal cells. *Biomaterials*, 245 :119973, 2020.

[363] Yongbo Lu, Baozhi Yuan, Chunlin Qin, Zhengguo Cao, Yixia Xie, Sarah L Dallas, Marc D Mckee, Marc K Drezner, Lynda F Bonewald, and Jian Q Feng. The Biological Function of DMP-1 in Osteocyte Maturation is Mediated by its 57-kDa C-terminal Fragment. *Journal of Bone and Mineral Research*, 26 :331–340, 2011.

[364] Shufan Zhang, Huixuan Wan, Peng Wang, Mengmeng Liu, Gongchen Li, Chunxue Zhang, and Yao Sun. Extracellular matrix protein DMP1 suppresses osteogenic differentiation of Mesenchymal Stem Cells. *Biochemical and Biophysical Research Communications*, 501 :968–973, 2018.

[365] Jesus Delgado-Calle, Amy Y Sato, and Teresita Bellido. Role and mechanism of action of Sclerostin in bone. *Bone*, 96 :29–37, 2017.

[366] E Michael Lewiecki. Role of sclerostin in bone and cartilage and its potential as a therapeutic target in bone diseases. *Therapeutic Advances in Musculoskeletal Disease*, 6 :48–57, 2014.

[367] Dragos C Ilas, Sarah M Churchman, Thomas Baboolal, Peter V Giannoudis, Joseph Aderinto, Dennis McGonagle, and Elena Jones. The simultaneous analysis of mesenchymal stem cells and early osteocytes accumulation in osteoarthritic femoral head sclerotic bone. *Rheumatology*, 58 :1777–1783, 2019.

[368] Naruhiko Sawa, Hiroki Fujimoto, Yoshihiko Sawa, and Junro Yamashita. Alternating Differentiation and Dedifferentiation between Mature Osteoblasts and Osteocytes. *Scientific Reports*, 9 :13842, 2019.

[369] M J Mc Garrigle, C A Mullen, M G Haugh, M C Voisin, and L M McNamara. Osteocyte differentiation and the formation of an interconnected cellular network in vitro. *European Cells and Materials*, 31 :323–340, 2016.

[370] Yutong Guo, Shufang Du, Shuqi Quan, Fulin Jiang, Cai Yang, and Juan Li. Effects of biophysical cues of 3D hydrogels on mesenchymal stem cells differentiation. *Journal of Cellular Physiology*, 236 :2268–2275, 2020.

[371] Carolina Da Silva Madaleno, Jerome Jatzlau, and Petra Knaus. BMP signalling in a mechanical context - Implications for bone biology. *Bone*, 137 :115416, 2020.

[372] Inkyung Kang, Dinesh Panneerselvam, Vassilis P Panoskaltsis, Steven J Eppell, Roger E Marchant, and Claire M Doerschuk. Changes in the Hyperelastic Properties of Endothelial Cells Induced by Tumor Necrosis Factor-alpha. *Biophysical Journal*, 94 :3273–3285, 2008.

[373] Grégory Francius, Joseph Hemmerlé, Jacques Ohayon, Pierre Schaaf, Jean-Claude Voegel, Catherine Pichart, and Bernard Senger. Effect of Crosslinking on the Elasticity of Polyelectrolyte Multilayer Films Measured by Colloidal Probe AFM. *Microscopy Research and Technique*, 69 :84–92, 2006.

[374] Zheng Dai, Jennifer Ronholm, Yiping Tian, Benu Sethi, and Xudong Cao. Sterilization techniques for biodegradable scaffolds in tissue engineering applications. *Journal of Tissue Engineering*, 7 :1–13, 2016.

[375] Raquel Galante, Terezinha J A Pinto, Rogério Colaço, and Ana Paula Serro. Sterilization of hydrogels for biomedical applications : A review. *Journal of Biomedical Materials Research Part B : Applied Biomaterials*, 106 :2472–2492, 2018.

[376] Nathaniel Huebsch, Michele Gilbert, and Kevin E Healy. Analysis of Sterilization Protocols for Peptide-Modified Hydrogels. *Journal of Biomedical Materials Research Part B : Applied Biomaterials : An Official Journal of The Society for Biomaterials, The Japanese Society for Biomaterials, and The Australian Society for Biomaterials and the Korean Society for Biomaterials*, 74 :440–447, 2005.

[377] Celine Chollet, Christel Chanseau, Murielle Remy, Alain Guignandon, Reine Bareille, Christine Labrugère, Laurence Bordenave, and Marie C. Durrieu. The effect of RGD density on osteoblast and endothelial cell behavior on RGD-grafted polyethylene terephthalate surfaces. *Biomaterials*, 30 :711–720, 2009.

[378] Christianne Gaudet, William A Marganski, Sooyoung Kim, Christopher T Brown, Vaibhavi Gunderia, Micah Dembo, and Joyce Y Wong. Influence of Type I Collagen Surface Density on Fibroblast Spreading, Motility, and Contractility. *Biophysical Journal*, 85 :3329–3335, 2003.

[379] C Echalier, R Levato, M A Mateos-Timoneda, O Castano, S Déjean, X Garric, C Pinese, D Noël, E Engel, J Martinez, A Mehdi, and G Subra. Modular bioink for 3D printing of biocompatible hydrogels : sol-gel polymerization of hybrid peptides and polymers. *RSC Advances*, 7 :12231, 2017.

[380] Sirisha Thippabhotla, Cuncong Zhong, and Mei He. 3D cell culture stimulates the secretion of in vivo like extracellular vesicles. *Scientific Reports*, 9 :13012, 2019.

[381] Anne Bernhardt, Violetta Österreich, and Michael Gelinsky. 3D co-culture of primary human osteocytes and mature human osteoclasts in collagen gels. *Tissue Engineering Part A*, 26 :647–655, 2020.

[382] Florian Boukhechba, Thierry Balaguer, Jean-François Michiels, Karin Ackermann, Danielle Quincey, Jean-Michel Bouler, Walter Pyerin, Georges F Carle, and Nathalie Rochet. Human Primary Osteocyte Differentiation in a 3D Culture System. *Journal of Bone and Mineral Research*, 24 :1927–1935, 2009.

[383] Soraya Rasi Ghaemi, Bahman Delalat, Alex Cavallaro, Agnieszka Mierczynska-Vasilev, Krasimir Vasilev, and Nicolas H Voelcker. Differentiation of Rat Mesenchymal Stem Cells toward Osteogenic Lineage on Extracellular Matrix Protein Gradients. *Advanced Healthcare Materials*, 8 :1900595, 2019.

[384] A G Castano, V Hortigüela, A Lagunas, C Cortina, N Montserrat, J Samitier, and E Martinez. Protein patterning on hydrogels by direct microcontact printing : application to cardiac differentiation. *RSC Advances*, 4 :29120, 2014.

[385] Dong Qin, Younan Xia, and George M Whitesides. Soft lithography for micro- and nanoscale patterning. *Nature Protocols*, 5 :491–502, 2010.

[386] Virginie Gauvreau and Gaétan Laroche. Micropattern Printing of Adhesion, Spreading, and Migration Peptides on Poly(tetrafluoroethylene) Films To Promote Endothelialization. *Bioconjugate Chemistry*, 16 :1088–1097, 2005.

[387] Louis Gagné, Gerardo Rivera, and Gaetan Laroche. Micropatterning with aerosols : Application for biomaterials. *Biomaterials*, 27 :5430–5439, 2006.

[388] Louis Gagne and Gaetan Laroche. Engineering Biomaterials Surfaces Using Micropatterning. *Advanced Materials Research*, 17 :77–82, 2007.

[389] S M Naqvi and L M McNamara. Stem Cell Mechanobiology and the Role of Biomaterials in Governing Mechanotransduction and Matrix Production for Tissue Regeneration. *Frontiers in Bioengineering and Biotechnology*, 8 :1375, 2020.

[390] Steve Stegen, Ingrid Stockmans, Karen Moermans, Bernard Thienpont, Patrick H Maxwell, Peter Carmeliet, and Geert Carmeliet. Osteocytic oxygen sensing controls bone mass through epigenetic regulation of sclerostin. *Nature Communications*, 9 :2557, 2018.

Appendix A

Scientific communications

A.1 Publications

Maryline Moreno-Couranjou, Jérôme Guillot, Jean-Nicolas Audinot, Jérôme Bour, Emilie Prouvé, Marie-Christine Durrieu, Patrick Choquet, & Christophe Detrembleur. Atmospheric pulsed plasma copolymerization of acrylic monomers : Kinetics, chemistry, and applications. *Plasma Processes and Polymers*, 2020, 17, 1900187.

Prouvé Emilie, Laroche Gaétan, & Durrieu Marie-Christine. 4 Hydrogels for mesenchymal stem cell behavior study. In *Superabsorbent Polymers*. De Gruyter, 2021. p. 103-142.

Prouvé Emilie, Drouin Bernard, Chevallier Pascale, Rémy Murielle, Durrieu Marie-Christine, & Laroche Gaétan. Evaluating Poly(Acrylamide-co-Acrylic Acid) Hydrogels Stress Relaxation to Direct the Osteogenic Differentiation of Mesenchymal Stem Cells. *Macromolecular Bioscience*, 2021, 2100069.

Prouvé Emilie, Rémy Murielle, Feuillie Cécile, Molinari Michael, Chevallier Pascale, Drouin Bernard, Durrieu Marie-Christine, & Laroche Gaétan. Interplay of matrix stiffness and stress relaxation in directing Mesenchymal Stem Cells osteogenic differentiation. In preparation.

A.2 Oral communications

Characterization of poly(acrylamide-co-acrylic acid) hydrogels stress relaxation to direct mesenchymal stem cells differentiation.
Young Scientist Symposium. 23-05-2019. Pessac, France.
E. Prouvé, B. Drouin, P. Chevallier, G. Laroche, M.-C. Durrieu

Evaluating stress relaxation of poly(acrylamide-co-acrylic acid) hydrogels.
Journée du CBMN. 28-05-2019. Pessac, France.
E. Prouvé, B. Drouin, P. Chevallier, G. Laroche, M.-C. Durrieu

Evaluating stress relaxation of poly(acrylamide-co-acrylic acid) hydrogels to direct hMSCs osteogenic differentiation.
30th Annual Conference of the European Society for Biomaterials. 09 to 13-09-2019. Dresden, Germany.
E. Prouvé, B. Drouin, P. Chevallier, G. Laroche, M.-C. Durrieu

Modulating poly(acrylamide-co-acrylic acid) hydrogels stress relaxation and bio-functionalization to control MSCs differentiation.
Journée Scientifique du département Sciences et Technologie pour la Santé. **(1st Presentation prize)** 01-10-2019. Pessac, France.
E. Prouvé, B. Drouin, P. Chevallier, G. Laroche, M.-C. Durrieu

Selected during the first selection phase of the competition **My thesis in 180 seconds** in Bordeaux University. 2019. Talence, France.

Modulating poly(acrylamide-co-acrylic acid) hydrogels stress relaxation to control MSCs osteogenic differentiation.
Journée Scientifique du département Sciences et Technologie pour la Santé. 20-11-2020. Pessac, France.
E. Prouvé, B. Drouin, P. Chevallier, M. Rémy, G. Laroche, M.-C. Durrieu

Synthesis of bioactive surfaces for the control of stem cells differentiation for bone regeneration purposes.
Séminaire de l'Axe Médecine Régénératrice du centre de recherche du CHU de Québec. 29-04-2021. Virtual conference.
E. Prouvé, B. Drouin, P. Chevallier, M. Rémy, G. Laroche, M.-C. Durrieu

The impact of hydrogel stress relaxation on mesenchymal stem cells osteogenic differentiation.
36th Annual General Meeting of the Canadian Biomaterials Society. **(CBS abstract merit award)** 13/15-05-2021. Virtual conference.
E. Prouvé, M. Rémy, P. Chevallier, B. Drouin, G. Laroche, M.-C. Durrieu

Synthesis of bioactive surfaces for the control of stem cells differentiation for bone regeneration purposes.
CBMN PhD students seminar. **(Jury Award)** 01-07-2021. Virtual conference.
E. Prouvé, M. Rémy, C. Feuillie, M. Molinari, P. Chevallier, B. Drouin, G. Laroche, M.-C. Durrieu

Study of the effect of hydrogel stress relaxation on Mesenchymal Stem Cells osteogenic differentiation.
Colloque conjoint CQMF-Nouvelle Aquitaine sur les matériaux pour l'énergie et la santé. 19-08-2021. Virtual conference.
E. Prouvé, M. Rémy, C. Feuillie, M. Molinari, P. Chevallier, B. Drouin, G. Laroche, M.-C. Durrieu

Study of mesenchymal stem cells osteogenic differentiation in response to hydrogels stiffness and stress relaxation.
19^{th} Brazil Materials Research Society Meeting & International Union of Materials Research Societies. 30-08/01-09-2021. Virtual conference.
E. Prouvé, M. Rémy, P. Chevallier, B. Drouin, G. Laroche, M.-C. Durrieu

Interplay of hydrogel stiffness and stress relaxation in directing mesenchymal stem cells osteogenic commitment.
GDR Bio-Ingénierie des Interfaces. 21/22-09-2021. Toulouse, France.
E. Prouvé, M. Rémy, C. Feuillie, M. Molinari, P. Chevallier, B. Drouin, G. Laroche, M.-C. Durrieu

A.3 Poster presentations

Control on hydrogel mechanical properties to direct HMSCs osteogenic differentiation.
8ème édition du colloque étudiant du CERMA (Centre de Recherche sur les Matériaux Avancés). 06-04-2018. Québec, Canada.
E. Prouvé, B. Drouin, P. Chevallier, M.-C. Durrieu, G. Laroche

The effect of hydrogel stiffness on osteoblastic differentiation of Mesenchymal Stem Cells.
Journée scientifique de la Fr TecSan. 15-05-2018. Pessac, France.
E. Prouvé, B. Drouin, P. Chevallier, G. Laroche, M.-C. Durrieu

The effect of hydrogel stiffness on the differentiation of Mesenchymal Stem Cells.
Young Scientist Symposium. 25-05-2018. Pessac, France.
E. Prouvé, B. Drouin, P. Chevallier, G. Laroche, M.-C. Durrieu

Study of the effect of matrix stiffness on hMSCs osteogenic differentiation.
Journée du CBMN. 31-05-2018. Pessac, France.
E. Prouvé, B. Drouin, P. Chevallier, G. Laroche, M.-C. Durrieu

Evaluating viscoelasticity and poroelasticity in poly(acrylamide-co-acrylic acid) hydrogels.
21ème journée de l'Ecole Doctorale de Sciences Chimiques. 08-06-2019. Talence, France.
E. Prouvé, B. Drouin, P. Chevallier, G. Laroche, M.-C. Durrieu

Directing Mesenchymal Stem Cells osteogenic differentiation by varying hydrogel stress relaxation.
31st Annual Conference of the European Society for Biomaterials. 05 to 09-09-2021. Virtual conference.
E. Prouvé, M. Rémy, C. Feuillie, M. Molinari, P. Chevallier, B. Drouin, G. Laroche, M.-C. Durrieu